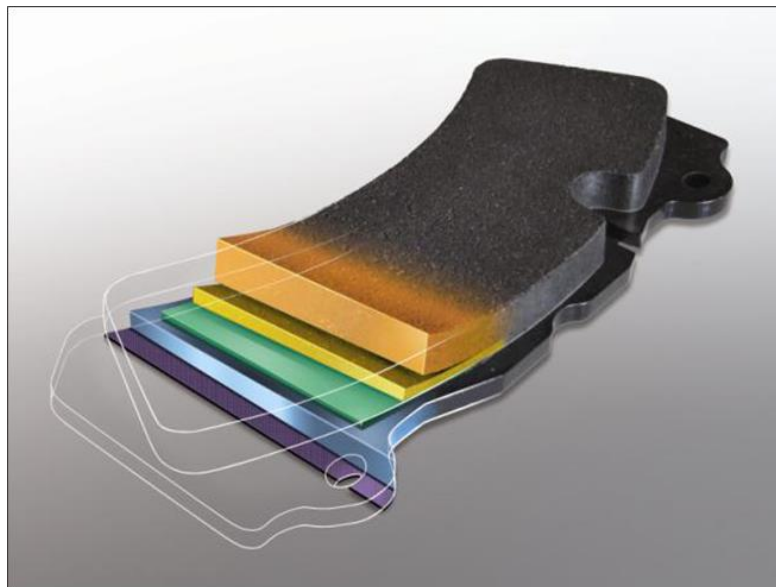# Low-impact friction materials for brake pads

Andrea Bonfanti

Low-impact friction materials for brake pads

Andrea Bonfanti

E-mail: andrea_bonfanti@brembo.it

Approved by:

Prof. Giovanni Straffelini, Advisor
Department of Industrial Engineering
University of Trento, Italy.

Ph.D. Commission:

Prof. Vincenzo Maria Sglavo,
Department of Industrial Engineering
University of Trento, Italy.

Prof. Nuno M. Neves
Department of Polymer Engineering
3B's Research Group , Portugal.

Prof. Cekdar Vakifahmetoglu
Department of Mechanical Engineering
Istanbul Kemerburgaz University, Turkey.

Thnks.

Abstract

State-of-the-art friction materials for applications in disc brake systems are constituted by composite materials, specifically formulated to ensure proper friction and wear performances, under the sliding contact conditions of braking events. The bases of typical friction compound formulations usually include 10 to 30 different components bonded with a polymeric binder cross-linked in situ. Main requests to be fulfilled during braking are an adequate friction efficiency and enough mechanical resistance to withstand the torque generated by forces acting on the disc brake. Generally, each component confers distinctive properties to the mixture and their primary function can be classified in the following categories: *binders* confer mechanical strength to friction material guaranteeing pad compactness during use, *abrasives* increase friction efficiency and improve compound wear resistance, solid *lubricants* are responsible for stabilizing friction coefficient and contrasting the build-up effect, *reinforcements* increase mechanical strength improving wear minimization and stabilization. Furthermore, other modifying components such as *fillers* and *functionalizers* are involved which are not directly related to friction efficiency, e.g. cheap materials, pigments, etc. (1) (2) (3).

Organic brake pads for disc-brake applications are based on phenolic resin binders, generally it requires three main manufacturing steps: raw material blending, where friction compound components are mixed by blenders. Hot-molding, where blended friction mix is pressed against a metallic support at controlled high pressure ($>2kN/cm^2$), temperature (150-200 °C) and pressing time (3-10 minutes). Brake pads post-curing, to complete the hardening of polymeric binder. This last step for phenolic resin is usually performed in a batch convective oven at temperature above 150 °C for 4-12 h, or alternatively using a continuous process, such as IR in-line tunnel ovens where the process time is 10-15 min, the oven heater temperature is between 500 and 700 °C and brake pad superficial temperature is easily above 300 °C (4).

Such kind of formulations and manufacturing process reflects the generally acknowledged state of the art as regards organic friction materials for passenger cars and light trucks. In this panorama the idea of introducing a completely inorganic binder matrix would represent nowadays an extremely appealing topic in the field (5) (6) considering potential improvements of this alternative approach.

The complete elimination of the organic binder would reduce emission of phenol-formaldehyde hazardous derivatives generated at high-temperature e.g. volatile organic compounds, highly toxic polyaromatic hydrocarbons etc… Nature and toxicity of the organic compounds released at high temperature was investigated on brake pads manufacturing and compared with preliminary studies recently published (7).

Introducing an inorganic hydraulically bonded matrix in place of the traditional organic-based binders would lead to a substantial reduction of the total embodied energy and water of brake pads considering low-temperature manufacturing process and inorganic binders properties. Primary production embodied energy for phenolic resin is estimated in the range of 75 - 83 MJ/kg (cradle to gate), while primary production water usage (embodied water) is in the range of 94 - 282 l/kg (8). As a matter of comparison, examples of the embodied energy for inorganic binders typically used for concrete construction are: Portland cements 4.9 MJ/kg, fly ash 9.3 MJ/kg, metakaolin 1.4 MJ/kg, silica fume 0.036 1.4 MJ/kg. The embodied water for these raw materials usually is less than 0.048 l/kg (9). Well-known properties of such peculiar inorganic materials (10) (11) exploiting the hydraulic activity of binders when exposed to water or alkaline environment. The only energy demanding compound was the alkaline solution (e.g. for sodium hydroxide and sodium silicate the embodied energy is respectively of 22MJ/kg and 16 MJ/kg (12))

New brake pad manufacturing process allowed the substitution of commonly implied highly energy-consuming procedures with low-temperatures steps. Friction material components except binders were blended together with conventional plow-blade blender forming a dry friction-mix, then this dry friction-mix is blended with the inorganic binder and water or alkaline activators in a planetary mixer forming a wet friction-mix. Eventually wet friction mix is cold-pressed onto a metal back-plate without the need for further treatments at high temperature. It immediately emerges the energetic benefit connected to the manufacturing process of this inorganic binder-based brake pads. After brake pad production, the behavior of these inorganic materials was compared to traditional phenolic-based friction materials. Brake pads were tested on a full scale automotive brake dynamometer and on a real vehicle (in terms of performance and particle emission) following custom and international standard procedures.

The aim of this work was to produce brake pad prototypes with friction material based on an inorganic hydraulic binder at performance comparable to commercial brake pads with organic-matrix based friction materials.

The results obtained so far resulted particularly promising and paved the way to further developments of these novel class of friction materials.

Table of Contents

1 General introduction

1.1 Introduction to brake systems

The aim of a brake systems is to generate a braking torque to retard the road wheel and thus the vehicle to which it is fitted. The purpose of friction brakes is to decelerate or to stop a vehicle by transforming the kinetic energy of the vehicle into heat, via friction, and dissipating that heat to the surroundings. For power-driven vehicles and their trailers this results can be achieved using two main types of brake systems:

- Disc brake system, consisting in pushing two brake pads on a disc.
- Drum brake system, consisting in pushing outwards brake shoes mounted inside a drum against the inner surface of the drum.

Modern light and commercial vehicles disc-pad brake systems are constitute by a brake disc, integral with the wheel hub, which is clamped by brake pads pushed on the disc by slave cylinders inside a caliper fixed to an hub bracket, see fig.1.1
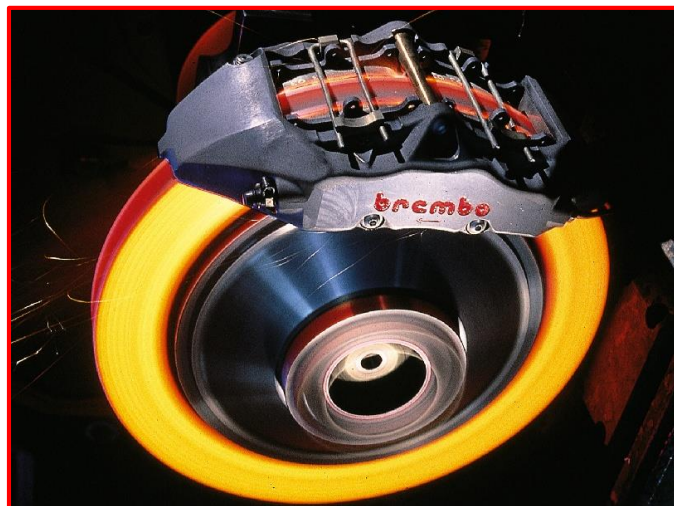
Fig.1.1 Brake disc system with fixed caliper tested on a full scale automotive brake dynamometer. (Courtesy of Brembo S.p.A.)

Slave cylinders force is controlled by a master cylinder behind the brake pedal which press a fluid in a hydraulic circuit where slave cylinders (pistons into the caliper) are connected. See fig.1.2
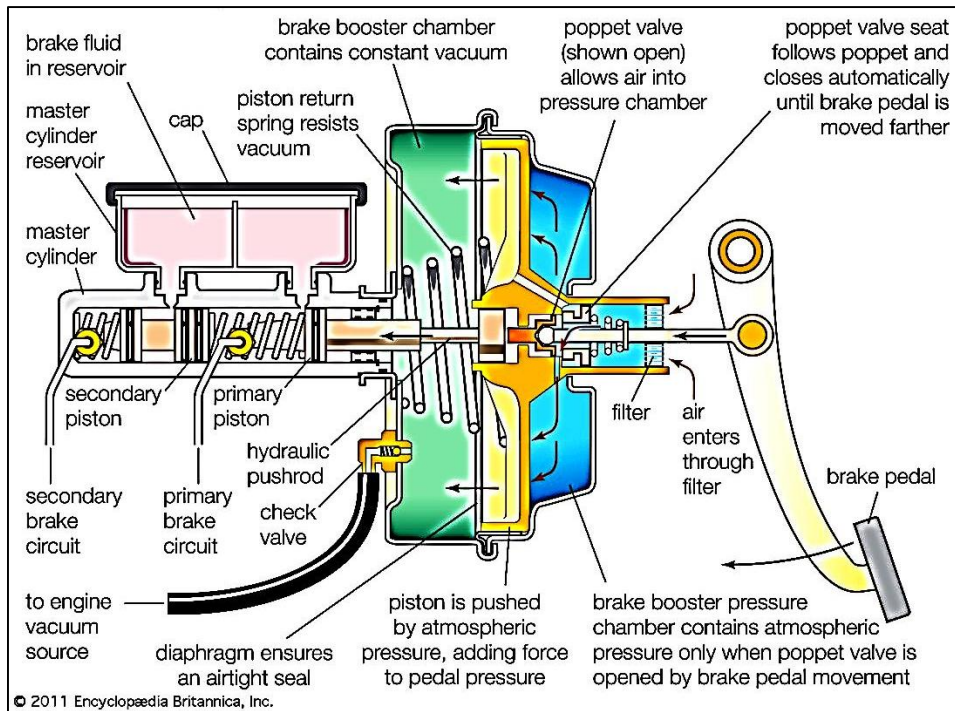
Fig.1.2 Vacuum-assisted power brake system (13)

1.1.1 Calipers

Calipers can be divided in floating or sliding calipers and fixed calipers.

Floating calipers have one or more pistons (slave cylinders) only on the inboard side of the rotor, caliper bracket is fixed to the hub bracket and the caliper frame (or housing) is free to slide on a pin set up, see fig.1.3 When pressure is applied on pistons, floating mechanism transferring load on the other side pushing pads on the brake disc. Good characteristics of floating calipers compared to fixed calipers are cheapness, small size, less brake fluid heating and different possible actuation systems, e.g. hydraulic, hydromechanics, mechanic, pneumatic and electric.
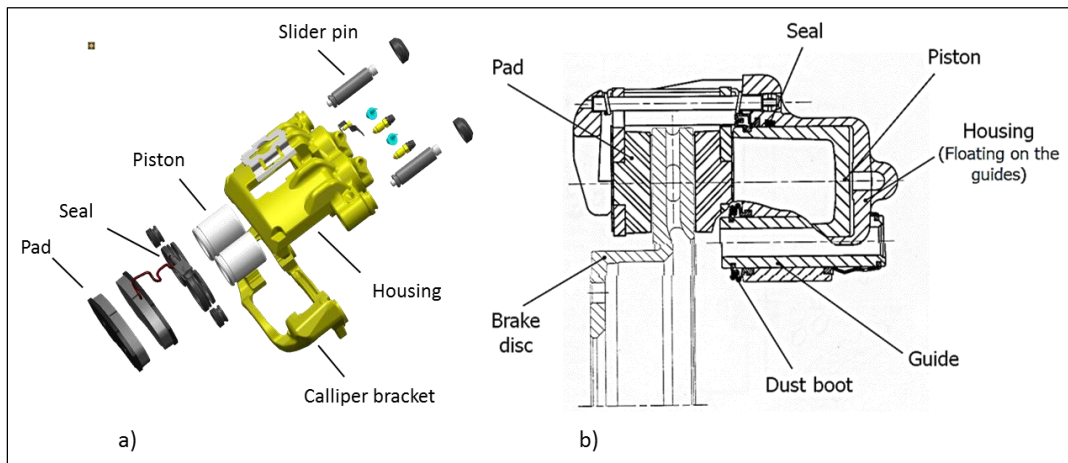
Fig.1.3 a) Exploded and b) section view of a floating hydraulic caliper. (Courtesy of Brembo S.p.A.)

2

Fixed calipers have hydraulically actuated pistons on both sides and no sliding parts. It can be made on single piece (monobloc) or in two pieces depending on production throughput, free installation space, car maker technical requirements, see fig.1.4. When pressure is applied on hydraulic circuit cylinders independently push pads on both sides of the disc.
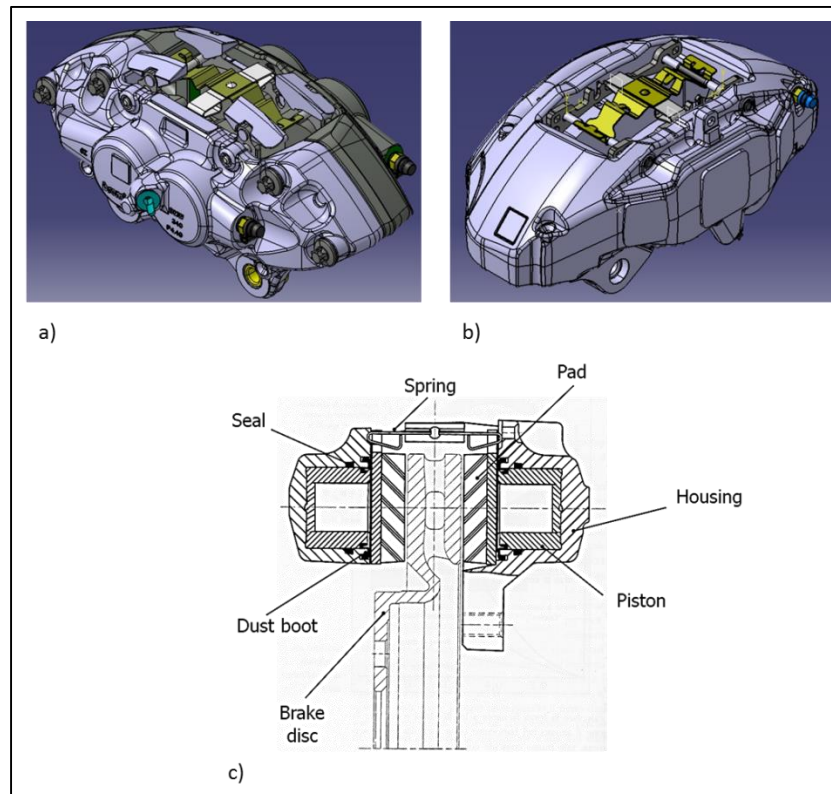
Fig.1.4 a) Two-piece and b) monobloc fixed caliper; c) section view of fixed caliper. (Courtesy of Brembo S.p.A.)

Compared to floating calipers good characteristics of fixed calipers are lightness, aesthetic, possible bigger pad superficial area, less residual brake clamping force and homogeneous pads wear.

1.1.2   Brake disc

Brake discs, or brake rotors in A.E., are commonly made of lamellar graphite structured grey cast iron. For some special application, e.g. high performance systems, brake discs can be made of different materials such as aluminum composites, carbo-ceramic, carbon-carbon etc. Cast iron is mainly used due to its stable performance, good noise dumping, raw materials low cost and easy manufacture.

A brake disc has two main functions: it transmits high mechanical force and disperses generated heat while operating at a high temperature.

More than 80% of the heat generated ends up in the disc and an excessively worn disc can impair the safety of the braking system, hence the disc needs to be cooled. Different disc design was studied for this purpose, for example improved air circulation caused by pillars compared to straight vanes or a full disc brings a more effective cooling of the braking surface see fig.1.5

Fig.1.5 Different brake disc design, from left to right: disc with curved vanes, with straight vanes and with pillars vane. (Courtesy of Brembo S.p.A.)

Wear is a normal phenomenon during disc use, on regular disc use it's recommended to do not delay in replacing discs once the minimum allowed thickness is reached. The pads do not work correctly if the disc thickness decreases and a reduction in disc mass increases disc temperatures. High temperatures cause the disc to expand, if it exceeds the material's elastic limit as soon as the disc cools down deformation begins and cracks occur after a certain number of cycles.

In particular for this work grey cast iron Brembo brake discs with pillar vein were used.

1.1.3   Brake Pads

Brake pads are used in disc brake systems and brake shoes are used in drum brake systems. It's called brake lining the consumable part sliding on disc/drum surfaces attached to pad/shoes backing plate.

There's a chronological sequence of the most common materials used for brake linings appearance (14) (15), see tab.1.1

Material Description	Application(s)	Approximate Year
Cast iron on steel	Railroad	prior to 1870's
Hair or cotton belting (limited by charring at about 300°F)	Wagon wheels and early automobiles	ca. 1897
Woven asbestos with brass and other wires for increased strength and performance	Automobiles and trucks	ca. 1908
Molded linings with shorter chrysotile fibers, brass particles, and low-ash bituminous coal	Automobiles and trucks	ca. 1926
Dry-mix molded material to replace cast iron brake blocks that produced metallic dust that shorted electric train rails	London underground	ca. 1930
Flexible resin binders developed along with more complex formulations	Brake drum linings	1930's
Resin-bonded metallic brake linings	Industrial and aircraft applications	1950's
Glass fibers, mineral fibers, metal fibers, carbon and synthetic fibers to provide semi-metallic with higher performance than asbestos (beginning of safety issues with asbestos)	Automotive and trucks	1960's
Non-asbestos (fiberglass) materials	Brake drums on original equipment cars	1980's Suggested use
Suggested use of carbon fibers	Automotive brakes	1991

Tab.1.1 Historical compositions of automotive friction brake materials (14)

Typical structure of brake pad is shown in fig.1.6, every part is responsible of a different task as reported in tab.1.2
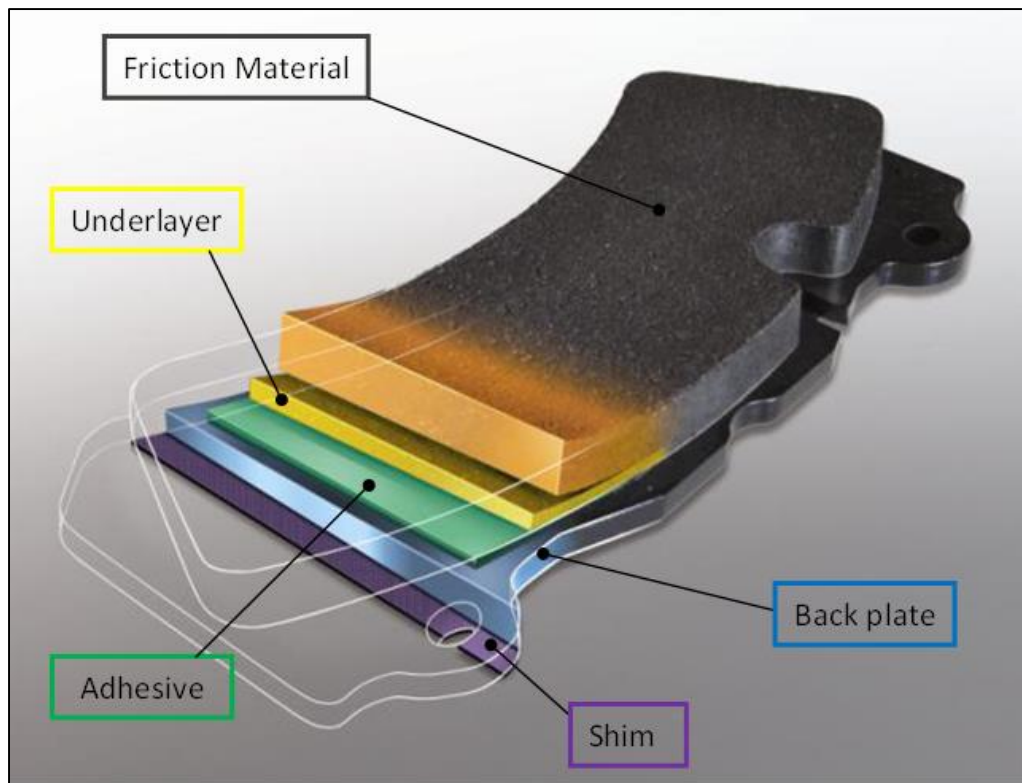
Fig.1.6 Typical components of a brake pad. (Courtesy of Brembo S.p.A.)

Layer	Main Properties
Friction material	Directly in contact with disc guarantees friction performance
Underlayer	Thermally insulate the backing plate and, therefore, the piston and brake fluid from the heat generated in the friction material. Improve comfort by limiting the transmission of vibration and noise from the friction material to the caliper. Good friction efficiency in any case required due to safety reason.
Adhesive	Ensure high shear strength between underlayer and back plate
Backing plate	Distribute the force exerted by the piston over the entire contact surface, dissipate the tangential force generated during braking by the contact between the friction material and the disc through the backing plate
Shim	Prevent the transmission of vibration to the rest of brake system

Tab.1.2 Main properties of brake pad components

State-of-the-art brake pads are constituted nowadays by resin-bonded composite friction materials, these are specially formulated to give good friction and wear performance. The basis of such formulations is usually a polymeric binder with addition of fillers and fibers that provide good friction efficiency during brakes and mechanical strength necessary to withstand at generated frictional forces. There is not a strict regulation to classify organic friction materials in terms of chemical composition, but they are commonly divided as reported in tab.1.3, where nomenclature varies from manufacturer to manufacturer, and also from country to country.

Material classification	Usual content	Main characteristics
NAO "Non-Asbestos Organic", sometime referred as "**Very low steel**" or "**Non-steel**" In aftermarket, NAO's are often referred as "**ceramic**" , this it should not be confused with *pre-ceramic* materials based on silicon resins.	Less than 10% of Cu, Fe and theirs alloys. Contain nonferrous metals, various abrasives and lubricants, mineral fibers and other reinforcements	- Low to medium-high friction coefficient 0.33 –0.40. - Excellent wear at lower temps. <200C. - Good for wheel dust. - Relatively poor wear under heavy duty conditions and at higher friction levels. - Good noise & roughness characteristics
"**Low Steel**" or "**Low-metallics**" also "**Low-met**" Sometimes referred as "**European**" or "**ECE**" (fulfil ECE regulation 90 requirements)	10-50% of Fe, Steel, Cu and Cu Alloys Contain some steel fibers and/or iron powder, various abrasives and lubricants, some non-ferrous metals.	- Medium high friction coefficient, typically 0.35-0.5 - Good pedal feel and braking confidence. - Good fade and high speed performance. - High pad/rotor wear. - Good for high speed wear. - Lots of wheel dust. - Can have "corrective" wearing action. - Can possibly "true-up" the rotor over time - Inferior noise and life.
"**Semi-metallic**" or "**Semimet**"	More than 50% Fe and Steel Primarily contain steel fiber, porous iron powder, abrasives and graphite/coke lubricants	- Low to medium friction coefficient 0.28 –0.38 - Relatively high mu variation (temperature, duty cycle) - Good fade characteristics. - Poor wear at low temps. <100C. - Excellent wear at temps. over 200C. - Good wear under heavy loads. - Poor wear at high speeds. - Generally inferior Noise, Vibration & Harshness compared to NAOs - Contains no copper - Low initial cost - High fluid temperatures can be an issue.

Tab.1.3 Organic friction materials nomenclature for light and commercial vehicles.

Due to the fact that asbestos is not allowed in modern friction materials, scientifically speaking all of classified material in tab1.3 are non-asbestos organic (NAO), different nomenclatures reported are for marketing purpose only.

Non organic friction materials are also possible, e.g. sintered metallic, carbon composite etc., but they are not considered in this work.

1.1.3.1   Organic friction materials

Typical friction material is a compound of 10 to 30 different subcomponents (1) (2) (3) (14) (16) (17), selected from thousands different materials; components are divided in classes depending on their functions. See tab.1.4

Material Function	Main tasks
Binders	Hold all others materials, conferee mechanical properties.
Reinforcements	Increase mechanical properties, reduce wear
Abrasives	Increase friction coefficient, clean the disc surface
Lubricants	Friction coefficient stabilizer, controls the friction film generation
Fillers and functionalizers	Manufacturing process aids, cheapen end products, corrosion protection, colorants, increase or reduce heat transfer, noise reduction, etc.

Tab.1.4 Description of friction material subcomponents functions

Abrasives: In this group there are materials with Mohs hardness higher than 5, usually metal oxides and ceramic material like carbides and nitrides. Abrasives components increase friction coefficient and keep clean the disc surface from rust or accumulated friction material.

Solid lubricants: In this group there are material with low friction coefficient like graphites metal sulphides and PTFE. Solid lubricant components are responsible to contrast the build-up effect of abrasives, reducing and stabilising the friction coefficient.

Reinforcements, the function is to confer mechanical resistance to friction material guaranteeing integrity of pad during the use.

Fillers and functionalizer: Organic and inorganic materials not directly related to friction efficiency, e.g. cheapen end products, corrosion protection, colors, increase or reduction of heat transfer, improving comfort during brake reducing noise and judder.

Some of the components could be placed into more than one category since they fulfil several functions, but generally they are identify from their main contribute.

1.1.3.2   Friction material identification

In compliance with applicable United States standards, market identification of organic commercial brake pads for passenger cars and light trucks is made by Automotive Manufacturers Equipment Compliance Agency AMECA trough an edge code^{TM} marking (18), see fig.1.7

Formulation identification code

ABC 1234 FG

Manufacturer's
identification code

Cold and hot friction coefficients
in accordance to VESC V-3 standard
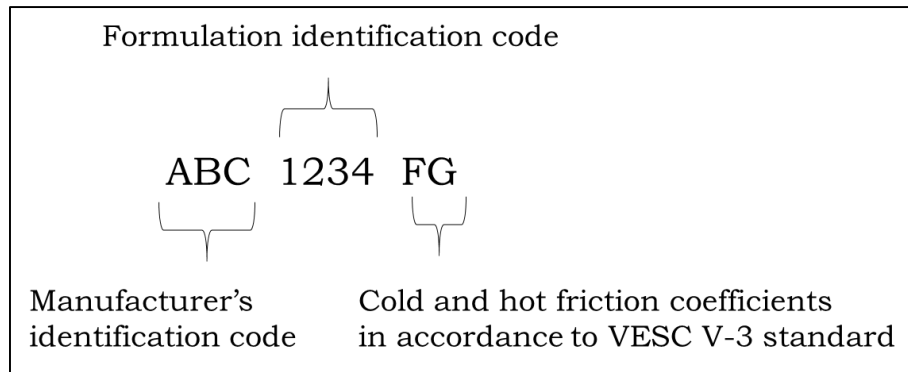
Fig.1.7 Edge code marking for commercial friction materials (19)

Edge code is indelibly marked on brake pad and is composed of three parts, the manufacturer's identification code, the formulation identification code and performance of friction materials in terms of friction coefficient in accordance to Vehicle Equipment Safety Commission regulation V-3 or VESC V-3 standard, see tab.1.5, where the first letter concerns "normal (cold) friction coefficient" in a temperature range from 200 to 400 F and the second letter concerns "hot friction coefficient" at temperatures from 400 to 650 F

Class Code	Coefficient of friction
C	Not over 0.15
D	Over 0.15 but not over 0.25
E	Over 0.25 but not over 0.35
F	Over 0.35 but not over 0.45
G	Over 0.45 but not over 0.55
H	Over 0.55

Tab.1.5 Minimum requirements and uniform test procedures for motor vehicle brake linings measured with a Friction Test machine as described in SAE J661A (20) **in compliance with VESC V-3 standard.**

Future of friction materials will be on "green" products. Due to environmental problems related to debris from friction materials wear, new regulations have been promulgated in different states; for California State legislation see tab.1.6

Regulation timing in California	Brake Manufacturers Council LeafMark	Brake friction material legislation requests
January 1, 2014	"Level A"	(a) On and after January 1, 2014, any motor vehicle brake friction materials containing any of the following constituents in an amount that exceeds the following concentrations shall not be sold in this state: (1) Cadmium and its compounds: 0.01 percent by weight. (2) Chromium (VI)-salts: 0.1 percent by weight. (3) Lead and its compounds: 0.1 percent by weight. (4) Mercury and its compounds: 0.1 percent by weight. (5) Asbestiform fibers: 0.1 percent by weight. (6) Motor vehicle manufacturers and distributors, wholesalers, or retailers of replacement brake friction materials may continue to offer for sale brake friction materials not certified as compliant with subdivision (a) solely for the purpose of depletion of inventories until December 31, 2023
January 1, 2021	"Level B"	On and after January 1, 2021, any motor vehicle brake friction materials exceeding 5 percent copper by weight shall not be sold in this state.
January 1, 2025	"Level N"	On and after January 1, 2025 any motor vehicle brake friction materials exceeding 0.5 percent copper by weight shall not be sold in this state

Tab.1.6 Brake friction material legislation requests from California State Senate Bill 346 (21).

Washington State Senate Bill 6557 is very similar (22).

The requirements for a friction material are: good thermal conductivity, good corrosion strength, low noise, low weight, long durability, steady friction, low wear rate, and a good price/benefit ratio. Influence of raw materials and production methods on brake system tribological behavior cannot be fully predicted a priori, but it requires big part of trials. For this reason most of friction materials formulations tent to be proprietary (23).

In following chapter relationship between chemical and physical properties of raw materials and brake fundamental mechanisms will be reviewed in order to describe the material selection criteria for friction materials formulation.

2   Friction material components

2.1   Abrasives

Despite the name of the category it's important to remark that the real duty of abrasives components in brake systems is not to wear, grind or cut away the brake disc/drum surface, but it's to fulfill two important roles:

- Increase friction coefficient at brake pad-disc interface
- Improve wear resistance of friction material.

To better understand the abrasive raw materials selection for friction materials it's interesting to review abrasive wear mechanism.

Wear is defined as "the progressive loss of substance from the operating surface of a body occurring as a result of relative motion of the surface " (24) and it can occur by adhesion, abrasion, erosion, oxidation, delamination, fatigue or a combination of these (25).

To describe abrasive wear many classifications are possible, one of the widely used models divides abrasion in "two-body" and "three-body" mechanisms (26).

Two-body abrasion: hard particles or asperities rigidly stuck on first body are able to penetrate in a second body during the rub of the two bodies under load.

Three –body abrasion: some material, whether autogenously generated or foreign matter, is present at the interface between first and second body during the rub of the two bodies under load.

It's interesting to see the effect of the two wear abrasion models on microscale (27). Looking at fig.2.1 (two body) it's easy to see grooves produced by a direct abrasion of second body on the first one. When large amount of particles are added on the interface micro multiple indentations are visible on first body surface without directionality (three body).
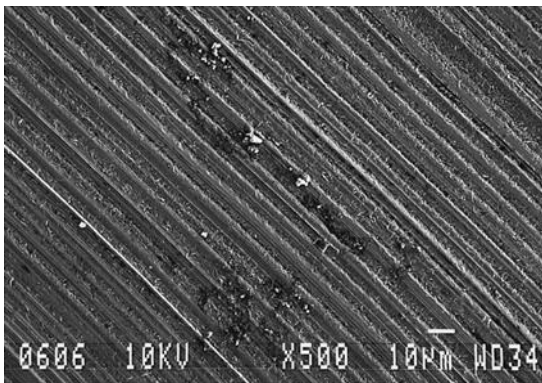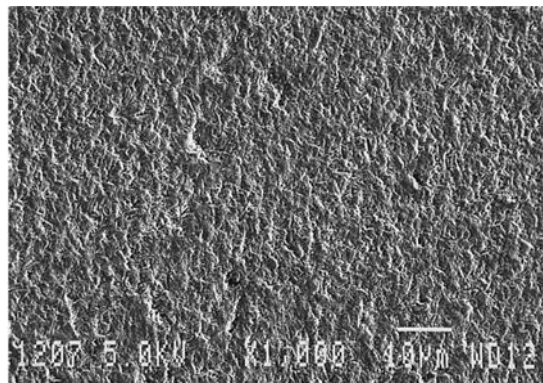
Two-body   Three-body

Fig.2.1 Worn surfaces of a quenched and tempered steel produced by hard martensitic steel ball and 3 μm diamond slurry 0.0009 %vol. for "two-body" and 0.237 %vol. for "three-body" wear mechanism (27).

In the main notation first body is referred to the surface that suffer wear, the second body is in relative motion with the first one such some force can be transmitted; second body can be in direct or indirect contact with the first one and it can suffer wear, even if wear is not its main concern.

In other notations second body is also called first body (especially if both bodies suffer wear), in this case they are called several first bodies. At other times first body is called "the body" and second body is called "the counterbody".

Four abrasive interaction mechanisms can be described: micro-cutting, fracture, fatigue and grain pull-out. (28) see fig.2.2
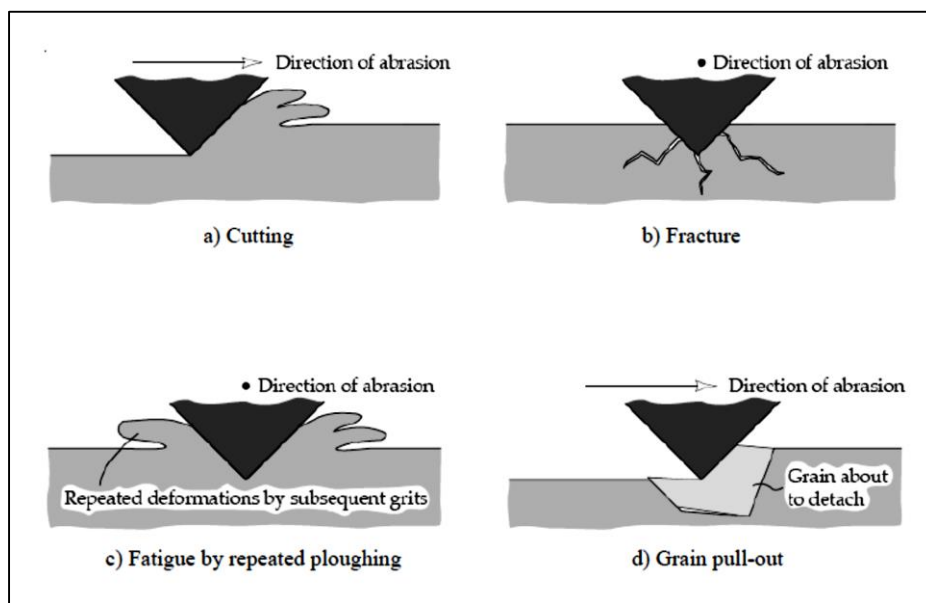
Fig.2.2 Mechanisms of abrasive wear: cutting, fracture, fatigue and grain pull-out (28)

Cutting and ploughing mechanisms involving predominantly plastic deformation of wear material. Conversely, fragmentation occurs for brittle materials where the nature of the contact change from elasto-plastic indentation to Hertzian fracture (29).

If f_{ab} is the ratio of the amount of material removed from the surface by the passage of a grit and the volume of the worn groove, $f_{ab} = 1$ for ideal micro-cutting, $f_{ab} = 0$ for ideal micro-ploughing and $f_{ab} > 1$ for micro-cracking. (30)

Considering that particles and bodies can be plastic deformed or crushed by cracking, and having chemical interaction during wear process, the solid state cohesion of materials should be considered to better explain abrasive wear.

2.1.1   Solid state cohesion

2.1.1.1   Hardness

It was shown the interaction between abrasives material and sliding surfaces, but when a material can be considered abrasive and how strong is the abrasion?

On a first approximation it's a good approach to compare hardness of surface material (H) and hardness of abrasive(H_a).

On fig.2.3 is reported the relative wear $\frac{1000}{\epsilon}$ of steel, hardened by tempering, grooved by abrasives with same size but different hardness; ϵ is the wear resistance relative to a standard material (31).
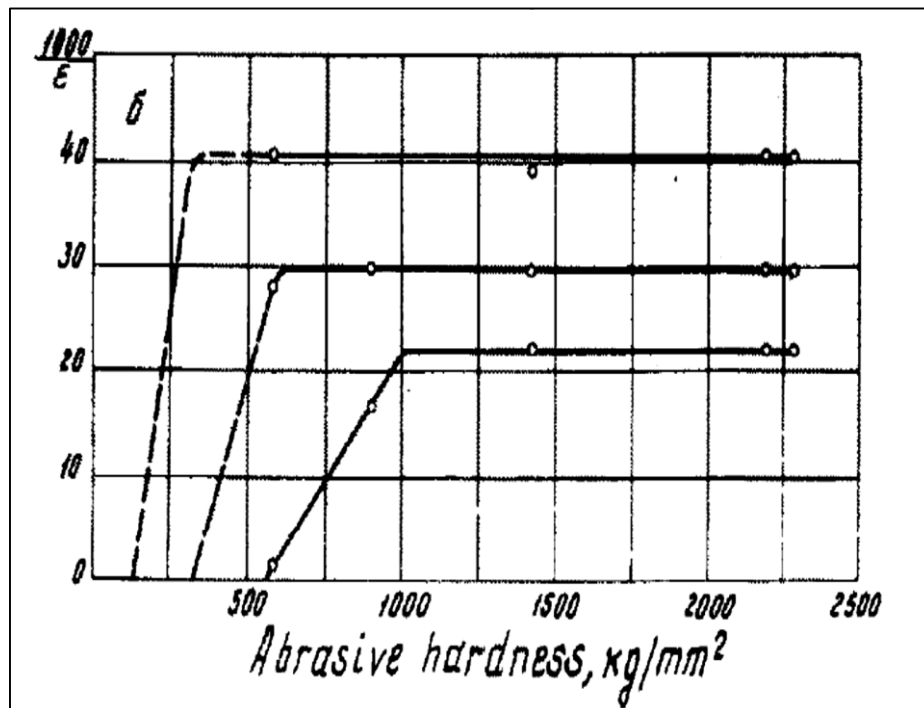
Fig.2.3 Relative wear of three steel 0.8% C martensitic hardened and tempered (186, 468 and 795 kg/mm² HV) worn by grains of the same size of glass (585 HV), flint (908 HV), garnet (1426 HV), railite (2198 HV) and electrolytically produced corundum (2290 HV) on a cloth (31).

It's interesting to see that after a certain hardness ratio value the wear doesn't change. This effect can be summarized as in fig.2.4
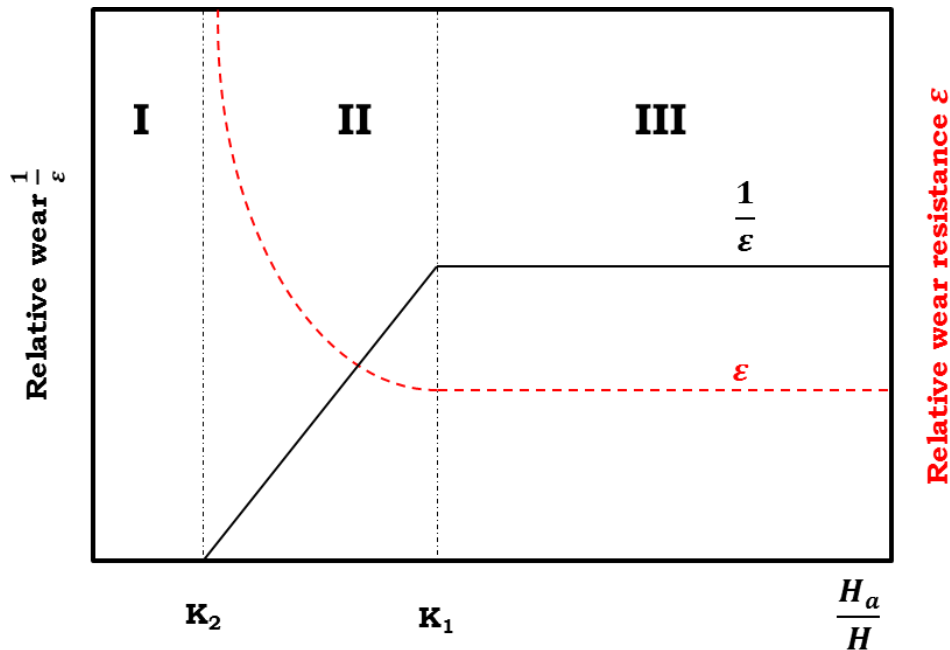
Fig.2.4 Dependence of relative wear and wear resistance on different hardness ratio (31).

Depending on hardness ratio, three different behaviors can be identified.

I)   *Not abrasive.* The hardness of abrasive is too low, $H < H_a K_2$
        No significantly wear. $K_2 = 0.7 - 1$

II)   *Mild abrasives.* The two hardness are comparable, $H_a K_2 < H < H_a K_1$.
        A linear dependence on H_a can be measured.

III)   *Hard abrasives.* The hardness of abrasive is significantly higher than the
        surface hardness, $H > H_a K_1$.
        Wear of surface is independent on H_a change.

A linear correlation between surface hardness or their modulus of elasticity and wear can be found (31).
For some specific cases like very ductile, extendable or brittle materials this relation is not always true, moreover the addition of alloying elements on metals doesn't raise the wear resistance in proportion to hardness increase (32).
A different approach has been proposed to on abrasive wear model, materials melting point has been to compare abrasive wear and material bonding energies.
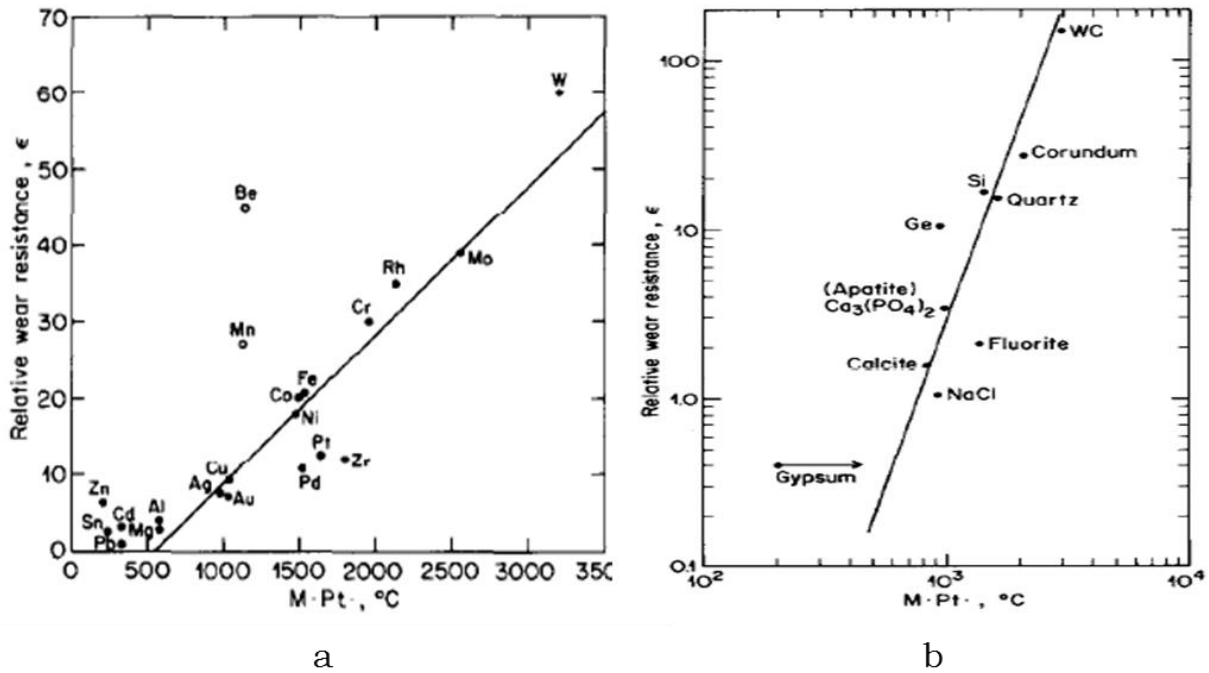
Fig.2.5 Correlation between melting points and relative wear for a) metals and b) non-metals.
(33)

Even if Be and Mn don't follow the relation, this research suggested that hardness is the first but not the only parameter to consider when describing abrasive wear (33).

2.1.1.2 *Fracture toughness*

Material fracture toughness is another parameter to consider in abrasives components choice. Particles size of abrasives can change during friction due to fragmentation of particles; decreasing the hardness and increasing the fracture toughness increases the critical abrasive size at which particle fragmentation occurs (34).

Toughness of abrasive materials can change depending on material nature, grain size and porosity, see tab.2.1

Da	Gb (µm)	Pc (%)	Toughnessd K ($MPa \cdot m^{1/2}$)					
			F	IF	I	CNB	NB	DT
Al₂O₃								
S	5	≥5		3.4	2.3			4.1
S	<10	<5		3.2-4				
TiB₂								
H	10	2		5.1 ± 0.5				6.7 ± 0.2
S	8	1		5.5± 0.6				8.0 ± 0.3
SiC								
H	<1	~1-2		3.8 ± 0.3				5.2 ± 0.3
α-S	4	~3-4		3.0 ± 0.1				3.0 ± 0.3
α-S		~1-2		2.8	3.0	3.1	4.2	
β-S		~1-2		2.6	3.0	3.4	4.0	
α-S		~2-3		3.3	3.6		4,8	
α-S	5	~1-2			3.8		4.6	
α-S	5		2-3	3.5			4.5-5	
H		~4		2.6-3.8				3.9
α-S			3.2					
RS				3.5 ± 0.4	4.1 ± 0.6			3.8 ± 0.4
Si₃N₄								
RS				2.1 ± 0.1	2.2 ± 0.3			2.1 ± 0.2
H			5.6					
S			3.3					
H	2	~0		6.1 ± 0.6	4 ±0.4			5.6 ± 0.9
H				3.5				4.1
S			6.0 ± 1.6				6.5 ± 1.2	
Se			3.8 ± 0.8				3.9 ± 0.8	

Tab.2.1 fracture toughness measured with different methods from various authors (35)
[a] *Materials* **and process: S=sintered, H=hot pressed, RS=reaction sintered**
[b] **G=Grain Size**
[c] **P=Volume fraction porosity**
[d] **F=fractography, IF=indentation flaw fracture, I=indentation, CNB=chevron notch beam, DT=double torsion**
[e] **SiAlON**

For non-cubic crystal systems a non-linear relation has been found from grain size and fracture toughness. Generally, in association with micro-cracks and crack growth resistance, a maximum in toughness and in fracture energy is measured for a certain grain size; this effect is less pronounced but also noticeable for cubic materials.
Fracture toughness depends also on porosity, a continuous decrease in toughness when porosity increase can be measured (35).

2.1.2　Particles size

When two-body and three-body models were described it wasn't consider that other materials in addition to abrasive can be embedded at interface between brake pad and disc. Indeed, relative soft elements can be released at interface due to the friction action. Tribofilm, third body layer, transfer layer, tribo-layer or friction layer

are often used as synonymous to describe the layer entangled at the interface between brake disc and brake pad.

Just for simplicity the tribofilm can be represented as a system where abrasive particles are mixed in a solid lubricant.

To describe what happened when particles are interposed in a lubricated contacts, a 2-D model can be used, where diamond shaped particles, characterized by a major axe D and an angle β, are embedded in the tribofilm with thickness h between two bodies A and B as reported in fig.2.6 (36)
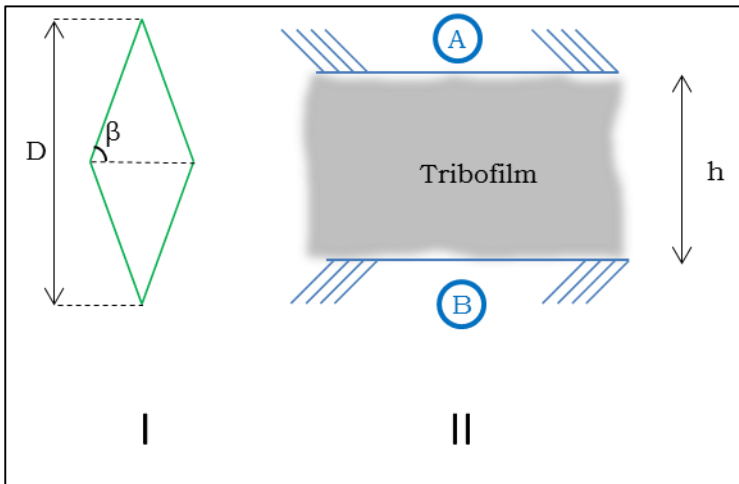
Fig.2.6 I) Abrasive diamond shape particles are described by parameters D and β. II) Embedded tribo-film with thickness h generated by relative motion of two surfaces in contact. (36)

Appling a relative motion between A and B three different cases are possible.

When D<h particles are free to move in the tribofilm, only occasionally contacts are possible and damage of surfaces is relatively low. See fig.2.7
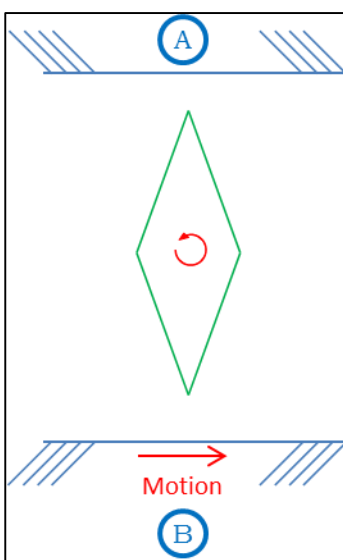
Fig.2.7 Abrasive particles are free to move in tribo-film $\frac{D}{h} < 1$ (36)

When B>h some considerations about the interaction from particles and surfaces have to be done.

There is a critic threshold $\left(\frac{D}{h}\right)_{crit}$, depending on β, beyond which at particles it is not permitted to rotate during the surfaces relative motion, see eq.2.1.

$$\left(\frac{D}{h}\right)_{crit} = sec\beta$$

Eq.2.1.

When $1 < \frac{D}{h} < \left(\frac{D}{h}\right)_{crit}$, particles are free to rotate indenting the surfaces; this produce a local pitting damage associable to an oblique hardness test, see fig.2.8
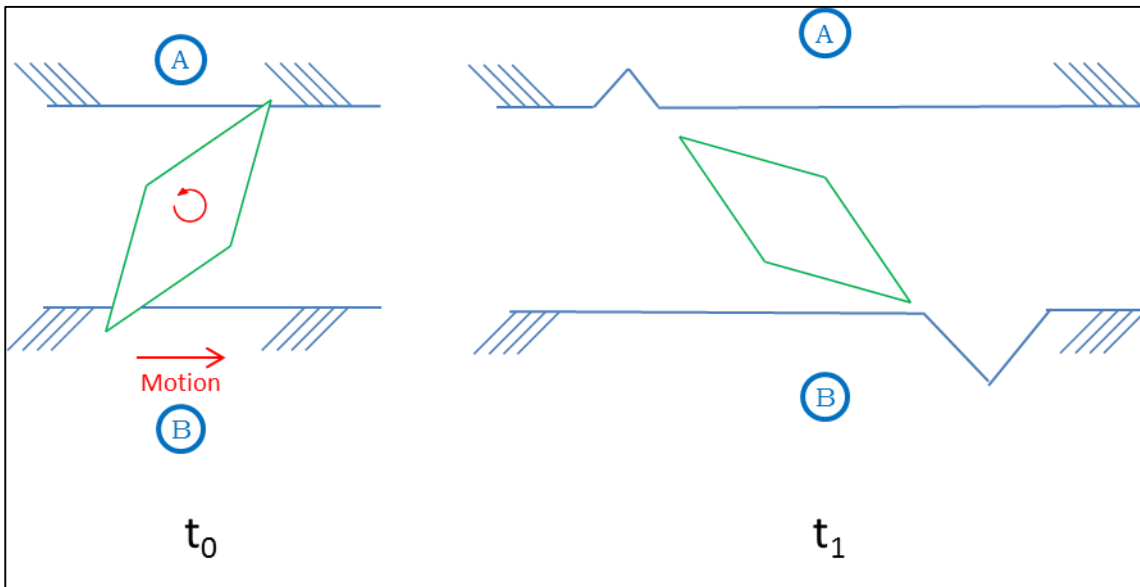
Fig.2.8 Abrasive particle with $1 < \frac{D}{h} < \left(\frac{D}{h}\right)_{crit}$. t₀) abrasive embedded particle rolls indenting surfaces. t₁) indented surfaces after mechanical action of particle during motion. (36)

When $\frac{D}{h} > \left(\frac{D}{h}\right)_{crit}$ particles rotate until a position of equilibrium, in this case there are two possibilities. See fig.2.9

I)   Both surface are grooved even if one is softer than the other. Considering the geometry of the system, particles start to rotate till they reach an equilibrium position. θ_1 is the inclination of the particles and it's related to $\frac{D}{h}$ by eq.2.2

$$\frac{D}{h} = \frac{[1 + tan^2(\beta + \theta_1)]tan\beta}{cos\theta_1 tan^2(\beta + \theta_1) - 2sin\theta_1 tan(\beta + \theta_1) - cos\theta_1}$$

Eq. 2.2

II) One surface is soft enough to firmly embed particles; during relative surfaces motion only the harder surface is grooved. θ_2 is the inclination of the particles at the equilibrium, and it's related to $\frac{D}{h}$ by eq.2.3 where $H = \frac{hardness_A}{hardness_B}$.

$$\frac{D}{h} = \frac{tan\beta}{cos\theta_2\left(1 - \frac{2(1 + H)}{1 + 2H}cos(\beta + \theta_2)\right)}$$

Eq.2.3
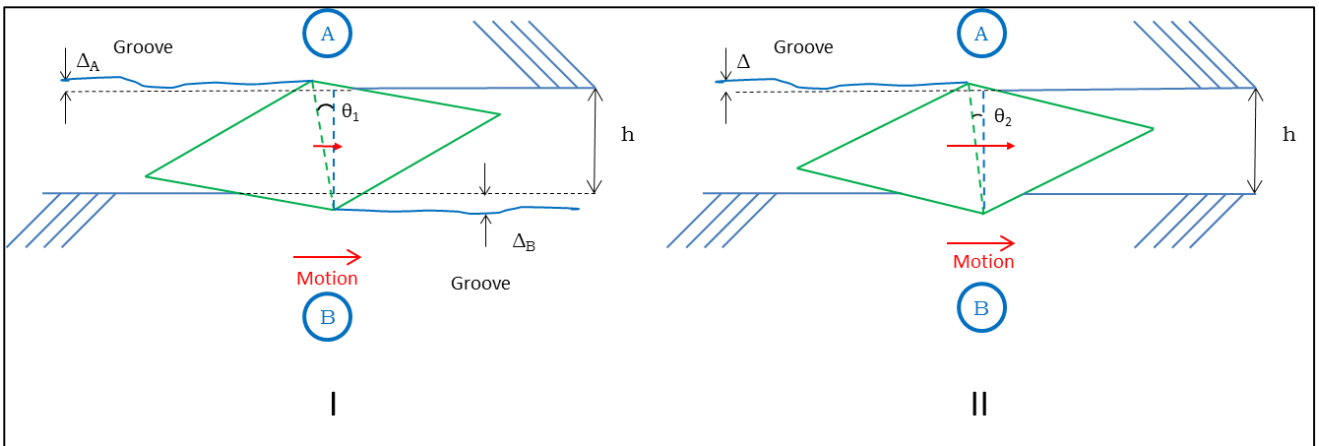
Fig.2.9 Abrasive particle with $\frac{D}{h} > \left(\frac{D}{h}\right)_{crit}$. θ_1 and θ_2 are particles inclination when a position of equilibrium is reached during motion. I) Embedded hard particle is dragged by relative motion of two bodies grooving both surfaces. II) Hard particle firmly embedded on a soft B surface grooving A surface only. (36)

Diamond like shape particles has been considered in the 2-D model but a similar approach can be used on a 3-D model to reach same conclusions on possible abrasion mechanisms.

A suitable system to describe the behavior of materials under wear is to plot "wear maps" (27) where a relation between load, speed and wear type it's considered; an example is reported in fig.2.10

19
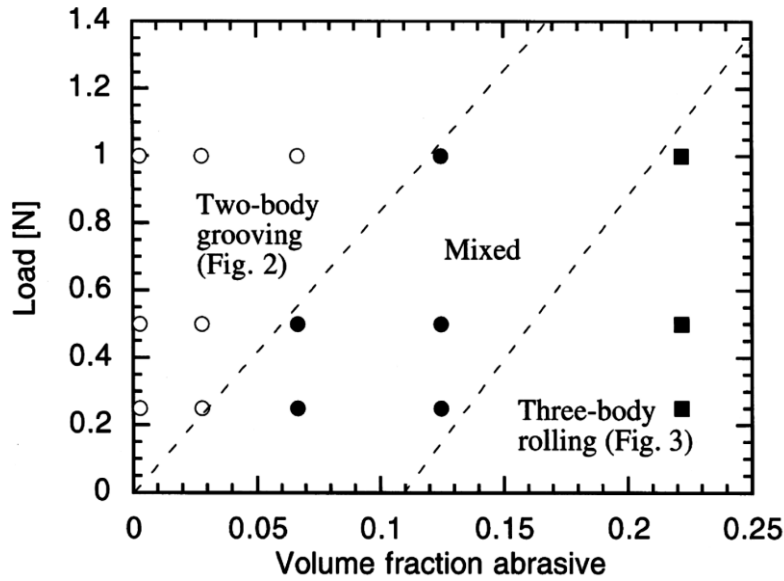
Fig.2.10 Wear map of tempered steel produced by hard martensitic steel ball and 3μm diamond slurry. (27)

In this map the areas of classical two-body and the three-body abrasive wear mechanism description are not well separated. There is a mixed area where grooving and rolling abrasive wear mechanisms notations are necessary to describe the system.

As already discussed $\frac{D}{h}$ ratio depends on shape of particles and on the distance of surfaces, when a load is applied the penetration of particles can regulate the distance of the two surfaces. Beside *two-body* and *three-body* models, *grooving* and *rolling* models can be considered to describe abrasive wear.

In Vickers hardness test, the measure of the hardness H depend on the surface diagonal length d of indented pyramid and the load P applied on the indenter as shown in eq.2.4

$$H = \frac{P}{d^2}$$

Eq.2.4

When more than one indenter is present, like in a multiple-particles system, the load P is distributed; in this case it's meaning to calculate the load for particle p, see eq.2.5, where A is the projected area of the wear contact, P the total load and υ the volume fraction of abrasive.

$$p \propto \frac{PD^2}{A\upsilon}$$

Eq.2.5

20

The new ratio $\frac{D}{h}$ equation became eq.2.6 where B is a constant for a given indenter geometry, and H the hardness of the surface

$$\frac{D}{h} = \frac{1}{1 - \frac{B}{D}\sqrt{\frac{p}{H}}}$$

Eq2.6

It is clear that different rolling or grinding abrasion mechanism is influenced by total load and number of particles present at surfaces interface. For low load and large amount of particles rolling wear mechanism is preferred; reducing the number of particles or increasing load, groove wear mechanism becomes dominant.

It's important to underline that rolling wear mechanism follows the classical Archard equation, see eq.2.7, where W is the wear volume, k is the Archard coefficient, P is the normal load and S is the total sliding distance.

$$W = k \cdot P \cdot S$$

Eq.2.7

For grooving mechanism the wear is proportional to some power of load less than 1. (27)

2.1.3 Particles Shape
Not only particles dimension affects wear, but also particles shape does (37), See fig.2.11

Sharp abrasive grit

Blunt non-abrasive grit
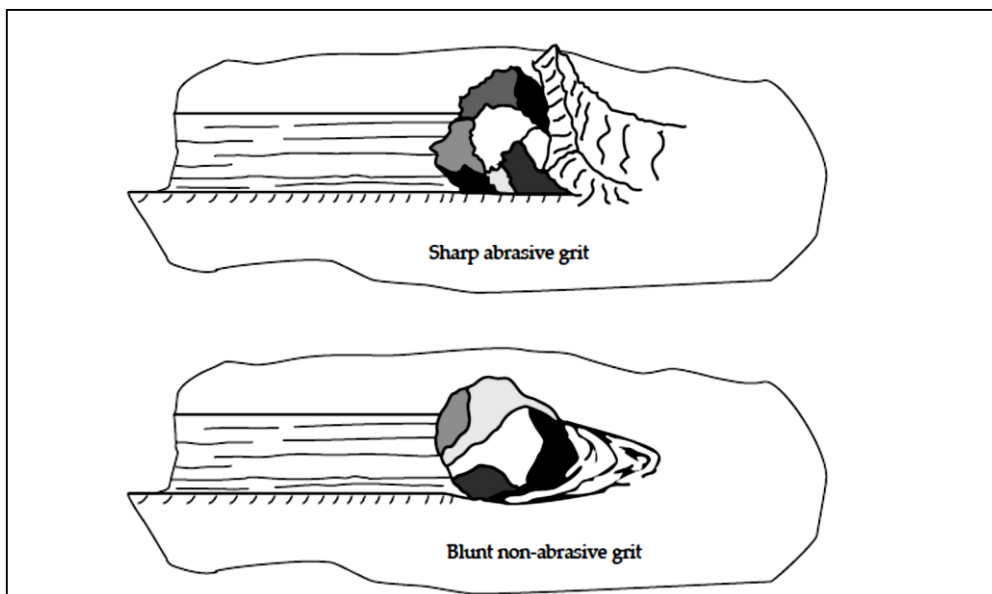
Fig.2.11 different abrasion mechanisms with increasing grit bluntness (30)**.**

Modification of superficial asperity can affect the deformation of a soft surface by hard wedge-shaped asperities, this can be described by three different models (30), see tab.2.2

Model	Description	Friction coefficient
Wave formation model (Rubbing model)	A soft surface is plastically deformed, forming a wave which is pushed away by a hard asperity. Wear debris may eventually be formed by fatigue processes. The model applies to smooth surfaces with weak interface between the asperities.	$\mu = \dfrac{A \sin \alpha + \cos(\arccos f - \alpha)}{A \cos \alpha + \sin(\arccos f - \alpha)}$ $A = 1 + 0.5\pi + arcos\, f - 2\alpha$ $-2 \arcsin[(1-f)^{-0,5}\sin \alpha]$
Wave removal model (Wear model)	A wave of plastically deformed material is removed from the surface producing wear particles. The process is characterized by high friction and high wear rates. The model applies to smooth surfaces with strong interface between the asperities.	$\mu = \dfrac{[1 - 2\sin\beta + (1-f^2)^{0.5}]\sin\alpha + f\cos\alpha}{[1 - 2\sin\beta + (1-f^2)^{0.5}]\cos\alpha + f\sin\alpha}$ $\beta = \alpha - 0.25\pi - 0.5\, arcos\, f$ $+\arcsin[(1-f)^{-0,5}\sin\alpha]$
Chip formation model (Cutting model)	The deformation of a soft material proceeds by a micro-cutting mechanism and a layer of material is removed as a chip. The model applies to rough surfaces.	$\mu = \tan(\alpha - 0.25\pi + 0.5\, arcos\, f)$

Tab.2.2 Deformation of a soft surface by hard wedge-shaped asperities models. μ is the friction coefficient, α is the asperity angle (angle between the two surfaces), f is the coefficient of interfacial adhesion between the asperity and the worn surface. (30)**.**

Following this model is possible to plot friction coefficient vs. asperity angle, see fig.2.12
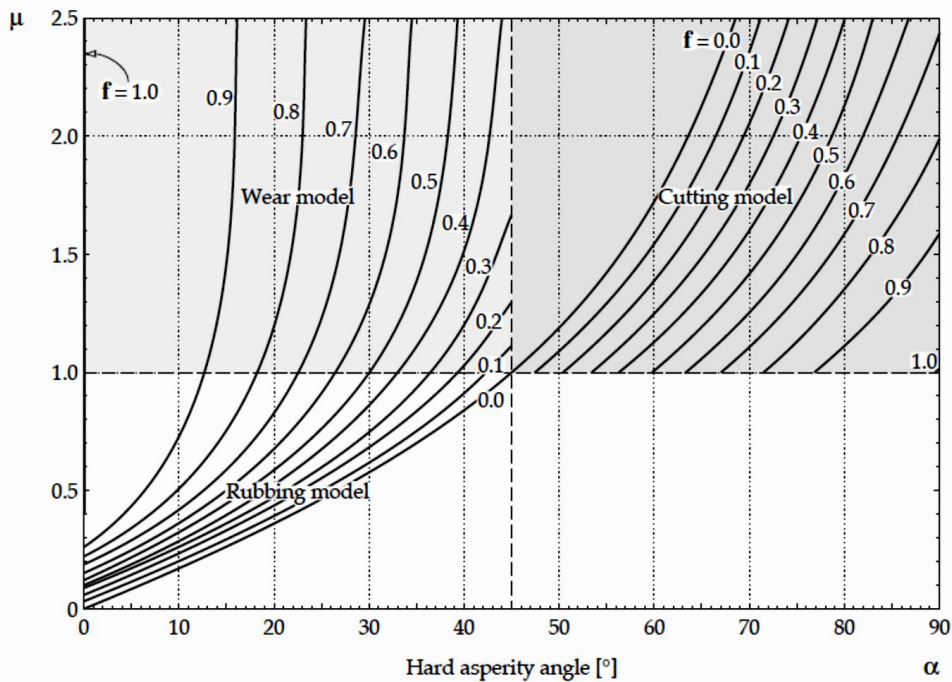
Fig.2.12 Variation of friction coefficient depending on wear model (30)

It's interesting to see that depending on wear model, fixed an asperity angle an increase of f has opposite effect on wear. This can explain why lubrication (defined by f value) may inhibit or promote wear depending on surface roughness.

How particles roughness can be measured?

Conventional methods to analyze particle shape are roundness factor and aspect ratio, roughness of particles surfaces can be correlated to *particles angularity*.

Spike parameter-linear fit (SP) it's a method based on fit triangles on particles boundary, fixed the base length of triangle (step size) triangles height h and apex angle θ spike values (SV), as showed in fig.2.13, are calculated around the boundary, see eq.2.8
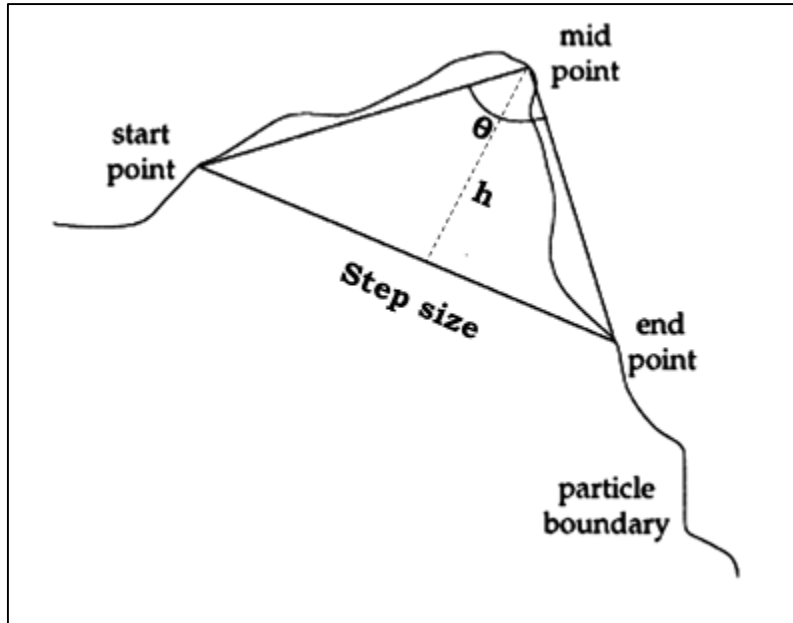
Fig.2.13 SV calculation by constructing triangles round the boundary, θ is the apex angle and h the height (38).

$$SV = h \, \cos\left(\frac{\theta}{2}\right)$$

Eq.2.8

Angularity is calculated in eq.2.9. Dividing SV by h.

$$Angularity = \frac{SV}{h} = \cos\left(\frac{\theta}{2}\right)$$

Eq.2.9

The combination of sharpness and height describes better particles influence on wear than sharpness only, for this reason, fixed the step size, only triangles with the maximum spike value (SV$_{max}$) are constructed.

The reckon of Angularity average (A$_{av}$) takes in account SV$_{max}$, the relative triangles heights (h$_{max}$) and the total number of triangles on the boundary (m) as described in eq.2.10

$$A_{av} = \frac{\sum_m \frac{SV_{max}}{h_{max}}}{m}$$

Eq.2.10

The procedure to calculate A_{av} can be repeated changing step size. The average of A_{av} on n different step sizes is called *spike parameter-linear fit* (SP) (39) and it's described in eq.2.11

$$SP = \frac{\sum_n \dfrac{\sum_m \dfrac{SV_{max}}{h_{max}}}{m}}{n}$$

Eq.2.11

SP is used to give a numerical characterization of *particle angularity,* however, SP value could overestimate particles sharpness for very small step sizes compared to the surface digitalization and for too large spot sizes used on convex-curved sides. Moreover, because small protrusions are not in contact with body surface during motion, some boundary features in angularity reckon should be neglected.

To avoid SP numerical model deficiency *spike parameter quadratic fit* (SPQ) has been proposed (40). The method consists in building a circle with center in the centroid of particle and an average radius, to exclude from calculus everything inside the circle and calculating spike values only on protrusion outside the circle as described in fig.2.14
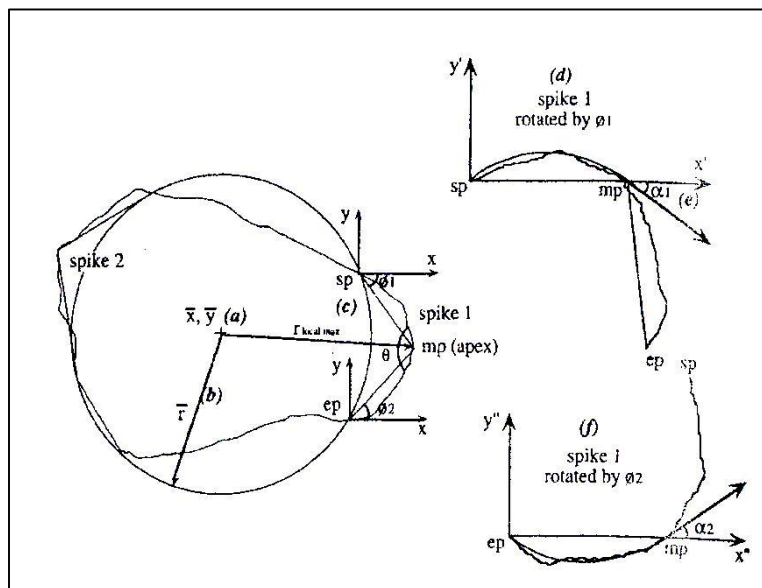
Fig.2.14 Fitting a quadratic function on rotated sp-mp and ep-mp particle boundary, α_1 and α_2 are calculated. Apex angles θ are estimated from related α_1, α_2, θ₁, θ₂ for every protruding sections. SPQ is the average of angularity on quadratic fitting calculated θ (38).

SPQ is calculate on quadratic fitting calculated angularity average of outer spike values; see eq.2.12

$$SPQ = Angularity_{Average}^{qf}$$

Eq.2.12

Spike parameter-linear fit (SP) and spike parameter quadratic fit are (SPQ) have been successfully used to describe abrasive wear mechanisms in both rolling and grooving conditions (40) (41) (42) (38). See fig.2.15
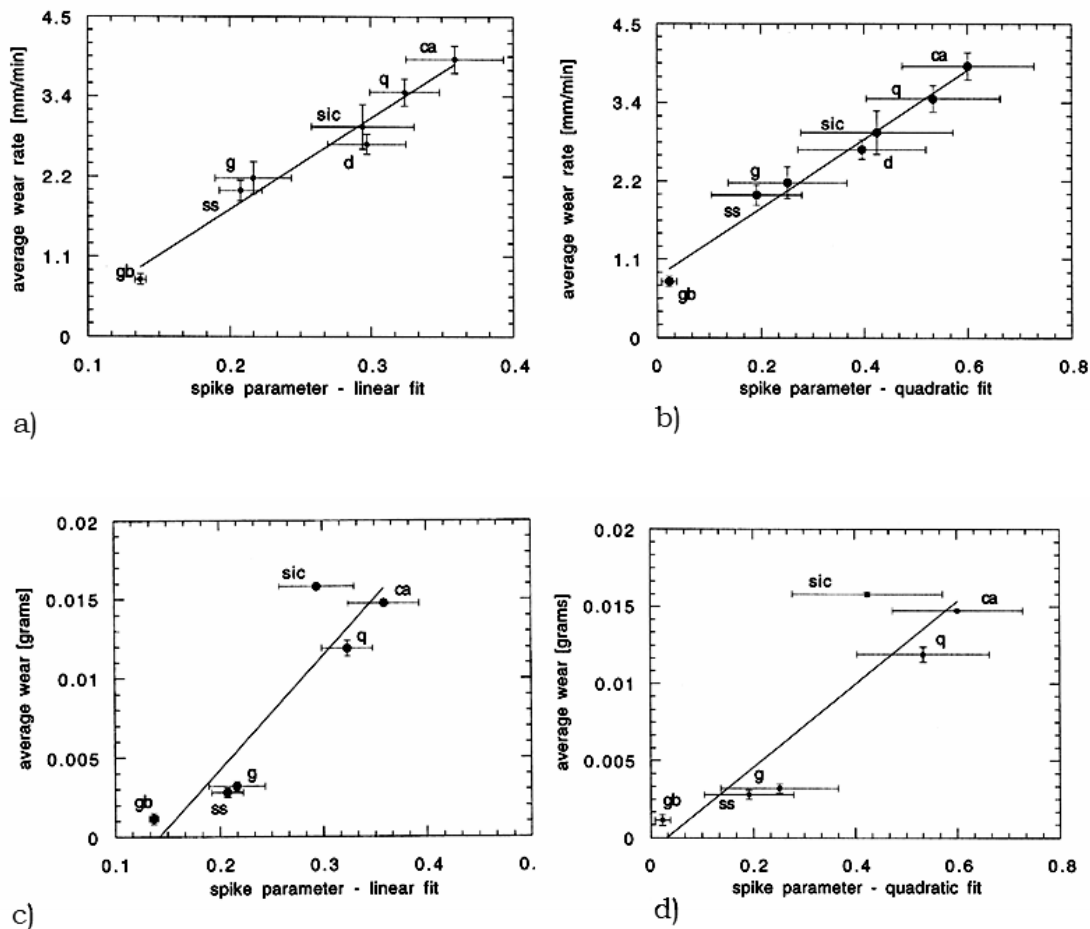
Fig.2.15 Effect of particles angularity of glass beads, silica sand, garnet, diamond, silicon carbide, quartz and crushed alumina on pin on disc two-body experiment for a) b) and on ball on disc three body experiment for c) d) (40).

It should be noticed that coexistence of grooving and rolling behavior in three-body experiment influences the results on angularity analysis, whereas two-body experiments provide more accurate information.

It's important to underline that particles toughness can change particles shape and size during wear, see fig.2.16
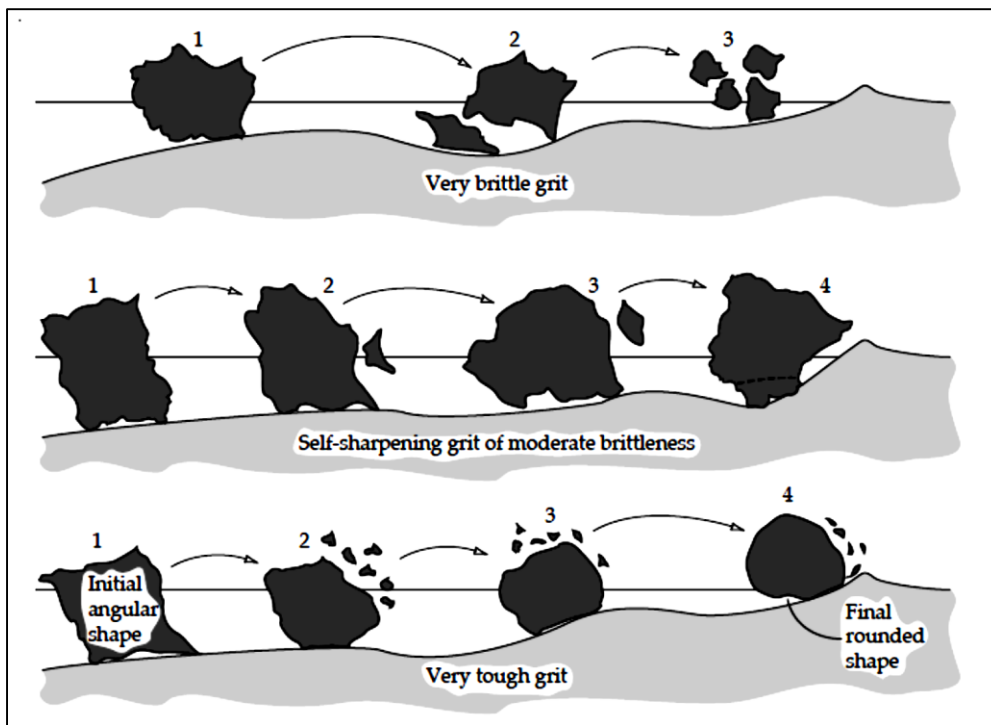
Fig.2.16 effect of grit toughness on particle shape and size

2.1.4   Abrasive wear models applied to a brake system

Regarding brake system, abrasion model it's important to describe the running-in phase. When new brake pad-discs surfaces come into contact are susceptible to groove abrasive wear; after particles release due to friction action both groove and rolling abrasive wear mechanisms are possible, depending on particles size, tribofilm thickness and brake pressure.

During brake event small particles can raise friction efficiency by rolling abrasive mechanism and increasing the real contact surface with the formation of secondary contact plateau, the composition of the friction layers observed at different temperatures and their stability are paramount to infer the composition of the particles and fragments emitted by the tribological system (43), see fig.2.17
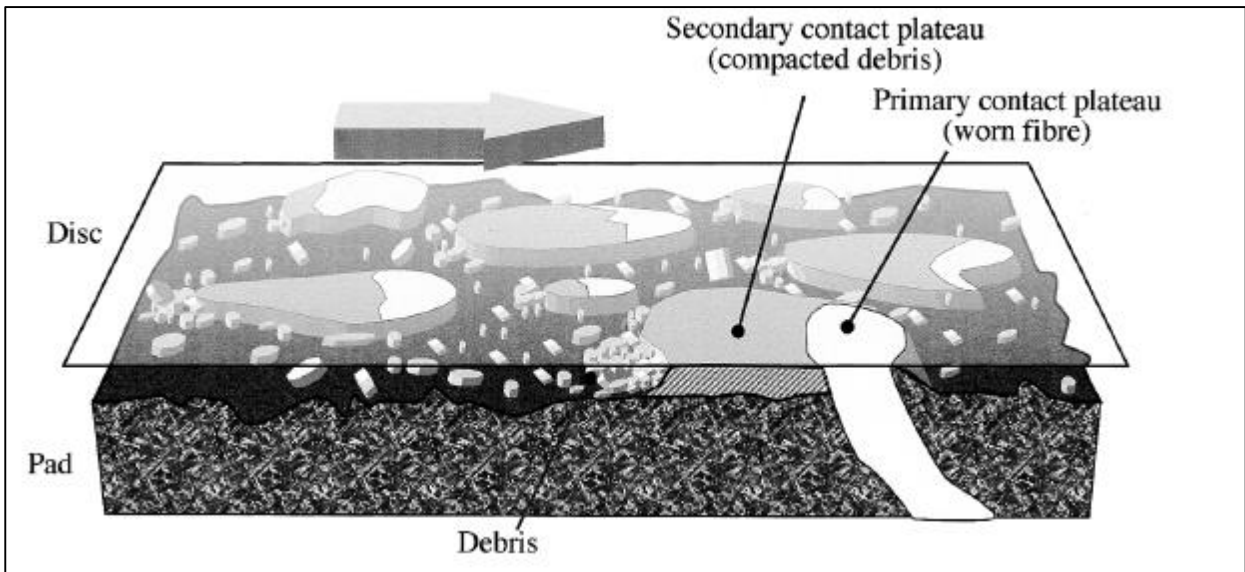
Fig.2.17 Generation of primary (white) and secondary (grey) contact plateaus at brake disc-pad interface. Secondary plateaus are generated by piled up debris compacted on stable primary plateaus by friction energy. (44)

Elevated relative speed of disc/pad surfaces can affect the rolling mechanism of particles. As a negative effect they are easily detached from friction material increasing brake pad wear (45).

Even if large particles increase friction coefficient less than small particles, they induce a more regular friction coefficient during brake due to the formation of more stable primary contact plateau, see fig.2.18
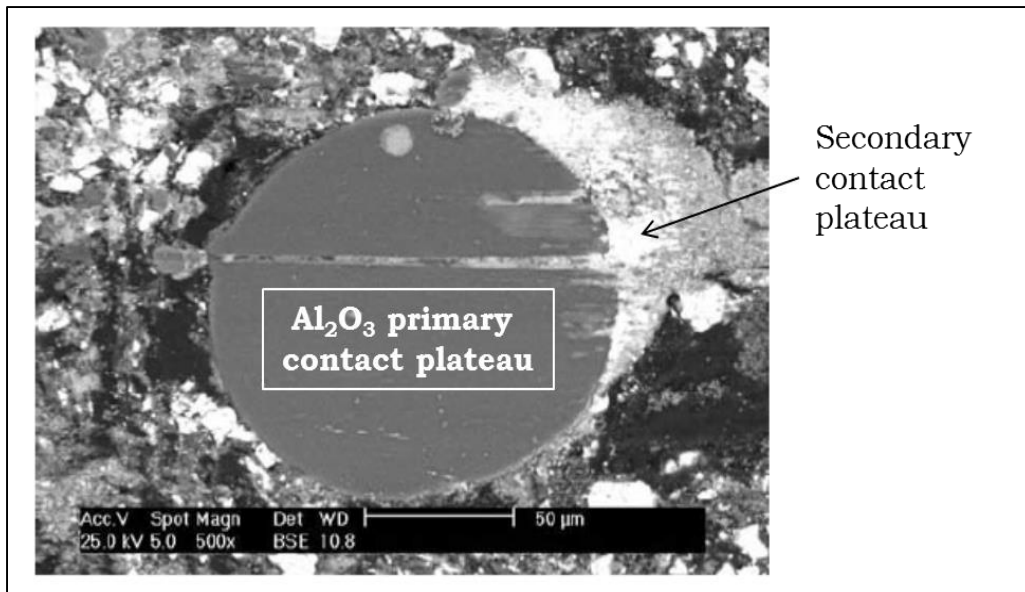
Fig.2.18 SEM view of a secondary contact plateau composed by small compacted particles generated by alumina primary contact plateau (46)

Large particles reduce brake pad wear, but, as a negative effect, they can increase disc wear and brake noise.

Generation, growth, and degradation of a micro-contact at the surface of a brake pad are summarized in fig.2.19
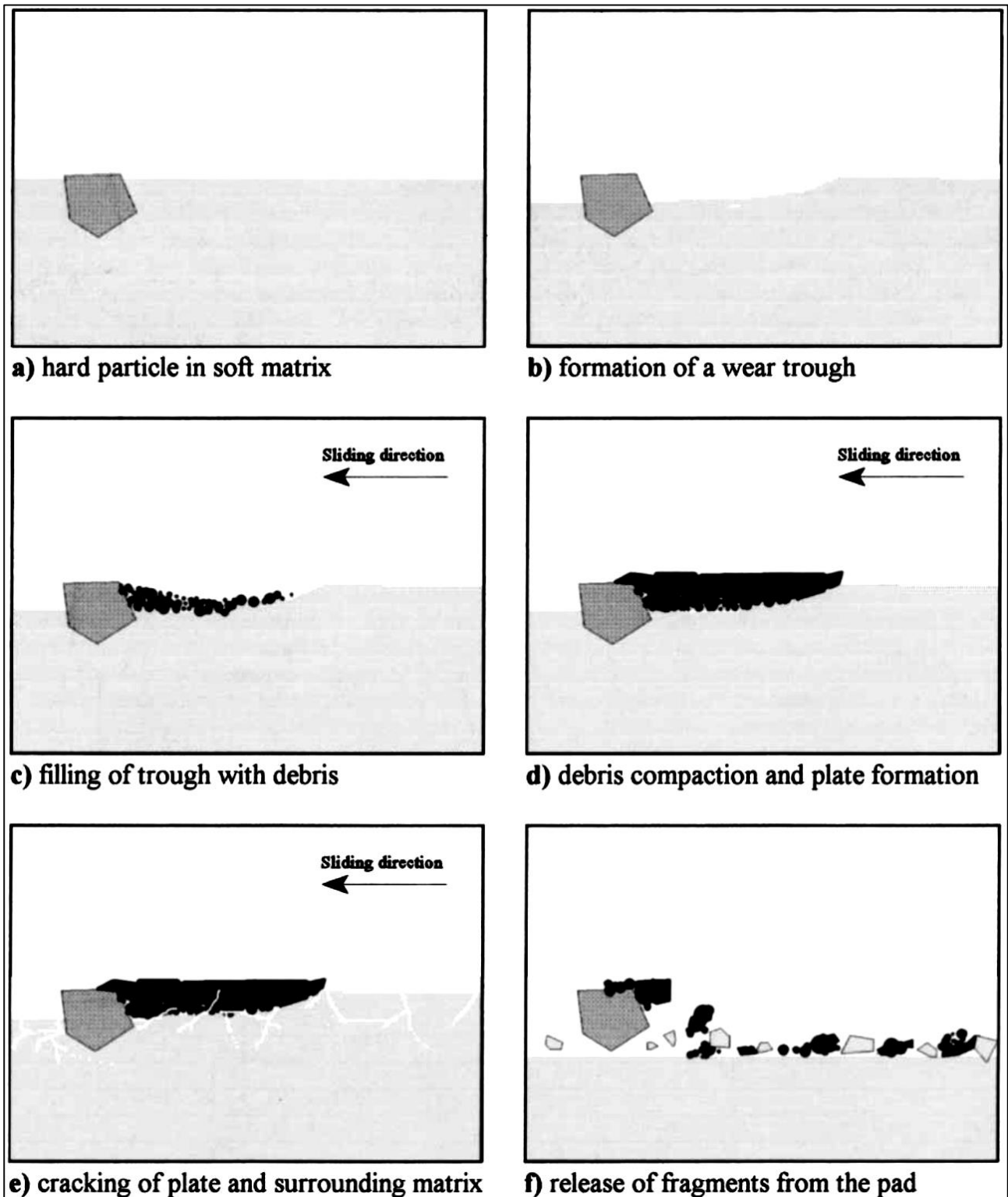
Fig.2.19 Generation, growth, and degradation of a micro-contact at the surface of a brake pad
(47)

An excess of third body layer thickness can reduce surfaces contact with abrasives, a lack or a non-homogeneous third layer thickness can produce a disc thickness variation (DTV) during brake due to the differential friction coefficient on different part of disc. DTV is lack of parallelism between its inboard and outboard braking surfaces and it's one of the main causes for brake judder.

Primary contact plateaus clean the disc surface reducing the third layer thickness, they regulate the equilibrium between generated and removed particles at brake disc/pad interface (48) (49) (46) (50).

As already mentioned brake disc/pad wear is not the aim of abrasive in friction materials. The best condition to increase the friction coefficient on brake system without significantly increase disc wear is to dissipate energy by rolling wear mechanism. On the other side to reduce brake pad wear large abrasive particles are necessary, moreover, depending on their nature, grits to be easily fragmented and temperature can change compactness of materials or third layer composition changing wear mechanism. For this reasons in friction material formulation it's convenient to select more than one abrasive materials with different hardness, particles sizes, shape and fracture toughness to take in account tribology of the brake system at different speed, pressure and temperature.

2.2 Abrasives (raw materials)

2.2.1   Carbides, nitrides, borides

High hardness, good thermal conductivity, good thermal shock resistance, high melting point and good resistance to oxidation and chemicals are the main characteristics for carbides used as abrasives in friction materials.

The type of the element bonded with carbon to form carbide determinates the properties of the compound (51) (52), see tab.2.3

Type	Elements	Main structures	Bonding	Properties
Salt-like or salinic Carbides	Groups I,II, and III	C^{4-} Methanides C_2^{2-} Acetylides C_3^{4-} Sesquicarbides	More than 50% ionic	Lack of electrical conductivity, high transparency, easily hydrolyzed forming methane, acetylene or propyne and metal hydroxide
Interstitial Carbides	Groups IV,V,VI	Not stoichiometric MeC_{1-x} X=0.5-0.97 Carbides are in interstitial position fcc, hcp, and hexagonal structures	Partially covalent and ionic, mostly metallic	Highest melting point and hardness, chemically stable, good electrical and thermal conductivity
Intermediate Transition Carbides	Groups VII,VIII	Distortion of metal crystal lattice. Multiple stoichiometries possible.	Partially covalent, ionic and metallic	Not chemically stable, easily hydrolyzed by water or dilute acids to produce hydrocarbons and hydrogen
Covalent Carbides	B, Si	*B_4C* boron icosahedrons (B_{12}) bridged by carbon atoms. *SiC* covalently bonded primary co-ordination tetrahedron	Essentially covalent Non metallic	High hardness, melting point, thermal and chemical stability. Low density

Tab.2.3 Carbide types and main properties

For friction material formulation salt-like and intermediate transition carbides are not recommended due to unstable chemical bonding easily hydrolyzed in water or dilute acids.

Interstitial carbides fulfill all the requirements for abrasive materials; they are often used in cutting tools and wear-resistant parts indeed, but price and density of this materials should be considered before using in friction materials, see tab.2.4

Group	Carbide	Density (g/cm³)	Vikers Hardness (GPa)	Major Compositions and structures
IV	TiC	4.91	28-35	TiC_{1-x} (fcc)
	ZrC	6.59	25.9	ZrC_{1-x} (fcc)
	HfC	12.67	26.1	HfC_{1-x} (fcc)
V	VC	5.65	27.2	V_2C (hcp), V_4C_3*, V_6C_5*, V_8C_7*, VC (fcc)
	NbC	7.79	19.6	Nb_2C (hcp) Nb_3C_2*, Nb_4C*, NbC (fcc)
	TaC	14.5	16.7	Ta_2C (hcp), Ta_3C_2*, Ta_4C_3*, TaC (fcc)
VI	Cr_3C_2	6.68	10-18	$Cr_{23}C_6$ (fcc), Cr_7C_3*, Cr_2C_2 (hex)
	Mo_2C	9.06	15.5-24.5	Mo_2C (hcp), Mo_3C_2*, MoC (hex)
	WC	15.8	22	W_2C (hcp), WC (hex)

Tab.2.4 Density and main composition of interstitial carbides

Covalent carbides can be made with the most similar carbon electronegativity elements, silicon and boron.

Boron carbide B_4C structure can be seen in fig.2.20 where boron atoms can form icosahedra, fully boron made (B_{12}) or partially substituted by carbon ($B_{11}C$), linked by 3-atom carbon (CCC) chains where 1 atom of carbon can be substituted by 1 atom of boron (CBC) (53).
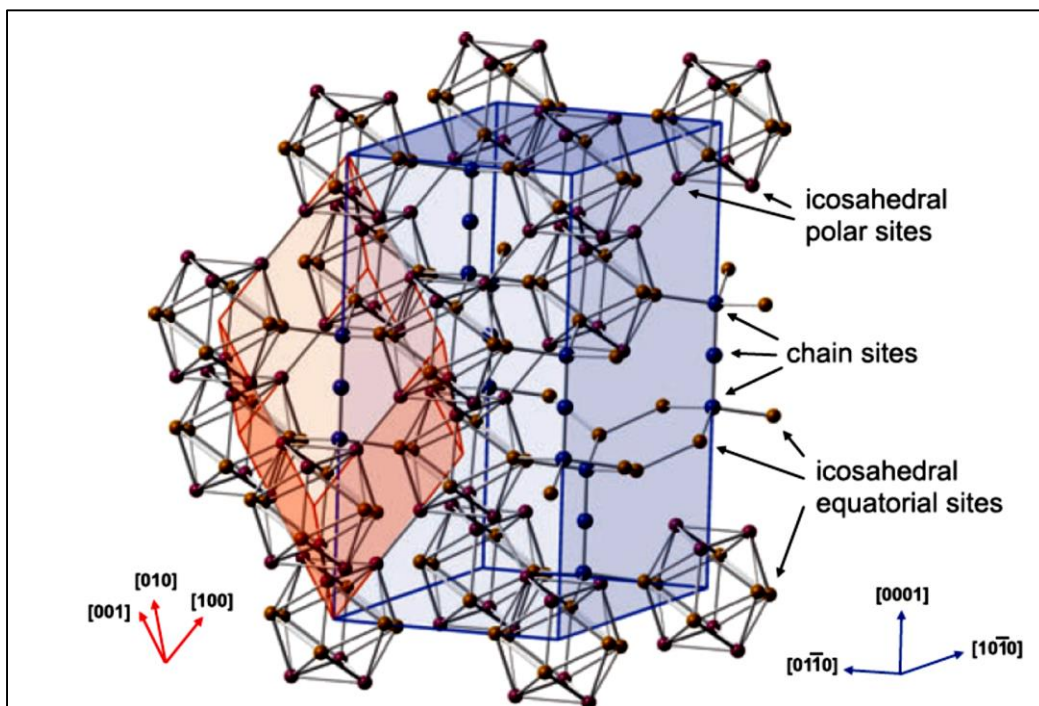
Fig.2.20 Boron carbide crystal structure. Icosahedra at the vertices of a rhombohedral (red) lattice of trigonal symmetry ($R\bar{3}m$) with 3-atom linear chains linking the icosahedra along the (111) rhombohedral axis. Equivalently can be describe with a hexagonal lattice (blu) where the [0001] hexagonal direction correspond to [111] rhombohedral direction. (53)

Silicon carbide SiC has two main different crystal structures (53) (54).

α-SiC has an hexagonal Wurtzite structure ($P6_3mc$), also rhombohedral structure ($R3m$) is referred as α-SiC

β-SiC has a fcc Zincblende structure ($f\bar{4}3m$)

More than 250 polytypes of SiC are possible. Polytypes are the one dimension variant of polymorphs, instead changing the entire crystal structure, polytypes differ only by the stacking sequence along one direction; a good approach to describe this system is to use Ramsdell notation.
β-SiC is a cubic structure with layer sequence of the [111] direction ABCABCABC. Ramsdell notation for β-SiC is 3C, where 3 is the number of Si-C bilayers in the primitive cell atoms necessary to produce a unit cell and C indicates the cubic symmetry. Hexagonal H and rhombohedral R combinations of these stacking sequences are also possible generating new polytypes, β-SiC for example has an hexagonal structure with 2 bilayer Si-C staked in [0001] direction and the Ramsdell notation is 2H

Main SiC polytypes are described in tab.2.5

Polytype Ramsdell notation	Structure	Sequence	Lattice parameters		Space group	Density (g/cm³)
			a_0 (nm)	c_0 (nm)		
3C (β-SiC)	Cubic	ABC	0.43596		$f\bar{4}3m$	3.214
2H (α-SiC)	Hexagonal	AB	0.30763	0.50480	($P6_3mc$)	3.214
4H	Hexagonal	ABAC	0.3076	1.0046		3.235
6H	Hexagonal	ABCACB	0.3080	1.5117		3.211
15R	Rhombohedral	ABDACBCABACABCB	0.3073	3.730	($R3m$)	3.274

Tab.2.5 Properties of main SiC polytypes

A comparison between covalent carbides is reported in tab.2.6

	Composition	X-ray Density (g/cm³)	Thermal Conductivity (W/mK)	Thermal Expansion (10-6/°C)	Vickers Hardness (GPa)	Melting Point (°C)
Silicon carbide	α-SiC	3.211	41.0	5.12	24.5-28.2	2545
	β-SiC	3.214	25.5	3.8		
Boron Carbide	$B_{11}C(CBC)$	2.52	30	4.3	27.3-34.3	2400

Tab.2.6 Covalent carbides main characteristics

Boron carbide is the carbide with the lower density, this can be appreciated on raw materials selection, due to the cost it's preferred for aerospace application, but can be used in automotive brake pad formulation.

Some borides and nitrides are also interesting as abrasives materials due to their properties, however cost and density, again, should be considered. Following the same considerations made for carbides, covalent bonded borides and nitrides are the most suitable for this purpose.

Tab.2.7 resumes main characteristics of this materials compared to diamond and silicon carbide (55).

	Density (g/cm^3)	Melting Point (°C)	Hardness (HV)
C (diamond)	3.52	3800	~8000
BN (cubic)	3.48	2730	~5000
B$_4$C	2.52	2450	3-4000
AlB$_{12}$	2.58	2150	2600
SiC	3.22	2760	2600
SiB$_6$	2.43	1900	2300
Si$_3$N$_4$	3.19	1900	1720
AlN	3.26	2250	1230

Tab.2.7 main characteristics of covalent bonded carbides nitrides and borides.

By comparing this materials it can be seen that borides and carbides are harder and less brittle than nitrides; they have higher melting points but lower thermal stability in oxidizing environment. Most of this materials are considered special technical ceramic materials due to high cost.

Significantly cheaper than other covalent borides and nitrides, low density, high hardness and melting point, good thermal shock resistance and chemically stability also at high temperature make silicon carbide (α-SiC) one of the most used abrasives in automotive brake pads friction materials formulation.

SiC naturally occurs as Moissanite, but it's a rare mineral; the main SiC is made by synthesis (52). Two process can be used for industrial production, the first is the "Solid Combustion Synthesis" where silicon and carbon powder are compacted, degassed and ignited in vacuum or inert atmosphere, see eq.2.13

$$Si + C \xrightarrow{\Delta} SiC \qquad \text{(eq.2.13)}$$

The most cheap process is the Acheson process. It's based on a carbothermal reduction where a carbon source like graphite, coal etc., is heated by graphite electrodes to a temperature higher than 1400°C in presence of silicon oxide in form of pure quartz, diatomaceous earth, sepiolite and other mountain leathers. SiC is produced by the reduction of silicon oxide passing through different sub-reaction in solid and vapor phases see eq.2.14-2.17.

$$SiO_2(s) + C(s) \rightarrow SiO(g) + CO(g) \qquad \textbf{(eq.2.14)}$$
$$SiO_2(s) + CO(g) \rightarrow SiO(g) + CO_2(g) \qquad \textbf{(eq.2.15)}$$
$$SiO(g) + C(s) \rightarrow SiC(s) + CO(g) \qquad \textbf{(eq.2.16)}$$
$$CO(g) + CO_2(g) \rightarrow 2CO(g) \qquad \textbf{(eq.2.17)}$$
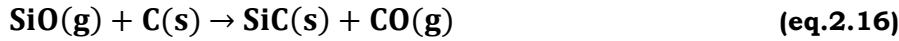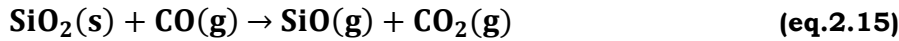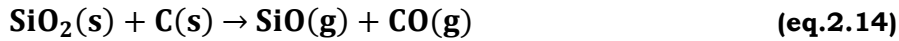
From 1400 to 1800°C β-SiC is produced, above 1800°C is produced α-SiC (56).

α-SiC and polytypes in Acheson process are synthetized in three grades:

- Metallurgical grade. SiC purity less than 97%
- Black grade. SiC purity from 97 to 99%.; hardness 9.1 in Mohs scale. The black color is derived from iron oxide impurity
- Green grade. SiC purity higher than 99%; hardness 9.4 in Mohs scale. The yellow-green color is derived from nitrogen impurities

2.2.2   Metal oxides and silicates

Oxides more are used in friction materials due to their low cost and high resistance to temperature in oxidizing environment.

Many oxides occur in nature and they can be classified as in tab.2.8

	Mineral Group name	Formula	Crystal System	Laue Group	Space group	Mineral name	Density (g/cm³)	Mohs Hard.
Hemi-oxide	Cuprite	Cu_2O	Isometric	$m\bar{3}m$	$Pn\bar{3}m$	Cuprite	6.104	3.5–4
		Ag_2O					7.318	-
Mono oxides	Periclase	MgO	Cubic	$m\bar{3}m$	$Fm\bar{3}m$	Periclase	3.585	6
		FeO				Wüstite	5.956	
		CaO				Lime	3.346	3.5
		NiO				Bunsenite	6.850	6.4-6.8
		MnO				Manganosite	5.365	5-6
	Zincite	ZnO	Hexagonal	$6mm$	$P6_3mc$	Zincite	5.712	5.56
		BeO				Bromellite	3.080	9
	Tenorite	CuO	Monoclinic	$2/m$	$C2/c$	Tenorite	6.515	3.5-4
	Montroydite	HgO	Orthorhombic	mmm	$Pnma$	Montroydite	11.193	1.5-2
	Corundum	Al_2O_3	Trigonal	$\bar{3}m$	$R\bar{3}c$	Corundum	3.986	9
		Fe_2O_3				Hematite	5.255	6.5
		Cr_2O_3				Eskolaite	5.224	8-8.5
		V_2O_3				Karelianite	5.021	8-9
	Bixbyite	$(Mn_{.983}Fe_{.017})_2O_3$	Isometric	$m3$	$Ia3$	Bixbyite	5.027	6-6.5
		Tl_2O_3				Avicennite	10.353	2
	Arsenic and antimony sesquioxides	As_2O_3	Isometric	$m3m$	$Fd\bar{3}m$	Arsenolite	3.870	1.5
		Sb_2O_3				Senarmontite	5.583	2
		As_2O_3	Monoclinic	$2/m$	$P2_1/m$	Claudetite	3.960	2.5
		Sb_2O_3	Orthorhombic	mmm	$Pccn$	Valentinite	5.844	2.5-3
	Rutile	TiO_2	Tetragonal	$4/mmm$	$P4_2/mnm$	Rutile	4.2743	6-6.5
		MnO_2				Pyrolusite	5.203	6-6.5
		SnO_2				Cassiterite	7.001	6-7
		SiO_2				Stishovite	4.287	7.5-8
	TiO_2 polymorphs	TiO_2	Tetragonal	$4/mmm$	$P4_2/mnm$	Rutile	4.2743	6-6.5
		TiO_2	Tetragonal	$4mm$	$I4_1/amd$	Anatase	3.895	5.5-6
		TiO_2	Orthorhombic	mmm	$Pcca$	Brookite	4.123	5.5-6
	Baddeleyite	ZrO_2	Monoclinic	$2/m$	$P2_1/c$	Baddeleyite	5.826	6.5
	MnO_2 polymorphs	MnO_2	Tetragonal	$4/mmm$	$P4_2/mnm$	Pyrolusite	5.203	6-6.5
		MnO_2	Orthorhombic	mmm	$Pnam$	Ramsdellite	4.874	3

	Mineral Group name	Formula	Crystal System	Laue Group	Space group	Mineral name	Density (g/cm³)	Mohs Hard.
	Uraninite	UO_2	Isometric	$m3m$	$Fm3m$	Uraninite	10.968	5-6
		ThO_2				Thorianite	9.987	6
	TeO_2 polymorphs	TeO_2	Orthorhombic	mmm	$Pbca$	Tellurite	5.749	2
		TeO_2	Tetragonal	422	$P4_12_12$	Paratellurite	6.043	1
Multiple Oxides	Ilmenite	$FeTiO_3$	Trigonal	$\bar{3}$	$R\bar{3}$	Ilmenite	4.786	5-5.5
		$MnTiO_3$				Pyrophanite	4.603	5
		$MgSiO_3$				Akimotoite	3.810	-
	Perovskite	$CaTiO_3$	Orthorhombic	mmm	$Pbnm$	Perovskite	4.044	5.5
		$MgSiO_3$				$MgSiO_3$	4.107	-
	Oxide spinel	$MgAl_2O_4$	Isometric	$m3m$	$Fd\bar{3}m$	Spinel	3.578	8
		$FeAl_2O_4$				Hercynite	4.256	7.5
		$MgFe_2O_4$				Magnesio-ferrite	4.547	6-6.5
		$FeFe_2O_4$				Magnetite	5.200	5.5-6
		$MnFe_2O_4$				Jacobsite	4.969	5.5-6
		$MgCr_2O_4$				Magnesio-chromite	4.414	5.5
		$FeCr_2O_4$				Chromite	5.054	5.5
		$TiFe_2O_4$				Ulvospinel	4.775	5-5.6
	Pseudobrookite	Fe_2TiO_5	Orthorhombic	mmm	$Bbmm$	Pseudobrookite	4.406	6
		Al_2TiO_5				Tialite	3.702	-
		$Mg_{.5}Fe_{.5}TiO_5$				Armalcolite	3.904	6
	Tungstate	$FeWO_4$	Monoclinic	$2/m$	$P2/c$	Ferberite	7.549	4.5
		$MnWO_4$				Huebnerite	7.265	4.5
		$CaWO_4$	Tetragonal	$4/m$	$I4_1/a$	Scheelite	6.115	4.5

Tab.2.8 Main parameters of natural hemi, single and multiple oxides. (57) (18)

To oxides all the silicate groups has to be added, and are classified as reports in tab.2.9

	Group	General chemical Formula	Crystal System	Laue Group	Space group	M^a, M^b, M^c or A,B,C,T	Mineral name	Density (g/cm³)	Mohs hard.
Nesosilicates or Orthosilicates	Garnet	$M_3^a M_2^b Si_3 O_{12}$	Isom.	$m3m$	$Ia\bar{3}d$	Mg,Al	Pyrope	3.559	7.5
						Fe,Al	Almandine	4.312	7-8
						Mn,Al	Spessartine	4.199	6.5-7.5
						Ca,Al	Grossular	3.600	6.5-7.5
						Ca,Fe	Andradite	3.850	6.5 -7
						Ca,Cr	Uvarovite	3.859	6.5-7
	Olivine	$M^a M^b SiO_4$	Orth.	mmm	$Bbnm$	Mg,Mg	Forsterite	3.227	6-7
						Fe,Fe	Fayalite	4.402	6.5
						Ca,Mg	Monticellite	3.040	5
						Ca,Fe	Kirschsteinite	3.965	5.5
						Ca,Ca	Ca-olivine	2.969	-
						Mn,Mn	Tephroite	4.127	6.5
						Co,Co	Co-olivine	4.719	-
						Ni,Ni	Liebenbergite	4.921	6
	Silicate spinel	$M_2^a SiO_4$	Isom.	$m3m$	$Fd\bar{3}m$	Mg	Ringwoodite	3.563	-
						Fe	Fe_2SiO_4	4.848	-
						Co	Co_2SiO_4	5.174	-
						Ni	Ni_2SiO_4	5.346	-
	Silicate zircon	$M^a SiO_4$	Tetrag.	$4mm$	$I4_1/amd$	Zr	Zircon	4.668	7.5
						Hf	Hafnon	6.976	7.5
						Th	Thorite	6.696	5
						U	Coffinite	7.185	5-6
	Willemite	$M_2^a SiO_4$	Trig.	$\bar{3}$	$R\bar{3}$	Zn	Willemite	4.221	5.5
						Be	Phenacite	2.960	7.5-8
	Aluminosilicate	Al_2SiO_5	Orth.	mmm	$Pnnm$	-	Andalusite	3.1425	6.5-7
					$Pnma$	-	Sillimanite	3.2386	7
			Tric.	$\bar{1}$	$P\bar{1}$	-	Kyanite	3.664	4-7
		$3Al_2O_3 \cdot 2SiO_2$	Orth.	mmm	$Pbam$	-	Mullite	3.11	6-7
		$Al_2SiO_4(OH,F)_2$			$Pbnm$	-	Topaz	3.492	8
	Humite	$Mg_3(SiO_4)$	Orth.	mmm	$Pbnm$	-	Norbergite	3.186	6-6.5

36

	Group	General chemical Formula	Crystal System	Laue Group	Space group	M^a, M^b, M^c or A,B,C,T	Mineral name	Density (g/cm³)	Mohs hard.
		$F_{1.8}(OH)_{0.2}$							
		$Mg_{4.95}Fe_{0.05}(SiO_4)_2$ $F_{1.3}(OH)_{0.7}$	Monoc.	$2/m$	$P2_1/b$	-	Chondrodite	3.158	6-6.5
		$Mg_{6.6}Fe_{0.4}(SiO_4)_3$ $F(OH)$	Orth.	mmm	$Pbnm$	-	Humite	3.159	6-6.5
		$Mg_{8.4}Fe_{0.6}(SiO_4)_4$ $F_{1.3}(OH)_{0.7}$	Monoc.	$2/m$	$P2_1/b$	-	Clinohumite	3.259	6
	Titanite	$M^a M^b SiO_5$	Monoc.	$2/m$	$P2_1/a$	Ca,Ti	Titanite	3.517	5-5.5
					$A2/a$	Ca,Sn	Malayaite	4.546	3.5-4
	Staurolite	$Fe_4Al_{18}Si_8O_{46}(OH)_2$	Monoc	$2/m$	$C2/m$	-	Staurolite	3.823	7-7.5
	Clinozoistite Epidoite	Ca_2Al_3 $Si_3O_{12}(OH)$	Monoc.	$2/m$	$P2_1/m$	-	Clinozoisite	3.321	7
		$Ca_2Al_{2.16}Fe_{0.84}$ $Si_3O_{12}(OH)$				-	Epidote	3.465	7
		$Ca_2Al_{2.6}Fe_{0.4}$ $Si_3O_{12}(OH)$				-	Epidote	3.392	7
		$Ca_{1.26}Re_{0.76}Al_{1.83}Fe_{1.17}$ $Si_3O_{12}(OH)$				-	Allanite	3.960	5-6.5
		Complex				-	Piemontite	3.38	6
		Complex	Orth.	mmm	$Ccmm$	-	Lawsonite	3.05	6
		Ca_2Al_3 $Si_3O_{12}(OH)$	Orth.	mmm	$Pnna$	-	Zoisite	3.336	6.5
		Complex	Monoc.	$2/m$	$A2/m$	-	Pumpellyite	3.16	5-6
	Melilite	$M^a M^b M^c SiO_7$	Tetrag.	$\bar{4}2m$	$P\bar{4}2_1m$	Ca,Na,Al	Na-Melilite	2.912	-
						Ca,Ca,Al	Gehlenite	3.006	5-6
						Ca,Ca,Mg	Akermanite	2.944	5-6
	Rankinite	$Ca_3Si_2O_7$	Monoc.	$2/m$	$P2_1/a$	-	Rankinite	2.96	5.5
	Tilleyte	$Ca_3Si_2O_7 \cdot 2CaCO_3$	Monoc.	$2/m$	$P2_1/a$	-	Tilleyte	2.84	-
	Wadsleyite	$M^a_2SiO_4$	Orth.	mmm	$lmma$	Mg	Wadsleyite	3.4729	-
						Co	Co_2SiO_4	5.044	-
	Lawsonite	$CaAl_2Si_2O_7(OH)_2H_2O$	Orth.	mmm	$Ccmm$	-	Lawsonite	3.088	7.5
	Tourmaline	Complex	Trig.	$3m$	$R3m$	-	Dravite	3.142	7-7.5
						-	Schorl	3.263	7.5
						-	Elbaite	3.063	7.5
	Vesuvianite	Complex	Tetrag.	$4mmm$	$P4/nnc$	-	Vesuvianite	3.429	6.5
	Beryl	$Be_3Al_2Si_6O_{18}$	Hexa.	$6/mmm$	$P6/mcc$	-	Beryl	2.645	7.5-8
	Axinite	Complex	Tric.	$\bar{1}$	$P\bar{1}$	-	Axinite	3.18	6.5-7
	Cordierite	$Mg_2Al_4Si_5O_{18}$	Orth.	mmm	$Ccmm$	-	Cordierite	2.499	7
Inosilicates or Chain silicates	Orthopyroxenes	$M^a_2Si_2O_6$	Orth.	mmm	$Pbca$	Mg	Orthoenstatite	3.204	5.5
						Fe	Orthoferrosilite	4.002	5-6
						Co	Co-Opx	4.222	-
	Primitive clinopyroxenes	$M^a_2Si_2O_6$	Monoc.	$2/m$	$P2_1/c$	Mg	Clinoenstatite	3.188	5-6
						Fe	Clinoferrosilite	4.005	5-6
						Mn	Mn-Cpx	3.819	-
	C-centered clinopyroxenes	$M^a M^b Si_2O_6$	Monoc.	$2/m$	$C2/c$	Ca,Mg	Diopside	3.279	6
						Ca,Mn	Johannsenite	3.27	6
						Ca,Fe	Hedenbergite	3.656	5-6
						Na,Al	Jadeite	3.341	6.5
						Na,Fe	Acmite	3.576	6-6.5
						Na,Cr	Ureyite	3.592	6-7
						Li,Al	Spodumene	3.176	-
						Ca,Al	Ca-Tschermaks	3.438	-
		Complex				-	Augite	3.19	5.5-6
							Aegirine	3.4	6
							Omphacite	3.16	5-6
	Pyroxenoids	$Ca_3Si_3O_9$	Tricl.	$\bar{1}$	$P\bar{1}$	-	Wollastonite	2.937	5
		$Mn_5Si_5O_{15}$				-	Rhodonite	3.752	6
		$Mn_7Si_7O_{21}$				-	Pyroxmangite	3.749	5.5-6
		$(Ca_{0.78}Mn_{0.12}Fe_{0.10})_3$ Si_3O_9			$I\bar{1}$	-	Bustamite	3.116	5.5-6.5
	Ortho-amphiboles	Complex	Orth.	mmm	$Pnma$	-	Anthophyllite	3.111	5-6
							Gedrite	3.184	5.5-6
	Clino-amphiboles	$A_{0-1}B_2C_5T_8O_{22}$ $(OH,O,F,Cl)_2$	Monoc.	$2/m$	$C2/m$	-,Mg2,Mg5,Si8	Cummingtonite	3.142	-
						-,Mg2,Mg3Al2, Si6Al2	Gedrite		

	Group	General chemical Formula	Crystal System	Laue Group	Space group	M^a, M^b, M^c or A,B,C,T	Mineral name	Density (g/cm³)	Mohs hard.
		Substitutions of Fe^{2+} for Mg, Fe^{3+} for Al in C sites, K for Na and similar not listed				-,Ca_2,Mg_5,Si_8	Tremolite-Actinolite	3.010	5-6
						-,Ca_2,Mg_4Al, Si_7Al	Hornblends	3.02-3.59	5-6
						-,Ca_2,Mg_3Al_2, Si_6Al_2	Tschermakite	3.14	5-6
						Na,Ca_2,Mg_5, Si_7Al	Edenite	3.00	6
						Na,Ca_2,Mg_4Al, Si_6Al_2	Pargasite	3.165	6
						-,$NaCa$,Mg_4Al, Si_8	Winchite	2.96	5.5
						-,$NaCa$,Mg_3Al_2, Si_7Al	Barroisite	-	5-6
						Na,$NaCa$,Mg_5, Si_8	Richterite	3.09	6
						Na,$NaCa$,Mg_4Al, Si_7Al	Katophorite	3.35	5
						Na,$NaCa$,Mg_3Al_2, Si_7Al	Taramite	3.5	5-6
						-,Na_2,Mg_3Al_2,Si_8	Glaucophane	3.125	6-6.5
	Aenigmatite	Complex	Tricl.	$\bar{1}$	$P\bar{1}$	-	Aenigmatite	3.869	5-6
	Pectolite	$Ca_2NaHSi_3O_9$				-	Pectolite	2.86	4.5-5
	Sapphirine	Complex	Monoc.	$2/m$	$P2_1/a$	-	Sapphirine	3.4	7.5
Phyllosilicates or Layer silicates	Talc	$Mg_3Si_4O_{10}$	Tricl. Monoc.	$\bar{1}$ $2/m$	$C\bar{1}$ $C2/c$ Cc	-	Talc	2.58-2.83	1
	Pyrophyllite	$Al_2Si_4O_{10}$	Tricl.	$\bar{1}$	$C\bar{1}$	-	Pyrophyllite	2.814	1.5-2
	Micas	Tri-octahedral Complex	Monoc.	$2/m$	$C2/m$	-	Annite	3.215	2.5-3
					$C2/m$	-	Phlogopite	2.875	2-2.5
					$C2/c$	-	Lepidolite	2.724	2.5-3
					$C2$	-	Zinnwaldite	2.986	3.5-4
		Di-octahedral Complex	Monoc.	$2/m$	$C2/c$	-	Muscovite	2.834	2-2.5
						-	Clintonite	3-3.1	3.5-6
						-	Paragonite	2.909	2.5
				m	Cc	-	Margarite	3.061	4
	Stilpnomelane	Complex	Tricl.	$\bar{1}$	$P\bar{1}$	-	Stilpnomelane	2.6	3-4
	Astrophyllite	Complex	Tricl.	$\bar{1}$	$P\bar{1}$	-	Astrophyllite	3.3	3-4
	Chlorite	Complex	Monoc.	$2/m$	$C2/m$	-	Chlorite	2.6	2-3
	Serpentine	$Mg_3Si_2O_5(OH)_4$	Tetrag.	$31m$	$P31m$	-	Lizardite	2.625	2.5
			Monoc.	$2/m$	Cm	-	Antigorite	2.5	3.5-4
			Orth.	$2/m$	$C2/m$	-	Chrysotile	2.55	2.5
	Clays	$Al_2Si_2O_5(OH)_4$	Monoc.	m	Cc	-	Nacrite	2.602	1
		$Al_2Si_2O_5(OH)_4$	Monoc.	m	Cc	-	Dickite	2.619	1.5-2
			Tricl.	1	$P1$	-	Kaolinite	2.601	1.5-2
		Complex	Tricl.	1	$C1$	-	Amesite	2.778	2.5-3
			Monoc.	$2/m$	$C2/m$	-	Illite	2.75	1-2
			Tetrag.	$4/mmm$	$P4/mmc$	-	Apopyllite	2.33	4.5-5
			Orth.	mmm	$P2cm$	-	Prehnite	2.9	6-6.5
			Monoc.	$2/m$	$C2/m$	-	Vermiculite	2.5	1.5-2
	Clays Group	Di-octahedral Complex	Monoc.	$2/m$	$C2/m$	-	Montmorillonite	2.3	1.5-2
							Beidellite	2.15	1-2
							Nontronite	2.35	1.5-2
	Smectite	Tri-octahedral Complex					Saponite	2.3	1.5-2
							Hectorite	2.5	1-2
							Sauconite	2.45	1-2
Tectosilicates or Framework silicates	Silica	SiO_2	Trig.	32	$P3_221$ $P3_121$	-	α-Quartz	2.648	7
			Monoc.	$2/m$	$C2/c$	-	Coesite	2.909	7.5
			Tetrag.	$4/mmm$	$P4_2/mnm$	-	Stishovite	4.287	7.5-8
			Tetrag.	422	$P4_12_12$	-	α-Cristobalite	2.318	6.5
			Monoc.	m	Cc	-	α-Tridymite	2.269	7
	Alkali feldspar	$M^aAlSi_3O_8$	Monoc.	$2/m$	$C2/m$	$K_{0.75}$ $Na_{0.25}$	Sanidine	2.578	6
						K	Orthoclase	2.571	6
						Rb	Rb-Feldspar	2.930	-
			Tricl.	$\bar{1}$	$C\bar{1}$	K	Microcline	2.567	6
						Na	Albite	2.610	7
		$M^aAl_2Si_2O_8$	Tricl.	$\bar{1}$	$P\bar{1}$	Ca	Anorthite	2.765	6

	Group	General chemical Formula	Crystal System	Laue Group	Space group	Mᵃ,Mᵇ, Mᶜ or A,B,C,T	Mineral name	Density (g/cm³)	Mohs hard.
	Alkaline earth feldspar		Monoc.	$2/m$	$I2/m$	Ba	Celsian	3.400	6-6.5
	Feldspar group	Albite $_{100-x}$ + Anorthite $_x$	Tricl.	$\bar{1}$	$C\bar{1}$	$x = 10 - 30$	Oligoclase	2.65	7
						$x = 30 - 50$	Andesine	2.67	7
	Plagioclase					$x = 50 - 70$	Labradorite	2.68	7
						$x = 70 - 90$	Bytownite	2.71	7
	Feldspathoid	$KAlSi_2O_6$	Tetrag.	$4/m$	$I4_1/a$	-	Leucite	2.461	6
		$KAlSiO_4$	Hexa.	6	$P6_3$	-	Kalsilite	2.621	6
		$KNa_3Al_4Si_4O_{16}$	Hexa.	6	$P6_3$	-	Nepheline	2.679	6
	Sodalite	$Na_8Al_6Si_6O_{24} \cdot x$	Cubic	$m\bar{3}m$	$P\bar{4}3n$	$x = Cl_2$	Sodalite	2.27	5.5-6
						$x = SO_2$	Nosean	2.3	5.5
		$(Na,Ca)_8Al_6Si_6O_{24} \cdot x$				$x = (SO_4,S)_{1-2}$	Haüyne	2.44	5.5-6
	Cancrinite	Complex	Hexa.	6	$P6_3$	-	Cancrinite	2.3	5-6
	Scapolite	Complex	Tetrag.	$4/m$	$P4_2/n$	-	Marialite	2.599	5.5-6
						-	Meionite	2.757	5-6
	Analcite	$NaAlSi_2O_6 \cdot H_2O$	Tetrag.	$4/mmm$	$I4_1/acd$	-	Analcite	2.264	5
	Zeolite	$Na_{16}(Al_{16}Si_{24}O_{80}) \cdot x$	Orth.	mmm	$Fdd2$	$x = 16H_2O$	Natrolite	2.2	5.5-6
		$Na_4Ca_8(Al_{20}Si_{20}O_{80}) \cdot x$			$Pnna$	$x = 24H_2O$	Thomsonite	2.3	-
		$Na_3KCa_2(Al_8Si_{40}O_{96}) \cdot x$			$Cmcm$	$x = 28H_2O$	K-Mordenite	2.132	5
		$Na_2Ca_2(Al_6Si_9O_{30}) \cdot x$	Monoc.	$2/m$	$C2$	$x = 8H_2O$	Mesolite	2.26	5
		$K_2(Ca_{0.5}Na)_4 (Al_6Si_{10}O_{32}) \cdot x$			$P2_1/m$	$x = 12H_2O$	Phillipsite	2.15	4-5
		$Ba_2(Al_4Si_{12}O_8) \cdot x$			$P2_1/m$	$x = 12H_2O$	Harmotome	2.4	4-5
		$CaAl_2Si_2O_8 \cdot x$			$P2_1/c$	$x = 4H_2O$	Gismondine	2.2	4-5
		$(Ca,Na_2,K_2)_4 (Al_8Si_{28}O_{72}) \cdot x$			Cm	$x = 24H_2O$	Heulandite	2.2	-
		$(Na,K)_6(Al_6Si_{30}O_{72}) \cdot x$			Cm	$x = 24H_2O$	Clinoptilolite	2.16	-
		$NaCa_2(Al_5Si_{13}O_{36}) \cdot x$			$C2/m$	$x = 14H_2O$	Stilbite	2.1	-
		$Ca_2(Al_4Si_8O_{24}) \cdot x$	Trig.	$\bar{3}m$	$R\bar{3}m$	$x = 12H_2O$	Chabazite	2.075	4
		$NaK_2MgCa_{1.5} (Al_8Si_{28}O_{72}) \cdot x$	Hexa.	6	$P6_3/mmc$	$x = 28H_2O$	Erionite	2.0	-
		$(Na_2,Ca)(Al_2Si_4O_{12}) \cdot x$			$P6_3/mmc$	$x = 6H_2O$	Gmelinite	2.1	4-5

Tab.2.9 Main parameters of rock forming silicate minerals. (18) (57) (58)

Reported oxides and silicates are rock forming minerals only.

Due to the fact that Mohs hardness of (cast iron) brake disc is around 5.5, on first approximation can be considered hard- abrasives all the materials with hardness equal or higher than 7, mild-abrasives materials with hardness included from 5 to 7 and low or non-abrasives or fillers all the materials with hardness lower than 5. Historically speaking quartz and his polymorphs have been largely used in friction materials as hard abrasive (59), but in1997 "*crystalline silica inhaled in the form of quartz or cristobalite from occupational sources*" has been classified as carcinogenic to humans (Group 1) by IARC (60), this limited the use of quartz in all his forms in friction material formulation; special attention must be paid to avoid quartz as mineral impurity in raw materials.

Not only hardness but also density, chemical and thermal stability, environmental and human health risk assessment, water insolubility and price/benefit ratio are parameters to be taken in account during raw materials selection.
A rapid overview of rock forming minerals show that only few of them can be considered hard abrasives, and some of this natural hard abrasives has high cost or low natural abundance. Most of them can be considered mild abrasives, fillers or, in some specific case, lubricants (see fillers and lubricants sections).

To overcome the shortcomings of natural oxides and silicate, hard abrasives synthetic oxides and silicates can be used in friction materials.

2.2.2.1 Alumina

Aluminum oxide, also called alumina is industrially produced by the Bayer process from bauxite ore, see fig.2.21. Bauxite is a natural mix of minerals mainly composed by Gibbsite, Boehmite, Quartz, Kaolinite/Halloysite, Hematite, Aluminian Goethite, Anatase and Rutile plus some minor componens (61).
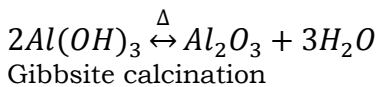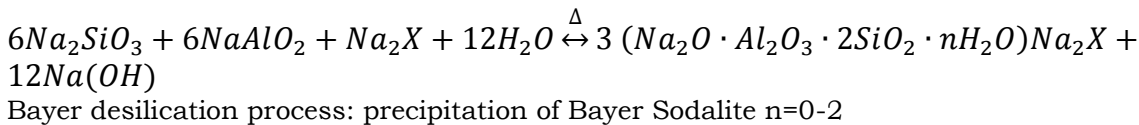
$$Al(OH)_3 + NaOH \overset{\Delta}{\leftrightarrow} Na^+ + Al(OH)_4^-$$
Gibbsite dissolution/precipitation

$$Na^+ + Al(OH)_4^- \overset{\Delta}{\underset{-bohemite\ seeds}{\longleftrightarrow}} AlOOH + Na(OH)$$
Boehmite precipitation

$$SiO_2 + 2NaOH \leftrightarrow 2Na_2SiO_3 + H_2O$$
Bayer desilication process: Quartz dissolution

$$Al_2O_3 \cdot 2SiO_2 \cdot 2H_2O + 6NaOH \leftrightarrow 2Na_2X + SiO_3 + 2NaAlO_2 + 5H_2O$$
Bayer desilication process: Kaolinite dissolution. $X = CO_3^=, SO_4^=, 2AlO_2^-, 2OH^-$

$$6Na_2SiO_3 + 6NaAlO_2 + Na_2X + 12H_2O \overset{\Delta}{\leftrightarrow} 3\,(Na_2O \cdot Al_2O_3 \cdot 2SiO_2 \cdot nH_2O)Na_2X + 12Na(OH)$$
Bayer desilication process: precipitation of Bayer Sodalite n=0-2

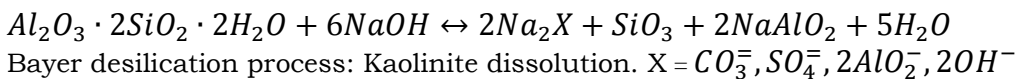$$2Al(OH)_3 \overset{\Delta}{\leftrightarrow} Al_2O_3 + 3H_2O$$
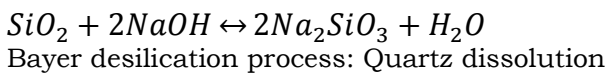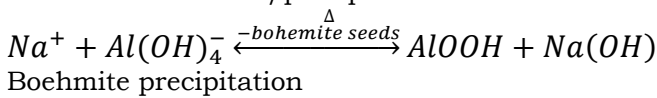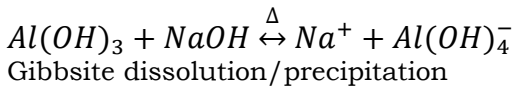Gibbsite calcination

Fig.2.21 Bayer process, Gibbsite precipitates from supersaturated sodium aluminate solution on gibbsite seed, silica is eliminated by desilication process. Gibbsite is calcinated to obtain Alumina. (61)

Alumina can be found in many commercial grades. See tab.2.10

Alumina grade	Production process	Main properties	Main use
Smelter or metallurgical	Aluminium hydroxide process dehydratated in a fluid flash processes at 180-600°C and then calcined at temperatures > 1000°C	α-Al_2O_3 form typically around 25%, relatively high specific area.	Manufacture of metallic aluminum
Calcined	Calcining aluminum hydroxide at temperatures higher than 1100°C Mineralizers, such as fluorine and boron can be used.	The crystallite size of α-Al_2O_3 in the calcined product can be varied from 0.2 to100 μm. Containing around 0.5% Na_2O	Ceramic and refractory applications
Low soda	Same as calcined alumina plus acid washing, chlorine addition, boron addition, and utilisation of soda adsorbing compounds	Same crystal size of calcined alumina. $Na_2O<0.1\%$.	Suitable for electric and electronic areas
Reactive	Manufactured by dry grinding calcined alumina to particle sizes smaller than 1 μm	The large surface area and very fine particles. High packing densities obtainable.	Sintered it's used where exceptional strength, wear resistance, temperature resistance, surface finish or chemical inertness are required.
Activated γ-Al_2O_3	Thermal controlled calcination of high purity boehmite gels and/or pseudoboehmite	γ-Al_2O_3 highly porous and exhibiting very large surface area	Catalyst support, absorbant adjuvant products, Abrasives, desiccating and filtration agent
Tabular	Manufactured by grinding, shaping and sintering calcined alumina	The thermal treatment at 1900–2150 K causes the oxide to recrystallize into large, tabular crystals of 0.2–0.3 mm.	Refractory applications
Fused	Manufactured by melting a suitable raw material in an electric arc furnace.	Calcined alumina from the Bayer process is used as a starting material for the highest quality fused alumina. Bauxites with varying levels of iron oxide, silicates, and titanium minerals are melted to produce the brown or less pure black qualities.	Abrasives and refractories
High-purity	Many methods	Purity higher than 99.99%	Manufacture of synthetic gem stones

Tab.2.10 Main properties of commercial alumina grades. (62) (63)

Depending on calcination temperature, see fig.2.22, many metastable phases can be achieved.

Face-centered cubic (fcc) arrangement of oxygen anions:

- γ-Al_2O_3 and η-Al_2O_3 (cubic) $Fd\bar{3}m$
- θ-Al_2O_3 (monoclinic) $C2/m$
- δ-Al_2O_3 (either tetragonal or orthorhombic) $P\bar{4}m2$ or $P2_12_12_1$

Hexagonal close-packed (hcp) arrangement of oxygen anions:

- α-Al_2O_3 (trigonal) $R\bar{3}c$
- κ-Al_2O_3 (orthorhombic) $Pna2_1$
- χ-Al_2O_3 (hexagonal) $P6/mm$ or $P6_3/mcm$

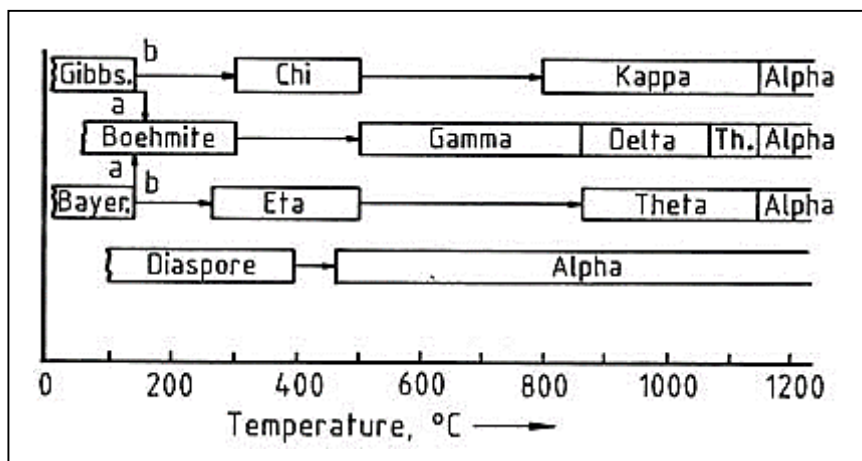Some additional monoclinic phases θ' θ" and λ have been identified. (64)

Fig.2.22 Alumina polymorphs generated at different temperatures (62)

Aluminum oxide is widely used in friction materials, α-Al_2O_3 has hardness 9 on mohs scale and lot of particle size/shape available.

A special mention for activated γ-Al_2O_3 due to its specific use for improvement provided with respect to fading phenomena. (65)

2.2.2.2 Zirconium oxide (Zirconia)

The main natural form of zirconium oxide is the Baddeleyite, as already reported it has a Monoclinic crystal system, (m-ZrO)space group $P2_1/c$ with Mohs hardness 6.5. Zirconium oxide has other two polymorphs, a tetragonal structure (t-ZrO) space group $P4_2/nmc$ stable from 1700 to 2370°C and cubic structure (c-ZrO) space group $Fm3m$, for temperature higher than 2370°C, see fig.2.23, the latter can be found in nature as rare mineral, Tazheranite, the mohs hardness is 7.5 (66).
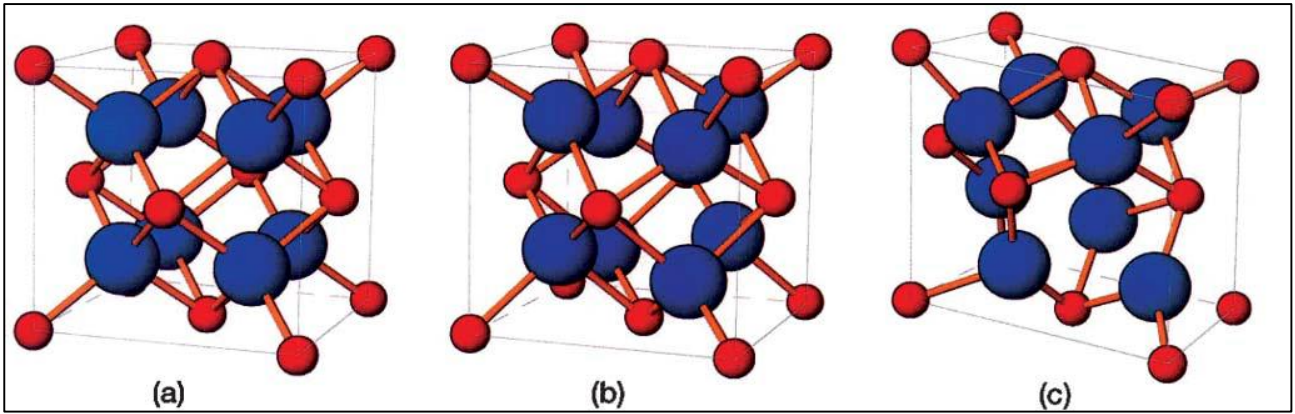
Fig.2.23 Schematic representation of the three polymorphs of zirconia (Zr in blue, O in red): (a) cubic $Fm3m$, (b) tetragonal $P4_2/nmc$, (c) monoclinic $P2_1/c$ (67)

To synthetize a temperature stable zirconia with high hardness, high toughness, good thermal conductivity and to avoid the transition between phases that involve a structural deformation with a large volume change, a structure stabilizer is needed (67). Stabilization is made by doping zircon with addition of trivalent dopants or tetravalent dopants into zirconia structure by creating oxygen vacancies to energetically favor tetragonal and cubic structures (68). Some example of stabilizer are yttrium oxide for yttria stabilized zirconia (YSZ), calcium oxide for calcia stabilized zirconia, magnesium oxide for magnesia stabilized zirconia, aluminum oxide for alumina stabilized zirconia, cerium oxide for ceria stabilized zirconia and hafnium oxide for hafnia stabilized zirconia.

2.3 Lubricants

In brake system there is contact between two surfaces, brake pads and brake disc. Static and dynamic contact between the two bodies generates stress on the interface, the stabilization of friction behavior requires the use of lubricants that generally fulfill the following purposes (69):

- Set the required friction coefficient in a desired range
- Formation of a continuous film having good elastic properties on the surface.
- Formation of a strong physical or chemical bond with the surface.
- Level off the friction curve
- Reduce wear and tear on disc and lining
- Reduce fading at high speeds and/or high temperatures
- Reduction of brake noise
- Good friction recovery after repeated application
- High thermal conductivity to avoid local melting due to frictional heating
- Reduce weight by using a material with low specific weight (carbon based lubricants)

As already seen in abrasive section a desired effect during brake events is the formation of a stable friction layer with strong physical or chemical interaction with the surfaces of tribo-couple. Friction layer should be a continuous film having good elastic properties which protects components from wear and corrosion to stabilize friction coefficient and to avoid sticking between brake disc and pads.

Lubricants are main players to determinate the friction layer characteristics in terms of adhesion and lubrication.

2.3.1   Fundamentals of adhesion

Different components are released at brake disc/pad interface due to the rubbing between components.

Release of particles by abrasive wear has already been reported in abrasive section, in this section adhesion and adhesive wear are discussed.

Special attention has to be paid during the running-in phase when the surfaces are clean and tribofilm generation begin.

More in general when tribofilm is not present, the small oxide layer that naturally covers metals can be removed by wear and cast iron gets in contact directly with brake pad materials in bulk and fiber form, at this condition many mechanisms are involved.

2.3.1.1 Metal-metal interaction

Many parameters influence adhesion between solids in contact, bond strength due to the surface characteristics like atomic or molecular orientation, chemistry nature, elastic and plastic deformation, impurities absorption from the environment or segregated from bulk etc.

Even if data on ideal interfaces is only the first step and oughtn't be considered exhaustive in adhesive studies, a theoretical approach through simplified models can provide some important information on materials interaction.

In a hypothetic adiabatic system, where two bodies are in contact at T=0 K the adhesive interaction energy $E_{ad}(a)$ is described as in eq.2.18, see fig.2.24 (70)

$$E_{ad}(a) = \frac{[E(a) - E(\infty)]}{2A}$$

Eq.2.18

Where A is the cross-sectional area and a is the separation between the two elements and the total energy $E(a)$ is a minimum functional of the electron density and atomic coordinates.
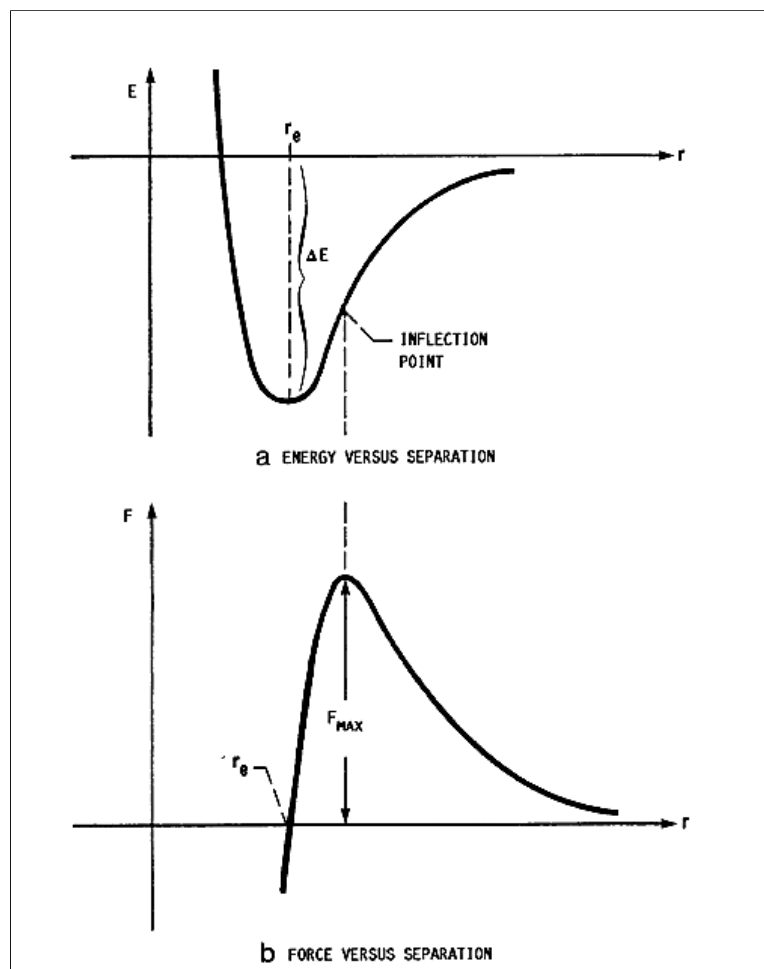

Fig.2.24 Binding energy curve a) energy vs. separation b) force versus separation (70)

Quantum mechanics first-principle calculation can be used to separate the contribution of different factor on total adhesion energy (71).
Total adhesion energy is function of electron density and is calculated by eq.2.19

$$E(\rho) = E_{ke}(\rho) + E_{es}(\rho) + E_{xc}(\rho)$$

Eq.2.19

Where $E_{ke}(\rho)$ is the kinetic factor, $E_{es}(\rho)$ is the electrostatic factor and $E_{xc}(\rho)$ is the exchange and correlation energy contribution.

Following this model it was calculated that the maximum adhesion force of metal pair (minimum on total energy in fig.) depend more on the exchange-correlation energy factor than on the kinetic energy factor (72), that determines the strength of an adhesive bond.
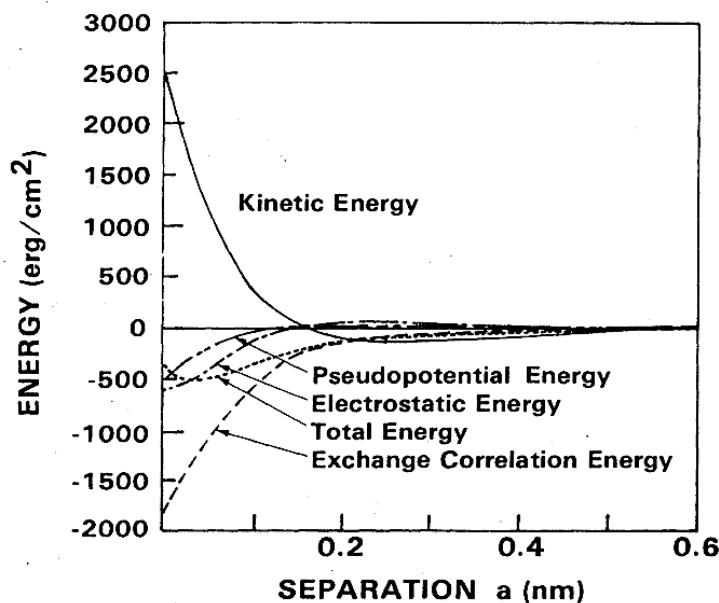

Fig.2.25 Self-consistent energy components of the binding energy calculated for an Al(111) - Mg(0001) contact. (72)

The critical separation distance where the adhesion force is maximized should be shorter than 3Å, the protective oxide layer that generally cover the metal surface when exposed to air is around 5 nm and this layer when removed by wear is fast reformed. To have metal-metal adhesion, metal surfaces have to be exposed to the contact and this is possible during the brake events only.

It's also important to underline the effect of crystal structure:

-   Within the same crystal some planes have higher modulus of elasticity and a lower resistant to deformation under a given load, thus, the real area of contact is less than those of the other less dense planes.

46

- On different crystal structures hexagonal close-packed results to be less ductile compared to face-centered and body-centered metals which, as a consequence, tend to be more adhesive, see fig.2.26
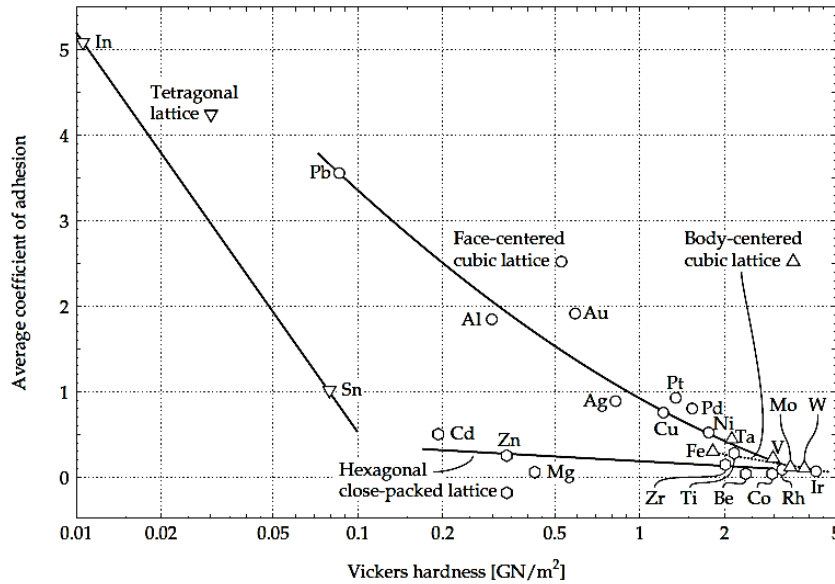

Fig.2.26 Adhesion coefficient of various metals defined as the ratio of rupture force and contact force vs. metal hardness (73).

Transferred metal can be highly work-hardened by friction. Interaction between hardened material and the original one can induce plastic deformation on the latter increasing real surface contact and consequently adhesion.

Not only electron density of two separated elements that get in contact is important on adhesive strength, electron transfer between metals as in acid-base interaction has to be evaluated.

Transition metals have an amphoteric behavior, due to their Fermi level calculated on filling of d orbitals, at short range a metal can act as a Lewis base accepting electron or Lewis acid donating electron and creating an intermetallic bonding. To a lesser extent also the contact electrification at long range can have an effect on metal-metal adhesion.

Not every metals pair has adhesive behavior, some intermediate phases at the contact can have a positive free energy of atomic bond formation, adhesion of metals can be predicted considering their reciprocal solubility as reported in fig.2.27 (74)
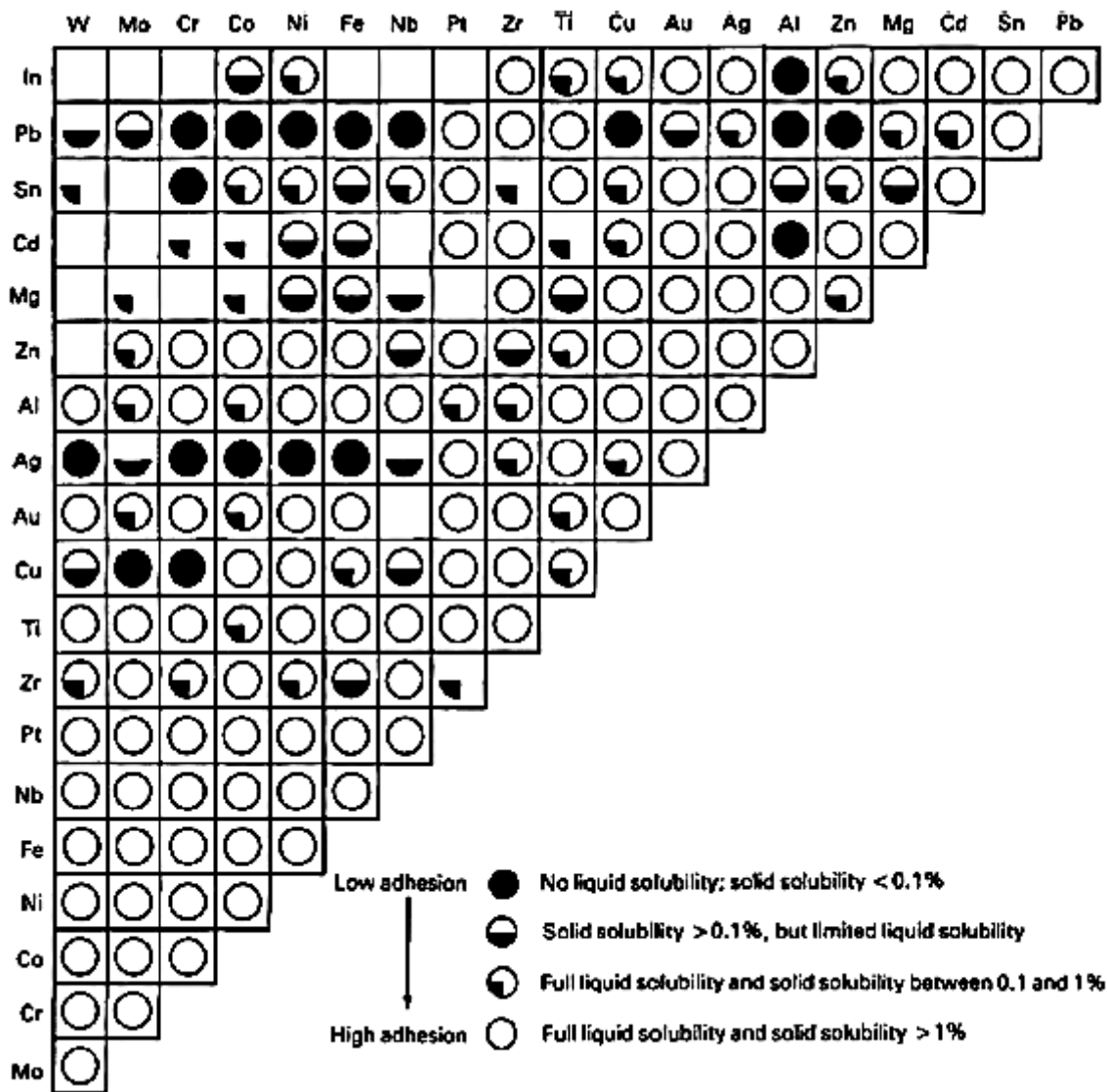
Fig.2.27 Chart indicates the degree of expected adhesion between the various metal combinations. (74)

Metals compatible with iron in brake system can contribute to the formation of a film with good tribological and physical properties.

2.3.1.2 Metal-ceramic interaction

As already seen transition metals have an amphoteric behavior.
The interaction energy ΔE between the HOMO highest occupied molecular orbital of a base (nucleophile) and the LUMO lowest unoccupied molecular orbital of an acid (electrophile) is describe in eq.2.20

$$\Delta E = -\underbrace{\frac{Q_{Nu}Q_{El}}{\epsilon R}}_{\text{Coulombic term}} + \underbrace{\frac{2(C_{Nu}C_{El}\beta)^2}{E_{HOMO} - E_{LUMO}}}_{\text{Frontier orbital term}}$$

Eq.2.20

Where Q_{Nu} and Q_{El} are the total nucleophile and electrophile charge, C_{Nu} and C_{El} are the respective coefficients of the atomic orbital, β is the resonance integral, ϵ is the permittivity and R is the distance between Nu and El. (70)

Following the Pearson's Hard-Soft Acid Base principle (HSAB) materials that react exchanging electrons can be described as in tab.2.11

HSAB	Reaction behaviour	Frontier orbital characteristic
Hard acid	Nucleophile	High energy LUMO
Soft acid	Nucleophile	Low energy LUMO
Hard base	Electrophile	Low energy HOMO
Soft base	Electrophile	High energy HOMO

Tab.2.11 Pearson's Hard-Soft Acid Base principle

On adhesion between metal and ceramics the bonding is due to the acid-base interaction, where the metal is considered soft acid and his HOMO is the Fermi level (see fig.2.28) and the ceramic is considered a base.
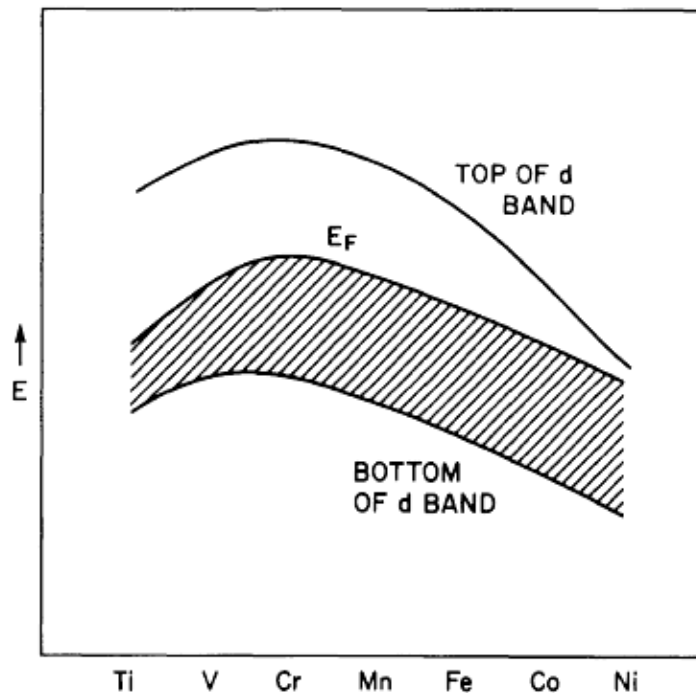

Fig.2.28 Fermi level of some transition metals (75)

An example of acid base interaction between metals and ceramics is the Fe-SiC bonding. In this case mechanical hardness of carbide induce plastic deformation on iron surface guaranteeing a good contact, electron from the HOMO of the carbide (soft base) are donated to iron generating the bonding (76).

Special attention has to be done on interaction between oxides and metals, oxides in fact can be considered as hard bases. Heats of formation of metal oxides determinate reactivity between metal and oxygen, when metal is directly in contact with a metal oxide reactive metals favor the adhesion.
For low-reactive metals like gold and silver only Lifshitz - van der Waals forces should be considered, this forces are two order of magnitude smaller than adhesion force of reactive metals (77).

2.3.1.3 *Metal-polymers interaction*

The prevalent mechanisms on interaction between polymers and metals are physisorption based on Lifshitz-van der Waals forces, molecular interactions, e.g. acid-base (or donor-acceptor) interactions, chemical interactions, and to a lesser extent electrostatic attraction (70).

It's convenient to classify polymers considering their wettability as described in tab.2.12

Wettability	γ_c Zisman's critical surface tensions	Examples of polymers and name abbreviations
Low	$10\frac{mJ}{m^2} < \gamma_c < 30\frac{mJ}{m^2}$	Fluoropolymers, polysiloxanes, polyolefins (PP,PE etc.) and some rubbers
Medium	$30\frac{mJ}{m^2} < \gamma_c < 40\frac{mJ}{m^2}$	Polyvinyl methyl ether PVME Polypropylene oxide PPO Polyethyl methacrylate PEMA Polyethyl acrylate PEA Polystyrene PS Polyvinyl acetate PVAc Polyvinyl alcohol PVA Polymethyl methacrylate PMMA Polyvinyl chloride PVC Polyvinylidene chloride PVCl$_2$ Some Rubbers
High	$\gamma_c > 40\frac{mJ}{m^2}$	Polycarbonate PC Poly 6-aminocaproic acid PA6 Polyethylene terephthalate PET Polyacrylonitrile PAN Polyhexamethylene adipamide PA66 Epoxy resins

Tab.2.12 Wettability and critical surface tension of some polymers

A general rule is the higher the wettability of the polymer the better is the adhesion.

2.3.2   Lubrication mechanisms in brake systems

Smearing is the release of material on surface forming a thin film. Failure of this film can lead to more and more critical situations, from scratching to scuffing and seizure depending on the chemical and physical interaction of the friction pair materials and on working conditions such as pressure temperature and speed.

To keep wear under control a lubricant system is needed; two main mechanisms are employed in dry lubrication for brake systems (78):

- Exfoliating solids
- Soft films

2.3.2.1   *Exfoliating solids*

The first method requires materials with structure that tend to exfoliate when interposed in two sliding surfaces such as lamellar solids. See fig.2.29
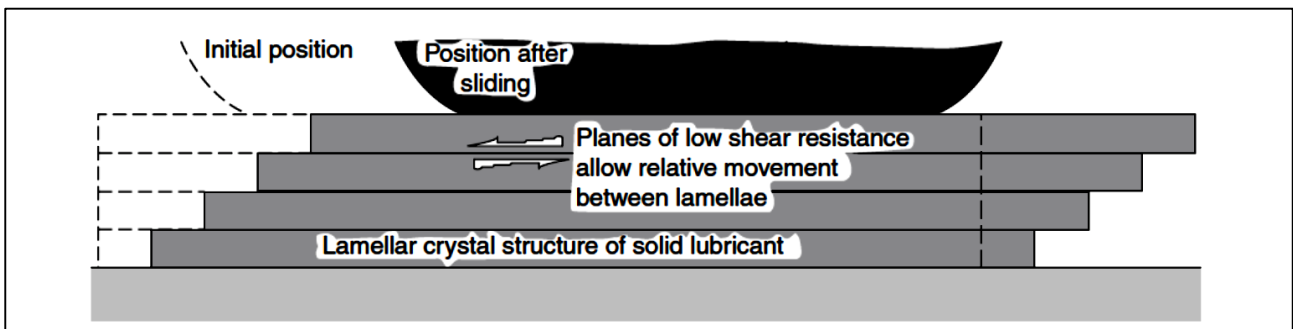
Fig.2.29 Mechanism of lubrication by lamellar materials (73)

Only low inter-lamellar bonding force materials are considered lubricants, materials with high inter-lamellar bonding force can be considered as mild abrasives. Lamellar solids have interesting tribological properties, they promote lubrication in brake systems at high speed and pressure condition. Example of lamellar solid lubricants are graphite and metals chalcogenides like sulfides, selenides and tellurides (69) (79).

Selected materials have to be resistant to temperature and to be insoluble in water, the limit of most of lamellar solids is their behavior at high temperature, over 500°C they can oxidize changing chemical composition and losing lubricant power (80).

2.3.2.2   *Soft film*

According to Bowden and Tabor model, friction coefficient μ can be described by eq.2.21 , where F is the friction force, L is the applied load, A_r is the real area τ is

the shear strength, τ_0 is the interfacial shear strength, a "velocity accommodation parameter" which is a property of the interface and α represents the pressure dependence of the shear strength.

$$\mu = \frac{F}{L} = \frac{A_r \cdot \tau}{L} = \frac{\tau}{P_H} = \frac{\tau_0}{P_H} + \alpha$$

Eq.2.21

Tribofilm not only prevent the direct contact between rubbing surfaces but also play the role of "peak load shifting" increasing the actual contact area and reducing local contact pressure (81).

The concept of interpose soft films into hard sliding surfaces is represented in fig.2.30
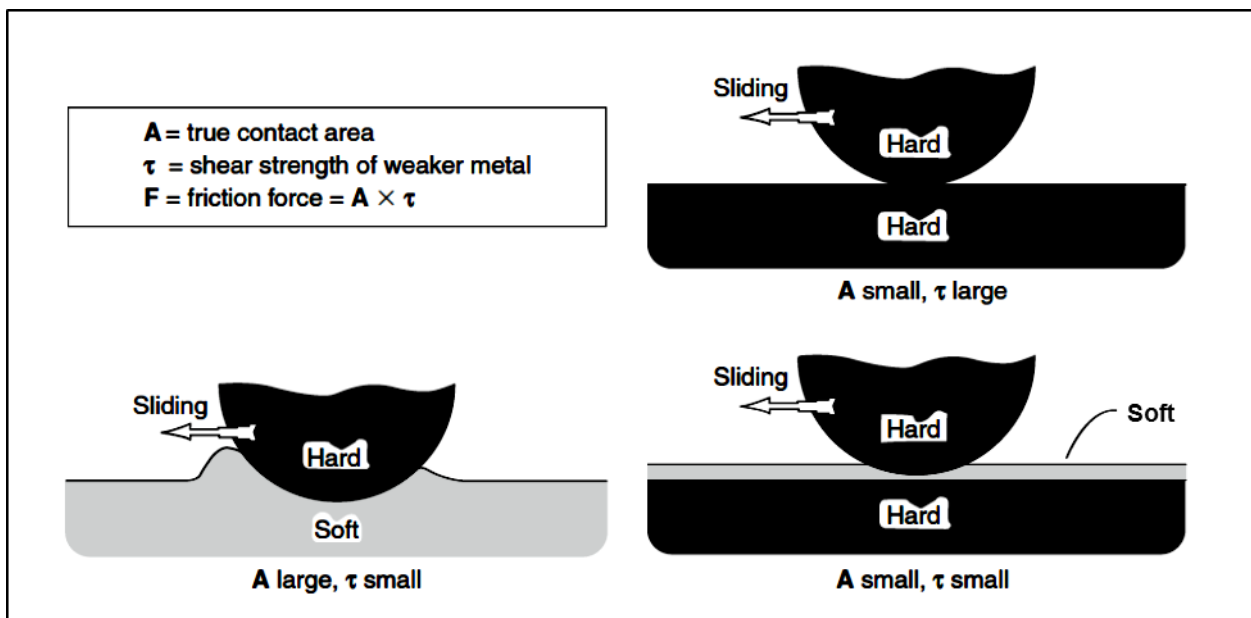
Fig.2.30 Mechanism of friction reduction by soft films on hard substrates (73)

When two hard surfaces are in contact small interaction area and high shear stress determinate an high friction coefficient. The same effect can occur when a hard surface is directly in contact with a soft surface, low shear stress and high contact surface can increase friction coefficient. When a soft film is interposed between two comparable hard surfaces the contact area is determinated by hard surfaces and the friction coefficient is regulated by "soft" interlayer, this is the ideal situation for friction coefficient reduction (74).

High temperature resistant polymers, metals, metal oxides and fluorides are suitable for this purpose.

2.4 Lubricants (raw materials)

2.4.1   Carbon based lubricants

Most of the lubricant properties of carbon based materials are due to the graphite, one of the carbon allotropic form.

Graphite is a crystalline, polymorphic form of elementary carbon and two types of spatial arrangement of carbon layers are possible (82), see fig.2.31

- Space group $P6_3/mmc$. The sequence ABABAB. . . is characteristic of the hexagonal structure of graphite, thermodynamically stable over a range of temperatures and pressures (T < ~ 2000 °C, p < 130 kbar). In plane C-C bond length is 1,42Å while interlayer distance is 3,354Å length.

- Space group $R3m$. The sequence ABCABC. . . occurs in the rhombohedral modification, it's a metastable phase that disappear at elevated temperatures (T>2000° C). This form has not been observed as a separate phase in the structure of natural graphite

P6$_3$/mmc graphite lattice has a heterodesmic layered structure consisting of six-membered rings in which each carbon atom has three near neighbors at the apices of an equilateral triangle. Within the large planar layers, there are linkages intermediate between atomic and metallic bonds. The layers in the crystal are held together by van der Waals bonding forces of energy of 0.2 eV/atom.
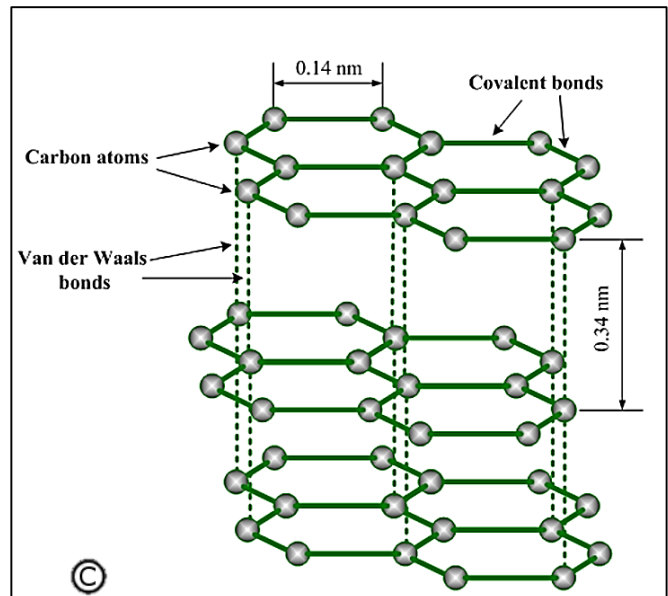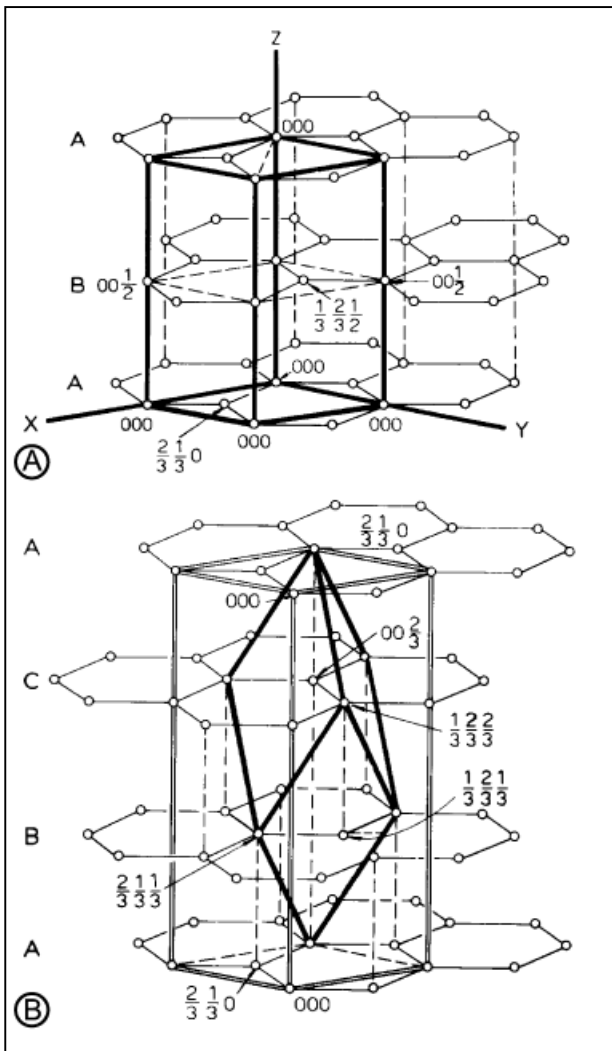
Fig.2.31 (A) P63/mmc hexagonal lattice of graphite; (B) R3m rhombohedral lattice of graphite. (82) (C) Hexagonal lattice of graphite with bond lengths (83)

Low-friction behavior in graphite is traditionally ascribed to the low resistance to shear between atomic layers bonded by weak van der Waals force (84). Under vacuum, graphite lattice has high inter-lamellar binding energy, which can be reduced by insertion of gases or liquids like water (85). The lubricating effects of inert gases are explained by a mechanical action of atoms inserted between crystallites and thus increasing their mobility, high temperature condition reducing the amount of volatile components increasing the friction coefficient of graphite that may perform as a mild abrasive (86).

Friction and wear behavior is also correlated with structural order/disorder in graphite. The density of states of π-electrons in a disordered stacking structure of carbon atoms usually is called turbostratic graphite (87), this is an irregular stacking of parallel graphitic monolayers with no periodicity along the c axis (axis perpendicular to the graphitic layers) (88). At low loading ranges chemical structure of graphite does not change providing a linear relationship between load and friction coefficient (due to related friction energy only). At high loading range friction

induced phase transformation in graphite is observed and friction coefficient increases significantly. This behavior at high load is explained by transformation of 3D graphite into a 2D turbostratic phase which constitutes high degree of stacking interlayer disorder (coke-like) leading to increase in friction coefficient. (89)

Generally carbon based solid lubricants are present until 30% in weight on friction material formulation, they are effective to build up a thick transfer layer (90).

2.4.1.1 Natural graphite

Graphite occurring in nature has a biogenic and inorganic origin, it's mainly formed under conditions of thermal or regional metamorphism. However, besides the temperature, graphitization of carbonaceous material also requires the input of shear strain and strain energy. The effects of pressure and shear promote molecular ordering of basic structural units in graphite and facilitate preferential alignment of aromatic lamellae and pore coalescence.

Graphite occurs in different forms in various types of rocks and deposits: (91)

- Dispersed cryptocrystalline pigment and cryptocrystalline dust
- Submicroscopic crystallites aggregated in scaly-granular forms
- Xenoblastic microfragments
- Distinct crystaloblasts, single flakes, scales, plates or lamellae, disseminated flakes
- Impregnations in the form of pyrolitic nodules or rosette forms
- Irregular patches enclosed within tonalities
- Lumps, pieces, fragments, and monocrystalline flakes
- Pseudomorphs spherical aggregates resulting from polycentric growth

"Amorphous" graphite so called due to his anhedral morphology it's not really amorphous but the structure is polycrystalline and near-isotropic in micro-crystalline particles (92). Generally found as massive lumps coal-like in flat fracture cleavage it's formed by thermal metamorphism of coal seams. Commercial grades of amorphous graphite are available from 75-85% purity in particle sizes from 4-inch lumps to 3-micrometer powder. The "graphite content" of 20-40 percent is low if compared to 90 percent for other natural graphite grades, however it's lower in cost than other types and it's still lubricious, conductive, and chemically stable. (93)

Vein Graphite, crystalline vein, Sri Lankan graphite, or Celyon graphite, is a naturally occurring form of pyrolitic carbon (solid carbon deposited from a fluid phase), massive platy intergrowths of fibrous or needle-like crystalline aggregates.

Flake graphite is fossil remnants which have been graphitized over time under extreme pressure and temperature. Found in metamorphic rock, these plate-like structures are liberated from ore through a flotation process

2.4.1.2   Synthesis, pyrolysis and carbonization.

Starting from organic/carbonaceous matter, heat treatment under inert atmosphere leads a modification of carbon structures depending on the temperature reached. See Fig.2.32 (94) On the first phase, from 200 to 600°, aliphatic hydrocarbons tend to cyclize and aromatize and in a second step aromatic hydrocarbon tend to condensate releasing low molecular weight molecules like CO_2, CO and CH_4. Above 800°C H_2 is formed leaving a carbonaceous solid which, depending on raw materials, can still contain elements like sulfur, nitrogen and oxygen.
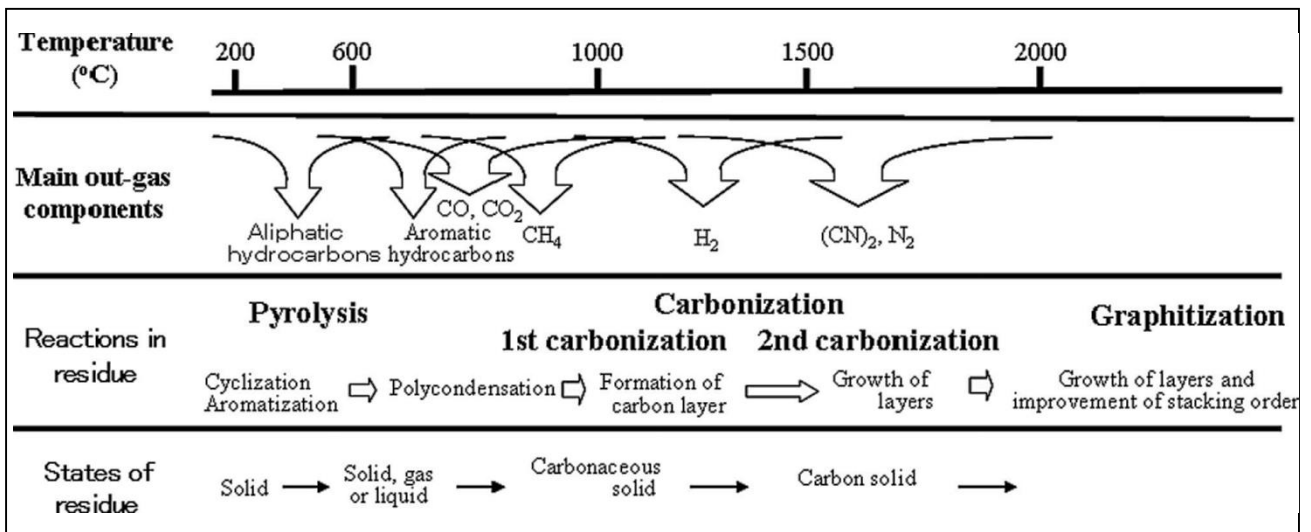

Fig.2.32 Scheme of out-gases, reactions, and state of residues during carbonization

The carbonization process can be conducted starting from different state of raw materials, in tab.2.13 are reported the main characteristics related to different structures produced from gas, liquid and solid state materials.

Carbonization process	Precursors	Carbon materials	Characteristics
Gas-phase carbonization	Hydrocarbon gases, decomposition in space	Carbon blacks	Fine particles, so-called "structure"
	Hydrocarbon gases, deposition on substrate	Pyrolytic carbons	Various textures, preferred orientation
	Hydrocarbon gases, with metal catalysts	Vapor-grown carbon fibers, Carbon nanofibers	Fibrous morphology, various nanotextures
	Hydrocarbon gases, without any catalyst	Diamond-like carbon	Thin film, sp^3 bond, amorphous structure
	Carbon vapor	Carbon nanotubes	Tubular, single-wall and multi-walled
	Carbon vapor	Fullerenes	Spherical, molecular nature
Solid-phase carbonization	Plants, coals, and pitches	Activated carbons	Highly porous adsorptivity
	Furfuryl alcohol, phenol resin, cellulose, etc.	Glass-like carbon	Amorphous structure, conchoidal fracture, gas impermeability
	Poly(acrylonitrile), pitch, cellulose and phenol resin	Carbon fibers	Fibrous morphology, high mechanical properties
	Polyimide films	Carbon films	Film wide range of graphitizability
Liquid-phase carbonization	Pitch, coal, tar	Cokes mesocarbon microbeads	Spherical particles
	Cokes with binder pitches	Polycrystalline graphite blocks, including high-density isotropic graphite	Various densities, various degrees of orientation

Tab.2.13 Carbonization Processes for the Production of Various Carbon Materials

Many of this products are used in formulation of friction materials not only as lubricant but also as fillers or fibers.

2.4.1.2.1 Cokes

There are different cokes used in friction materials, they are produced by different feedstock sources:

Met Coke. The coke-making process involves carbonization of coal to temperature of 1100°C in an oxygen deficient atmosphere in order to concentrate the carbon. Metallurgical Coal, mainly used for reduction of iron ore tab.2.14 , has to be more pure than steam coke (burned to produce electricity): (95)

Met. coal characteristics	Preferred Values
Ash	>10%
Sulfur	<1%
Phosphorus content	≤0.06 %
Volatile matter (dry, ash free basis).	22-31%
Rank (level of coal metamorphism)	≥0.82 R_0
Reflectance	≥0.95 Ro max
Ash acid/base ratios	>3.5

Tab.2.14 Typical Met-coke parameters (95)

Pet Coke. Calcined petroleum coke is formed from the by-product (tar) of crude oil distillation, that is the process of carbon rejection from the heavy residues producing lighter components lower in sulfur, since most of the sulfur is retained in the coke (96). These materials have a dark, flat sheen and are high in carbon low-temperature-treated carbons is quite different from well-crystallized graphite, because it consists of random stacking of small layers, as shown on a petroleum coke heat-treated up to 1000°C (94).

Calcined petroleum cokes are characterized by a higher friction coefficient and low wear - especially by contrast with other petroleum and metallurgical coal grade.

Calcined Needle Coke. The name needle coke arises from the acicular shape of the coke particles that reflects the anisotropic nature of the coke structure, in fact, to give excellent needle cokes with developed anisotropy and low thermal expansion highly aromatic coal tar pitch is required. (97) Mainly used for the production of Graphite electrodes due to its high level of carbon and low level of ash and metal it can be used in friction materials. It has a better developed layer structure than standard calcined coke giving it unique friction and wearing properties.

2.4.1.2.2 Synthetic graphite

Synthetic graphite is generally obtained from calcined petroleum cokes, the material started out as carbon with limited long range crystalline order defined by the mesophase from which it was composed. To obtain good products, graphitization is done at temperatures above 2700°C, it's fundamental that oxygen be excluded from the furnace, some oxygen scavenging material can also be added to this purpose (98).
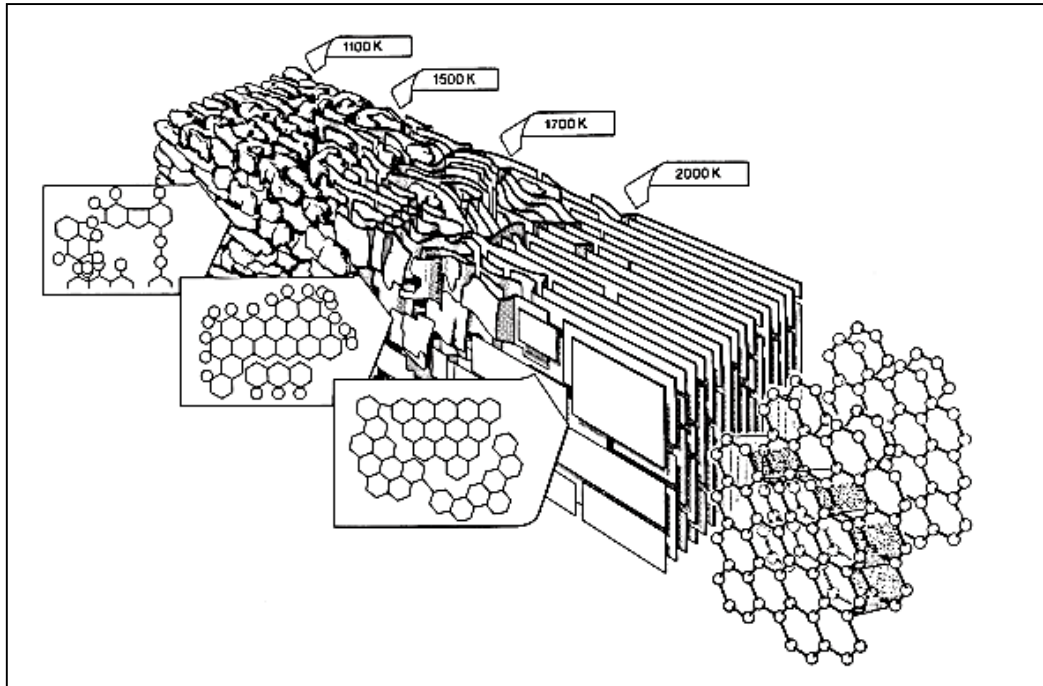
Fig.2.33 Molecular structures of carbon at different temperatures (99)

During graphitization phase no macro morphology significant change occurs, the microstructure of the graphite, however, will differ in the size and extent of the crystals that make up the polycrystalline structure of synthetic graphite. (100)

Crystallinity is not the only parameter that influence the tribo-performance, also particle size of lubricants has been demonstrated that change wear and friction coefficient at different load and speed (101).

2.4.1.2.3   Graphite fluoride
Fluorination of graphite produce substoichiometric graphite fluoride with structural formula $(CF_x)_n$ where $0 < x < 1.24$.

It's also called polycarbon fluoride and when $x = 1$ polycarbon monofluoride or carbon monofluoride.

Graphite fluoride is prepared by reaction between gaseous fluorine and graphite, as in graphite structure, interlayer weak Van der Waals bonding is responsible of lubricant properties of the material, fluorine increases the spacing between planes reducing graphite layers shear strength and making it a good solid lubricant. (102)

Both, boat and chair cyclohexane-like structures are possible, with covalent bonding between fluorine and carbon atoms, see fig.2.34.

The boat structure is favorite, it has an orthorhombic crystal lattice with a= 2.47 Å, b= 4.11 Å, and c= 5.76 Å (103).
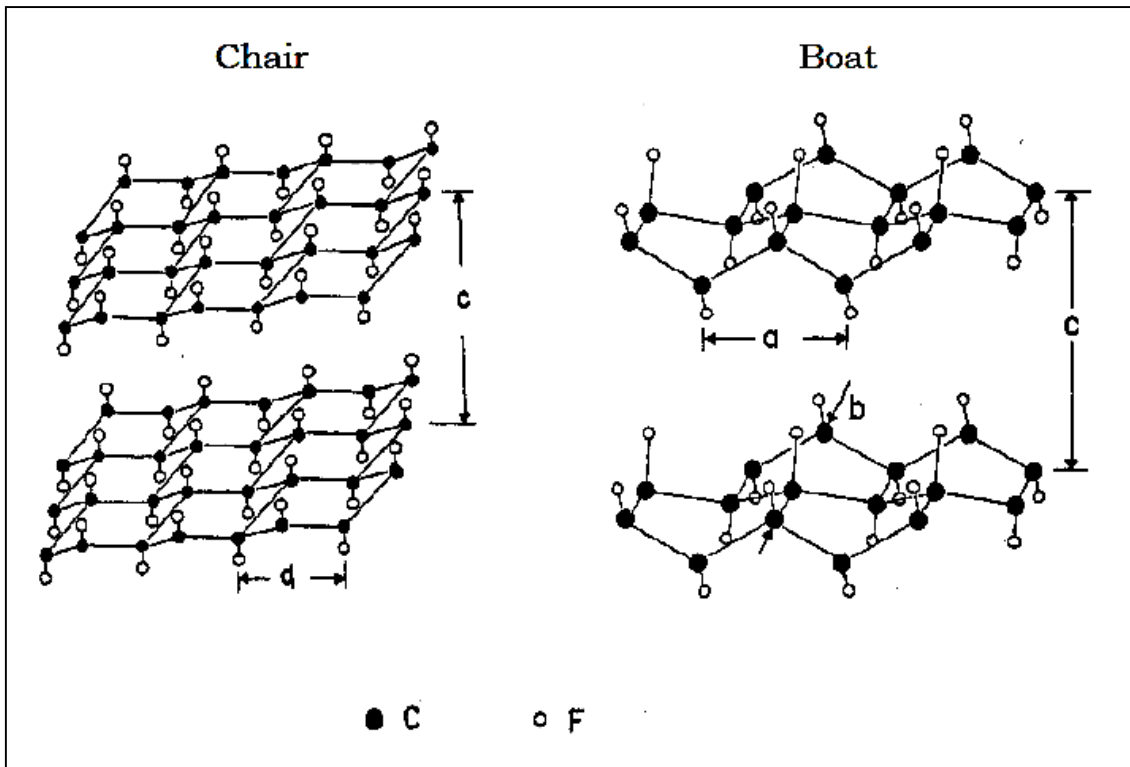
Fig.2.34 Structure of chair and boat (CF$_x$)$_n$. "a", "b", and "c" refer to the unit cell axes. (103)

Graphite fluoride has friction coefficients equal to or lower than MoS$_2$ and graphite (104).
Even if it's not considered suitable for use in heavy load application (105), it can be added in friction materials for low loads noise prevention.

2.4.2   Metal sulfides

Oxidation of metal sulfides starts at 400-500°C, diselenides has a significantly lower oxidation resistance and, from a tribological point of view, ditellurides are not so well-performing.

For this reasons in the group of chalcogenides, metal sulfides are mainly used for friction materials formulation. See tab.2.15

60

Chemical formula (mineral name)	Crystal structure (*H-M*) *Space Group*	Mohs Hard.	Density (g/cm³)	Ionic %	$\Delta_f G^0$ (KJ/mol)	Evaporation – decomposition in inert gas (°C) and melting point (m.p.) (°C)	Temperature of oxidation in Air (°C)
Sb_2S_3 (Stibnite)	Orthorhombic - Dipyramidal *(2/m 2/m 2/m)* *Pbnm*	2	4.63	6	-156	600 546 (m.p.)	380 (Forming of Sb_2O_3) 570 (Forming of Sb_2O_4)
Sb_2O_3 (Senarmontite)	Isometric (Cubic) –Hexoctahedral *(4/m $\bar{3}$ 2/m)* *F d3m*	2-3	5.25	44	N.L.	660 656 (m.p.)	570 (Forming of Sb_2O_4)
Sb_2O_4 (Cervantite)	Orthorhombic - Pyramidal *(mm2)* *Pbn21*	4-5	6.64	44	-706	1150 n.a. (m.p.)	-
MoS_2 (Molybdenite)	Hexagonal - Dihexagonal Dipyramidal. *(6/m 2/m 2/m)* *P 6₃/mmc*	1-1.5	5.06	22	-225.2	950 n.a. (m.p)	450
MoO_3 (Molybdite)	Orthorhombic - Dipyramidal. *(2/m 2/m 2/m)* *Pbnm*	3-4	4.72	63	-666.8	805 795 (m.p.)	-
PbS (Galena)	Isometric (Cubic) –Hexoctahedral *(4/m $\bar{3}$ 2/m)* *F m3m*	2.5-2.75	7.4	12	-92.5	900 1114 (m.p.)	515, 725, 825 Oxidation in 3 steps
PbO (Litharge)	Tetragonal - Ditetragonal Dipyramidal *(4/m 2/m 2/m)* *P 4/nmm*	2	9.24	51	-188.5	1000 890 (m.p.)	-
ZnS (Sphalerite) *with Fe*	Isometric (Cubic) - Hextetrahedral *(4 3m)* *F$\bar{4}$3m*	3.5-4	4.05	9	-196	600 n.a. (m.p)	650
ZnS (Wurtzite) *with Fe*	Hexagonal - Dihexagonal Pyramidal *(6mm)* *P 6₃mc*	3.5-4	4.03	-	-	-	-
ZnO (Zincite) *with Mn*	Hexagonal - Dihexagonal Pyramidal. *(6mm)* *P6₃mc*	4.5-5	5.56	47	-318	1050 n.a. (m.p.)	-
TiS_2	Trigonal *($\bar{3}m$)* *P$\bar{3}$m1*	N.L.	3.22	22	N.L.	200 n.a. (m.p)	280
TiO_2 (Rutile) *(Brookite and Anatase also possible)*	Tetragonal - Ditetragonal Dipyramidal *(4/m 2/m 2/m)* *P 4/mnm*	6-6.5	4.25	63	-888	1100 n.a. (m.p.)	-
SnS (Herzenbergite)	Orthorhombic – Dipyramidal *(2/m 2/m 2/m)* *Pbnm*	2	5.2	9	-99.86	855 850 (m.p.)	700

Chemical formula (mineral name)	Crystal structure (*H-M*) *Space Group*	Mohs Hard.	Density (g/cm³)	Ionic %	$\Delta_f G^0$ (KJ/mol)	Evaporation – decomposition in inert gas (°C) and melting point (m.p.) (°C)	Temperature of oxidation in Air (°C)
SnS₂ (Berndtite)	Trigonal – Hexagonal Scalenohedra *(3 2/m)* *P 3̄m1*	1-2	5	9	-167	710 Forming of SnS and S n.a. (m.p)	470
SnO (Romarchite)	Tetragonal - Ditetragonal Dipyramidal *(4/m 2/m 2/m)* *P 4/nmm*	2-2.5	6.25	47	-256.8	1200 1130 (m.p.)	530 Forming of SnO₂
SnO₂ (Cassiterite)	Tetragonal - Ditetragonal Dipyramidal *(4/m 2/m 2/m)* *P 4/mnm*	6-7	6.85	47	-519.6	1000 n.a. (m.p.)	-
MnS (Alabandite)	Isometric (Cubic) – Hexoctahedral *(4/m 3̄ 2/m)* *F m3m*	3.5-4	3.99	12	-212.2	600 n.a. (m.p)	600
MnO (Manganosite)	Isometric (Cubic) – Hexoctahedral *(4/m 3̄ 2/m)* *F m3m*	5-6	5.18	50	-362	n.a. (m.p.)	-
WS₂ (Tungstenite)	Hexagonal - Dihexagonal Dipyramidal *(6/m 2/m 2/m)* *P 6₃/mmc*	2.5	7.4	18	-193	800 n.a. (m.p)	420
WO₃	Monocline *(2/m)* *P2₁/n*	N.L.	7.16	59	-760	n.a. (m.p.)	-
FeS (Troilite)	Hexagonal - Dihexagonal Dipyramidal *(6/m 2/m 2/m)* *P 6₃/mmc*	3.5-4	4.61	12	-98.4	800 1195 (m.p)	475
FeS₂ (Pyrite) *(Marcasite also possible)*	Isometric (cubic) – Diploidal *(2/m 3̄)* *Pnnm*	6.5	5.01	12	-166.5	420 na (m.p)	400
Fe₂O₃ (Hematite)	Trigonal – Hexagonal Scalenohedral *(3̄ 2/m)* *R 3̄c*	6.5	5.25	51	-740.8	1100 n.a. (m.p.)	-
Bi₂S₃ (Bismuthinite)	Orthorhombic – Dipyramidal *(2/m 2/m 2/m)* *Pbnm*	2	7.0	9	-145.4	700 685 (m.p)	480
Bi₂O₃ (Bismite)	Monoclinic – Prismatic *(2/m)* *P 2₁/c*	4-5	8.93	47	-560	1000 815 (m.p.)	-

Chemical formula (mineral name)	Crystal structure (*H-M*) *Space Group*	Mohs Hard.	Density (g/cm³)	Ionic %	$\Delta_f G^0$ (KJ/mol)	Evaporation – decomposition in inert gas (°C) and melting point (m.p.) (°C)	Temperature of oxidation in Air (°C)
CuS (Covellite)	Hexagonal - Dihexagonal Dipyramidal *(6/m 2/m 2/m)* *P 6₃/mmc*	1.5-2	4.68	6	-48.8	452 (Forming of Cu_2S) n.a. (m.p)	300
CuO (Tenorite)	Monoclinic – Prismatic *(2/m)* *C 2/c*	3.5-4	6.48	44	-137	n.a. (m.p.)	-
Cu₂S (Chalcocite)	Monoclinic – Prismatic *(2/m)* *P 2₁/c*	2.5-3	5.65	6	-90	1100 1085 (m.p.)	400
Cu₂O (Cuprite)	Isometric (cubic) – Hexoctahedral *(4/m 3̄ 2/m)* *P n3m*	3.5-4	6.1	44	-148.8	> 1200 1230 (m.p.)	450 (Forming of CuO)
CuFeS₂ (Chalcopyrite)	Tetragonal – Scalenohedra *(4̄ 2m)* *I 4̄ 2d*	3.5	4.19	10	N.L.	450 n.a. (m.p)	450
CuFeO₂ (Delafossite)	Trigonal – Hexagonal Scalenohedral *(3̄ 2/m)* *R 3̄ m*	5.5	5.4	47	N.L.	700 n.a. (m.p.)	700 (Forming of CuO and CuFe₂O₃)

Tab.2.15 Typical metal sulfides used as solid lubricants in friction materials with associated metal oxides (106).

Some sulfides show lubricant properties according to their lamellar lattice structure, others sulfides, like those with hexagonal structure, can easily slip along the close-packed planes. As reported in tab.2.15, oxides are thermodynamically more stable than sulfides, starting oxidation temperature and properties of formed oxides at brake operating temperatures should be considered in raw materials selection.

Beside lubrication mechanism, a good adhesion between sulfides and cast iron can be required; when iron and sulfides in air are in contact under load and temperature different reaction are possible depending on their reaction Gibbs free energy . For example when zinc sulfide is in contact with iron in presence of oxygen and water vapor different phases can be formed at the equilibrium like (in order of reaction energy from low to high) iron oxides, FeO(OH), zinc oxide, iron hydroxides iron sulfides and intermetallic compound of Fe-Zn (107). A good adhesion is done through the reaction between iron and sulfur at interface, but the reaction is competitive with others. The higher is the metal sulfide formation Gibbs free energy ΔG_f the better is for adhesion, when a metal sulfide has a ΔG_f lower than iron

sulfide there is no interaction with iron unless secondary reaction reduce sulfur to atomic form.

In opportune conditions, e.g. at high temperatures, sulfuration is possible also on iron of steel fibers, the reaction transforms fibers in powder reducing the fiber reinforcement effect to the matrix.

Some metal sulfides, like lead and antimony sulfides, are nowadays avoided for potential health hazards or environmental issues. Historically speaking they were largely used due to the lubricant effect of their oxides at high temperatures (108), moreover stibnite has a relative low melting point, around 500°C, that lead to the formation of a soft film on the surface providing exceptional tribological properties. Other sulfides will be replaced or strongly limited in future, like copper containing sulfides, due to new international regulations on copper content in brake pads.

To replace forbidden sulfides, synthetic multiphase metal sulfides have been developed, with formula:

$$M_l^1 M_m^2 M_n^3 S_x$$
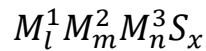
Where M^1, M^2 and M^3 are Ti, V, Mn, Fe, Cu, Zn, Mo, W, Sb, Sn or Bi with l=1-5, m=1-5, n=0-5 and x=2-8.

They are produced by heating metal powder with a source of sulfur, like S, polysulfides, ammonium sulfide or hydrogen sulfide according to wet or dry chemical methods. (109)

2.4.2.1 Molybdenum disulfide

Graphite and molybdenum disulfide are the widely used material as solid lubricants (78), as an example of sulfides layered structures it's interesting to see MoS_2 molecular structure. MoS_2 has two possible crystal forms: hexagonal and rhombohedral. The hexagonal system has the same crystal group of hexagonal graphite $P6_3/mmc$, see fig.2.35
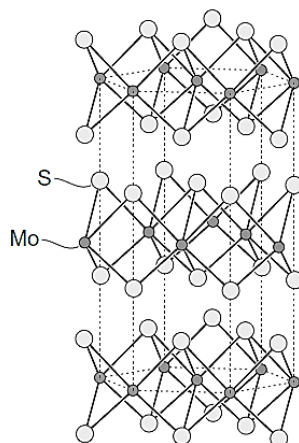
Fig.2.35 Cristal structure of molybdenum disulfide (73).

As for graphite weak Van der Waals forces give rise to inter-lamellar mechanical weakness and hence easy shear (slip) between the planes and is the main responsible for lubricant behavior.
For this reason, orientation of basal plane in sulfides grain is fundamental for good lubrication, lower friction coefficient is achieved when basal plane is parallel to the sliding surfaces.

Running-in phase promotes the mechanism of sulfide transfer at brake disc-pad interface and a basal plane re-orientation, moreover under load an amorphous to crystalline structure transformation is possible as shown in fig.2.36
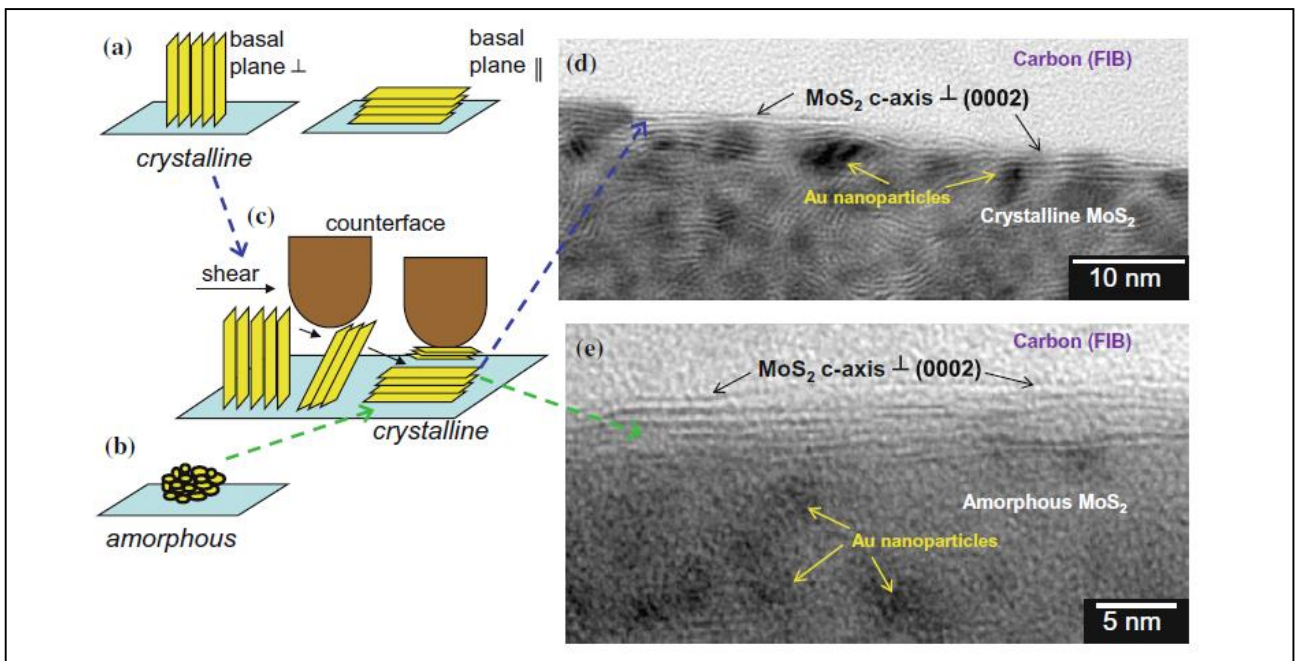

Fig.2.36 (a) → (c) Reorientation of MoS$_2$ basal plane due to the friction force. (b) → (c) Amorphous to crystalline structure transformation. (d) TEM images inside the wear track of d crystalline MoS2/Au coating (1000 sliding cycles, Pm = 0.3 GPa), and (e) amorphous MoS2/Sb2O3/Au coating (10,000 sliding cycles Pm = 0.7 GPa)

Contrary to graphite, it's been shown that the friction coefficient decreases when condensable vapors are removed from the atmosphere, see fig.2.37, indeed water penetrating in MoS2 layers increasing their shear strength (110).

Reduction of moisture content in MoS$_2$ can explain the reduction of friction coefficient increasing temperature, loads or sliding speeds, indeed the same friction coefficient variation is not registered if tests are conducted in dry condition (111).
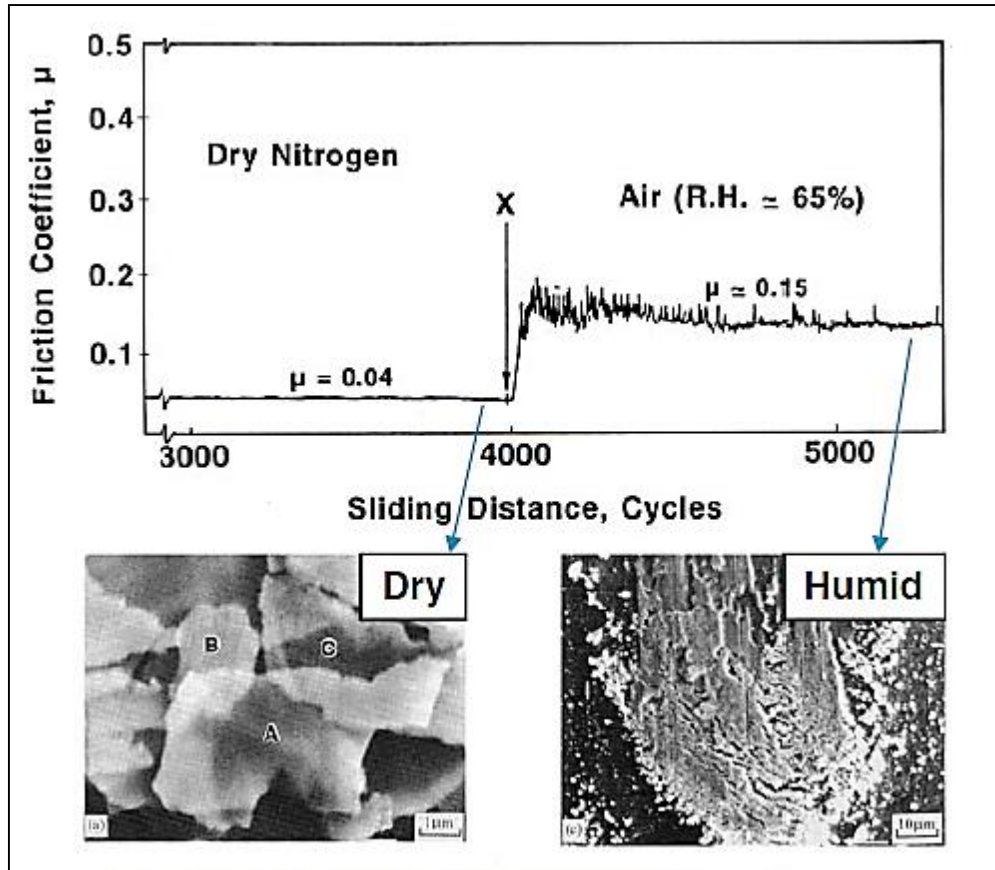
Fig.2.37 Variation in friction coefficient of MoS$_2$ from dry nitrogen to air 65% relative humidity and wear tracks on 440C SS counterface. (110)

Molybdenum disulfide is one of the best performing solid lubricants for friction materials but fluctuation related to molybdenum cost should be considered in raw materials selection.

2.4.2.2   *Metal sulfides in brake pads*

Sulfides can be commercialized standalone or multiphase, mix of tin sulfides SnS and SnS$_2$ is a well-known example.

Some modification on chemical composition can be done to improve the sulfides lubricant effect; carbon and sulfides can be intrinsically embedded reacting carbon, metal and an excess of sulfur, premixed at temperature up to 1500°C; phosphates and other sulfides can be also added as process aids. As already mentioned due to environmental issues antimony sulfides have to be substituted; comparing a brake pad where antimony sulfide is substituted 1:1 with carbon-sulfides mix, a wear reduction of 40% has been measured on brake pads till 400°C. (112)

Another strategy in sulfide based lubrication is to use a cheap material like FeS blended with metals, e.g. tin, that can exchange with Fe in sulfide structure during the brake, generating metal sulfide *in-situ*. (113)

It must be stressed the fact that it doesn't exist one lubricant which fulfill all the requirements for a friction material, combination of two or more lubricants is commonly used, this can generate a non-linear synergic effect on friction coefficient. As example a combination of graphite and MoS_2 is shown in fig.2.37 (114)

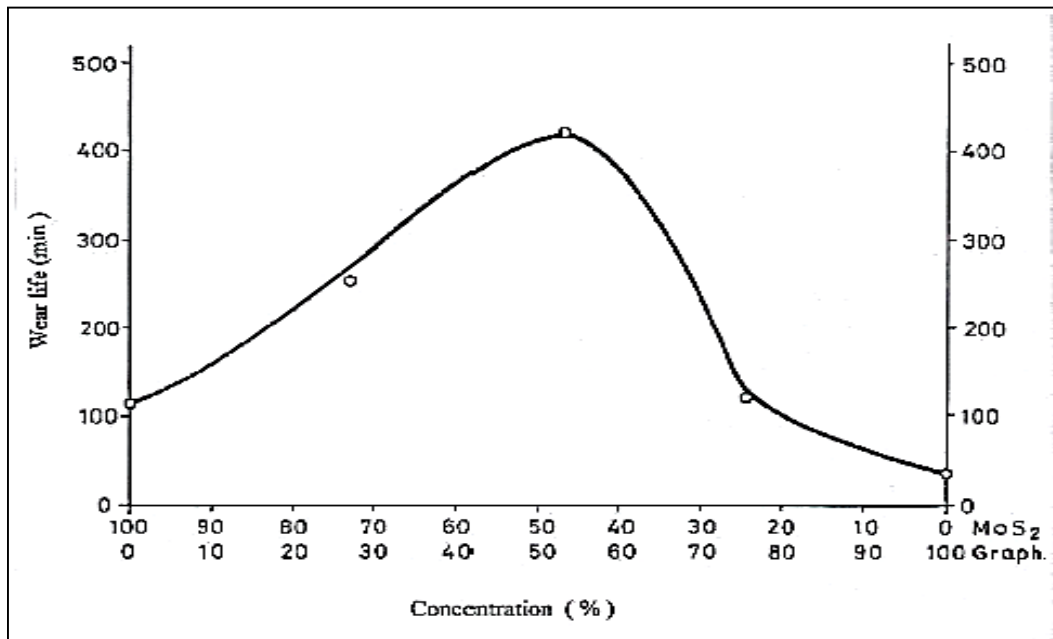**Fig.2.38 Recording of wear life of a composite containing graphite and molybdenum disulfide at various ratios** (114)

Even if MoS_2 is more efficient in lubrication respect graphite it suffer a so called blistering failure mechanism, see fig.2.39 due to low lamella distortion resistance and to oxidative crinkling of molybdenum disulfide.
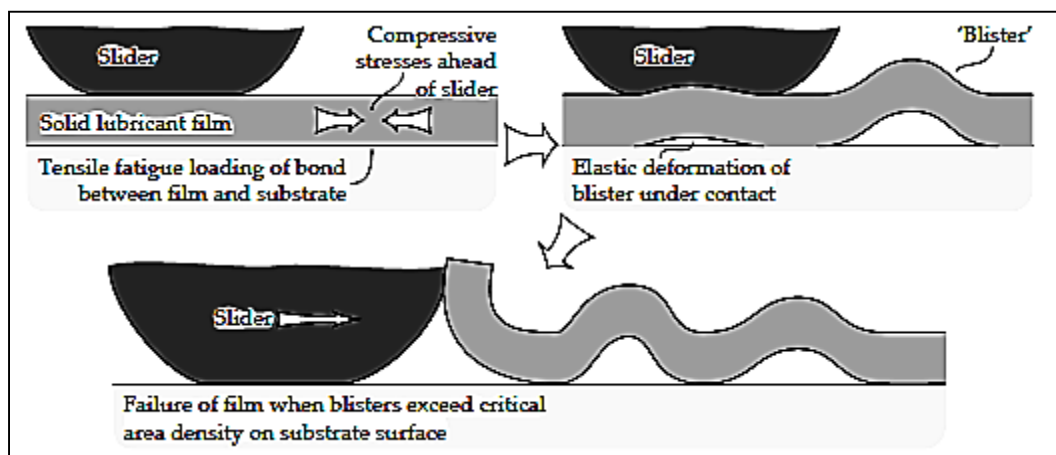

Fig.2.39 Tribofilm blistering failure mechanism (110).

The graphite due to its high lamella distortion resistance suppresses the effect of blistering mechanism and increases wear resistance, moreover, even if graphite are more thermally stable, it can in part act as oxygen scavenger protecting molybdenum disulfide from oxidation (110).

Not every layered material is suitable for lubrication in friction materials, some of them are load sensitive, some temperature sensitive. Talc, for example, has a Monoclinic - Prismatic layered structure (space group $C\,2/c$), but over 100°C gradually lose his lubricating power, see fig.2.39
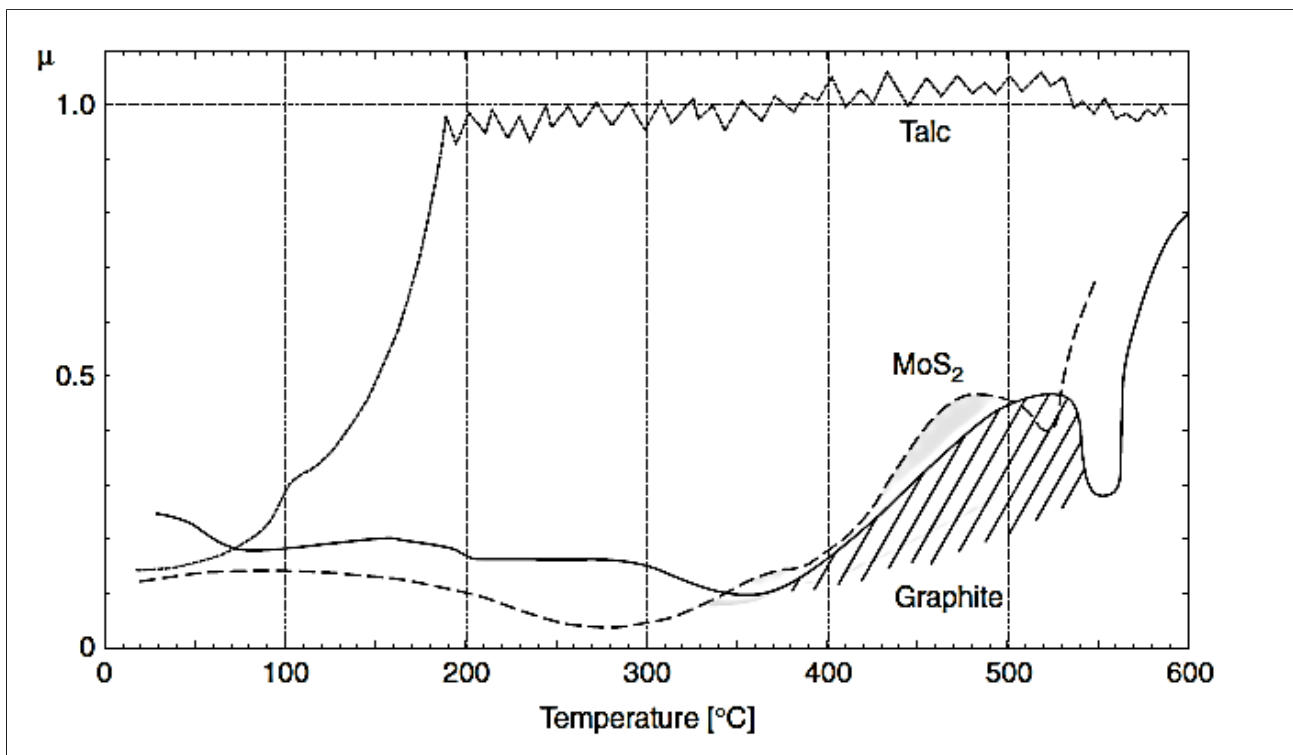
Fig.2.39 Coefficient of friction vs. temperature for graphite, talc, and molybdenum disulfide (73)

2.4.3   Hexagonal boron nitride

Unlike abrasive boron nitride with cubic lattice hexagonal, layered boron nitride (h-BN, α-BN, g-BN or graphitic BN) has the same space group of graphite and MoS_2 ($P6_3/mmc$), see fig.2.40, recently it has been considered as a possible component for friction materials. BN lubrication mechanism follows the same rules for other layered material, with week Van der Waals bonding between basal planes
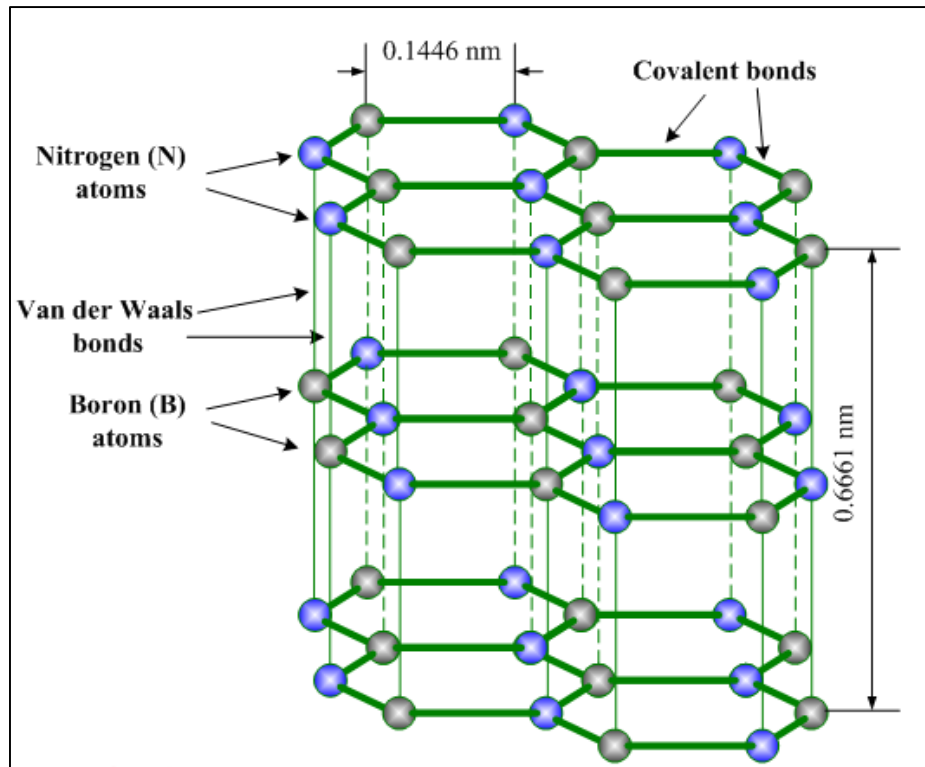
Fig.2.40 Cell crystal lattice of hexagonal boron nitride (83)

h-BN is very stable in oxidizing atmosphere (up to 870°C) chemically inert to most acids, alkalis and solvents and provides good adhesion to metal surfaces. It has been proved to be a good candidate as lubricant substitute of metal sulfides (115).

2.4.4   Fluorides

2.4.4.1   Organic fluorides
Considering lubricant organic fluorides, polytetrafluoroethylene is the most important, see fig.2.41

TFE
tetrafluoroethene

PTFE
Polytetrafluoroethilene
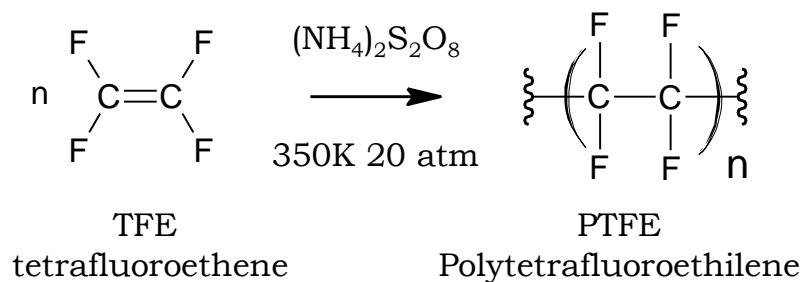
Fig.2.41 PTFE synthesis from TFE

Four different crystalline phase of PTFE are possible depending on temperature and pressure (116), see fig.2.42
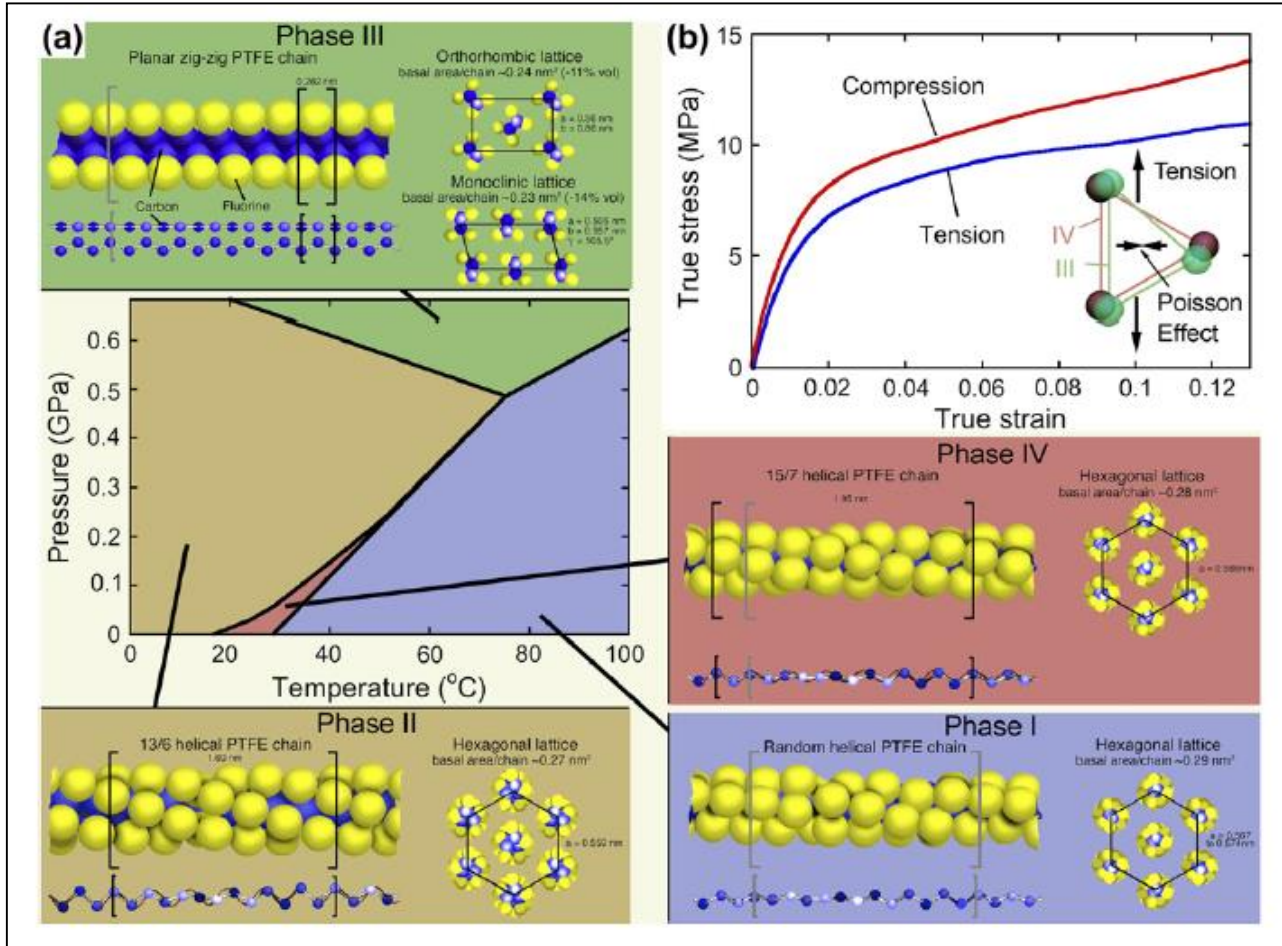
Fig.2.42 Hydrostatic and uniaxial PTFE structural responses. (a) Temperature - pressure phase behavior of crystalline PTFE with the inter- and intra-polymer chain crystalline structures. (b) Bulk stress-strain response of PTFE at ambient temperature and pressure (116).

At different conditions in a friction material Phase I, II and IV are involved, moreover an additional phase transformation occurs at 150°C (1 bar) where the trans conformation 15_7 helix became gauche (117) (118) , see tab.2.16

Phase	Temperature (°C)	Molecular conformation	Crystal system Space Group	Unit cell constants
II	<19	13_6 helix	Triclinic Pseudohexagonal	a=b=5.54 c=16.8 γ=119.5
				a=b=5.59 c=16.88 γ=119.3
			Triclinic	a=4.882 b=4.875 c=5.105 α=90 β=86-87 γ=86-87
			Monoclinic P2$_1$	a=5.59 b=9.76 c=16.88 β=90
		54_{25} helix	Monoclinic	a=9.6 b=5.62 γ'=91.4
IV	>19,<30	15_7 helix	Hexagonal P3$_1$	a=b=5.66 c=19.50
		15_7 helix, left and right handed	Triclinic	a=11.02 b=11.42 γ=121
I	>30, <150	Disordered 15_7 helix	-	-
	>150	Excitation from trans to gauche conformation in the disordered15_7 helix	-	-

Tab.2.16 Structural details of the thermally activated phases of PTFE from different studies (118) (13_6 helix is a twisted zigzag arrangement, the twist being 180° after every 13 –CF$_2$-units which form the repeat unit)

There is a great debate about lubrication mechanisms of PTFE (119), that, in part, it is not well understood. PTFE friction coefficient can change from 0.05 to 0.3 depending on sliding speed, it decreases with contact pressure and it suffers high wear (116).

Low friction coefficient at low speed can be explained by a crystal lattice deformation along prismatic planes by shearing; temperature and pressure, modifying the PTFE crystal phases and dimension, can influence the deformation mechanism. Low friction coefficient has been also associated to the smooth profile of stiff rod-like molecules.

At high speed, plasticization of the surface is not enough fast, so friction coefficient increases.

Regarding high wear rate, two factors have to be taken in account:

- Initial removal from sliding PTFE (primary wear).

- Secondary removal from transferred film (secondary wear).

As seen PTFE has a low wettability, adhesion between fluorinate molecules and metals is not very high, only week Van der Waals bonding can be established. This means that during running in process, to prevent a failure of friction layer, new matter is drawn out from the PTFE rider surface to substitute fast worn transferred film causing an high wear rate.

Reducing PTFE particles size increases the residence time of debris on the surface, indeed higher specific surface area can lead an easier polymer degradation by oxidation improving adhesion and reducing secondary wear. (119)

2.4.4.2   *Inorganic Fluorides*

Friction materials, on contact with disc, can locally reach temperature above 1000°C , this decrease the lubricant action first drying graphite and then oxidizing lubricant components. As already described organic fluorides and sulfides can't be used for temperature above 400-500°C.

Some metal fluorides from alkali or alkaline-earth groups (LiF, CaF_2, BaF_2, NaF), from rare earth elements (LaF_3, CeF_3) and their combination have lubricant action at temperature above 500°C (120).

Calcium fluoride (sometimes mixed with barium fluoride) is the main used inorganic fluoride as lubricant for friction materials, it has an isometric (cubic)-hexoctahedra crystal system and space group *F m3m.*

Some studies have been carried on CaF_2 behavior at different temperatures, see fig.2.43
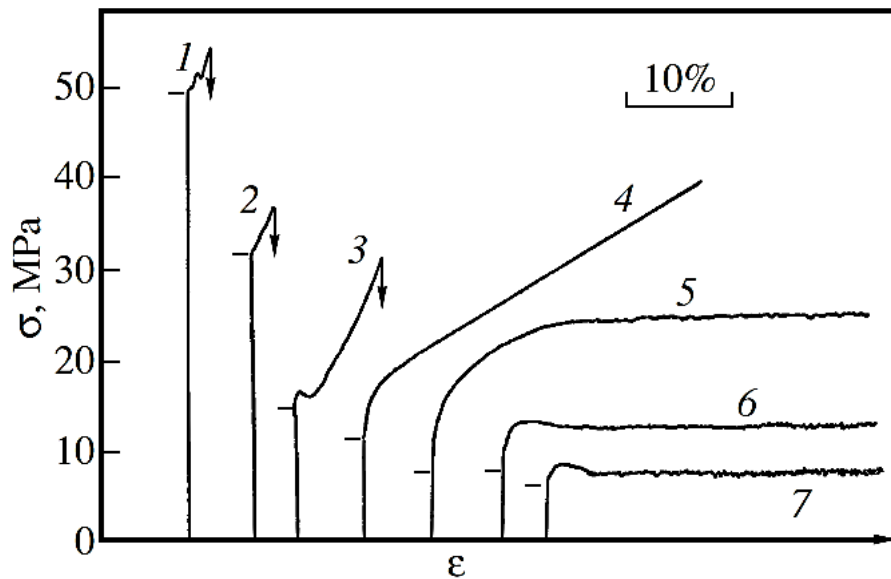
Fig.2.43 Compressive-stress–strain curves for CaF$_2$ single crystals at temperatures of (1) 100, (2) 200, (3) 300, (4) 400, (5) 600, (6) 800, and (7) 980°C. The scale of the total average strain ε is shown. σ is the applied stress (121).

At room temperature calcium fluoride it's a brittle material with conchoidal fracture type, but at T>400°C it shows plastic deformation, different mechanisms have been proposed to explain this behavior (121):

1) Dislocation motion
2) Fast autocatalytic process of dislocation multiplication and formation of non-equilibrium point defects (vacancies)
3) Correlated motion of large groups of dislocations and self-organization of an ensemble of micro-shears
4) Dramatic softening and the occurrence of θ-type instability
5) Deformation stratification and the formation of enlarged rough slip bands
6) Ductile fracture.

Purity of fluorides and more generally of ore minerals, is an important parameter to keep under control. Calcium fluorite for example is available in three main grades, metallurgical grade with CaF$_2$<85%, ceramic grade 85%≤CaF$_2$<97% and acid grade CaF$_2$≥97%

2.4.5   Metals and metal oxides

Metals can be used as lubricant through soft film mechanism.

Mechanical hardness and compatibility with cast iron elements are fundamental parameters to select metals as lubricant for friction materials. The better the reactivity with oxygen the stronger is the adhesion with oxides on brake disc surface, therefore oxidation resistance and relative metal oxide hardness should be considered.

For example, copper and copper alloys have been largely used in friction material. They provide ductility to friction layer and enhance friction material thermal conductivity and generated oxides are not so abrasives (122) (123).

Copper will be strongly limited by law in future, copper replacement in friction materials is ongoing (124).

A general rule to select metal oxides as lubricant for high temperatures is to find the relationship between friction coefficients, hardness and ionic potentials, see fig.2.44
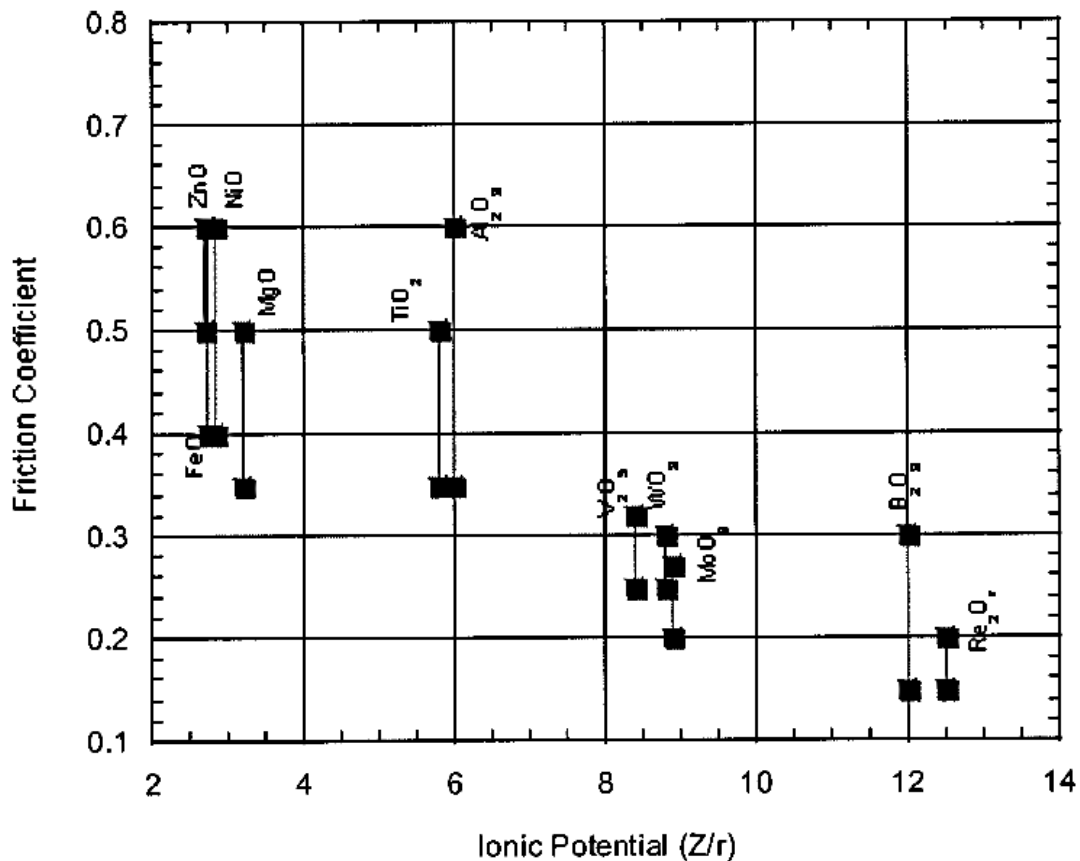
Fig.2.44 Metal ionic potential vs. friction coefficient of some oxides considering different literature data (125)

As for abrasives, hardness is not the only parameter to consider on solid cohesion. Lubricant efficiency of metals oxides is generally dependent not only on hardness but also on melting point.

To reduce oxide melting point and relative friction coefficient, a mix of them can be used, see fig.2.45
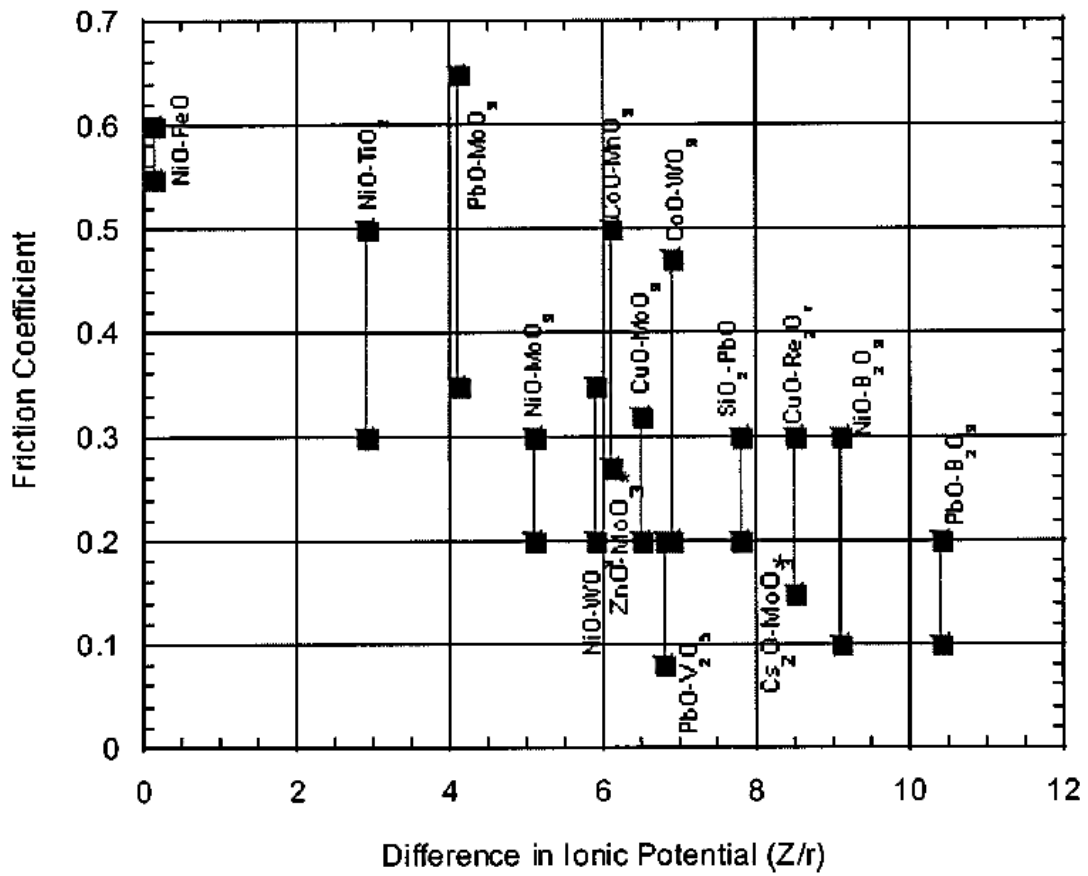
Fig.2.45 Metal ionic potential vs. friction coefficient of some binary oxides considering different literature data (125)

Most of soft metal oxides, e.g. lead, antimony, boron, arsenic oxides etc., are banned from friction materials due to their toxicity.

2.5 Reinforcements

The main contribution of reinforcements to friction material are:

- Wear minimization
- Wear stabilization at any operating condition, e.g. different speed, temperature (low fade), pressure, braking duration
- High and stable friction coefficient
- Increasing mechanical strength, improving stability of brake pad edges and increasing fracture toughness
- Dimensional stability

As showed in fig.2.46 in composite materials different additive shape can be used as reinforcements.
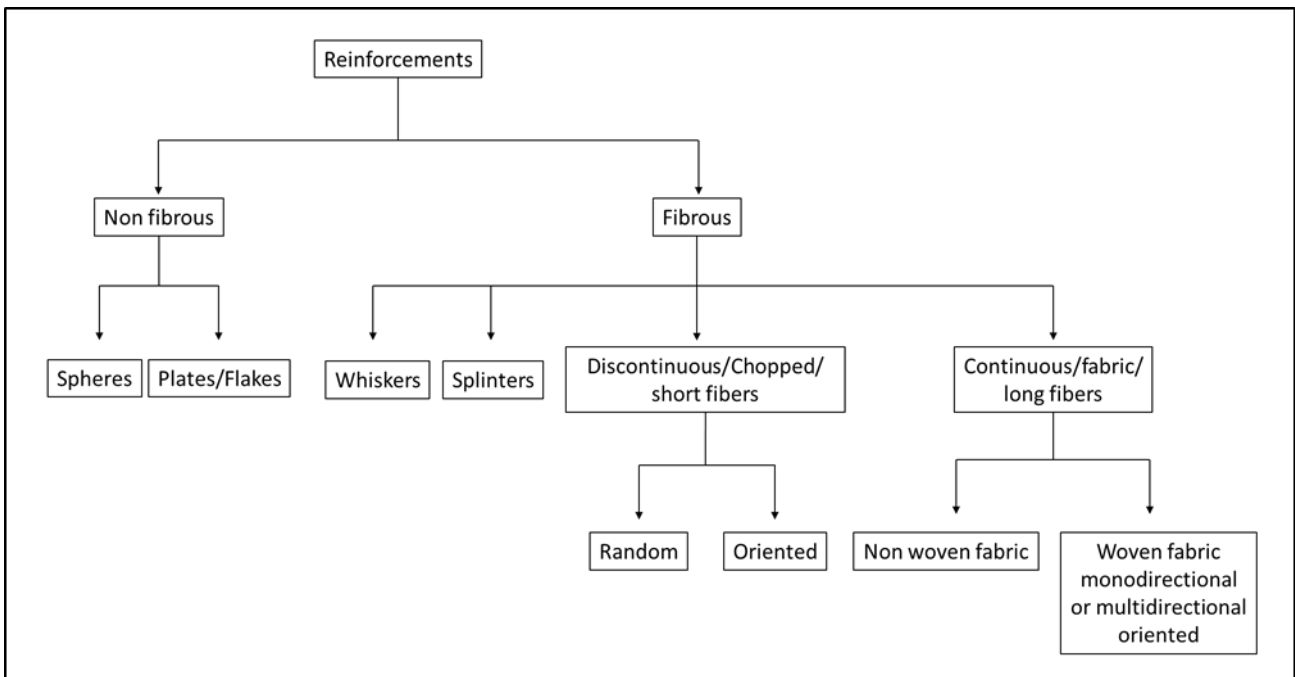
Fig.2.46 Typical reinforcements for thermoplastic and thermosetting matrices, adapted from (126)

2.5.1   Fibrous reinforcements

Someone choose to define a fibre (BrE) or fiber (AmE) as an object with an aspect ratio of three or greater (127), but following this definition many crystalline substances can be classified as fibers, so other authors prefer to use an aspect ratio greater than ten (126). In addition, for our purpose only, it can be arbitrarily defined as an object having a maximum diameter no greater than 1 mm, where: when the diameter is greater than 200 μm is generally known as rod, when it is from 100 to 200 μm is known as very large diameter structural fiber, when it is

from 1 to 25 μm is known as microfiber and when it is from 1to 100 nm is known as nanofiber (128). Diameter is of critical importance in regard to the tensile strength, indeed all materials showing brittle fracture increase in strength as the diameter decrease. To obtain an higher cross section without increase fiber diameter, it's possible to group filaments in bundle with a sizer. Then it's possible to obtain a chopped bundle of short fibers, chopped woven fabric, chopped fiber tow or chopped roving.

Regarding fibrous reinforcements mechanism it's important to analyze the fiber-matrix interface where the load is transferred. Applied stress on composite material is transferred from matrix to fiber, the higher is the fiber aspect ratio, the higher is the load contact from matrix and fiber following eq.2.22

$$\sigma_f = \frac{2\tau l}{r} + \sigma_m$$

Eq.2.22

Where σ_f is the contact stress, l is the length and r the radius of fibers considered circular cylinder, τ is the tangential stress and σ_m is the compressive stress due to the load applied on composite. (129)
In a polymer-fiber composite, as occur in friction material, critical strain of fiber is lower than the one of matrix, when a critical stress is applied fibers can be broken or pulled out from the matrix as shown in fig.2.47.
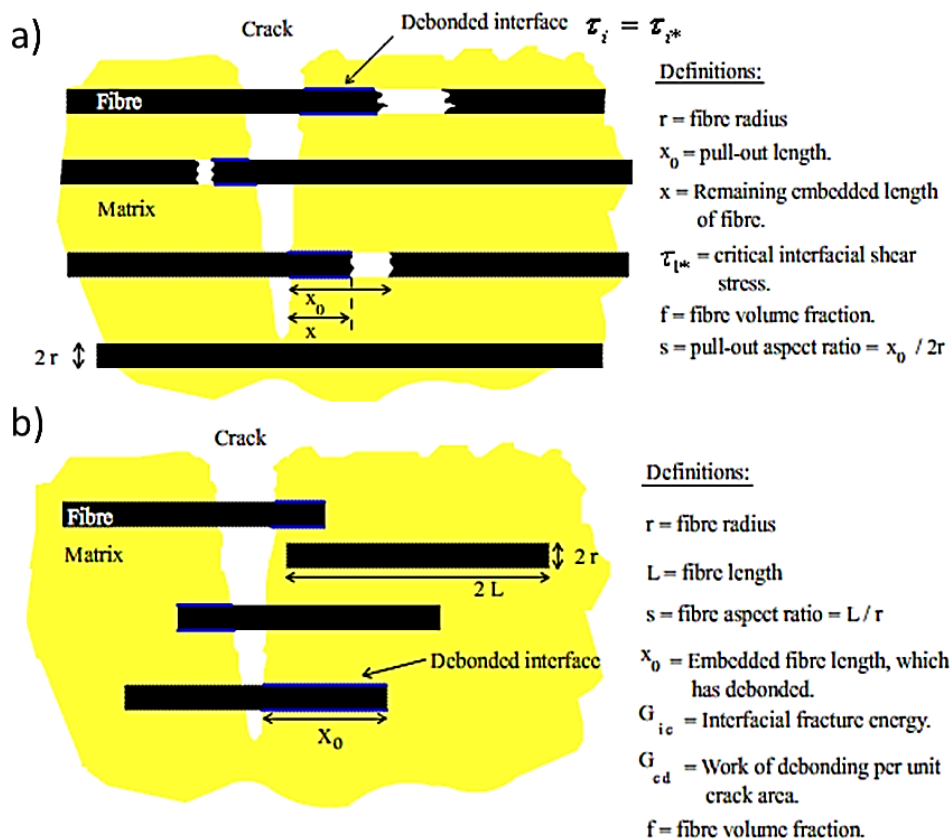

Fig.2.47 a) matrix-fibers partial debonding after fibers brake. b) matrix-fibers interfacial debonding before fiber brake (130)

Critical fiber length depend on good adhesion between fibers and matrix and it's the minimum length where fibers start to brake or, equivalently, the maximum length where fibers are capable of maintaining its integrity, debonding from matrix. High aspect ratio and few fibers ends lead to have for long/continuous fibers a better impact resistance and higher stiffness better dimensional stability and enhanced creep and fatigue resistance, however the use of short fibers is recommended for the lower cost of composite manufacturing. Fibers normal oriented to sliding surface provide the best reinforcements in friction materials; introduction of short fibers random mixed, even if slightly orientated in a undesirable direction during press molding, it's in any case effective.

Fibers can be chemically divide in two classes: amorphous and crystalline fibers, when a fiber is made of a single crystal it's called whisker. Each group can be divided in four classes: natural mineral, synthetic inorganic or man-made inorganic (sometime referred improperly as mineral), natural organic and synthetic organic or man-made organic fibers.

In the past asbestos fibers serpentine and amphibole forms were widely used in friction material formulation due to their optimum properties in term of chemical and thermal stability and good improvement in wear resistance. Asbestos is proposed in two forms (131):

- A long, curly and pliable serpentine form.
  Crysotile (white asbestos) $[Mg_3Si_2O_5(OH)_4]_n$,

- A short, straight, and stiff amphibols form.
  Amosite (brown asbestos) $[(Fe^{2+})_7Si_8O_{22}(OH)_2]_n$,
  Crocidolite (blue asbestos) $[NaFe_3^{2+}Fe_2^{3+}Si_8O_{22}(OH)_2]_n$,
  Anthophyllite (azbolen asbestos) $[(Mg)_7Si_8O_{22}(OH)_2]_n$,
  Actinolite $[Ca_2(Mg,Fe^{2+})_5Si_8O_{22}(OH)_2]_n$
  Tremolite $[Ca_2Mg_5Si_8O_{22}(OH)_2]_n$

When fibers are breath and reach lungs different effects can be found: effusions; plaques, local areas of fibrosis of the parietal pleura, diffuse pleural fibrosis, extensive visceral pleural fibrosis, often with fusion of both pleural surfaces and rounded atelectasis that occurs when an area of visceral pleural fibrosis extends into the parenchyma and renders a portion of the lung airless.
Even if chrysotile fibers are less harmful than amphiboles, both increase the incidence of malignant mesothelioma and occasionally the peritoneum after exposure (132).
Due to its health hazards, asbestos replacement was one of the main activities on friction compounds, mineral and synthetic fibers have to demonstrate the non-toxicity in term of human health to be used for current friction material formulation. To complete replace all properties of asbestos a mix of different fibers is generally required.

2.5.2   Non fibrous reinforcements

Materials with different shape, like particles, sphere, plates and flakes, can be used as reinforce for friction material.

Assuming that reinforcements have better mechanical properties respect to the polymeric matrix, the main difference from non-reinforcing and reinforcing fillers is that the latter increase mechanical performance of composite material respect the matrix alone in terms of toughness and strengthens. (133)

Considering that adhesion between filler and matrix is the key point of load transfer, compatibility of materials and actual contact area are parameters to determinate if the filler is reinforcing or non-reinforcing. The lower the particles size the higher the interface extension, moreover the smaller the particles the higher is the particle fracture energy; for this reason, usually, big particles are considered non-reinforcing. (134)

Particles and microspheres have no orientation effect providing isotropic properties to the compound, the lesser reinforcement compared to fibers due to the unitary aspect ratio is compensated introducing an higher filler fraction.

Plates and flakes guarantee a reinforce action on two directions and space orientation of 2D structure is fundamental to determinate the reinforcement effect.

2.6 Reinforcements (raw materials)

2.6.1   Synthetic organic fibers

Low weight, good strength and toughness are the most prominent features of these fibers.

Since there are many polymers available, continuous operation temperature resistance should be considered on raw material choice. Low melting point thermoplastic polymers like polyethylene, polypropylene, polylactide, polyvinyl alcohol etc. have been also used but effective at low temperature only. On the contrary thermoset polymer fibers and some high melting point thermoplastic are commonly used for high performance friction materials formulation.

2.6.1.1   Aramid fibers
Para-aramid polymer, see fig.2.48, it's commonly used in friction material due to its good stiffness-weight ratio, high thermal stability and good wear resistance (135).
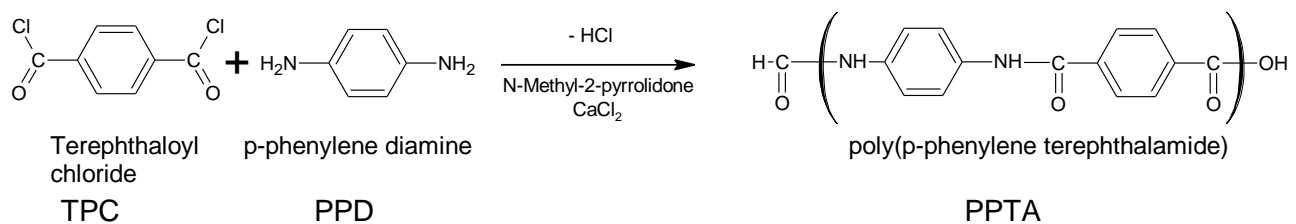
Fig.2.48 Synthesis of PPTA a para-aramid polymer used to produce aramid fibers

Different morphology of aramid fiber can be used, but generally it's added on friction materials in a fibrillated form called pulp.

Fibrillated fibers are fibers longitudinally partially split in thinner fibrils as showed in fig.2.49 this guarantee respect a non-fibrillated fiber of same aspect ratio and diameter a lower bulk density an higher matrix to fiber coupling area. Fibrillation is useful to binds dust, helps guarantee a homogenous mixture, and prevents segregation in production, the degree of fibrillation is the average of effective number of fibrils into which a typical fiber is split.
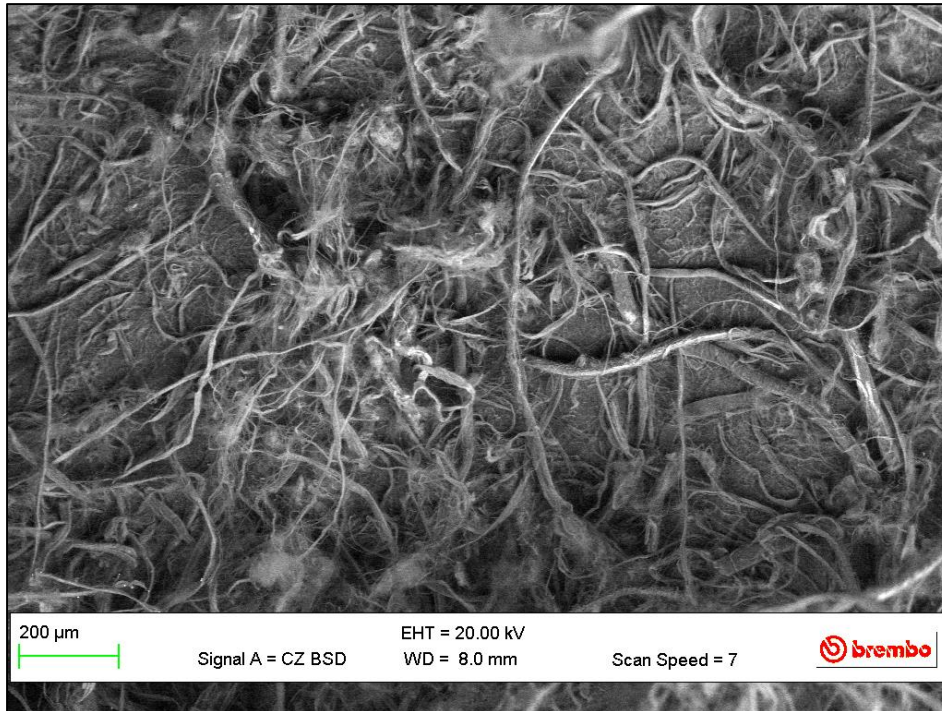
Fig.2.49 SEM image of fibrillated aramid pulp

Besides general request for reinforcements, aramid fibers lend other properties to friction material:

- Reduced noise, judder, fading and vibration
- Less corrosion respect to metallic fibers
- Low specific weight
- Increase of porosity
- Improved pre-form stability (green strength) for cold pre-pressing
- Low thermal conductivity

Improving the tear strength of fiber-reinforced rubber compounds, fibrillated aramid fiber is often used in rubber premix, moreover many synergistic effect with other fibers was reported.

Critical points of aramid fibers are low resistance to compression and high sensitivity to moisture.

2.6.1.2   *Polyacrylonitrile*
Polyacrylonitrile (PAN) fibers can be used in friction materials by itself or as precursor of oxidized and thermally stabilized polyacrylonitrile OPAN (sometime referred as PANOX™), see fig.2.50
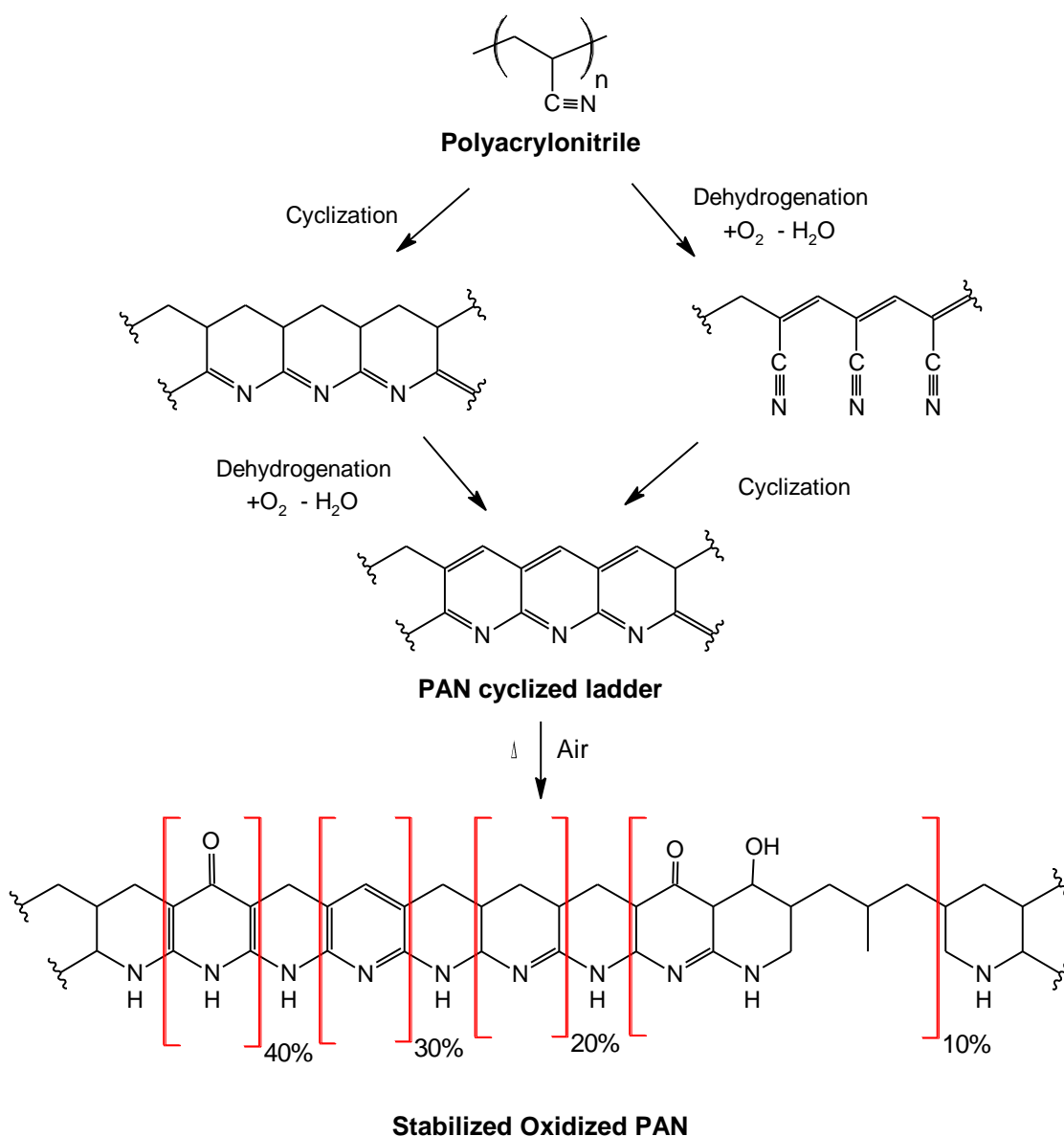
Fig.2.50 Proposed structures of oxidized polyacrylonitrile (OPAN) by oxidation of polyacrylonitrile (PAN). PAN cyclized latter is synthetized by a dehydrogenation and cyclization of PAN. (136)

The presence of oxygen promote the dehydrogenation of structures by elimination of water. Thermal stabilized PAN cyclized ladder is one of precursor of carbon fibers.

PAN is a thermoplastic material, an oxidation treatment is necessary to make it infusible, in this phase different structures can be generate containing bridging ether links, carbonyl groups, and those in which each nitrogen atom donates its lone pair of electron to an oxygen. OPAN respect PAN does not burn, melt, soften or drip. The increase of limiting oxygen index (LOI) over 50% due to its capability to thermally decompose forming an expanded foam which fill voids and cracks and preventing gas transfer, it's a property used in flame retardant compound. In friction materials this property can affect temperature fading resistance of leading a lower friction coefficient at high temperature compared to materials reinforced with aramid fibers. (137)

As for aramid acrylonitrile based fibers can be used fibrillated in pulp form. (136)

2.6.2 Natural organic fibers

There are many products derived from vegetable source such as seed hair, bast fibers, and leaf fibers, many of them were used for plastic composites such as cotton, kapok, wood flour/fiber, jute, sisal, abaca, pineapple, sunhemp, oil palm, kenaf, coir, banana, flax, wheat straw, bamboo.

Generally a natural fiber is composed by crystalline cellulose micro-fibrils in an amorphous matrix of lignin and hemicellulose, see fig.2.51
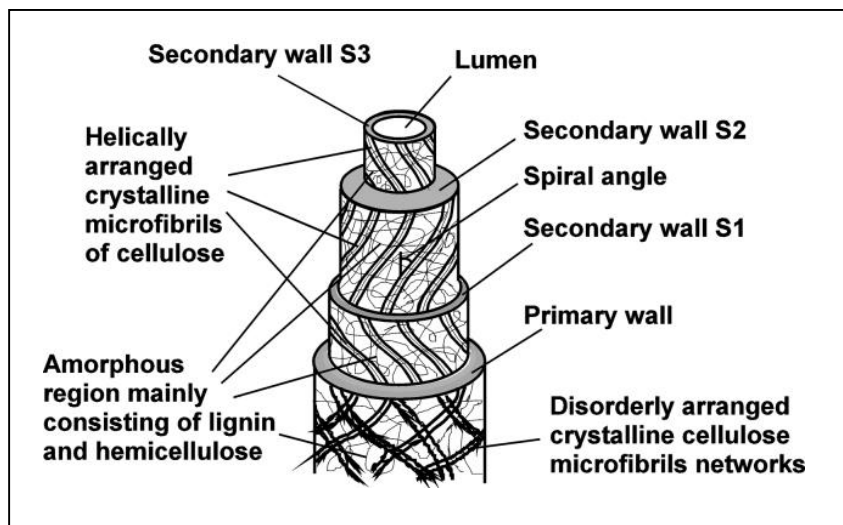
Fig.2.51 Structural constitution of a natural vegetable fiber cell. (90)

Thermogravimetric analysis demonstrated that thermal degradation of natural fibers evolve in two steps, in the range 220–280°C there is the degradation of hemicellulose and at 280–300°C the degradation of lignin; low thermal resistance is evident if compared to a synthetic organic fiber, such as aramid fiber, where the thermal degradation start at temperature over 400°C.

High modulus/specific gravity ratio, low cost and renewable source are the strong points of this fibers, instead low thermal resistance and variable mechanical properties depending on moisture content are the weak points. Compatibilizers or surface treatments can be used to increase adhesion between fiber and polymeric matrix. (138) (139)

Besides general request for reinforcements, natural organic fibers lends other properties to friction materials (140):

- Aid mixing and dispersion of raw materials
- Low specific weight
- Noise and judder reduction
- Bio-degradable
- Low cost

It has been demonstrated good efficiency in term of wear reduction and friction coefficient stabilization in friction materials natural organic fibers reinforcements, but their real limit is the loss of mechanical properties for thermal fading at temperatures over 300°C (141) (142) (143). Over this temperature cellulose fibers, can be used as pore generator, indeed, polymer degradation lead the formation of cavity permitting at generating gas to escape from inner and contrasting temperature fade effect and imparting friction stability.

Some patents has been made on friction materials based also on animal fibers based on hydroxyproline (144) or α-keratinous fibers but are not commonly used.

2.6.3   Inorganic fibers

Inorganic fibers can be divide in man-made and natural fibers as described fin fig.2.52

Fig.2.52 Inorganic fibers taxonomy adapted from (145)

A large number of ceramic fibers are available on the market, here are review the most used for friction material.

2.6.3.1   Metal fibers

Short metal fibers have been widely used in friction material formulation due to their good strength, toughness and thermal diffusivity. As already described in lubricant chapt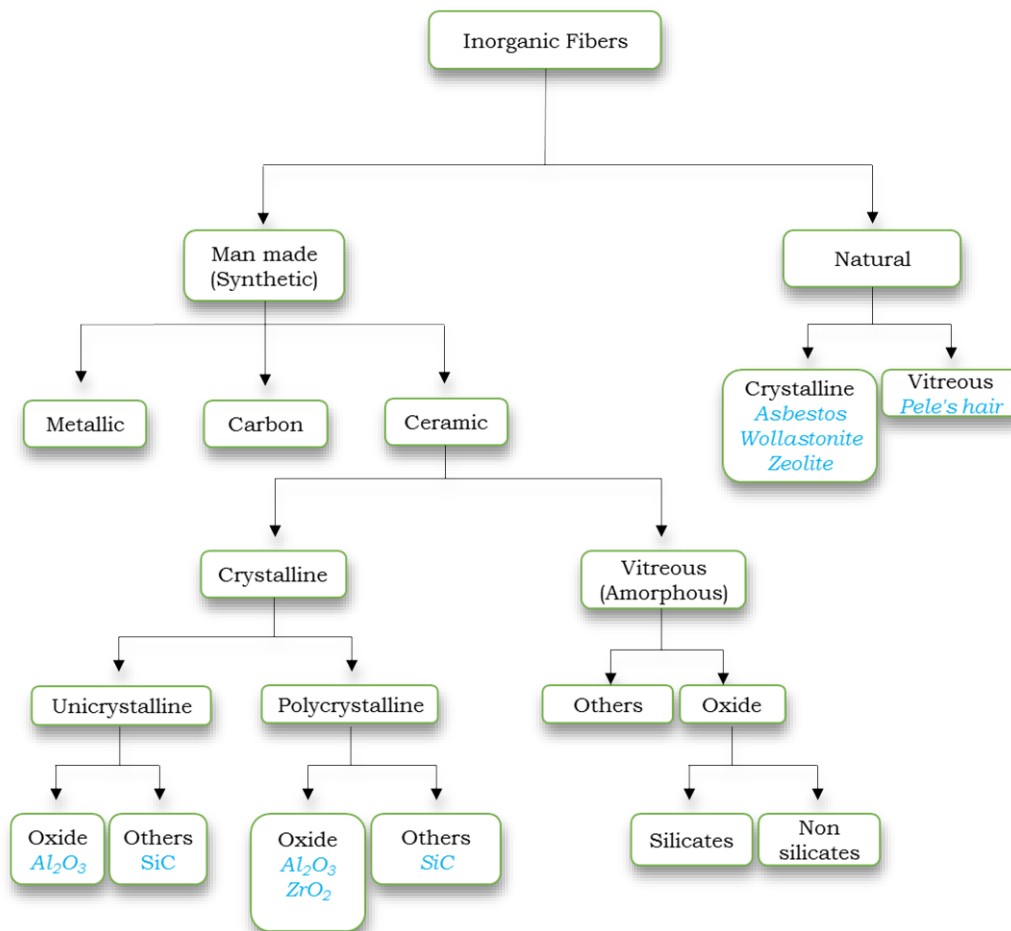er, adhesive wear is proportional to the adhesion of sliding counterfaces materials. For cast iron brake discs, hardness and compatibility of fiber metals with iron establish the aggressiveness of friction materials against the brake rotor. (146) Oxide formation on metal surface can decrease the adhesion phenomena, rupture of this oxide can be easily achieved under small loads leading metallic interaction for hard oxides on soft metals e.g. aluminum oxide on aluminum. Copper, iron and other harder metals can prevent the oxide rupture at higher load, see tab.2.17

Element	Vickers hardness (Kg/mm)		Load at which appreciable metallic contact occurs. (g)
	Metal	Metal oxide	
Gold	20		0
Silver	26		0.003
Tin	5	1650	0.02
Aluminum	15	1800	0.2
Zinc	35	200	0.5
Copper	40	130	1
Iron	120	150	10
Chromium plate	800	2000	>1000

Tab.2.17 Breakdown of oxide films produced during sliding, measure to detected by electrical conductance measurements for a spherical slider on a flat. Results relative to copper (1 g) measure (147).

Thermal stability is an important parameter to consider on metal fibers choice. At high temperature reactivity of the surfaces increase with metals inter-diffusion and alloy formation, surface melting can also occur decreasing friction coefficient and metal oxidation can lead to the opposite effect; moreover rapid heating and cooling can provide metallurgical changes. (147)

A decrease in friction during brake application is called fade, resistance to fade at high temperatures is a critical requirement for commercial friction materials. High thermal diffusivity is important removing heat from brake disc-pad contact surface during the brake reducing fading effects. A good and isotropic thermal conductivity it's also important during hot press molding of pad production. Indeed, reducing thermal gradient between external and inner brake pad part allows to avoid cracks formation on brake pads (148).

Hardness, expected adhesion with cast iron, thermal diffusivity and expected behavior in temperature are the main parameters to consider in metal fibers choice.

Toxicity aspects have also to be taken in account, in the past for example lead fibers was used due to their low hardness, non-adhesion with iron and a soft lead oxide formation at high temperature as friction stabilizing. Lead is nowadays forbidden in friction materials and, as already mentioned, in next future copper and its alloys, like brass and bronze, will be banished. Copper fibers substitution is an important task in present day, good copper properties in terms of ductility, friction coefficient stabilization, high thermal diffusivity and poor adhesion with iron cannot be replaced by one material only (149) (150).

- *Steel Fibers*

Steel fibers are commonly used on friction materials formulation to improve high temperature fade resistance and to reduce brake pads wear. Different grades are available such as fibers, wools or wires; generally for friction materials they are used in short fibers form. Melt spun fibers can be produced by melt extraction, where molten metal is extracted from a melt a wedge-shaped edge of a rotating disc. Fibers with circular cross section produces by melt extraction are not commercially available, see fig.2.53.
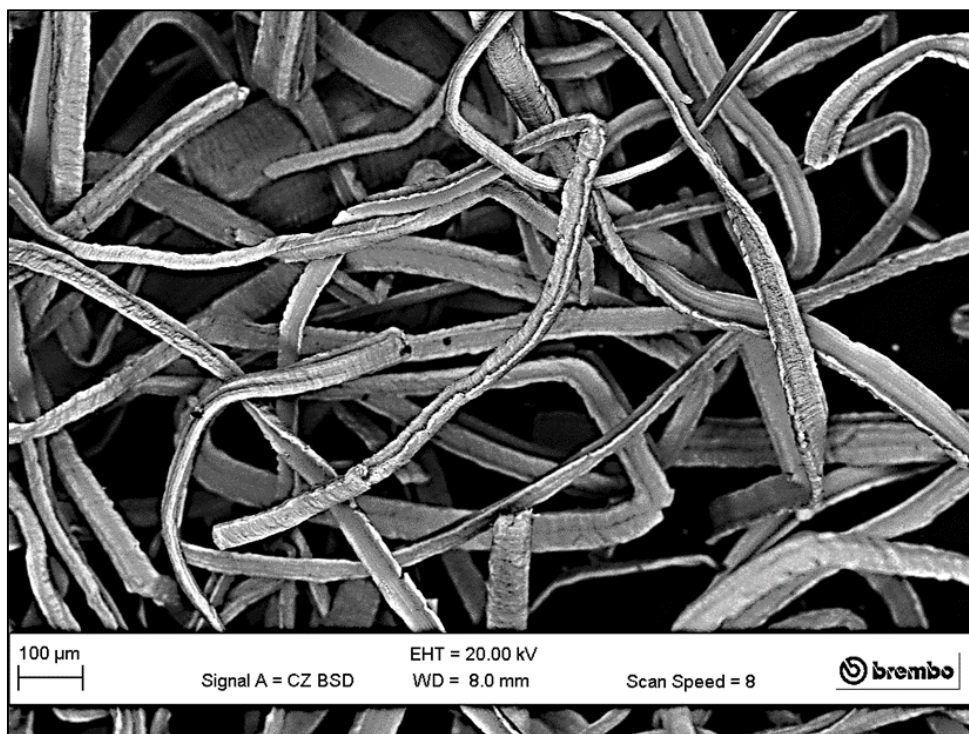
Fig.2.53 SEM image of melt spun steel fibers

Steel fibers were widely employed for asbestos replacements in semi-metallic formulation, they increase the friction coefficient of composite material and reduce fading by thermal diffusivity. It's expected an increase of pad wear compared to the unreinforced material due to their low adhesion with polymer (151), moreover due to high metal hardness and high adhesion with cast iron they induce excessive wear on brake disc generating DTV (Differential Thickness Variation) and causing vibration or judder. For this reasons the fraction of steel fibers has been gradually reduced on low-met and NAO materials.

2.6.3.2 Ceramic fibers

Ceramic fibers are higher melting, heat and chemical resistant and in any case nonflammable. Respect metallic fibers are stiffer and more brittle.

Wear mechanism of ceramic fibers is mainly abrasive and it's different from other fibers due to the material brittleness. Wear mechanism can be summarized in fig.2.54
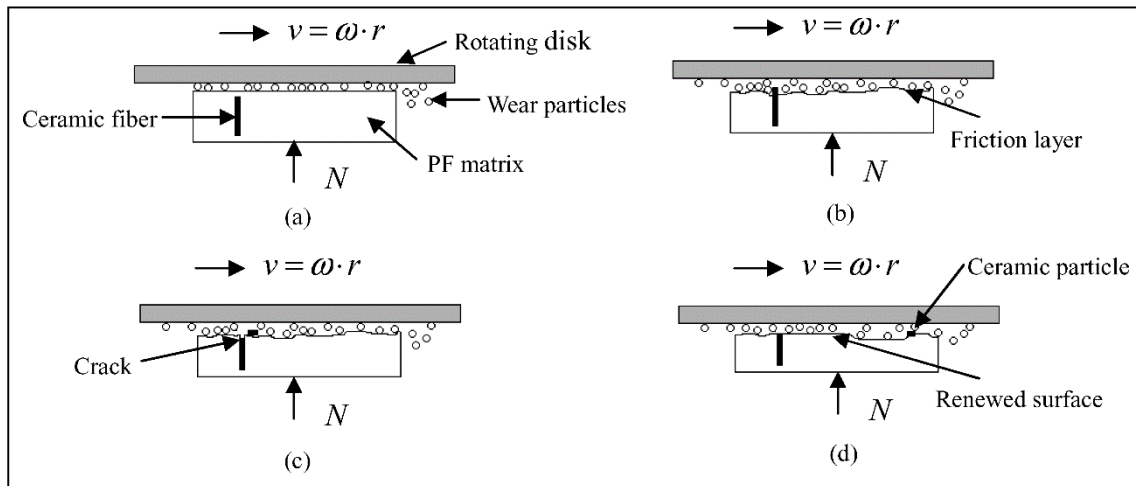
Fig.2.54 Wear mechanism of friction materials reinforced with ceramic fibers (a) Wear of matrix, (b) growth of ceramic fiber, (c) cracking of ceramic fiber, (d) renewed contact surfaces. (152)

The use of ceramic as a structural material has always been limited by its susceptibility to brittle failure due to small cracks or flaws acting as stress concentrators. For friction materials the increase of friction coefficient with introduction of ceramic fibers is explained by fibers rupture during brake which produces small abrasive particles with a resulting abrasive action on disc metal surface (151). Hard fibers are also responsible on generation of primary contact plateau during wear as reported in abrasive section.

Ceramic fibers can be classified in vitreous (or amorphous) fibers, monocrystalline fibers (or whiskers) and polycrystalline fibers

2.6.3.2.1 Man-made vitreous fibers MMVF

Natural mineral asbestos fibers replacement leaded to the use of inorganic synthetic fibers called man-made vitreous fibers. MMVF are inorganic not crystalline fibers manufactured from glass, rock, minerals, slag and inorganic oxides.

Amorphous silica is described as a random network of SiO_4 tetrahedra, some random relative orientation of SiO_4 tetrahedrals can occur over short-range order (1–2 nm). The oxygen atoms at the corners of the tetrahedra are shared between two tetrahedral, thus, the overall chemical composition is that of SiO_2 (153). Atoms of first and second group of periodic table of elements are commonly added to silica in oxide form to change physical and mechanical properties, see fig.2.55
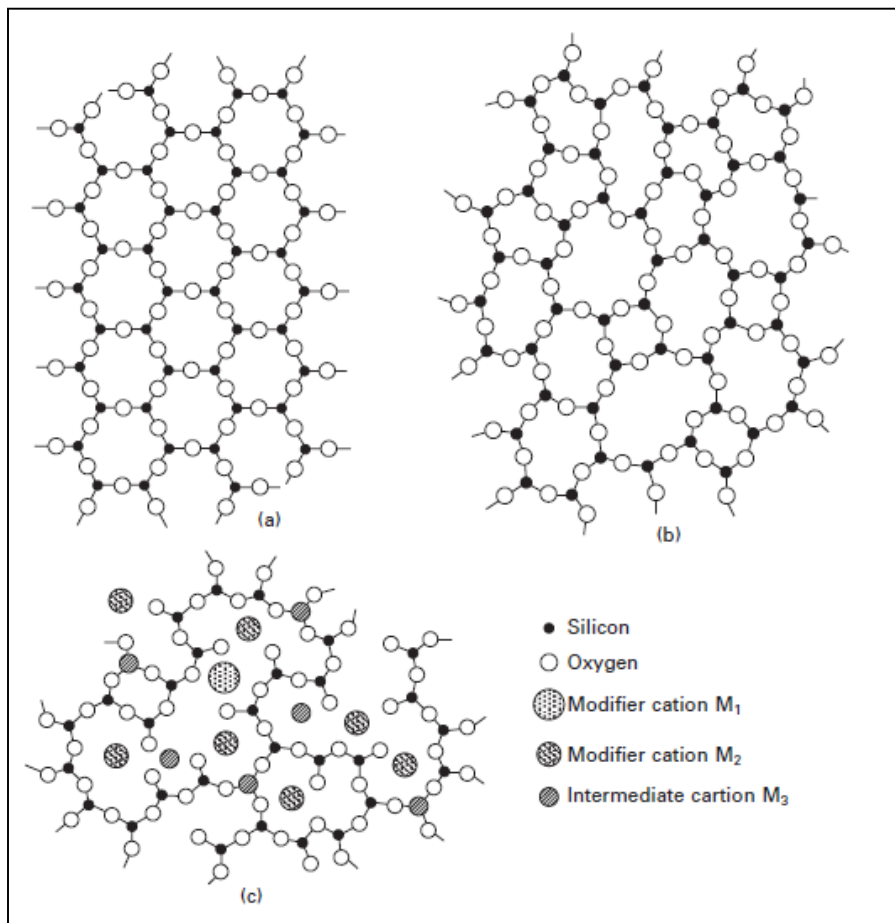
Fig.2.55 2D schematic structure of a) crystalline silica, b) amorphous silica and c) multicomponent glass (153)

Sodium, potassium calcium and magnesium oxides for example are terminal elements linking through one oxygen only to the silicon that interrupt silicon oxide network, they are added to lowering viscosity and increasing workability of glass even if they reduce chemical durability of acidic solutions. It's also possible to substitute silicon atoms with other network formers such as aluminum and boron. The complete homogeneity is lost when modifiers are added and there are regions of relatively higher or lower concentrations of different elements, in borosilicate glasses, for example, boron with sodium can form rich areas drop-shaped in the matrix which reduce thermal expansion and help to increase glass thermal shock resistance.

Glass fibers can be classified by their properties depending on their chemical composition, see tab.2.18

Type of glass	Multi-purpose	Acid resistant			Alkali resistant	High strength		Good dielectric properties	
	E	A	C	E-CR	AR	R	S	D	Quartz
SiO_2	53-55	70-72	60-65	58	60	60	60-65	73-74	100
Al_2O_3	14-15.5	0-2.5	2-6	12-13	0.7	25	20-25		
CaO	20-25	5-9	14	21	5	6		0.5-0.6	
MgO	20-25	1-4	1-3	4.5		9	10		
B_2O_3	6.5-9	0-0.5	2-7	≤0.1			0-1.12	22-23	
F	0-0.7			≤0.15					
Na_2O	≤1	12-15	8-10	0.6	14		0-1.1	1.3	
ZrO_2	≤1				18				
K_2O	≤1	1		0.4				1.5	
Fe_2O_3	≤1			0.3	0.1				
TiO_2	≤1			2.1					
Density (g/cm³)	2.61	2.46	2.46	2.7	2.68	2.53	2.48	2.14	2.2
Modulus of elasticity (GPa)	73	74	71	72	76	86	85.5	55	6.2-7.2
Tensile strength (GPa)	3.4	3.1	3.1	3.33	3.7	4.4	4.59	2.5	0.4-0.5
Dielectric constant at 1MHz	5.8-6.4	6.8	7			5.6-6.2	4.9-5.3	3.85	3.78

Tab.2.18 Chemical composition and typical values of fiber glasses commercial grade. Adapted from (154)

Glass fibers thermal stability is an important parameter for friction materials, indeed fiber mechanical strength not only decrease at high temperature due to flow processes at low viscosity, but also for hydrolysis of siloxane groups, see fig.2.56
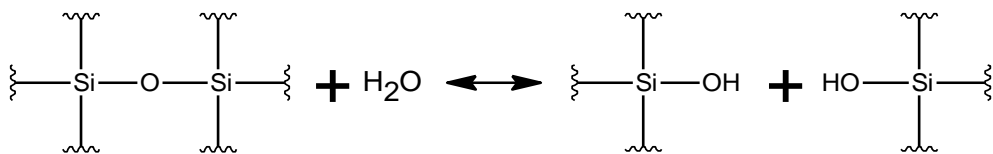
Fig.2.56 At high temperature hydrolysis of siloxane bonds became predominant respect condensation of silanol groups

The presence of alkali metal oxides catalyzes hydrolysis, at temperature over 250°C rate of hydrolysis is higher than rate of silanol condensation, affecting negatively fibers mechanical strength.

Sizing of fibers has been largely use to improve matrix adhesion and chemical resistance of vitreous fibers, but toxicological aspects on biopersistence have to be considered.

During years dangerousness of this mineral fibers was investigated, nowadays the main request for brake pad production is to use fibers not-hazardous for human health, according to the dangerous substances directive (67/548/EEC) (155):

- *Category 1. Known to be carcinogenic to man*
- *Category 2. should be regarded as if they are carcinogenic to man*
- *Category 3. Cause concern for man owing to possible carcinogenic effects, but in respect of which the available information is not adequate for making a satisfactory assessment*

Regarding dimensions textile glass fibers are classified in ISO 6355:

1) *A glass filament* is a textile glass fiber of practically unlimited length of a given diameter drawn from molten glass.

2) *A glass staple fiber* is a textile fiber of limited length (spun fiber) and of a given diameter.

All inorganic with critical dimensions (length L > 5 µm, diameter D < 3 µm and an aspect ratio L:D> 3:1) are suspected of having a carcinogenic potential and therefore are classified a priori as category 3 carcinogens and for larger diameters is required that fiber do not split longitudinally; glass staple fiber is subject to this directive.

As already seen for asbestos inhaled fibers can leads to both inflammatory and fibrotic processes depending on deposited dose in the lung and their chemical composition. Fibers dimension and fibers biopersistence are key points in their toxicity, for Man-made vitreous (silicate) fibers with alkaline oxide and alkali earth oxide ($Na_2O + K_2O + CaO + MgO + BaO$) content greater than 18 % by weight the "Nota Q" of "91/69/CE Directive" outlines specific criteria in relation to biopersistence and that determine when the classification do not need to be applied, "Nota R" of the same directive outlines dimensional criteria.

(Nota Q). A short-term biopersistence test by inhalation showing that the longer than 20 µm have a weighted half-life of less than 10 days; or a short-term biopersistence test by intratracheal instillation showing that the longer than 20 µm have a weighted half-life of less than 40 days; or an appropriate intraperitoneal test showing no evidence of excess carcinogenicity; or absence of relevant pathogenicity or neoplastic changes in a suitable long-term inhalation test.

(Nota R). Classification as a carcinogen need not apply to fibres with length weighted geometric mean diameter less two standard geometric errors greater than 6 µm.

MMVF with high melting point are historically produced as thermal insulator by melt spun of natural rocks like basalt , rhyolite or diabase. This fibers are called man-made mineral fibers (MMMF). As a result, chemical composition of mineral fibers varies significantly from one geographical region to another, fiber length

distribution was not under control and lot of not fibrous elements called shots, beads or slugs were present (154), see Fig.2.57

Fig.2.57 SEM image of a Man Made Mineral Fiber, big spherical shots can be easily distinguished from fibrous elements.

Particular attention must be paid on presence of shots in fibers; shots are generally very hard particles and their presence in large number and dimension can increase friction coefficient highly affecting disc wear.

Nowadays vitreous fibers can be manufactured in different ways, see fig.2.58.

Glass fibers preferably by Owens and rotatory processes, mineral fibers by Owens and rock wool processes and slag fibers from centrifugal blowing process. Raw materials are a mix of natural and chemical sources such as limestone, dolomite, honolite, feldspar, nepheline-syenite, kernite, colemanite, ulexite, heavy spar (barite), kaolin and furnace slug (154).
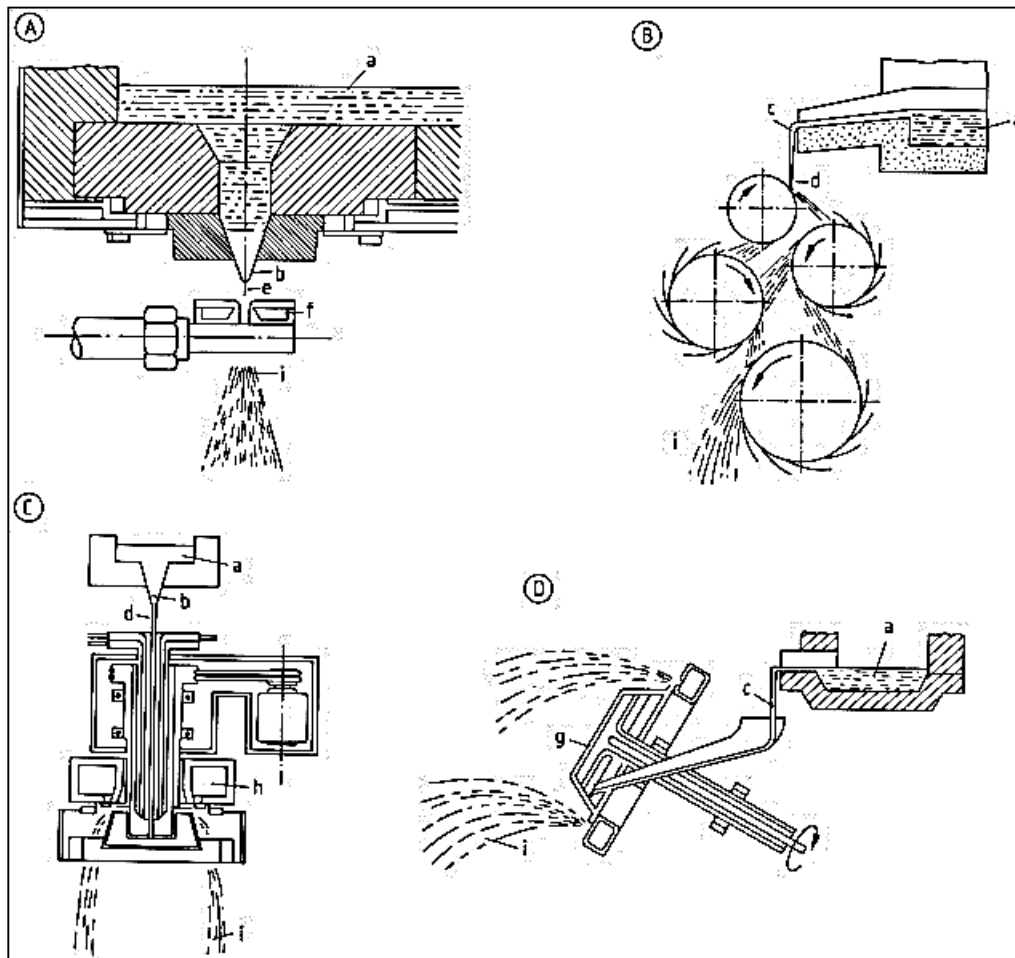
Fig.2.58 A) Owens process B) Rock wool process C) Rotary process D) Centrifugal blowing process. a) Melt; b) Bushing; c) Spout; d) Melt stream; e) Primary fiber; f) Jet; g) Centrifugal spinner; h) Burner; i) Fiber stream (154)

All general request for friction material fibrous reinforcements are satisfied by mineral staple fibers (sometime called Lapinus™ from a commercial name), in particular they provide high friction performance and stability, good fade recovery and low friction fluctuations. (156)

2.6.3.2.2 Crystalline ceramic fibers

Differently from synthetic or mineral aluminosilicate fibers, crystalline ceramic fibers can be used as refractory until temperature in excess of 1000°C. By a mechanical point of view single crystals (whiskers) are preferable to polycrystalline reinforcements, the absence of grain boundary or structure close to dislocation-free crystals ensures better creep resistance in composite and higher temperature capability.

Generally all ceramic crystalline materials can be used, but, commercially, for thermal isolation and high-temperature reinforce, boron, boron nitride, silicon

carbide, silicon nitride, sialon, alumina, high alumina ($Al_2O_3:SiO_2 > 0.6$), aluminum borate, zirconia and mullite in form of fibers or whiskers are mainly used.

Production cost and material toxicology strongly limiting use of ceramic crystalline fibrous reinforcements, indeed, directive (67/548/EEC) is applied also to this class of products.

Despite the toxicological aspect two crystalline ceramic reinforcements still be used for manufacture of friction materials due to their high cheapness: potassium titanates and wollastonite.

- *Titanates*

Titanates have been considered as reinforcement for polymers. They can be synthetized mixing metal oxides and titanium dioxides in different proportion, $M_2O \cdot nTiO_2$, where M is an alkaline metal and n can be 2, 4, 6 or 8. They are synthetized by different techniques like calcination, hydrothermal reactions, flux evaporation, flux growth (melting) and the slow-cooling process. For an high alkaline content, like dititanate $M_2O \cdot 2TiO_2$ or tetratitanate $M_2O \cdot 4TiO_2$, the layered structure is not suitable for reinforcements purpose. For low alkaline content, like hexatitanate $M_2O \cdot 6TiO_2$ and octatitanate $M_2O \cdot 8TiO_2$, a tunnel structure exhibits good thermo-insulation properties and good chemical stability.

Potassium hexatitanate $K_2Ti_6O_{13}$ has been widely use in friction materials it demonstrated to have good wear, high temperature and chemical resistance then remarkable mechanical and fire-proof properties. It's also relatively cheap compared to octatitanate. (157) (158)

The crystal structure is monoclinic, with spatial group $C2/m$ see fig.2.59

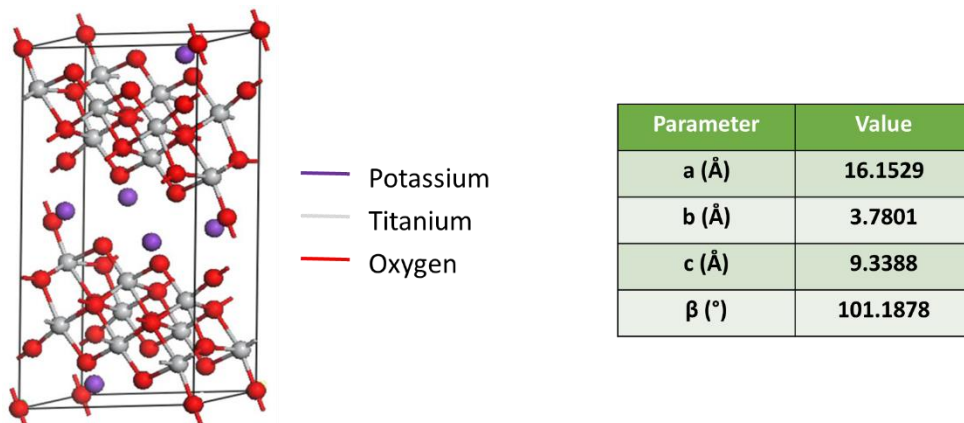| Parameter	Value
a (Å)	16.1529
b (Å)	3.7801
c (Å)	9.3388
β (°)	101.1878

Fig.2.59 Crystal model of potassium hexatitanate s.g $C2/m$ and equilibrium lattice constant (157).

TiO_6 octahedrons form a tunnel structure where potassium ions are embedded, potassium ions cannot easily escape from the tunneling structure, this conferees chemical resistance at the material.

Different shape of potassium hexatitanate has been considered to reinforce friction materials, as reported in fig.2.60
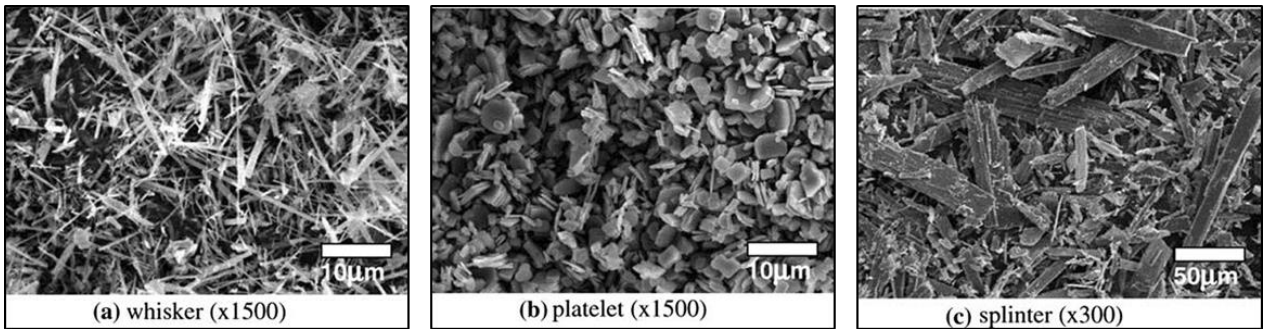
Fig.2.60 Potassium hexatitanate in a) whisker b) platelet c) splinter forms (159)

From different tests it was demonstrated that morphology of potassium hexatitanate makes a big difference on friction material tribological properties, splinter forms shown the lower wear rate and best friction stability at high temperature (159). Heat-insulating property is used to reduce the heat transfer between disc and caliper reducing the brake fluid temperature in different condition.

Potassium hexatitanate is widely used in non-asbestos organic (NAO) and very low steel (VLS) friction materials and in general is used with other fibers like aramid pulp due to strong synergistic effects. Even if aramid pulp alone demonstrates an higher wear rate of friction material compared to $K_2Ti_6O_{13}$ whiskers, it has a good electrostatic effect on it succeeding in keep potassium hexatitanate well dispersed in friction mix and obtaining an high cohesive strength of the friction layer (160) (161).

As already seen, potassium hexatitanate is not completely free of risks, indeed, it's under investigation as potential cause of mesothelioma and classified by IARC as possibly carcinogenic to humans (Group 2B) (162). Many efforts has been made to avoid this classification introducing new forms like small granulated powder from fibers, but problem on health classification stays open.

- *Wollastonite*

Wollastonite is a natural mineral silicate $CaSiO_3$ with triclinic crystal structure, space group $P\bar{1}$ and hardness 5 on Mohs scale. Acicular natural morphology of wollastonite leads naturally to form ores with high percentage of long needles, a separation of this needle-like particles with air permits to produce wollastonite with length/diameter aspect ratios of 15:1 – 20:1, tensile modulus of individual crystals is almost as good as those of aramid fibers. Coupling agents like silane, aminosilane, organo-silicone and titanate can be used to increase compatibility with plastic matrix (102)

As for potassium titanates due to low cost is still used for NAO materials and sometimes in underlayer, it enhances wear and recovery performance and reduces friction coefficient variability. As for titanates health hazard classification of wollastonite still be an open point.

2.6.3.3   *Carbonaceous reinforcements*

2.6.3.3.1   Carbon fibers

Carbon fibers are based on graphite-like structures with sp³ crosslink bonding between basal planes (163).

Carbon fibers historically started to be produced by carbonization of natural fibers based on cellulose sources such as cotton, linen, ramie, sisal and heme or chemicals derived from cellulose, such as Rayon, with better results in terms of mechanical properties. (164). As already seen for synthetic graphites high temperatures are required for a rearrangements of carbonaceous structures.
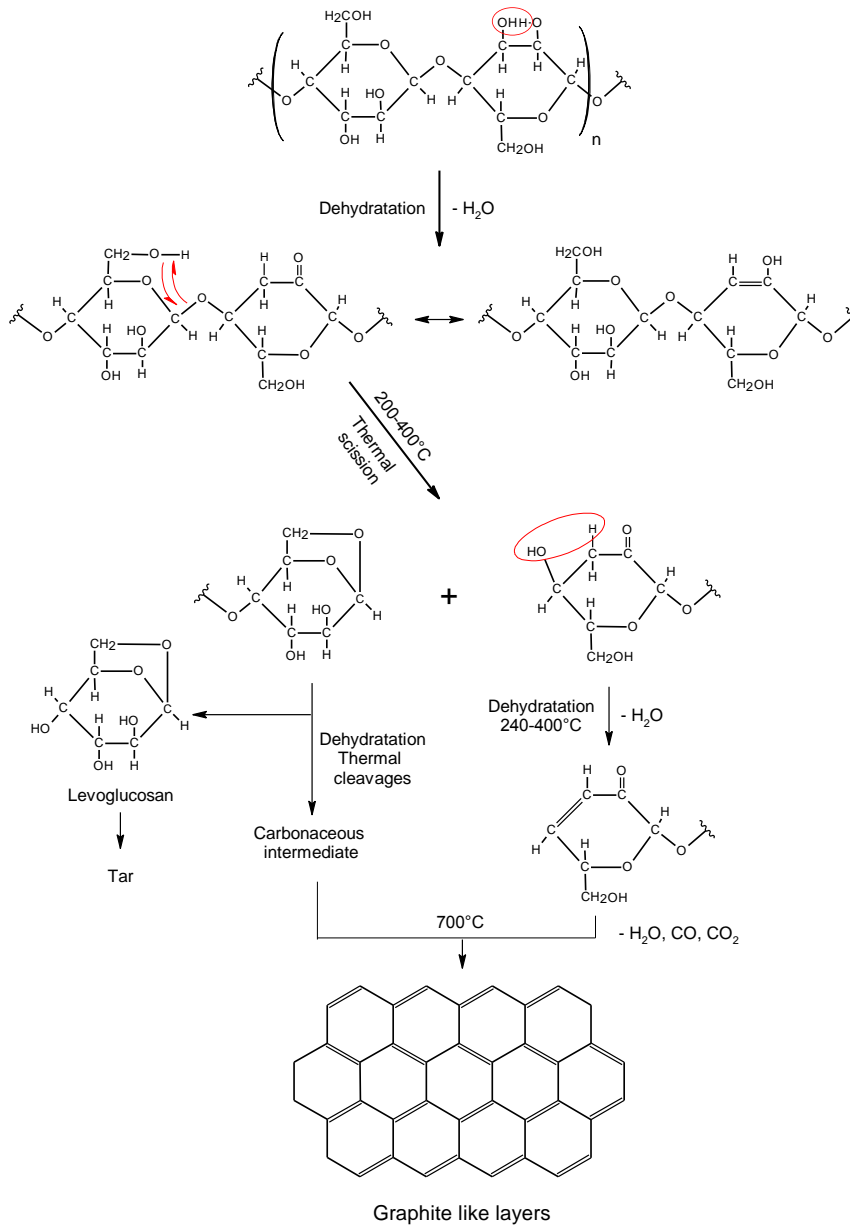
Fig.2.61 Carbon fiber synthesis path from cellulose, adapted from (164).

95

Carbon fibers based on cellulose amounts only 1–2% of the total carbon-fiber production but research of low cost natural materials, such as lignin or cellulosic precursors, for mass production of carbon fibers in automotive industry is ripe for further improvement.

Not every source is suitable for carbon fibers, alignment of graphitic layers along the fiber axis and cross-sectional microstructure are responsible of final strength and modulus. In plain orientation of precursors guarantees a good graphitizability of structures; cellulose does not produce long-range parallel order of graphene structures and it has a low theoretical carbon yield (44%). To overcome this point synthetic sources have been historically used such as PAN, polyacrylonitrile, and pitch, an high molecular weight carbonaceous material preferably derived from coal tar or crude oil distillation. Petroleum pitch is preferable to coal tar pitch as it has a lower proportion of undesirable lighter components. (165)

PAN fibers are made by wet spinning polymer solutions in highly polar solvents and afterwards separated in a water-based coagulation path. The PAN ladder structure generation is an exothermic process, and polyacrylonitrile decomposes below his melting temperature, to protect fibers from a degradation during this phase copolymers can be used.
Pitch fibers can be made by melt spinning, when no mechanical or chemical means are applied to achieve preferred orientation of the polyaromatic molecules in the fiber direction isotropic low modulus pitch-based carbon fibers are obtained, low cost of this materials permits the use of carbon fibers in large scale production.
After oxidation and thermal stabilization a carbonization of fibers under inert atmosphere proceeds in two steps as described in fig.2.62; high mass hydrocarbons, hydrogen cyanide, ammonia, nitrogen, methane, carbon mono and dioxide, ethane, ethylene, hydrogen and water are produced in this steps. Application of tension during carbonization and graphitization improves mechanical properties of the final carbon fibers.

Fig.2.62 Carbonization of PAN fibers by pyrolysis in inert atmosphere.

At the end of carbonization a structure described as graphite like crystals with stacked layers of graphene inside an amorphous or glassy carbon matrix and some voi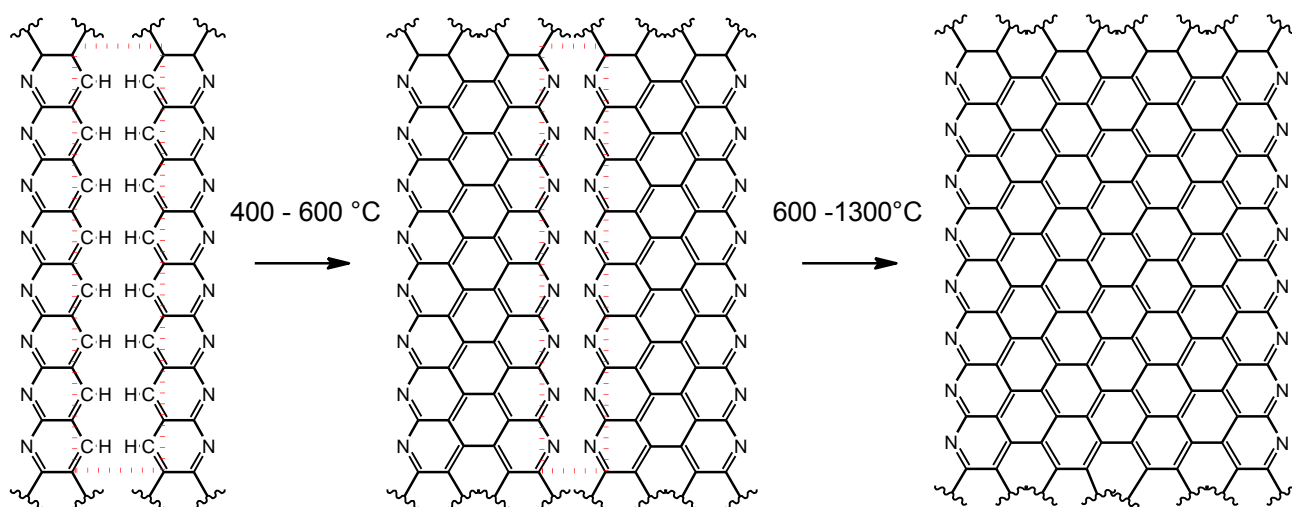ds is achieved. Compressive properties of carbon fibers are governed by sp^3 crosslinks between the basal planes. (166) (167) (168)

Main differences between carbon fibers are reported in tab.2.19

Carbon fiber grades	Main properties	Tensile strength (GPa)	Tensile modulus (Gpa)	Elongation at break (%)
PAN based CF	- Graphene "turbostratic" layers non high-oriented in stacking - Low graphite like crystal lengths - Some wrinkled structures - By varying the processing conditions, better alignment of graphene layers can be achieved leading to stiffer, higher-modulus PAN fibers, but with lower strength	3.5–6.3	200–500	0.8–2.2
Pitch based CF	- Good orientation of the crystalline phase into fiber direction - High graphite like crystal lengths - High electric and thermal conductivity - Low cost for isotropic pitch version (general grade). - 80% of total CF world production	1.3–3.1	150–900	0.3–0.9
Cellulose based CF (Rayon)	- Short-range parallel order of graphene structures - Large void content and inter-filament de-bonding - Low theoretical carbon yield (44%) - Low cost - Renewable raw materials	0.9–1.1	90–100	1.0–1.1

Tab.2.19 Main carbon fibers grades (164) (165) (166) (167)

Fibers undergoing graphitization process at T>2000°C are commercially called graphite fibers, they are used for their high tensile modulus and thermal diffusivity. Temperature improves the orientation of the basal planes increasing the fiber stiffness. The carbon structure never reaches a three-dimensional crystallinity so the fiber never consist of a polycrystalline graphite, so the name "graphite fibers" is formally incorrect.
Due to poor adhesion between polymers and carbon fibers surface treatments has been studied to importantly contribute at properties of the fiber-matrix interface.
Main surface treatment of carbon fibers are oxidative by gaseous and liquid phases, and non-oxidative such as whiskerization, plasma polymerization and carbon deposition, but the exact nature of treatment is a trade secret.
Small adhesion at interface does not guarantees a good load transfer between fiber and matrix and a strong adhesion decrease the fracture toughness of a composite, so the right degree of superficial treatment should be use. (169)

Besides general requests for reinforcements, carbon fibers lend other properties to friction material:

- Good thermal diffusivity
- Very high stiffness/weight ratio
- Fatigue resistance
- Low linear coefficient of thermal expansion
- Chemical inertness
- High damping

Friction coefficient of carbon fiber reinforced friction material is not expected to be higher than unreinforced material, indeed, carbon fibers are not hard and brittle but they have a lubricant graphite-like structure.

2.6.3.3.2 Other carbonaceous fibrous reinforcements

Due to their important mechanical properties carbon nanofibers and carbon nanotubes are under evaluation for friction materials. Main differences in structures are reported in fig.2.63
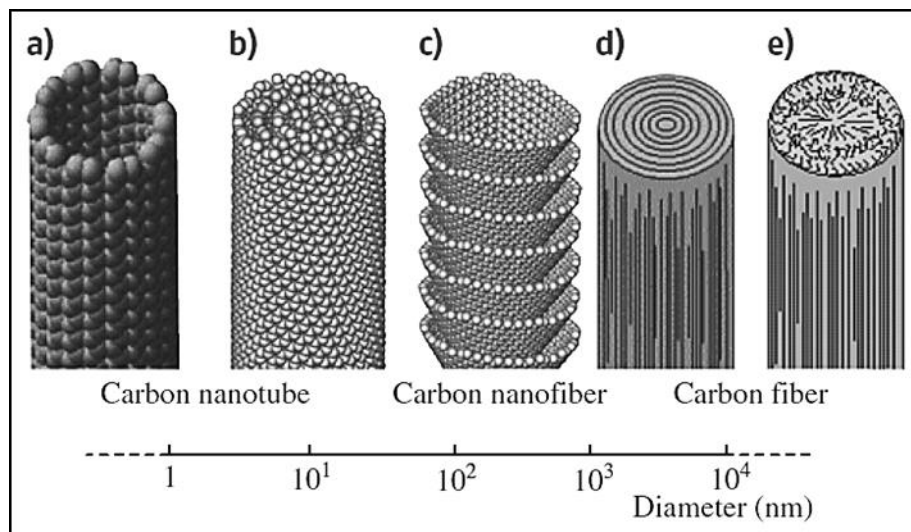
Fig.2.63 Fibrous carbon reinforcements a) Single-walled carbon nanotube b) multi-walled carbon nanotube c) d) e) carbon fibers prepared under different processing conditions (167)

Even if CNT-added friction materials showed improved fade resistance and friction stability, difficult to disperse nanomaterials with conventional mixing system leads to have undispersed bundles which act as lubricant lowering friction coefficient (170).

Carbon whiskers has been produced in condition next to triple point of graphite (T = 4100 K, p = 123 kbar) or by chemical vapor deposition of ethane in the presence of Cu – Ni catalyst. a carpet-rolling structure of graphite sheets gives to the material

98

high mechanical strength and modulus along the fiber axis next to pure graphite crystal.

Carbon nanomaterials have been studied in elastomeric composites for a wide range of potential applications (171), they could be used in rubber premix, but cost of nanomaterials is not negligible and should be evaluated for their use in friction materials.

2.6.4 Particulate reinforcements

For thermoplastic materials like phenolic resin the effect of particulate reinforcements is to increase stiffness and hardness of the compound (when hard materials are used) reducing the deformation at brake. A different behavior can be seen on elastomers, simultaneous increase modulus and deformation at break can be achieved by use of particulate reinforcements. (133)

2.6.4.1 Carbon black

Generally they are derived from incomplete combustion in an oxygen deficient atmosphere of gaseous or mist of hydrocarbons; during carbonization process the spherical nanostructure of formed material is nano-texturized as hexagonal carbon layers preferentially oriented along the surface as showed in (172) fig.2.64(a)
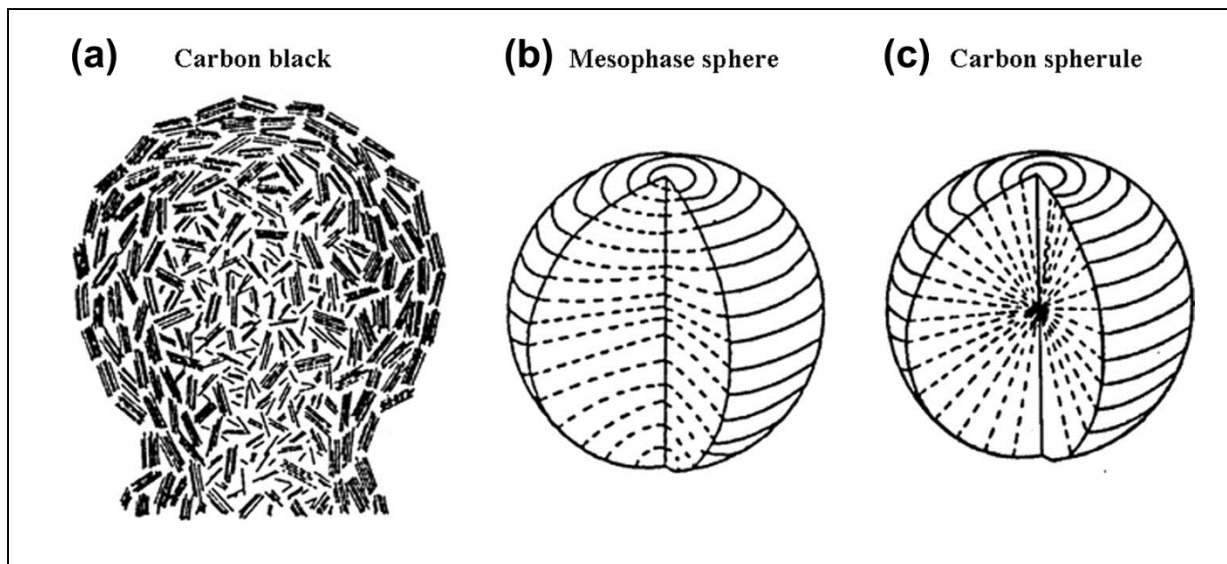
Fig.2.64 Nanotextures in three spherical carbon materials (172)

Strong interaction between polymers and carbon black bonds part of polymeric chain on particles surface. The best reinforcing condition is when any chain is directly in contact with at least one carbon aggregate, therefore high reinforce load and adequate dispersion are required. For this reason carbon black is not added

directly on friction materials (produced by a blender at low shear rate), but can be added on a premixed rubber compound. Rubber premix is manufactured with a batch internal mixer which provide sufficient shearing to correctly disperse fillers in the matrix. Surface area/particle size, structure (particles aggregation) and surface chemistry are properties that characterize carbon black reinforce effect on compounds (173), see fig.2.65
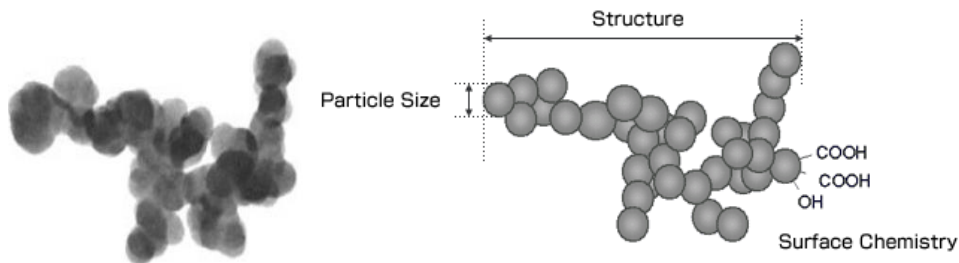
Fig.2.65 The three main properties which characterize carbon black, particle size, structure and surface chemistry. Original TEM image and relative structure sketch adapted from (83)

In elastomeric compounds carbon black is largely used to increase mechanical properties, thermal stability and UV protection (174) (175).

2.6.4.2   *Activated Carbon*

Activated carbons are generating in two phases (176). In the first phase, called stabilization, a solid resins carbonization process generates closed shells (consisting of carbon hexagonal layers) called glass-like carbons due to their mechanical properties; in the second phase, called activation, it's the oxidation of glass like carbons. Pores grow from the particles surface forming CO and CO_2. Pore size depend on oxidation condition, see fig.2.66
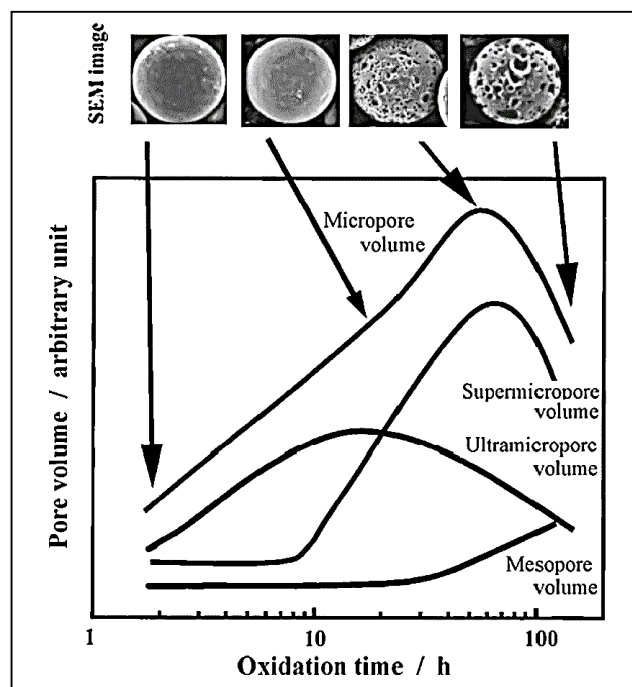
Fig.2.66 Pore development during gas activation on glass-like carbon sphere.

Well-developed pore structure allows effective flow of viscous fluids; in plastic compound is used for odor and smoke adsorption, in friction materials porosity reduces fading effect at high temperature, increases pedal feeling and reduces noise (93).

2.6.4.3   *Silica*

Silica vitreous particulate in friction materials has been used to increase brake pad wear resistance and to reduce noise level during brake in form of microspheres or porous glass beads; in both cases silica particles are not a reinforcement.

Conversely, a large use of silica as particulate reinforcement has be done in rubber technology where it's used in two main forms (133):

a) Precipitated silicas, where alkaline glass is solubilized in water at high temperature and precipitated by acid
b) Fumed Silicas, where fluffy form of silica particles are obtained by thermal oxidation of silane or silane methyl hydride precursors. Some silanols formed during oxidation are formed, and they can guarantee good dispersion in rubber matrix.

To increase the compatibility with the polymeric matrix silica can be doped or grafted by different chemical species.

2.7 Fillers and functionalizers (raw materials)

In friction materials every ingredient is responsible to the behavior of final friction coefficient, so every raw material could be considered as a friction modifier, however it's convenient to classify materials following their main contribution to the final compound properties. In this section raw materials not belonging to abrasive, lubricants, reinforcements or binder groups are classified two main subgroups:

- *Fillers.* Thermally stable inexpensive materials have minimum impact on friction performance and occupying the volume improve brake pad manufacturing process.

- *Functionalizers*, all the materials not included in precedent groups which provide specific properties to final friction compound such as noise suppressors, colorants, corrosion inhibitors, etc.

2.7.1   Fillers

A composite can be defined as a product arise from the incorporation of some basic structural material into a substance called matrix (177). In the past all the incorporated materials in friction compound was simply called fillers (178), most recently fillers has been considered only materials which reduce cost/benefit ratio (179).

Main properties of fillers are high thermal stability, minimum impact on friction performance, water insolubility and low cost; generally they are scarcely compatible in term of adhesion with the matrix; a specific superficial treatment or a use of coupling agent to convert them in reinforcements could be expensive. By brake pads manufacturing point of view presence of particulate fillers in friction compound reduces the shrinkage during molding and curing (180).

Material from mineral sources are suitable for this purpose due to their low cost, a review of rock forming minerals not already considered in previously chapters such as carbonates, sulfates, nitrates and phosphates is reported in tab.2.20

Crystal Group	Formula	Crystal System	Laue Group	Space group	Mineral name	Density (g/cm³)	Mohs hard.
Calcite	$MgCO_3$	Trig.	$\bar{3}m$	$R\bar{3}c$	Magnesite	3.010	3.5-4.5
	$ZnCO_3$				Smithsonite	4.434	4.5
	$FeCO_3$				Siderite	3.973	4-4.5
	$MnCO_3$				Rhodochrosite	3.720	3.5-4
	$CdCO_3$				Otavite	5.024	3.5-4
	$CaCO_3$				Calcite	2.7106	3
	$NaNO_3$				Nitratine	2.261	1.5-2
Dolomite	$CaMg(CO_3)_2$	Trig.	$\bar{3}m$	$R\bar{3}$	Dolomite	2.868	3.5-4
	$CaFe(CO_3)_2$				Ankerite	3.293	2.5-4
Aragonite	$CaCO_3$	Orth.	mmm	$Pmcn$	Aragonite	2.930	3.5-4
	$SrCO_3$				Strontianite	3.843	3.5
	$PbCO_3$				Cerussite	6.577	3-3.5
	$BaCO_3$				Witherite	4.314	3-3.5
	KNO_3				Niter	2.079	2
Malachite	$Cu_2(OH)_2CO_3$	Monoc.	$2/m$	$P2_1/a$	Malachite	3.8	3.5-4
Azurite	$Cu_3(OH)_2(CO_3)_2$	Monoc.	$2/m$	$P2_1/a$	Azurite	3.83	3.5-4
Barite	$SrSO_4$	Orth.	mmm	$Pbnm$	Celestine	3.961	3-3.5
	$PbSO_4$				Anglesite	6.321	2.5-3
	$BaSO_4$				Barite	4.467	3-3.5
Gypsum	$CaSO_4 \cdot 2H_2O$	Monoc.	$2/m$	$I2/a$	Gypsum	2.313	2
Anhydrite	$CaSO_4$	Orth.	mmm	$Amma$	Anhydrite	2.953	3.5
Apatite	$Ca_5(PO_4)_3OH$	Hexa.	$6/m$	$P6_3/m$	Hydroxyapatite	3.153	5
	$Ca_5(PO_4)_3F$				Fluorapatite	3.201	5
	$Ca_5(PO_4)_3Cl$				Chlorapatite	3.185	5
Monazite	$CePO_4$	Monoc.	$2/m$	$P2_1/n$	Monazite	5.226	5-5.5

Tab.2.20 Main properties of carbonate sulfates and phosphates rock forming minerals (57) (18) (58)

To have a minimum impact on friction coefficient value only materials not belonging to abrasives and lubricants groups have to be considered; all reported minerals with Mohs hardness between 3 and 4.5 can be eligible as fillers (depending also on the cost). Oxides and silicon based materials in this range have already been reported in abrasive section, see tab.2.8-2.9.

Sulfates and carbonates well satisfies cheapness and hardness requirements and both are widely used in friction materials formulations. Sulfates are more chemical and thermal resistant than carbonates, even if the latter are cheaper. (179)

Some contamination in minerals is inevitable. Barium sulfate $BaSO_4$, e.g., also called barite or baryte, it has strontium sulfate as common impurity (181), then, as commercial grades, it's common not to find pure barium sulfate but a $(Sr, Ba)SO_4$ solid solution.

2.7.2 Functionalizers

2.7.2.1 Noise suppressor
One of main problems on brake system is comfort in terms of noise, vibration, and harshness (NVH) (182) and in terms of pedal feeling during the brake. Frequency from 20 Hz and 20kHz represent human range of audibility, NVH studies divide noise events depending on their frequency, see fig.2.67
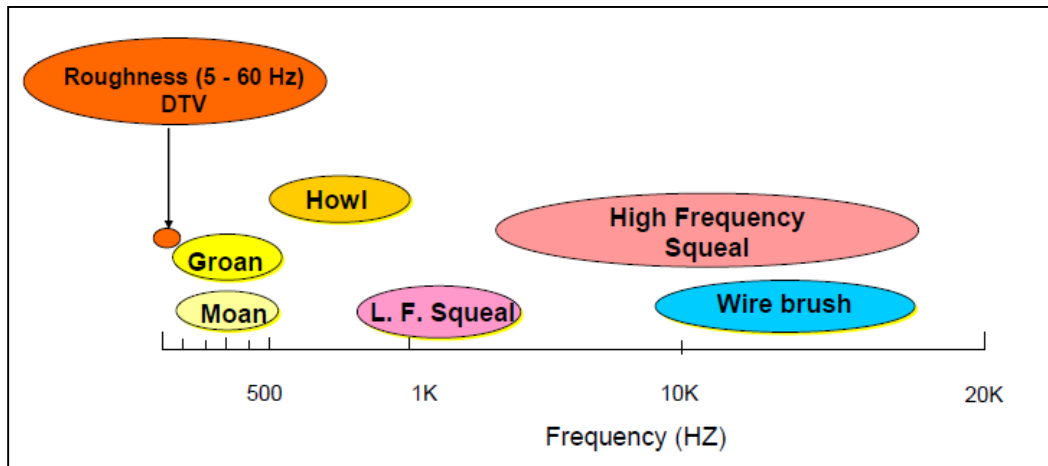
Fig.2.67 Basic terminology referred to brake noise (183)

Different strategies have been studied to reduce unstable friction coefficient and noise, for example in other chapters it was considered how friction stabilizers can contribute to increase the brake comfort. Other methods related to friction material composition used to achieve this result are reviewed in this section. Friction coefficient and brake/disc wear at different pressure speed and temperatures are the main characteristic required to a friction material. Noise suppressors can be used directly in the friction mix, but it's better to use it in a separate layer in between from friction material and back-plate. This underlayer, also called backing layer (184), is directly in contact with the brake disc only at end-life of brake pads, this permits to formulate a completely different composite material with properties focused not on brake efficiency, but, e.g., on noise damping.

2.7.2.1.1 Porous particles

Friction material porosity plays an important role in sound absorption, number, indeed, size and type of pores are the important factors on studies of sound absorption mechanism (185). Often used as gas absorbers, particles with porous structures can reduce density and increase the porosity of friction compounds. Beside noise reduction, porosity can increase the thermal fade resistance and recovering, indeed their structures facilitate the evacuation of formed gases at high temperature. (186) (187)

As for other the components of friction materials, thermal resistance and water insolubility are essential. Porous materials can be selected from synthetic or natural sources such as activated carbon, porous silica, diatoms micro-shells, zeolites, porous glass microspheres, or other synthetic crystalline ceramics (188) (189) (190).

Low cost of materials from natural sources increased their use in friction material formulations, furthermore noise reduction, raise of friction efficiency and brake pad wear reduction can be achieved with the use of this materials.

2.7.2.1.2   Layered structures

Inorganic materials having a plane netlike crystal structure act as sound dumpers (191). Phyllosilicates mineral also called layered silicate, reviewed in abrasive chapter, are suitable for this purpose. In this mineral category clays and micas have been widely used for friction materials. On micaceous structures dry-ground phlogopite mica $KMg_3AlSi_3O_{10}F(OH)$ is preferred due to its cheapness, good heat resistance and good properties of noise reduction (192) (193) (194).

On clays special attention must be paid to vermiculite minerals $(Mg, Fe^{2+}, Al)_3(Al, Si)_4O_{10}(OH)_2 \cdot 4(H_2O)$. In particular, exfoliated or expanded vermiculite has been used in the past as asbestos substitute in industrial applications for thermal insulation (195). On heating, vermiculite exfoliates due to interlaminar steam release (196),see fig.2.68
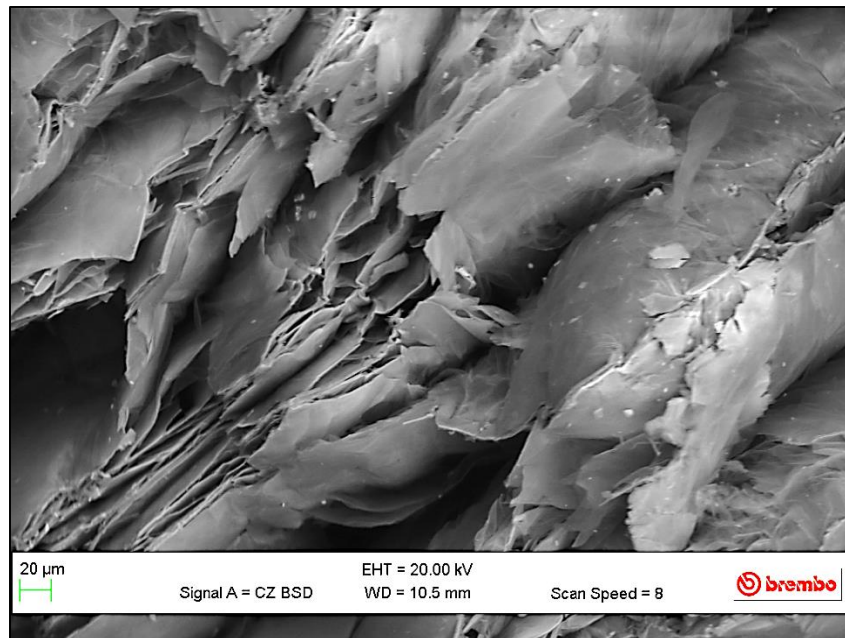
Fig.2.68 SEM image of expanded vermiculite

This special form of vermiculite is particularly efficient in friction mix as noise suppressor and thermal fade recovery (197).

2.7.2.1.3   Elastomers

Elastomers, also called rubbers, are mainly used in composite materials to increase elasticity and reducing thermal diffusivity on final compound. High compressibility, flexibility and noise dumping are expected by addition of this ingredient in friction materials (4)

Elastomers can be added in liquid or solid granulated form to friction mix by itself or in a premixed compound (198), common commercial rubbers are reported in fig.2.69

Most of rubbers are soft-sticky materials, not resistant in terms of wear or breaking load and they don't maintain the shape after a large deformation, when rubber particles are exposed to friction forces poor adhesion with phenolic resin and poor mechanical strength of elastomers can compromise the brake leaving undesirable holes on surface. Car operating temperature can reasonably reach -40°C, then noise behavior at low temperature can change depending on thermos-mechanical behavior of friction compound; low glass transition temperature of elastomers is a parameter to consider on rubber choice.

Rubber high temperature and mechanical resistance can be achieved in different ways such as using reinforcements, fillers and functionalizers. As already seen fibrous and particulate reinforcements can increase rubber mechanical strength and elasticity. Other components i.e. carbon black can act as antioxidant increasing rubber thermal resistance (199). The Rubber premix (called also rubber block or simply premix) can be manufactured by an internal rubber mixer, also called Banbury® mixer (from trade name), where intermeshing rotors intensively mix rubber with other ingredients. At the end the mixed rubber block is granulated, at the selected particle size.

Another method to increase thermomechanical resistance of rubber is the vulcanization process.

Vulcanization is a chemical process where rubber macromolecules are crosslinked forming a three-dimensional network, the net-like structure reduces the amount of permanent deformation increasing elasticity and decreasing plasticity of the original rubber. Different vulcanization process can be done on rubbers, for example sulfur and peroxide vulcanizations are used for "high diene" rubbers such as Natural rubber NR, synthetic isoprene rubber IR, butadiene rubber BR, styrene butadiene rubber SBR, butyl rubber or isobutylene-isoprene rubber IIR, halobutyl rubbers (bromo BIIR and chlorobutyl rubber CIIR), ethylene-propylene-diene monomer rubber EPDM and nitrile rubbers (normal NBR or hydrogenated HNBR) (200)

Sulfur vulcanization can require different components such as vulcanizing agents, accelerators, activators, retarders and inhibitors.

CH₃ — Natural Rubber NR / Polyisoprene (cis) rubber IR

Cl — Chloroprene rubber CR

Butyl rubber or isobutylene-isoprene IIR

C≡N — Nitrile rubber NBR

Halobutyl rubber CIIR BIIR
X = Cl,Br

Polybutadien rubber BR

Styrene butadiene rubber SBR

Chlorinated polyethylene CM

Ethylene-Propylene Diene Monomer Rubber EPDM

Silicone MQ

Chlorosulfonated polyethylene CSM

Fluorocarbon FKM

Epichlorohydrin ECO

Polysulfide T

Urethane rubber AU

Polyacrylate ACM

Fig.2.69 Structures and abbreviations of common commercial elastomers, adapted from (201)

Vulcanizing agents include elemental sulfur or organic sulfur donors like 4,4'-dithiobismorpholine (DTDM) and tetramethylthiuram disulfide (TMTD), zinc oxide is vulcanization system activators and fatty acids are coactivators.

At 140°C unaccelerated reaction between sulfur and natural rubber can require several hours, and higher temperatures risk to damage rubber structures. Accelerators agents are commonly used to reduce curing time from several hours to some minutes, common accelerators for sulfur vulcanizing are reported in fig.2.70
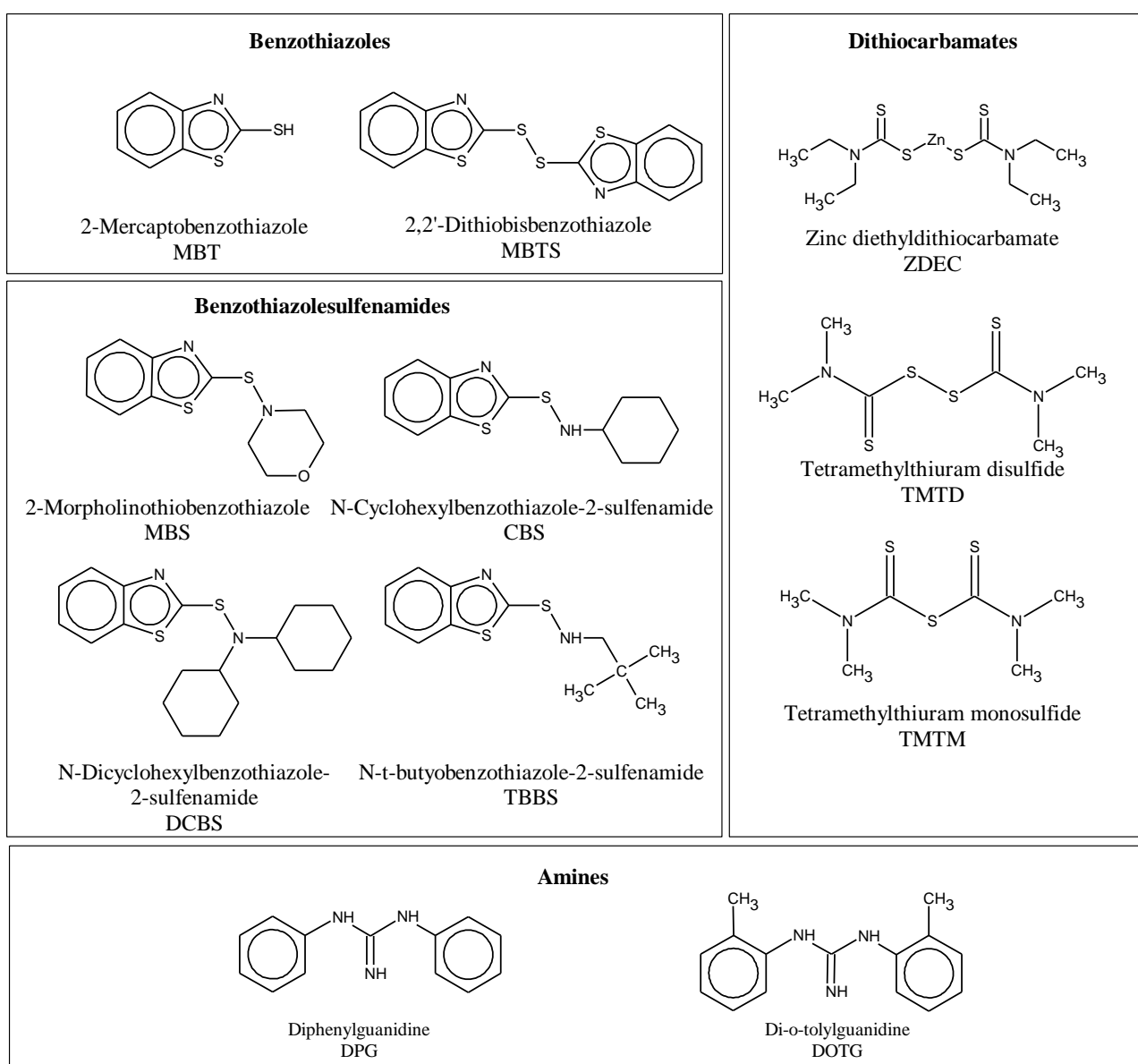
Fig.2.70 Structures and abbreviations of common accelerators for sulfur vulcanizing, adapted from (200)

Sulfur vulcanization reaction mechanism can be divided in three steps. In the first step initiators and activators react with sulfur structures. In the second step sulfurating agents interact with rubber chains producing polysulfidic pendant groups terminated by accelerator groups. In the third step rubber crosslinks is formed. (202)

1) $Ac + S_8 \rightarrow Ac - S_x - Ac$ *Sulfuration of accelerator agent*
2) $Ac - S_x - Ac + RH \rightarrow R - S_x - Ac + AcH$ *Polysulfidic pendant groups*
3) $R - S_x - Ac + RH \rightarrow \boldsymbol{R - S_x - R} + AcH$ *Crosslinking*

Where Ac is the accelerator agent and RH is the rubber chain

Sulfur can attack via ionic or free-radical intermediates on the isoprene structure in different points see fig.2.71
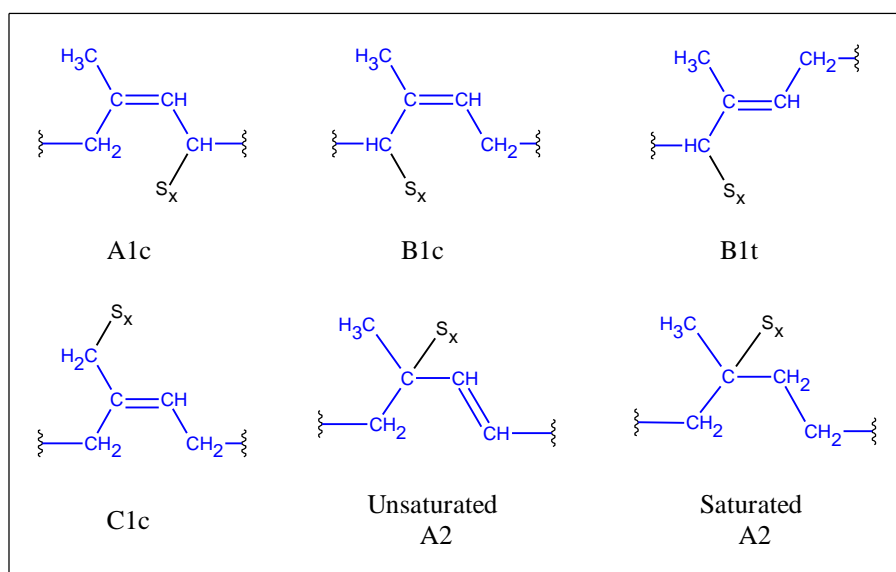
Fig.2.71 Designation of nomenclature for vulcanized NR and cis-polyisoprene structures, adapted from (202)

Generic structures from sulfur crosslinking is reported in fig.2.72
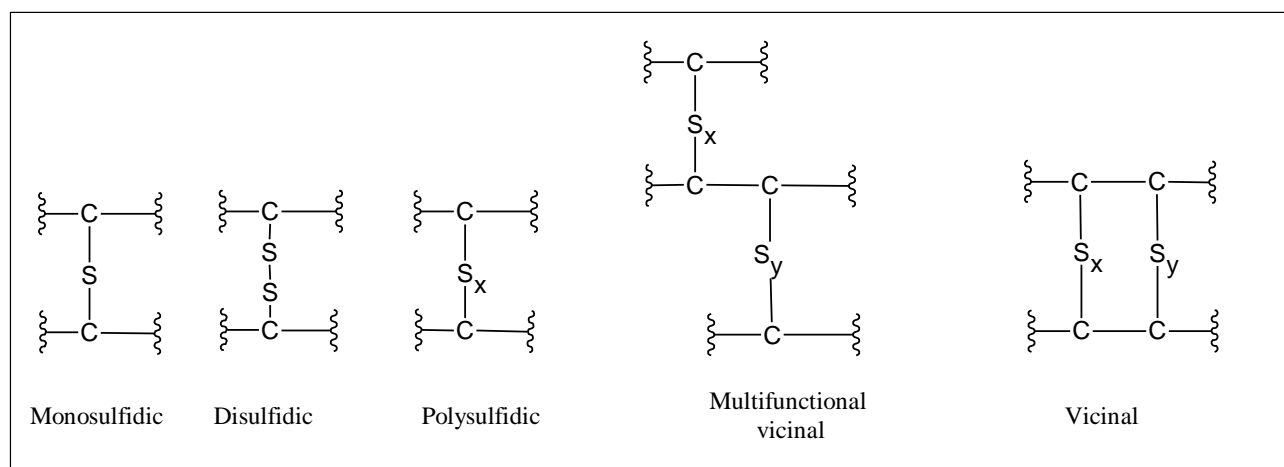
Fig.2.72 Generic structures in sulfur-vulcanized natural rubber (203).

Scorching time is the time elapsed before crosslinking starts rapidly increasing viscosity of cured material. To delay initiation process in order to handle or shape the rubber before vulcanization start, some delay agents such as N-(cyclohexylthio) phthalimide (CTP) or bisalkylpolysulfides can be used.

Others vulcanizing agents like peroxides on diene elastomers can be used, but the cost of peroxides and low mechanical strength of products limited this choice for friction material rubber premix (204).

Other possible crosslink systems are reported in tab.2.21

Rubber	Crosslink agents
Fluoro-rubber (FKM)	Polyamines, polyols, peroxides, diol-amines and radiation-induced.
Chlorinated and brominated butyl rubber	Quinoid, resin, metal-oxide, metal-dithiocarbamate and thiourea
Chloroprene rubber and epichlorohydrin rubber	Metal-oxide-, amine-, thiourea-, and thiuram-based crosslinking

Tab.2.21 crosslinking systems for different rubbers. (204)

Vulcanized rubber changes mechanical properties depending on crosslink density, an idealization of final properties can be seen in fig.2.73
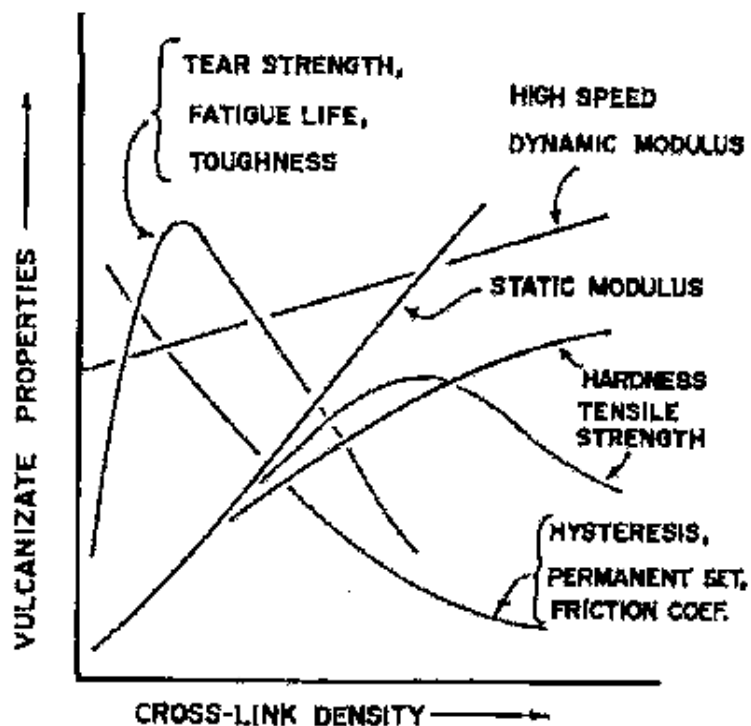
Fig.2.73 Major effects of vulcanization on rubber mechanical properties (205)

It's also possible using liquid rubbers, but their main contribute on friction compound is not noise suppression. Generally liquid rubbers are used to create a coating on premixed particles to avoid local aggregation and to prevent their dropping. (206)

2.7.2.2   Others functionalizers

The following is a quick overview of other functionalizers for friction materials.

Colorants are request in order to identify different layers composing a lining, indeed at components end-life it's good practice to have a visual indicator to recognize the end of friction material and the begin of underlayer. Thermal resistant dyes or pigments are mixed in underlayer for this purpose

Corrosion protectors. Corrosion is the main cause of brake disc-pad sticking. Iron oxides formed on disc and pad surface can act as adhesive when the two components are in contact in a steady state as it can happen for parking brake. In this case after oxidation at disc-pad interface even when parking brake is released, components stay stacked causing a complete block of the vehicle. To prevent this event a cathodic protection by addition of metallic zinc or tin to friction material formulation can be used. Moreover an alkaline environment can reduce cast iron oxidation rate, compounds like calcium hydroxide are typically used for this purpose.

2.8 Binders (raw materials)

2.8.1   Organic Binders

2.8.1.1   Phenolic resins

Phenol formaldehyde resin is one of main used binder for friction materials. The first commercial phenolic resin plant, Bakelite GmbH, was started on 25 May 1910 by Riitgerswerke AG at Erkner near Berlin (207).

Phenolic resins are produced by the reaction of phenols with aldehydes, for friction materials a phenol - formaldehyde polymer is used (3).

The synthesis can be performed following three steps

-   *Step1: Methylolated phenols formation.*

Formaldehyde addition to phenol follow the mechanism in fig.2.74 for alkaline condition.
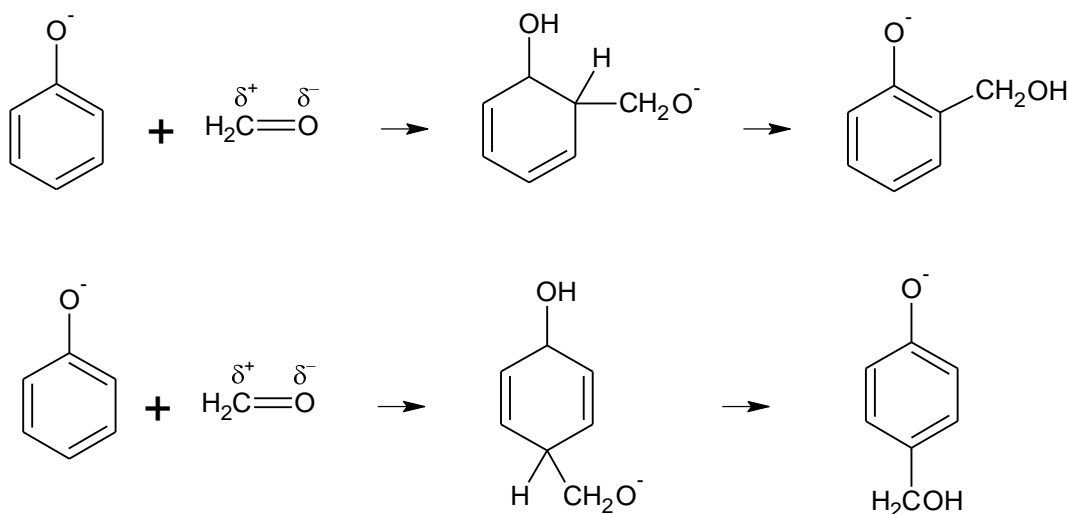
Fig.2.74 Phenol formaldehyde reaction in alkaline condition

For formaldehyde/phenol ratio >1 besides the monomethylol phenols, some dimethylol phenols and trimethylol phenol are obtained following scheme in fig.2.75 (208)
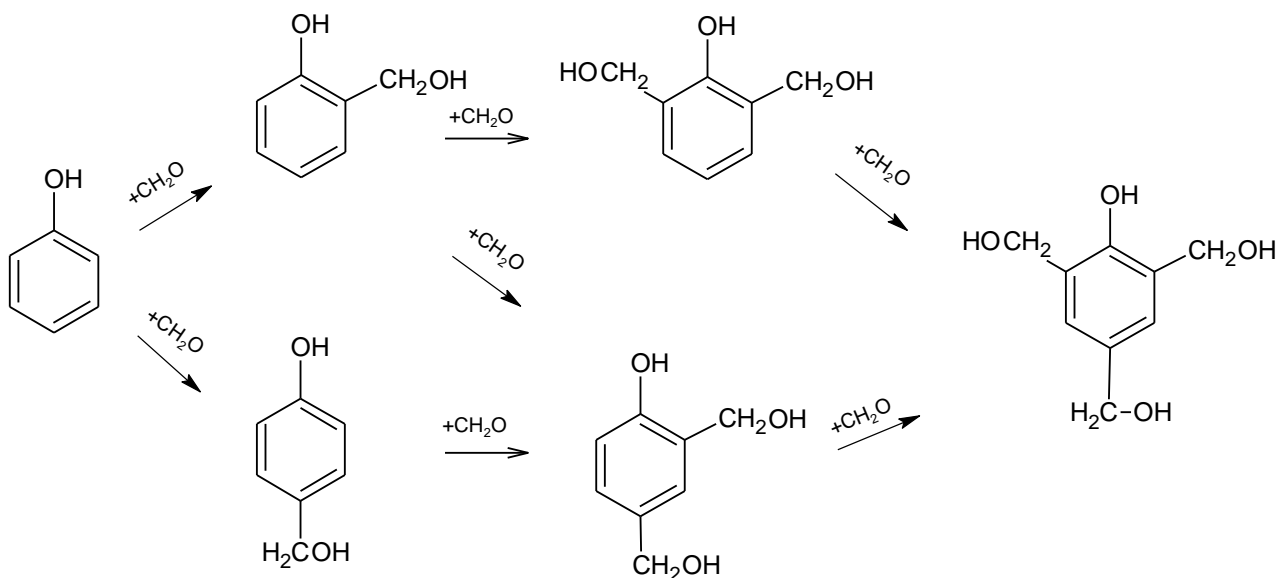
Fig.2.75 Methylolated phenols synthesis from phenol and formaldehyde in alkaline solution

$$H_2C=O \ + \ H_2O \ \rightleftharpoons \ HO-CH_2-OH \qquad\qquad 1)$$

$$HO-CH_2-OH \ + \ H^+ \ \rightleftharpoons \ H_2\overset{+}{C}-OH \ + \ H_2O \qquad\qquad 2)$$
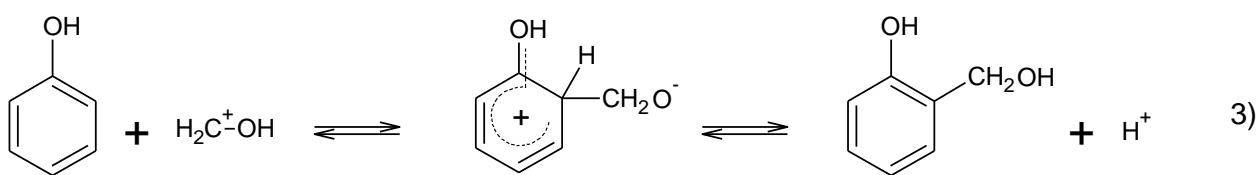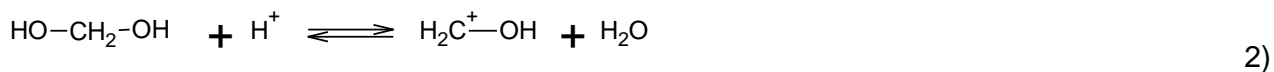
Fig.2.76 Phenol formaldehyde reaction in acid condition

Formaldehyde is dangerous to human health tab.2.22,

113

Hazard statements	Description
H301	Toxic if swallowed
H311	Toxic in contact with skin
H314	Causes severe skin burns and eye damage
H317	May cause an allergic skin reaction
H331	Toxic if inhaled
H335	May cause respiratory irritation
H341	Suspected of causing genetic defects
H350	May cause cancer
H370	Causes damage to organs

Tab.2.22 Hazard statements for formaldehyde
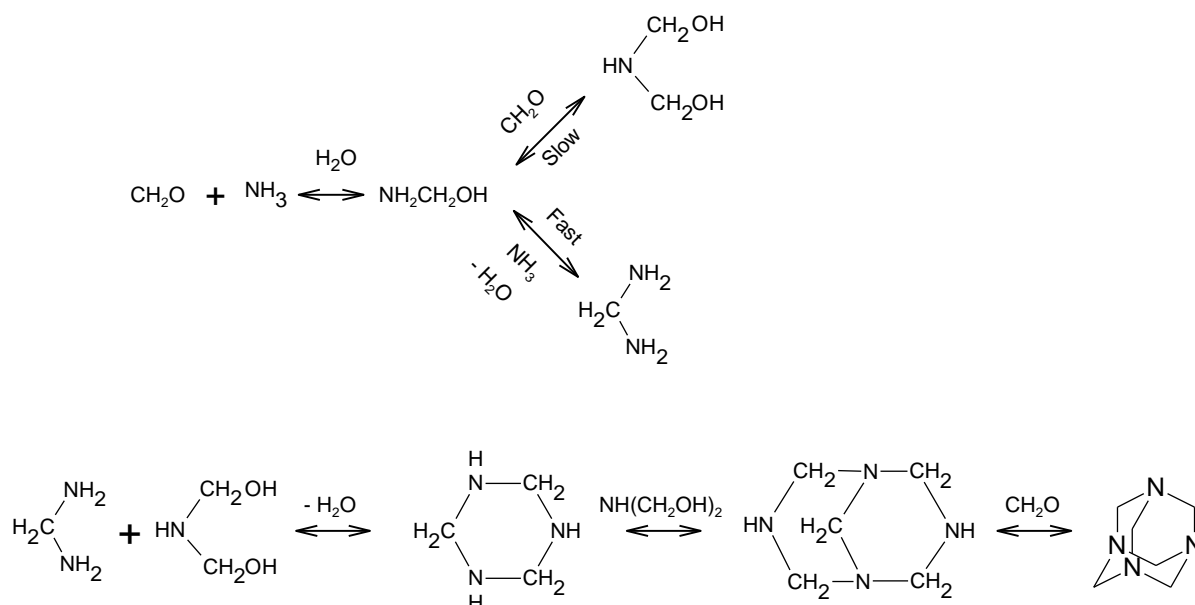
Fig.2.77: Hexamethylenetetramine synthesis, all reaction steps are reversible (209).

For industrial application is preferred using pentaerythritol [2,2-bis(hydroxymethyl)-1,3-propanediol] or hexamethylenetetramine (HMTA; 1,3,5,7-tetraazatricyclo[3.3.1.1]decane) Fig.2.77.

HMTA can be hydrolyzed to ammonia and formaldehyde. (210)

- *Step 2*: *Synthesis of oligomers.*

In alkaline conditions the absence of ortho-ortho bridges on the formation of oligomers is in accordance with a kinetic study of the self-condensation of tri(hydroxymethyl)phenol (211).

114

A first-order reaction in alkaline solution was interpreted as the formation of quinone methides.
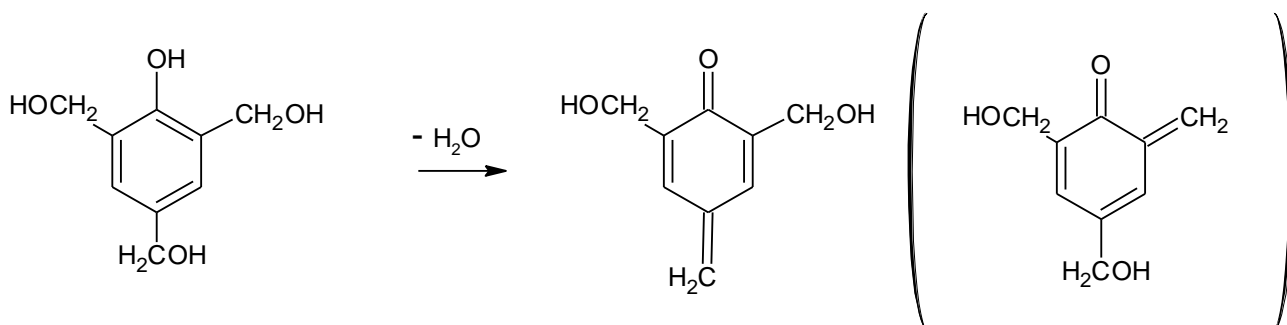
Fig.2.78: Quinone methides syntesis from dehydration of methylolated phenols

Quinone methides''' (212) formed as intermediates may react with free ortho or para positions to form methylene bridges, or with hydroxymethyl groups to form dimethylene ether links, which again may lose formaldehyde to form methylene bridges. A direct displacement of formaldehyde (ipso substitution) seems possible too Fig.2.79
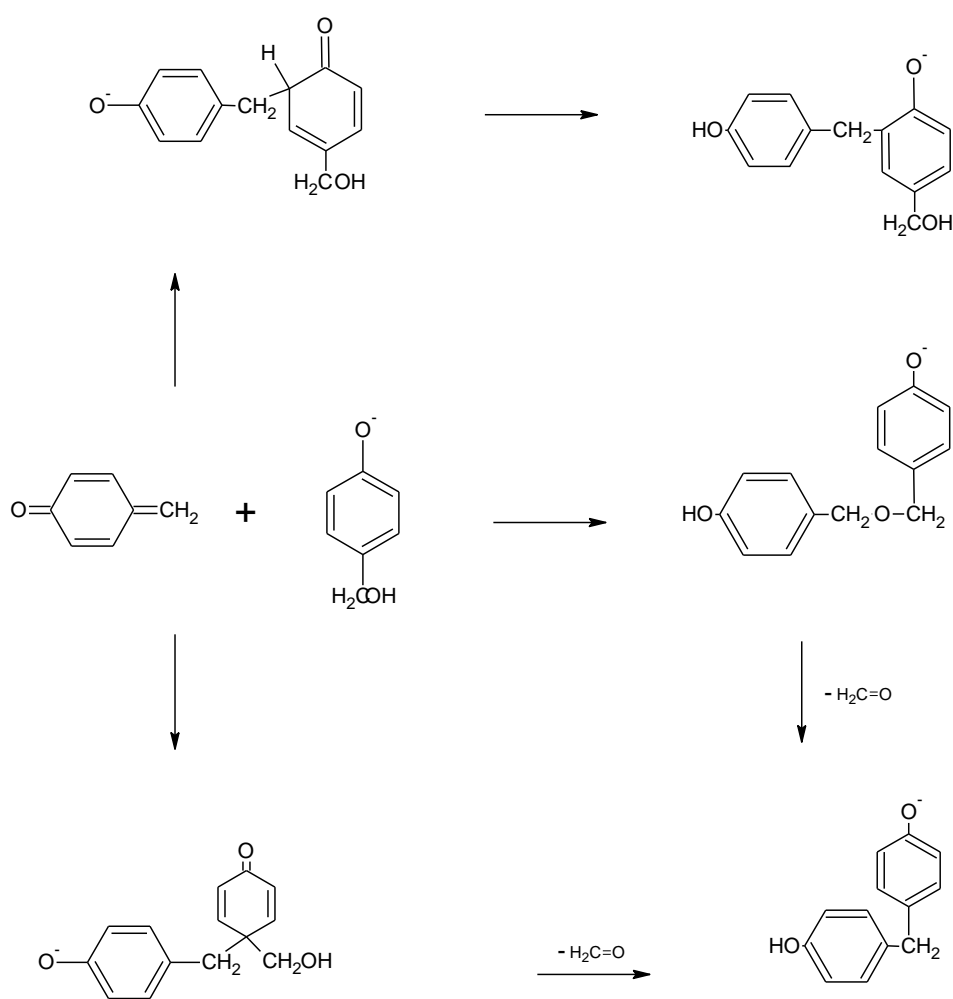
Fig.2.79 Phenolic resin dimers synthesis from p-quinone methide in alcalyne solution

In acid solution the main reactions are possible to connect phenolic units by methylene bridges are the condensation of hydroxymethyl derivatives with other phenols, which can also generate non-symmetrical structures, and the direct condensation with formaldehyde Fig.2.80 , that lead to symmetrical structures. (207)
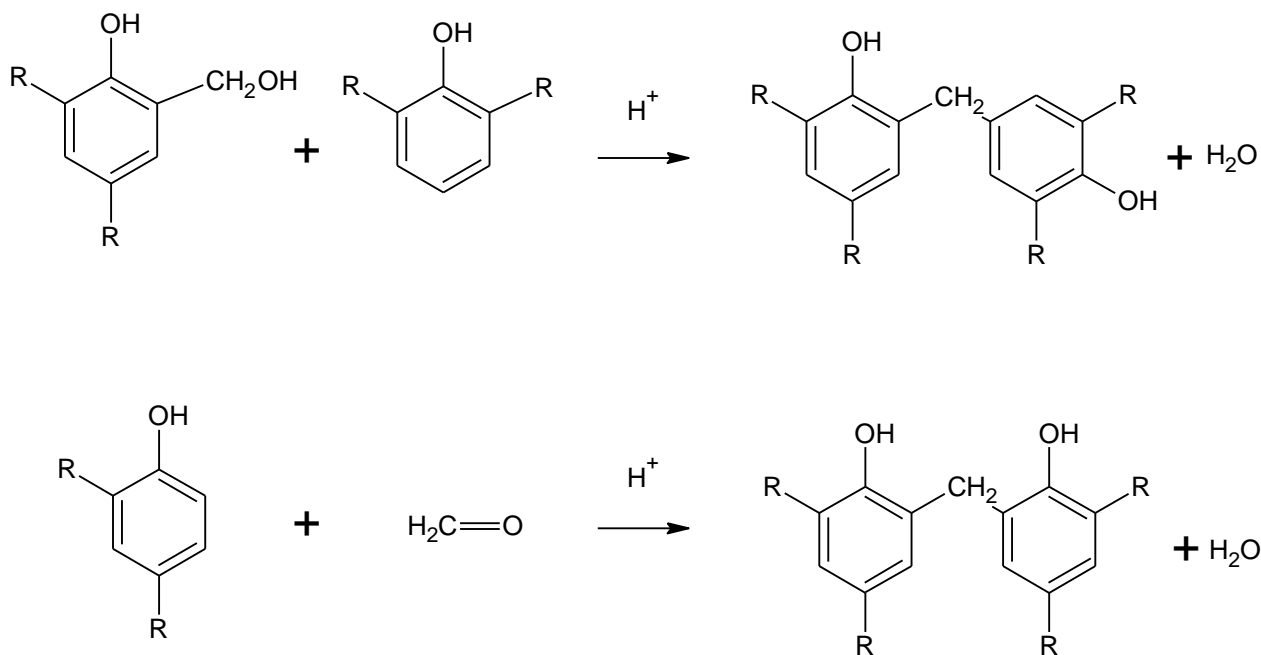
Fig.2.80 Phenolic resin dimers synthesis in acid solution

High proportion of ortho–ortho links needs a low curing activation energy, and temperature and reduce cure time (fast curing resins). To obtain a higher proportion of ortho–ortho links of the resins, it should be chosen the bivalent metal salt of an organic acid as the catalyst, especially the salts of Zn^{2+}, Mg^{2+}, Mn^{2+}, Cu^{2+}, Cd^{2+}, and Ca^{2+}; ZnAc2 has been proved to be an excellent catalyst (213).

Alkaline synthesis with phenol- formaldehyde molar ratio of 1 leads to form resol resins, acid synthesis with phenol-formaldehyde molar ratio less than 1 leads to form Novolak resins Fig.2.81.
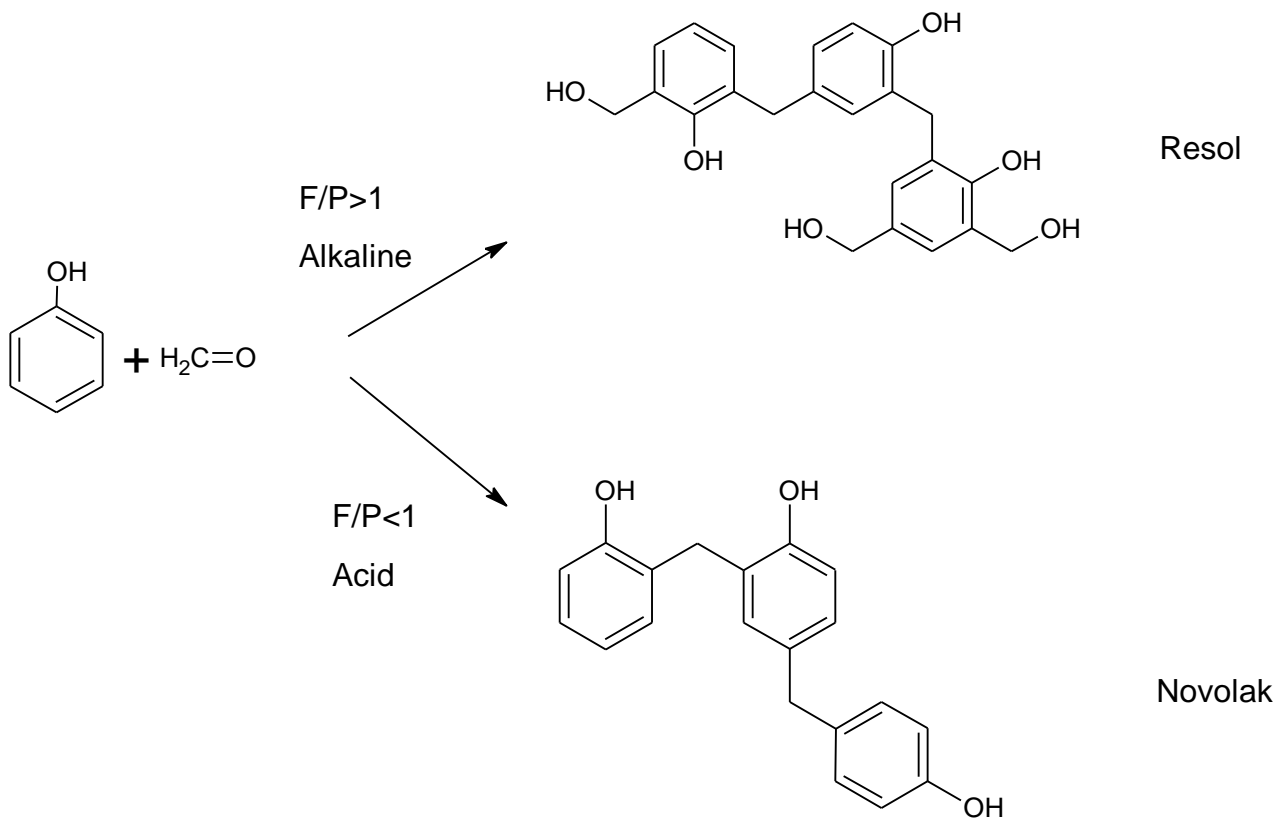
Fig.2.81: Novolac and resol formation from phenol and formaldehyde

- *Step 3: Curing*

Commercial resins are available in solid and liquid form, generally for friction materials a mix of novolak and resol resin, HMTA is used as cross-link agent; heating up the system it's formed a three-dimensional network thereby generating a very compact arrangement in the crystalline state (207) (208). Considering the hydrolysis products of HMTA as first step, benzoxazine and benzyl amines form as the initial intermediates, in a second step these initial intermediates are transformed into methylene bridges between phenol rings (210) (214), see fig.2.82
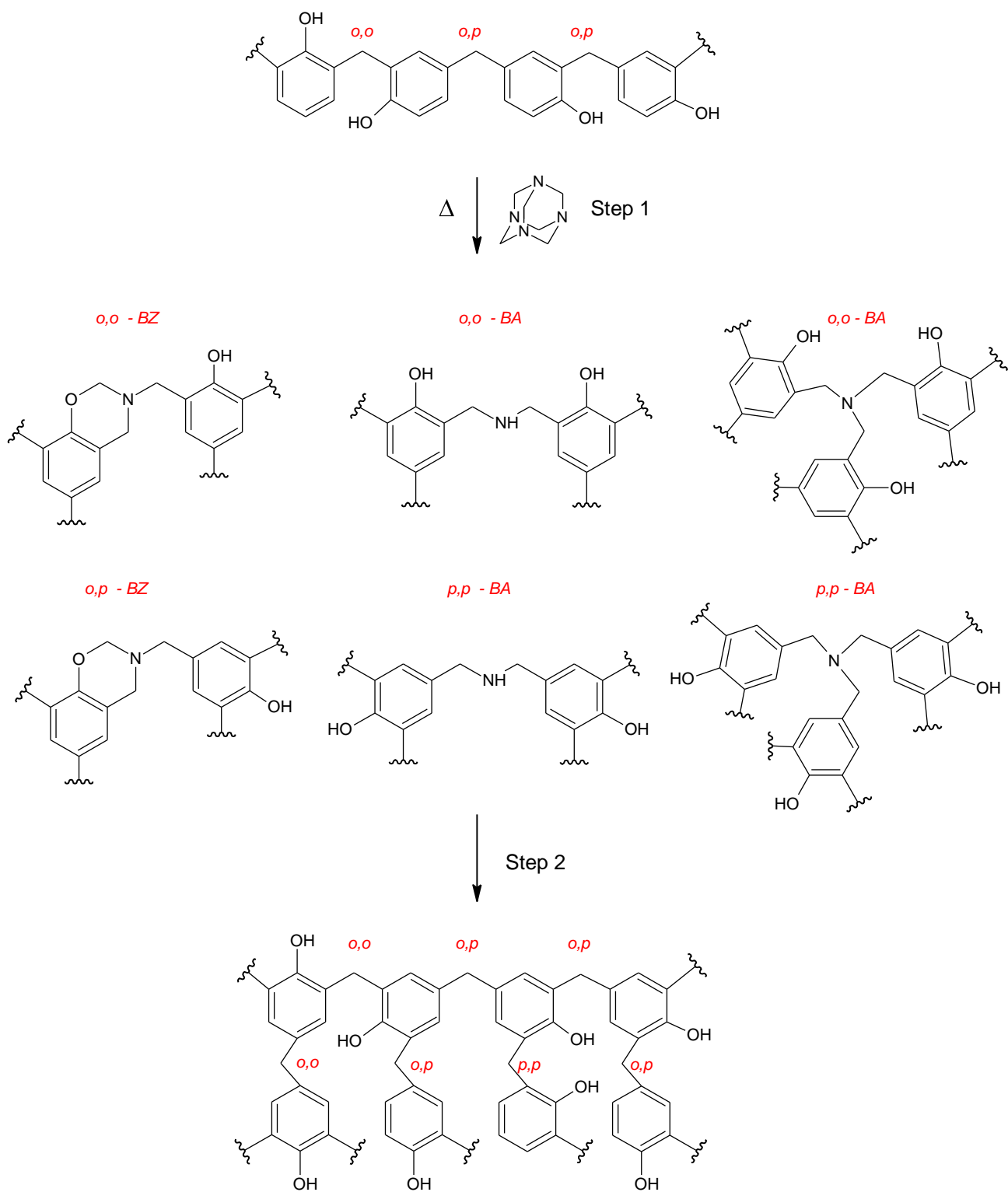
Fig.1.82 Curing process of novolak resin

Resole is called a single-step resin, indeed its thermoset can be obtained by simple heating the resin without addition of curing agents (215). Resole cross-linking can be accelerated using a cure accelerator such as resorcinol (10% based on phenol) anhydrides, amides, carboxylic acid esters, and carbonates.
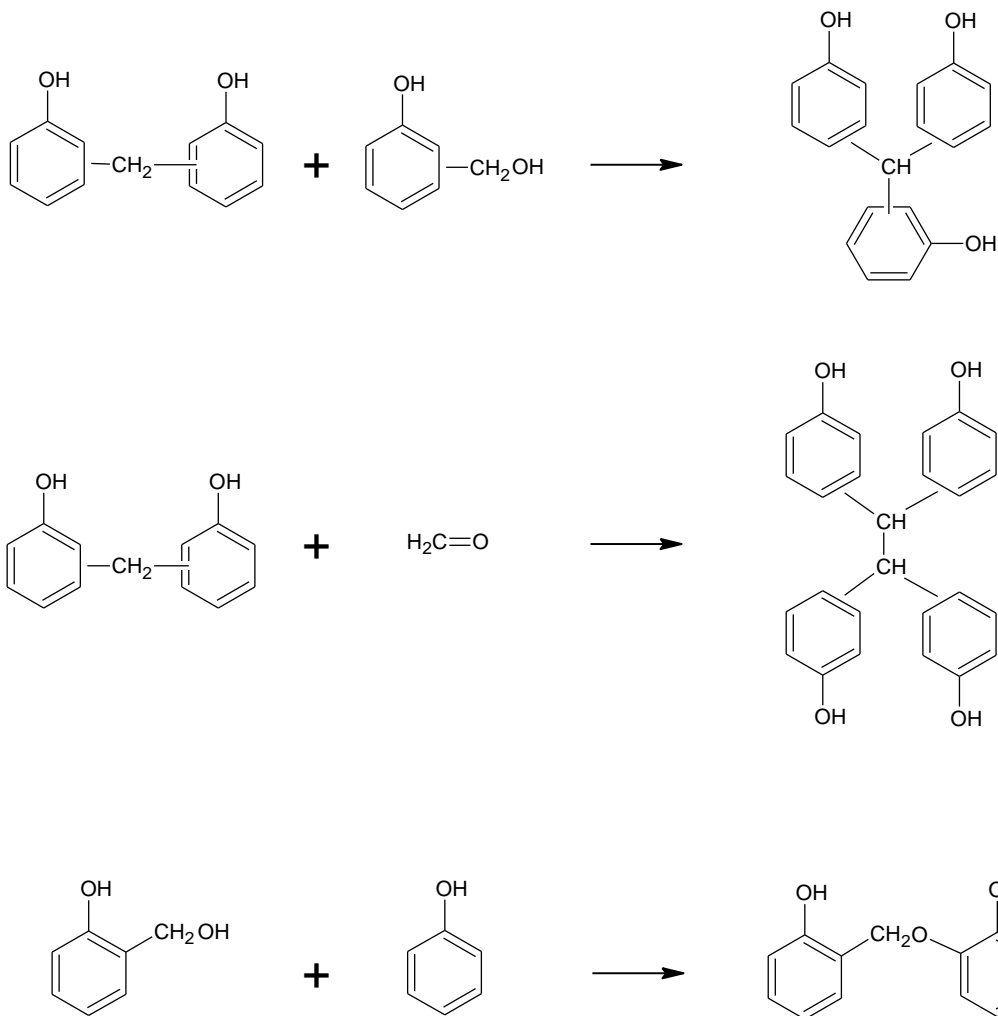
Fig.2.83 Curing of resol resin.

Complete cure of phenolic resol fig.2.83 leads to a highly crosslinked material exhibiting high modulus, excellent moisture and heat resistance (210).

2.8.1.1.1 Modified phenolic resin

To improve properties of phenolic resin some modification of the structure is possible.

- Phenolic resin modified *cashew nut shell liquid* (CNSL), containing Cardanol that improved flexibility, good drying after baking, high electric insulation properties and thermal stability, it increases also resistance to softening action of mineral oils and it has high acid and alkali resistance (216). Considering ecological and economical issue, CNSL is an excellent natural phenol-like source for polymer synthesis (217). It can be also polymerized separately with formaldehyde to form friction dust, also called cashew friction dust or CNSL dust, its flexibility contributes to brake noise reduction. (218)

119

- *Furfural* can be used as linking agent instead of formaldehyde, the curing time increase (slow resin) with increasing molecular weight of aldehyde. Phenolic resin builds its crosslinked network around each additive and "flows" in the interstitial spaces between particles during hot-press molding, slow resins can flow for more time before being hardened increasing his boding effect. Phenol/furfural resins yields products of greatly increment of toughness and hydrocarbon solvents resistance (219). Phenolic resin can also be CNSL-furfural simultaneously modified, see fig.2.84 (220)
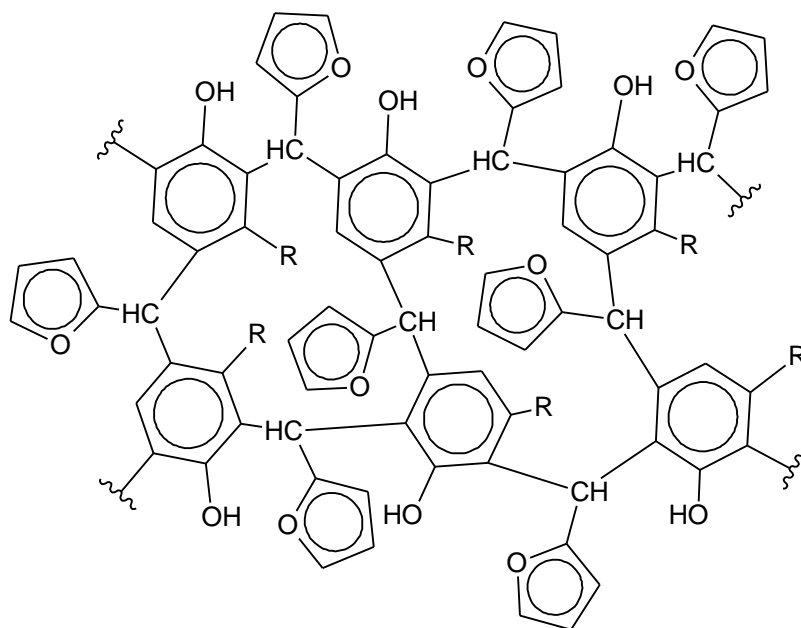
Fig.2.84 Proposed structure of cardanol furfural resin.

- *Boron modified* phenolic resin is synthetized from phenol formaldehyde and boric acid, it proves higher thermal resistance and superior mechanical strength respect common phenol-formaldehyde resins due to B-O bonding (221) (222).
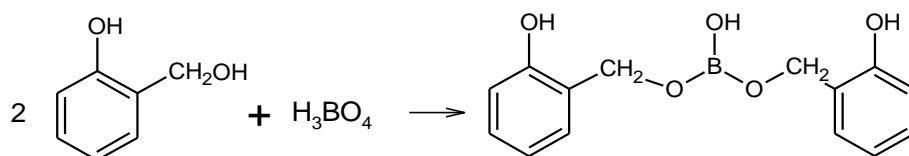
Fig.2.85 Boron modified phenolic resin

According to the European Classification, labelling and packaging of chemicals regulation (1272/2008/EG), boric acid and preparations that contain more than 5.5% boric acid have to be classified and labelled as toxic

to reproduction, category 2, this can limit the use of Boron modified phenolic resin in the future.

- *Acrylic rubber* modified resins providing excellent flexibility and vibration absorption. Due to relative high glass transition temperature (~ -10°C) so it is difficult to reduce the brake noise at this temperature using a general acrylic rubber. Special Acrylic rubber modified phenolic resins have been developed to keep a good flexibility until temperature of -30°C (223)

- *Silicone Rubber* modified Resin are polymers having good thermal stability, chemical and impact resistance, electrical insulation, water repellancy and anti-adhesive properties.
  Silanol groups undergo condensation reactions with the phenolic hydroxyls or with phenolic methylol hydroxyl groups of the cured phenolic resin to introduce Si-O groups into the phenolic polymer (224). See fig.2.86
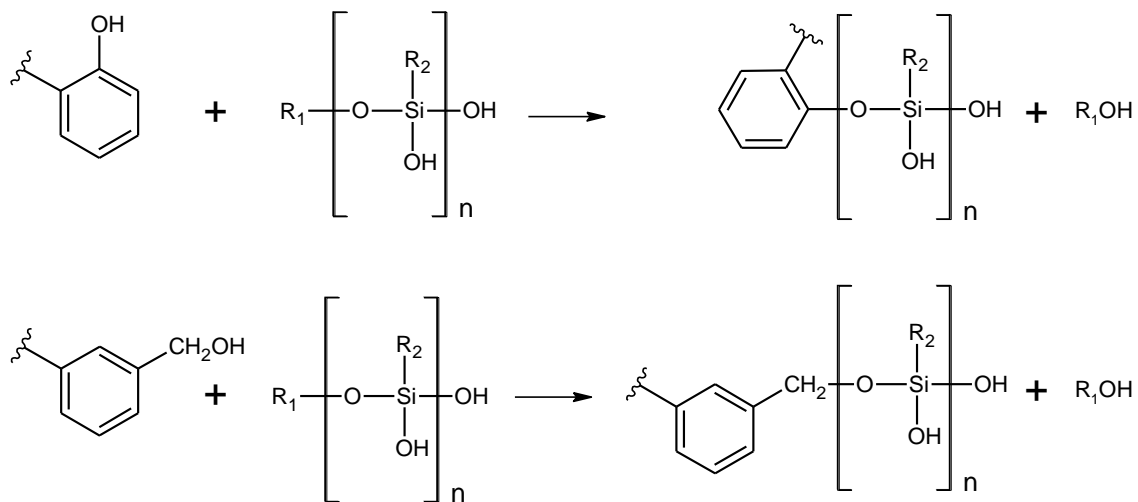
Fig.2.86 Silicon modified phenolic resin synthesis

- *Phenol Aralkyl* Resins have stable friction coefficient and wear, excellent heat and chemical resistance, anti-noise and vibratory qualities. Synthesis of Aralkil novolac resin is reported in fig.2.87
  To increase anti-noise and increasing thermal shock resistance (225) a silicone rubber-modified aralkyl novolac epoxy resin can also be used, see fig.2.88
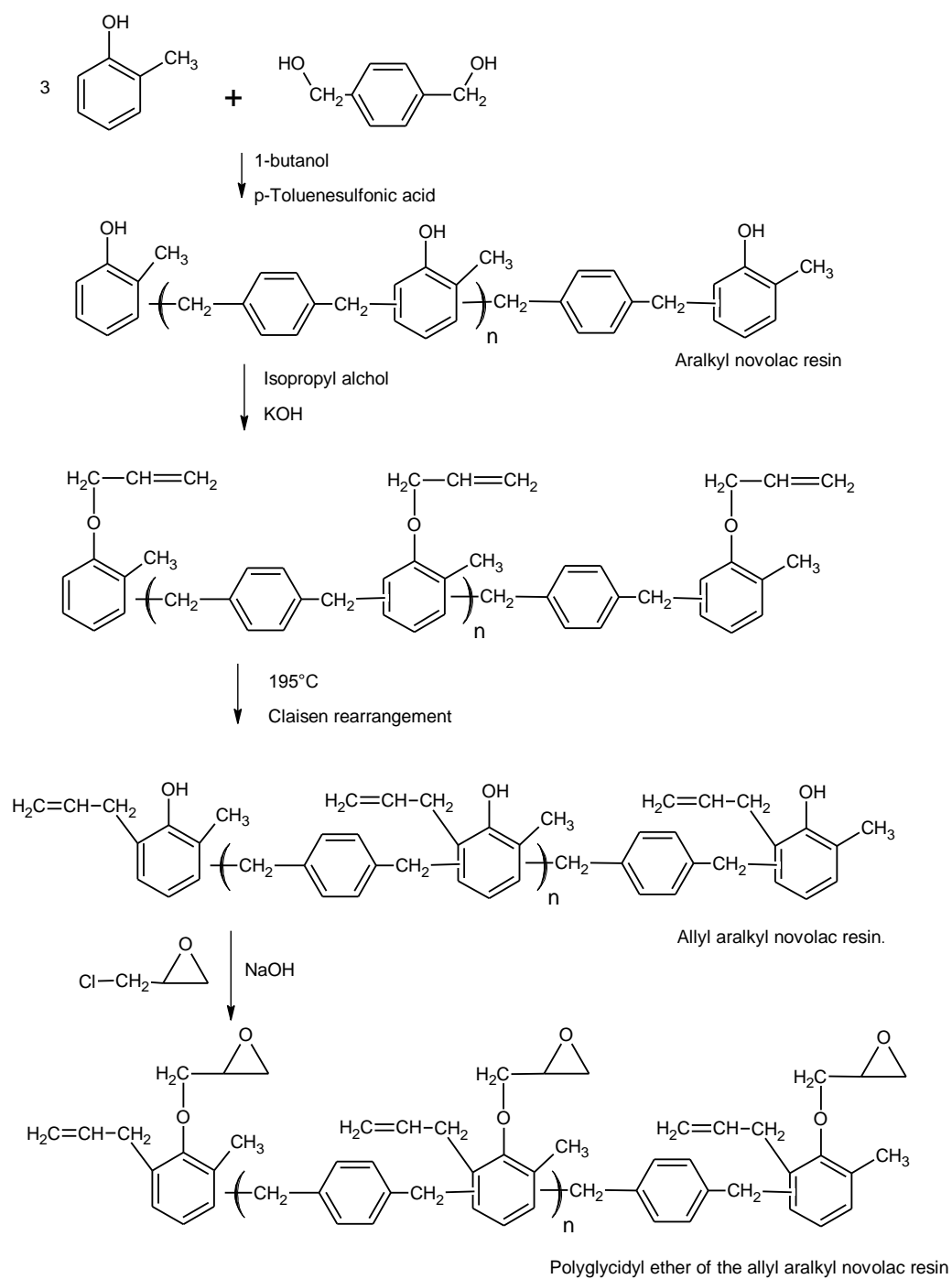
Fig.2.87 Aralkil novolac resin and polyglycidyl ether of the allyl-aralkyl novolac resin syntesis

122
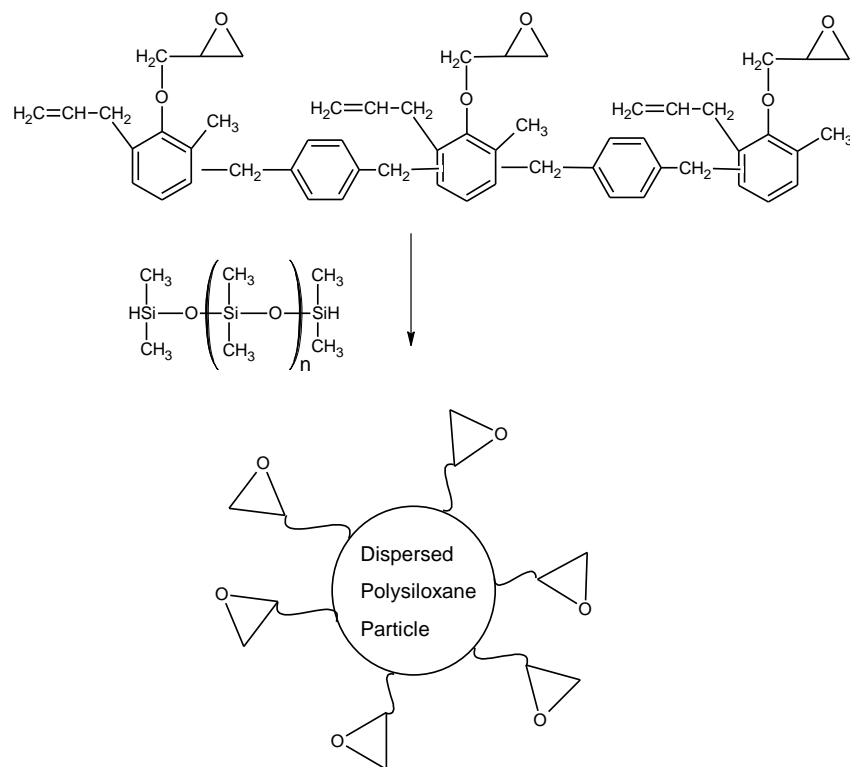
Fig.2.88 Silicone rubber-modified aralkyl novolac epoxy resin synthesis

- *Cyanate ester* modified resins are introduced due to their high temperature degradation resistance, other names for cyanate ester resins are cyanate resins, cyanic esters, or triazine resins. The synthesis is based on –OCN functional group that trimerizes in the course of resin formation to yield a highly branched heterocyclic polymeric network based on the substituted triazine core structure (226).
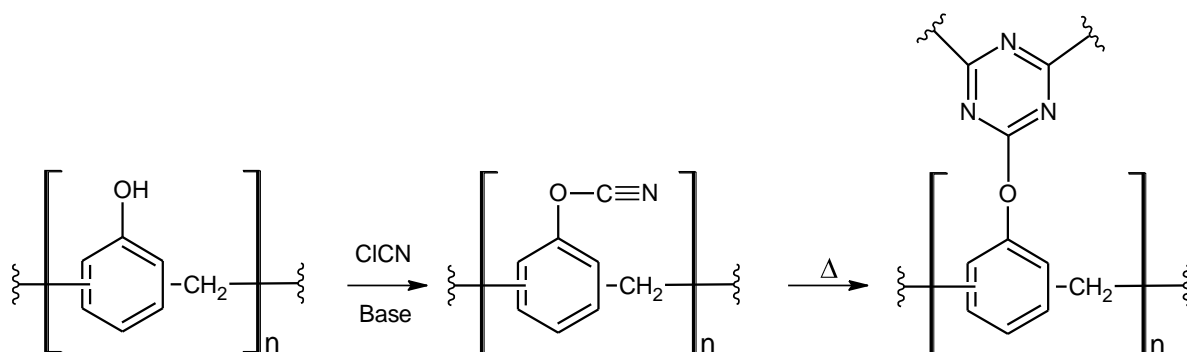
Fig.2.89 12 Poly phenol novolac cyanate ester synthesis and thermal curing

Cyanate esters modification confer high heat resistance, chemically inert and vibration dampener good properties to phenol formaldehyde resin but as negative aspect getting brittle, low-impact resistance material.

2.8.1.2   Silicone resins

For a special group of high performance brake pads, silicon resin binders have been studied in order to increase thermal resistance of friction material. A process of pyrolysis is required in order to achieve ceramisation by a process of pyrolysis of a preceramic silicon based binder at 400-600°C (5). This ceramic friction material has not to be confused with "ceramic material" labelled for after-market NAO based materials.

The synthesis of silicon resins can be achieved starting from different monomers (227).

Polymeric materials composed of a (Si-O) back bone with two monovalent organic radicals attached to each silicon atom as shown in fig.2.90, are generally called silicones (228).
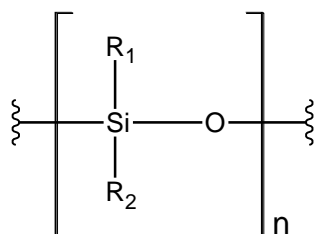
Fig.2.90 silicones backbone structure

The (Si-O-) repeat unit is also called as the "siloxane" bond or linkage, other terms can be used to describe these types of polymers such as siloxane polymers or polysiloxanes.

Synthesis starts from chlorosilanes and organoclorosilanes they easily react with water producing silanol, polysiloxanes can be achieved by polycondensation of silanol (229). Some silicones chemical structures with non-reactive substituents are reported in fig.2.91

I)   II)   III)   IV)
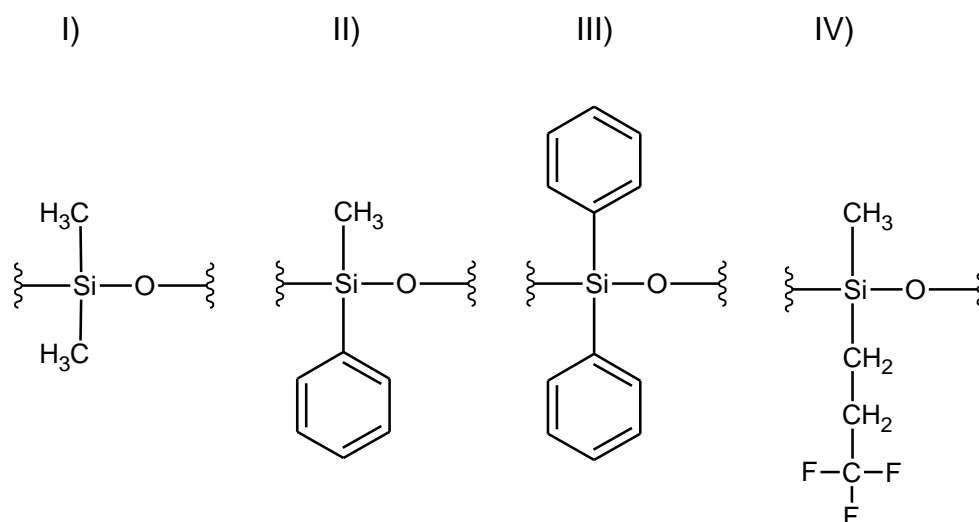
Fig.2.91 Some silicone polymer structures: I) Dimethylsiloxane, II) methylphenylsiloxane, III) diphenylsiloxane, and IV) 3,3,3-trifluoropropylmethylsiloxane.

Silicon resin based friction materials are commonly used for carbo-ceramic brake discs, after pyrolysis shows high and stable performance but low comfort in noise, vibration, and harshness (NVH) studies, this is acceptable for racing brake systems only. To improve NVH properties in non-racing application some hybrid silicon-phenolic resins based friction materials have been developed.

2.8.2   Inorganic hydraulic binders

The idea of using inorganic hydraulic binders in friction materials is not new, since the beginning of twentieth century brake blocks for railway were based on ordinary Portland cement (OPC). In more recent years many attempt were made friction materials based on cements and waterglass (230). In 1993 Kapl at. all developed a friction lining, based on mixtures of soluble silicates and reactive oxides such as those used in high temperature resistant cements, produced at low temperatures and without the need for high pressure equipment (231). Even if these materials are supposed to be highly heat resistant, in present days inorganic hydraulic binders are not widely used due to the inflexible nature of binders prone to brittle fracture (230).

The aim of this thesis work was to developed a friction material with a matrix based on an inorganic hydraulic binder and performance comparable to commercial organic-matrix based friction materials. Finely tuning of friction compound components and brake pads manufacturing process at high pressure and low temperature were required to achieve this results.

Inorganic binders were selected among Portland cements and among mineral admixture such as natural pozzolans, fly ash, calcined shale, calcined clay, silica fume, ground granulated blast-furnace slag and metakaolin

Portland cements are hydraulic cements composed primarily of hydraulic calcium silicates where setting and hardening is obtained by chemically reaction of cement clinker phases and water, see fig.2.92

$$2(3CaO \cdot SiO_2) + 11\,H_2O \rightarrow 3CaO \cdot 2SiO_2 \cdot 8\,H_2O + 3(CaO \cdot H_2O)$$

| Tricalcium silicate (C₃S) | Water | Calcium silicate hydrate (C-S-H) | Calcium hydroxide |

Tricalcium silicate (C$_3$S) Water Calcium silicate hydrate (C-S-H) Calcium hydroxide

$$2(2CaO \cdot SiO_2) + 9\,H_2O \rightarrow 3CaO \cdot 2SiO_2 \cdot 8\,H_2O + CaO \cdot H_2O$$

Dicalcium silicate (C$_2$S) Water Calcium silicate hydrate (C-S-H) Calcium hydroxide

$$2(3CaO \cdot Al_2O_3) + 6CaO \cdot Al_2O_3 \cdot 3SO_3 \cdot 32H_2O + 4\,H_2O \rightarrow 3(4CaO \cdot Al_2O_3 \cdot SO_3 \cdot 12H_2O)$$

Tricalcium aluminate (C$_3$A) Ettringite Water Calcium monosulfoaluminate

$$3CaO \cdot Al_2O_3 + CaO \cdot H_2O + 12\,H_2O \rightarrow 4CaO \cdot Al_2O_3 \cdot 13H_2O$$

Tricalcium aluminate (C$_3$A) Calcium hydroxide Water Tetracalcium aluminate hydrate

$$4CaO \cdot Al_2O_3 \cdot Fe_2O_3 + 10\,H_2O + 2(CaO \cdot H_2O) \rightarrow 6CaO \cdot Al_2O_3 \cdot Fe_2O_3 \cdot 12H_2O$$

Tetracalcium aluminoferrite (C$_4$AF) Water Calcium hydroxide Calcium aluminoferrite hydrate

Fig.2.92 Portland cement clinker phases hydration reactions (primary transformations only) (232)

Alternatively, mineral admixtures can be used with Portland cements or individually as alkali-activated binders (10) (11).

3   Experimental procedures and results

3.1 Proposal for innovative friction materials

The aim of this work was to investigate the feasibility to produce a new and alternative friction materials for passenger car disc brake pads with a low environmental impact respect to traditional friction materials based on organic binders. The idea was to substitute organic friction materials focusing on developing new braking materials based upon innovative friction mixes and inorganic hydraulic binders with enhanced properties, and subsequently testing the their friction performances. The use of inorganic binders can be considered more environmentally-friendly respect the use of traditional organic thermoset resin in terms of brake pad embodied energy and chemical emission during their manufacturing and use.

This thesis work was developed in different phases:

- *Raw material selection*

In this phase the raw material used for the production of organic and inorganic brake pads have been selected and controlled.

- *Organic brake pad manufacturing*

All organic brake pads were manufactured in the production site of Brembo Stezzano. It's reported here a quick overview of main production steps.

- *Chemical emission*

In collaboration with IRFMN IRCCS chemical emission of organic friction materials during the manufacturing process was measured. The analyses were focused on high temperature treatments.

- *Inorganic brake pad manufacturing*

Formulation of new friction material have been proposed on the consolidated experience an outstanding scientific and technological know-how of Brembo S.p.A. and the group technical center (CTG) part of Italcementi S.p.A. group. Various explored mixes were produced using the laboratory-scale approach where formulation of new inorganic materials required a fine tuning of friction components and binders so to maximize the final matrix-additives compatibility and the overall composite material performances. Beside organic matrix substitution, it was possible to achieved material formulations which envisaged the exclusion of any other organic components, maintaining only sources of inorganic carbon, i.e. graphites and cokes.

Not only chemical composition, but also the entire brake pad manufacturing technology had to be reconsidered due to different physicochemical properties of new binders.

Over this part of thesis work one patent (233) and one pending unpublished patent (234) were submitted.

- *Brake system testing*

Friction materials for brake pads need to have a composition such as to ensuring consistent and reliable performances in a wide range of operative conditions, in particular as the disc brake pads for vehicles operate under extreme and hard working conditions, providing at the same time reliability and a long life, therefore friction materials performances must be subject to rigorous and severe testing procedures which regulate their use.

Since it was estimated that up to 55 wt.% of non-exhausted traffic related PM10 emissions are due to brake wear alone (235), new materials should pay specific attention to this issue. Inorganic materials were expected to be more environmental friendly in terms of chemical emission respect to organic traditional ones, therefore wear particle emission during their use has been measured

On this part of thesis work, two unpublished papers have been submitted (236) (237).

3.1.1   Raw material selection

In the previous chapter components generally used in friction material formulation were described. Considering that for each proposed ingredient are available many commercial grades the selection was made on thousands possible raw materials.

Hundreds raw materials have been selected and every material batch was analyzed to verify conformity with the manufacturer specifications. Each material required different analytical equipment and methods depending on its chemical nature, shape, size and physical state. All this data is part of Brembo S.p.A. know-how, it's shown here as example a copper fibers analysis (different commercial grades) and phlogopite mica analysis (different batches of one selected grade). In raw material selection process, saving of embodied energy and embodied water due to new friction material binders was also considered.

3.1.1.1 Copper fibers analysis (different material grades)

As example of analysis of different material grades, it's shown the difference of some copper fibers commercially available. The main properties analyzed were

properties declared on suppliers specifications such as density, size, chemical composition and morphology.

Bulk density of fiber (or powders) is the ratio of the mass of a sample and its freely settled volume including the contribution of the void volume measured with a graduated cylinder. This information is useful during friction mix preparation to calculate the final volume of friction mix, and therefore to calculate the maximum weight of friction mix to prepare considering the mixers volume.

Tapped density or jolting density is the ratio of the mass of a sample and its volume after it is tapped in a graduate cylinder until a little volume change is observed. To determinate tapped density of fibers has been used a jolting volumeter STAV II according to ISO 787/11, except where the standard procedure foresees that the sample is dried in an oven before the test.

Sieves analysis. Even if it is not the most reliable method to evaluate the real fiber dimension due to their non-spherical shape, sieves analysis is one of the most used on quality control on metal fibers. To evaluate fiber size distribution, sieves with different meshes were used on a Retsch vibratory sieve shaker of the series AS 200 according to ASTM B214.

Chemical composition of fibers was measured using a wave dispersive X-ray fluorescence spectroscopy. Samples of 3 mm in diameter had been prepared with a laboratory press where fibers had been compressed at room temperature on an aluminum sample holder for 5 min with a pressure of 345 bar. The WDX-XRF analytic instrument used was a RIGAKU ZSX Primus II equipped with 4kW Rh target x-ray tube AFX88L, LiF200, Ge, Pet, RX-25 analyzing crystals suitable for elements from F to U, as detector a gas flow proportional and a scintillation counter. The analytical procedure was the qualitative EZ-Scan standard-less method provided by ZSX Primus II software. Chemical analysis was important to measure Cu purity in order to guarantee the absence of undesired toxic elements such as lead, cadmium arsenic and antimony.

Morphology of different samples was investigated with the aid of a scanning electron microscope Zeiss EVO MA 10, all the images were compared at the same magnification scale.

Eight copper fiber grades from different suppliers were analyzed, see tab.3.1

Copper fiber	Density ISO 787/11		Sieve Analysis ASTM B214							Chemical composition
Grade code	Bulk (untapped) density (g/cm3)	Tapped density (g/cm³)	710 μm (%)	425 μm (%)	212 μm (%)	150μm (%)	125μm (%)	106 μm (%)	Pan (%)	Cu (wt. %)
F12	3.79	4.24	0	0.9	94.72	-	4.38	-	-	99.82
F1	4.02	4.29	-	1.08	-	-	-	98.92	-	99.38
F9	4.08	4.39	-	3.07	-	96.93	-	-	-	99.15
F15	2.62	3.18	0.3	5	26.93	-	67.77	-	-	99.93
F13	2.38	3.05	1.05	8.55	31	-	-	-	59.4	99.95
F11	2.42	2.67	1.4	15.7	38.1	-	-	44.8	-	99.8
F5	1.81	2.32	4.19	18.47	-	51.13	-	-	26.21	99.77
F14	1.81	2.12	4.14	17.28	26.42	32.28	-	-	19.88	99.82

Tab.3.1 Density, sieve analysis and chemical composition of different copper fiber grades.

Comparing the residues at 425μm a general trend where for high residue correspond a higher tap density can be seen, fig.3.1
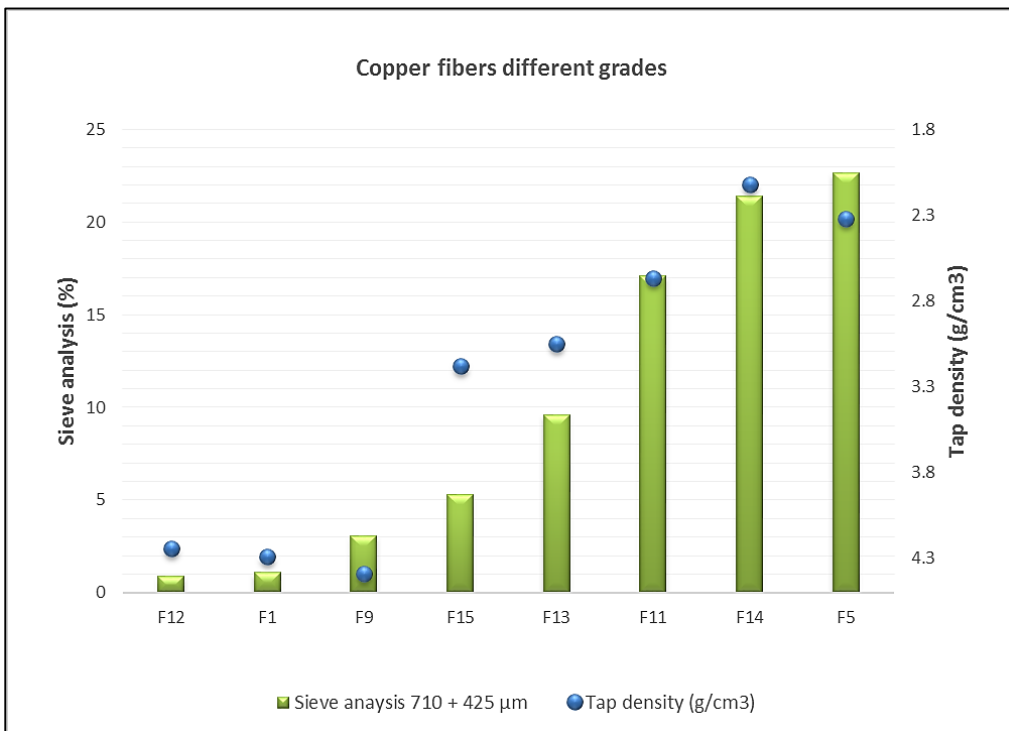
Fig.3.1 Tap density and sieve analysis results for different copper fibers grades.

An overview of SEM sample images shown how entangled fiber bundles F15, F13, F11, F14, F15 have higher reside for high sieves mesh even if thinner than F12, F1 and F9, see fig.3.2
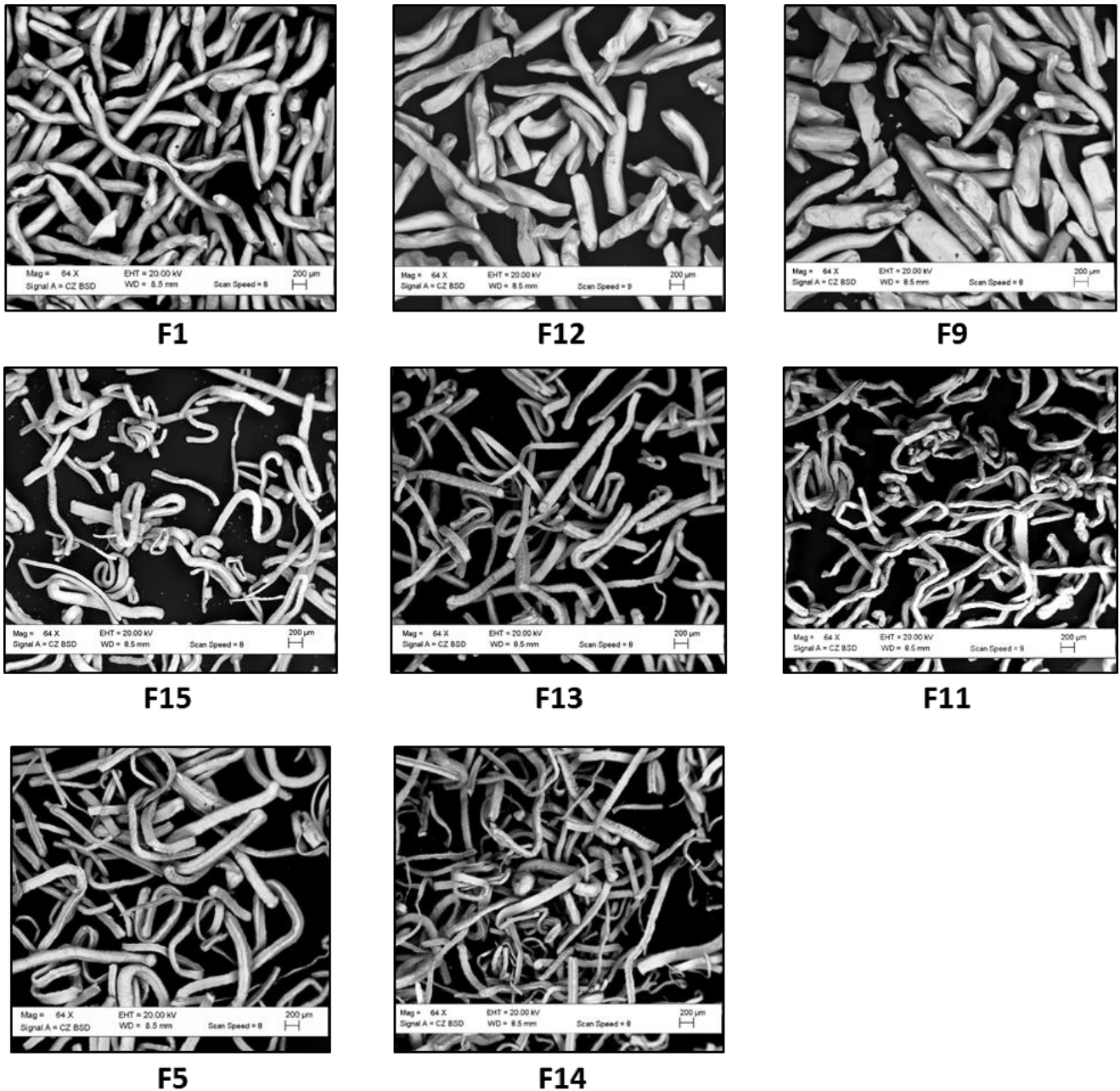
Fig.3.2 Copper fibers of different grades. Scanning electron microscope images compared at same magnification

Sieve analisys is not appropriate to measure fiber dimension (238), but can be correlated to the flowability of fibers during the mixing process and it's a fast and reliable quality control test that ensures the conformity at supplier specifications.

3.1.1.2 Analysis of phlogopite mica (different batches of selected grade)

Reliability of brake pads performance is related to the constance of raw materials specification and manufacturing process repetibility. Every raw material was analised to check the conformity at supplier specification.

The origin of material is not known, a material distributor provide his own technical and medical safety data sheet reporting only the main characteristics of the material on specifications. Even if a supplier assure that the material came from the same mine, the extracted material composition is not the same in the whole mine site, so that different batches can give different chemical composition.

Fig.3.3 Phlogopite mica, powder aspect on the left and SEM-BSD images on the right

Sample #	Si (wt.%)	Mg (wt.%)	K (wt.%)	Al (wt.%)	Fe (wt.%)	Ti (wt.%)	F (wt.%)	Ba (wt.%)	Ca (wt.%)	Cr (wt.%)
1	29.82	17.74	19.10	9.47	14.79	3.22	1.40	1.41	0.82	0.80
2	34.00	20.12	14.87	10.56	10.58	2.16	1.89	1.26	2.32	0.55
3	32.73	19.72	16.41	10.53	11.00	2.44	1.89	1.27	1.96	0.61
4	32.80	19.93	15.77	10.40	11.05	2.36	1.86	1.31	2.40	0.59
5	32.30	20.28	17.16	10.64	11.29	2.56	2.01	1.22	0.67	0.64
6	32.60	19.91	17.46	10.73	11.32	2.64	1.84	1.06	0.60	0.65
7	32.60	19.90	17.43	10.68	11.24	2.64	1.82	1.16	0.70	0.64
8	32.62	19.93	17.01	10.57	11.36	2.57	1.76	1.14	1.17	0.62
9	31.73	18.59	15.53	10.02	13.56	2.70	1.16	1.52	1.39	0.72

SAMPLE #	Na (wt.%)	Ni (wt.%)	Mn (wt.%)	Cl (wt.%)	S (wt.%)	P (wt.%)	Rb (wt.%)	Sr (wt.%)	Zn (wt.%)
1	0.24	0.53	0.12	0.00	0.00	0.00	0.00	0.00	0.00
2	0.37	0.34	0.12	0.22	0.17	0.16	0.12	0.10	0.00
3	0.31	0.34	0.12	0.22	0.09	0.09	0.11	0.08	0.00
4	0.36	0.33	0.12	0.21	0.09	0.12	0.11	0.09	0.00
5	0.29	0.36	0.09	0.23	0.04	0.02	0.12	0.03	0.00
6	0.30	0.35	0.09	0.23	0.02	0.01	0.12	0.02	0.00
7	0.28	0.36	0.10	0.23	0.03	0.02	0.12	0.03	0.02
8	0.29	0.35	0.10	0.22	0.05	0.04	0.12	0.05	0.03
9	0.35	0.42	0.15	0.19	0.09	0.10	0.14	0.13	0.03

Tab.3.2 Phlogopite mica WDX-XRF analysis of 9 different batches temporally ordered from the older (1) to the last sample received (9).

Chemical composition of eight different batches was analyzed with WDX-XRF technique. Results of analysis are shown in tab.3.2

Even if all the batches are in supplier specification range, due to high amount of elements measured is not simple to define a data trend.

To emphasize variation and bring out strong patterns in chemical analysis dataset "R" software to performs a principal components analysis on main 9 elements was used see fig.3.4
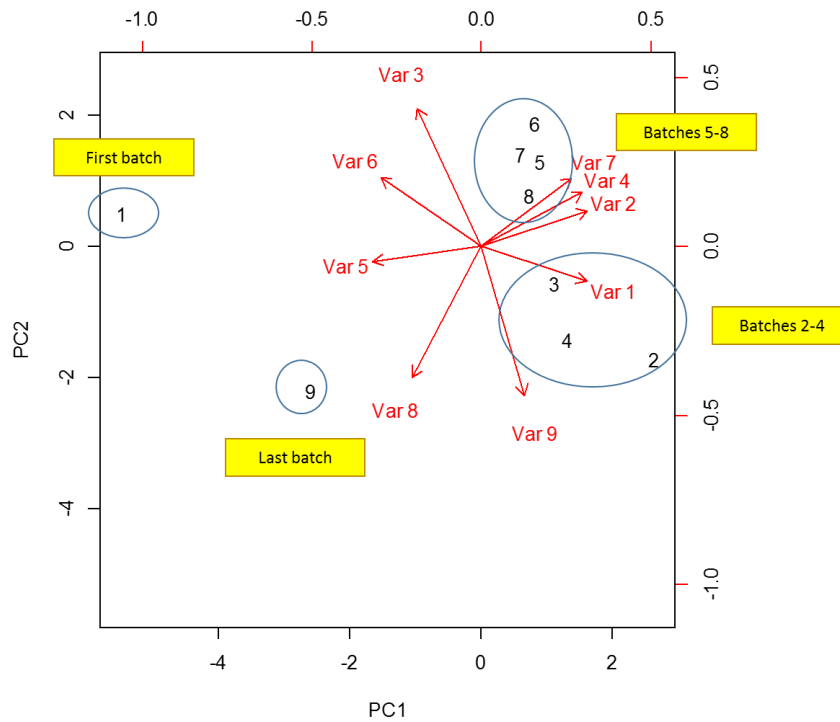
Fig.3.4 Correlations between WDX-XRF measures on phlogopite mica samples mapped onto first two principal components. Black numbers are batches and red vectors are variables

On PCA plot similar observations are close to each other and similar variables are close to each other. Projection of sample batches on first two principal components shown as first (prototype) batch was quite different from batches 2 to 4 and again different from following batches 5 to 8 and 9. Plotted data could discriminate a temporal trend of chemical analysis performed on subsequently batches.

3.1.1.3   *Evaluation of embodied water and energy*

Introducing inorganic binders in place of the traditional phenolic resin lead to a substantial reduction of the total embodied energy of brake pads only considering raw materials selection. Primary production embodied energy for phenolic resin is estimated in the range of 75 - 83 MJ/kg, while primary production water usage (embodied water) is in the range of 94 - 282 l/kg (8).

As a matter of comparison, examples of the embodied energy for inorganic raw materials typically used for concrete construction are: Portland cements 4.9 MJ/kg, silica fume 0.036 1.4 MJ/kg, metakaolin 1.4 MJ/kg and fly ash 9.3 MJ/kg. The embodied water for these raw materials usually is less than 0.048 l/kg (9).

Some of this inorganic materials required an alkali-promoted-hardening, it is in fact widely accepted, that these alkali activated material (e.g. natural volcanic ash, blast furnace slag...) exhibit enhanced thermal properties and fire resistance with respect to common Portland cement, so the well-known properties of such peculiar inorganic materials to come to a complete hardening at high pH values was considered (10) (11).

Energy demanding raw materials involved in this alkali-activated inorganic binder formulations were the alkali activators (e.g. for sodium hydroxide and sodium silicate the embodied energy is respectively of 22MJ/kg and 16 MJ/kg (12)). The estimated embodied energy for the inorganic binders (included alkaline agents) employed in tested formulations resulted less than 1.5 wt.% of phenolic resin counter-part, whilst the embodied water (included water of alkaline water solution) corresponded to less than 0.15 wt.%, both calculated using literature average values (8) (9) (12). Considering that the use of phenolic resin in literature organic low-met friction materials is from 7 to 12 wt.% (239), embodied energy and water saving on binder materials was guaranteed.

3.1.2   Brake pads manufacturing

3.1.2.1   *Organic brake pad manufacturing*

Organic brake pads can be produced in many ways; here, it's reported the method that was used to produce brake pad based on phenolic resin.

1. Friction material mix preparation

- Weighting of components

Following the friction material receipt each component is weighted on Sartorius Master LA2200P or CPA34001P balances depending on weight range, precision and accuracy required.

- Rubber premix

To produce rubber premix, discontinuous (single batch) Harburg internal mixer with capacity of 3,5 l was used. A special intermeshing rotor system resistant to abrasion has been used to intensive blend rubber and other components see fig.3.5. An internal cooling system was required to keep temperature under control during the exothermal vulcanization process and to compensate heat generated by intensive shearing.
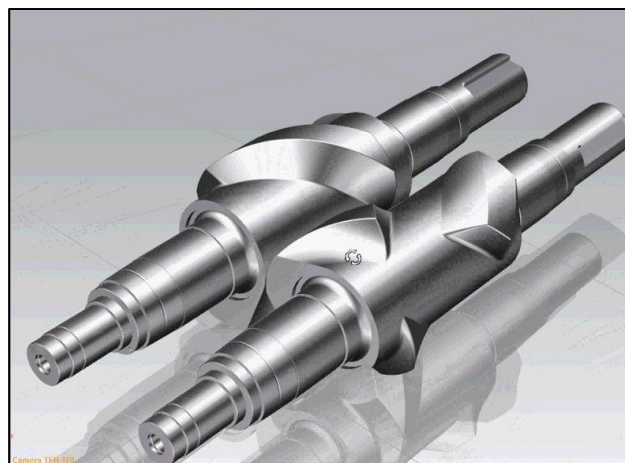
Fig.3.5 Example of intermeshing rotor system, the rotor of each shaft meshes with the other. Mixing is performed not only between the two rotors, but also between the rotors and the chamber wall (240)

After the mixed rubber compound had been discharged and cooled, Rapid granulator AB. was used to mill rubber premix to a defined particle size.

- Friction mix

Friction material components (included rubber premix when required) was dry blended by Eirich intensive batch mixers R05 type equipped with choppers and plow blades.
For short blending time components still agglomerate and unmixed, moreover fiber bundles are not adequately disentangled, for long blending time materials with different nature and shape can segregate, therefore a correct blending time is fundamental to reach an homogeneous mix.

2. Backing plate preparation

Backing plate is the steel plate where the lining is bonded by adhesive or mechanical attachment.

- Sandblasting

Sandblasting process is necessary to remove oxides formed during components shipment and other possible surface contamination.

- Adhesive application

For organic brake pads an adhesive coating was applied on sandblasted surface by a roll coater; the excess was deburred. Adhesive was an epoxy resin, it was activated by thermal curing on high temperature steps.

- Marking

Material edge code or experimental batch code is permanently marked on back of steel plate by means of a punching machines.

3. Hot press molding

In organic brake pads the raw materials cohesion is ensured by the intrinsic characteristic of the phenolic resin which essentially "flows" in the interstitial spaces between particles during hot-press molding and builds its crosslinked network around each additive. In this way the thermosetting behavior of the resin ensures the incorporation of each materials into a final compact hard material.

All organic brake pads was manufactured by IAG laboratory press mod. 633 with a double cavity mold. Alfa Romeo 939 (front axle) braking system type was the archetype for all the experimental investigations. the. Blended friction mix was distribute in the hot mold (150-200 °C) and pressed against backing-plate at controlled pressure (>2,5kN/cm^2), for the required time (3-10 minutes), the brake pad superficial area was 77 cm^2. When an underlayer was required the underlayer mix was distribute between friction mix and backing plate. During hot pressing molding cycle, the pressure can be reduced for some seconds to permit at water and other volatiles released at high temperature to degassing from the lining. The selection of press parameters depends on friction material composition and influences the final brake pad properties (241). An excess of material was used to produce pads thicker than required, then pads were grinded to reach good flatness and parallelism.

4. Thermal treatments

- Oven

A thermal treatment was required to complete phenolic resin cross-linking reaction on the inner part of molded pads. Wear test conducted by Hentati et all. (242) showed that material post cured for short duration presented higher levels of friction and lower wear resistance. This step is usually performed in a batch convective oven at temperature above 150 °C for 4-12 h, or alternatively using a continuous process, in a IR in-line tunnel ovens (process time 10-15 min, oven heater temperature between 500 and 700 °C, with a brake pad superficial temperature easily above 300 °C).

- Scorching

Thermal fade is the process where brake linings exposed to high temperature reduce their friction efficiency. Two main factors affected friction efficiency at high temperature (143):

a) Gas emission at interface due to material thermal degradation (243)
b) High rate of friction film formation which increases the true contact area, reducing applied pressure on pad surface. (244)

Scorching is used only when a stable performance is required from the early stage of brake pad usage. The intensive thermal treatment on pad surface simulate the thermal fade during pad use, it was made pressing hot plate (T>520 °C) on friction surface for 15–60 s. IR in-line tunnel ovens can also be used for this purpose. After scorching a final grinding was necessary to respect dimensional tolerances in terms of flatness, parallelism and pad height.

5. Painting

To protect metallic pad parts by corrosion, pads were painted on the edges and on backing plate using an electrostatic coating manufacturing process.

After the cleaning of surfaces with a shoot peening process the epoxy paint was electrostatic deposed. Epoxy was cured in an IR tunnel oven where the temperature, measured at pads back-plate, was linearly raised from 25 to 230°C in 6.6 min, then pads were cooled in a tunnel equipped with an extractor fan system.

6. Finishing

There are some parts that can be added at the end of pad manufacturing process.

- Shim

Shim or insulator plate is an anti-noise that can be attached on back of the backing plate. This device is made by different combinations of layers of rubber, carbon steel, stainless steel, fibre glass, cold adhesives (acrylic or silicone based) and hot sensitive glues, see fig.3.6

Fig.3.6 Example of multilayered shim (245)

- Labelling

Commercial pads required other information besides edge code, such as batch number, company name, bar code etc. Pad printing or paper labelling can be used in this manufacturing step

Fig.3.7 Main manufacturing steps of commercial organic brake pads. (Courtesy of Brembo S.p.A.)

3.1.2.2   *Inorganic brake pad manufacturing*

3.1.2.2.1   Laboratory samples

The preliminary work was conducted on the laboratory scale by preparing 13mm height x 40mm diameter cylindrical samples, see fig.3.8, based upon the various introduced formulations to be tested. Following this approach it was possible to screen and then select the best possible formulation candidates, both from the mechanical and thermal point of view, before the need for any brake pad production.
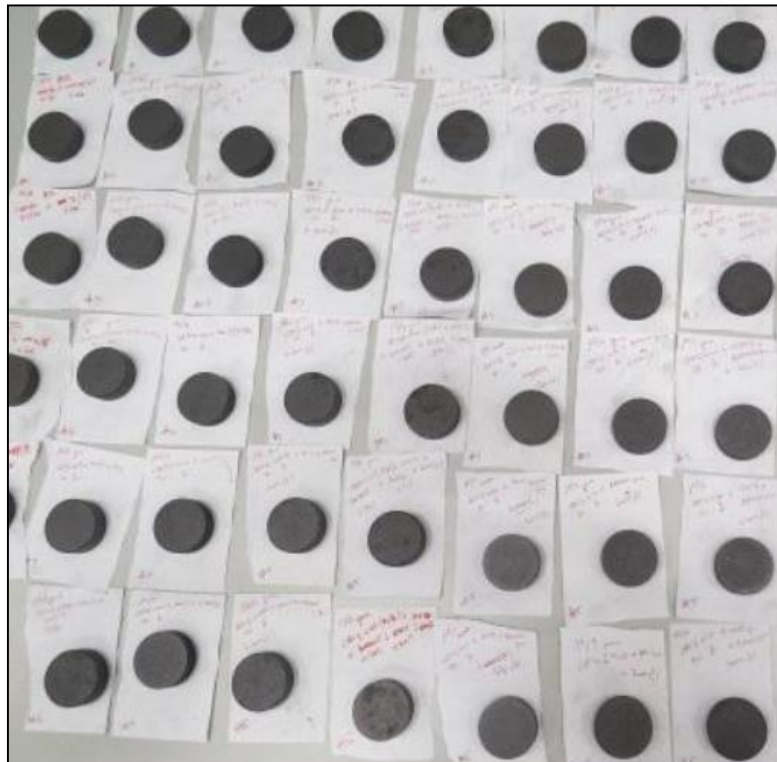
Fig.3.8 Cylindrical specimens based upon different friction material formulations, prepared for preliminary laboratory tests

The laboratory specimens were prepared using a laboratory press under the same pressure/time conditions employed during inorganic pads production, see fig.3.9

Fig.3.9 : Pressing machine E-Z™ 40 used for laboratory scale samples preparation

The samples were then tested after 9, 18 and 27 days from the preparation date in order to check the effect of the setting period on the resulting cementitious composite behavior, with the collateral aim of reducing the required brake pad production time. Starting from what is usually done for traditional brake pads, the sample hardness was measured (Rockwell Hardness Scale R) to gain information about the bonding properties of the chosen matrix as well as the composite resistance against external loads. After this first screening, only the best formulations were employed for the realization of the chosen prototype brake pads

3.1.2.2.2 Full scale prototypes
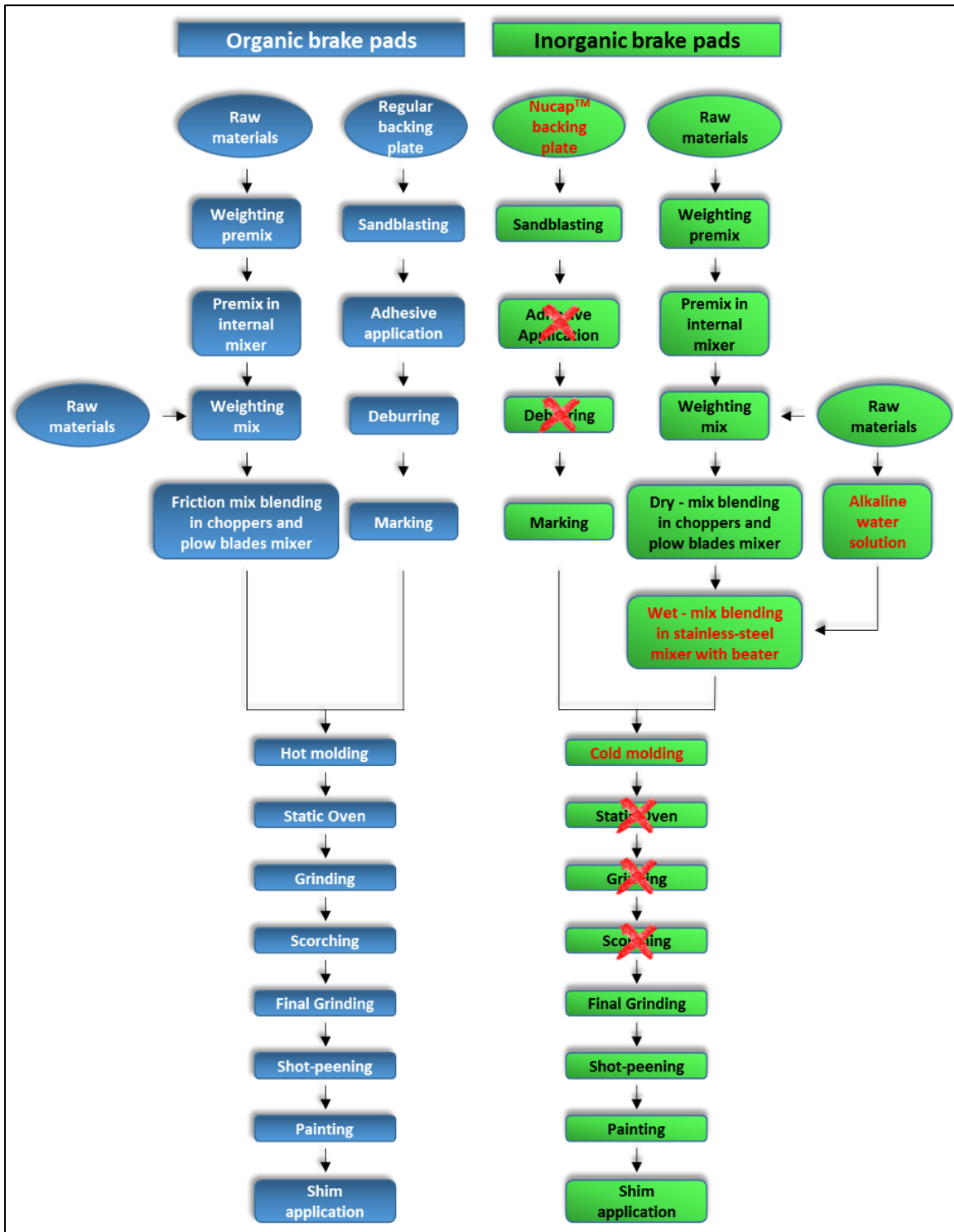
Fig.3.10 Brake pads manufacturing process flowchart for typical organic friction material compared to new inorganic friction material. Main differences are highlighted in red.

In fig.3.10 is shown a flowchart overview of typical organic brake pads manufacturing process compared to the inorganic friction material one.

There are many differences on two manufacturing process:

1. Friction mix

Wet friction mix for inorganic pads was prepared in three steps.

On the first step all the components (included any rubber premix when required) except binders and water solution was blended as for organic friction mix in the mixer equipped with choppers and plow blades Eirich intensive batch mixers R05 type to produce a dry friction mix.

On the second step binders were amalgamated for 15 min with alkaline water solution. The used binder was a laboratory scale stainless-steel mixer equipped with beater.

On the third step the previously prepared dry-mix was finally added in the laboratory mixer and blended for 5 minutes to produce the final wet friction mix.

2. Backing plate

In order to ensure the required adhesion of the friction lining to the support metal back-plate, a standard NRS™ Nucap mechanical retention system was used. See fig.3.11
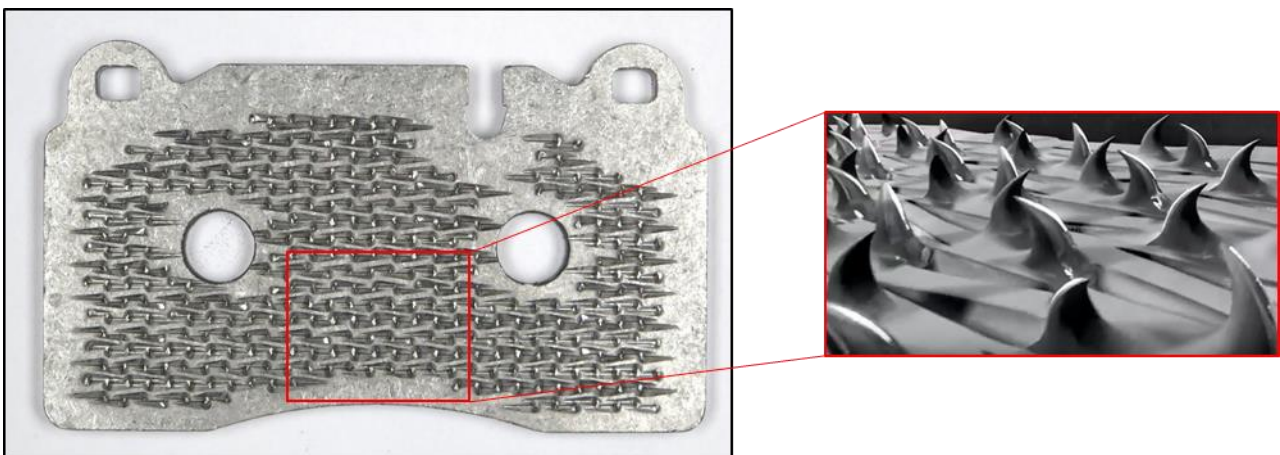
Fig.3.11 Alfa Romeo 939 model front axle pad backing plate with NRS™ Nucap mechanical retention system and a 3D simulation of hooked surface (246)**.**

A chemical adhesive such as epoxy resin needs high temperature curing to be activated. Inorganic hydraulic binders don't require thermal treatments, therefore a mechanical retention system replaced the thermoset adhesive.

3. Press molding

Inorganic material binder exploiting the hydraulic activity of specific components when exposed to water or alkaline environment, mold temperature was set at 50°C, Pressure and time set-up were similar to those used for organic pads.

Inorganic pads required custom-engineered molding set-up for the press in order to avoid water leakage during manufacturing. Indeed when wet friction mix was pressed on the backing plate, part of water solution could be wrung out. A draining system was designed and manufactured to fulfill this requirement collecting leaked water solution in a tank.

In view of future potential industrial production, a full automatic prototypal pilot line pressing station is currently in the state of advanced project to launch the pre-industrialization of this materials.

4. Thermal treatments (curing)

No thermal treatments were required in manufacturing process of inorganic brake pads. It immediately emerges the energetic benefit connected to this low temperature manufacturing process of this inorganic binder-based brake pads respect to the traditional organic one. Moreover every emission during high temperature manufacturing process was avoided.

Curing time for inorganic brake pads was 28 days at T=22 ±1 °C and RH<50% in order to gain an almost complete hardening of the cementitious matrix. After this time a final grinding was necessary to meet dimensional tolerances in terms of flatness, parallelism and required pad final height.

5. Painting
6. Finishing

Brake pads were painted and finished following regular procedure usually adopted for traditional brake pads.

3.2 Testing procedures

3.2.1 Chemical emission over brake pad manufacturing process

The aim of this part of research consisted in the determination of the air concentrations of the chemical emission during scorching treatment of organic brake pads. This analysis was done in collaboration with IRFMN IRCCS and it was part of a survey of industrial hygiene to research organic and inorganic substances released by organic brake pads during the manufacturing processes (247).
In order to reach this target a sampling campaign was carried out, collecting emission samples from the scorching air extraction system during typical industrial activities or commercial low-met organic pad manufacturing. Temperature of scorching plate was 520°C and, at full capacity, 28 low-metal organic brake pad

are simultaneously treated on the heat plate. Emission gas samples were isokinetically collected (which means that the sampling airflow velocity is equal to the scorching extractor airflow velocity) using a sampling systems comprising a filter (silica glass microfiber thimble, Whatman), followed by a condensing system maintained at a working temperature of -40 °C with or containing different sorption materials such as XAD-2, XAD-7, Silica gel, Polyurethane Foam and activated coal.

Sampled chemicals were determined using the following analytical procedure.

- *Polycyclic aromatic hydrocarbons (PAHs)*

Samples were spiked with the deuterium-labeled surrogate standard and then extracted with a mixture of pesticide-grade acetone/n-hexane (80/20) (Carlo Erba, Milano, Italy) (at 100 °C, 10 MPa, 5-min static time, 3 cycles for a total time of 1 h with a 34-mL pressurized liquid extractor (Dionex ASE 300) cells were packed with 3 g of anhydrous Na_2SO_4. After 0.5 mL using a rotary evaporator, each extract was cleaned by passing through a silica gel-alumina column containing baked anhydrous sodium sulfate (1 cm), neutral silica gel (3 cm, 3% deactivated), and neutral alumina (3 cm, 3% deactivated) from the top to the bottom using an eluent of 20 mL hexane/DCM (1:1, v/v). These elute were concentrated to approximately 0.1 mL using a gentle stream of N_2 prior to the instrumental analysis.
Samples were analyzed by a SUPELCO 28472-U column (60 m 0.25 mm 0.25 mm) coupled with an Agilent 7890 GC-5975 Mass Spectrometer, operating in the electron impact ionization (EI+) mode at 70eV and a temperature source of 230°C. 2 μl of each sample was injected in splitless mode, at a temperature of 250 °C. Helium was used as carrier gas. The temperature program for analysis was 100°C for 1 min, 10°C/min increase up to 320°C, 8°C/min increase up to 330°C.

- *SemiVolatile (SVOCs) and Volatile Organic Compounds (VOCs)*

Samples were extracted with organic solvents, and then concentrated to approximately 0.1 mL using a gentle stream of N_2 prior to the instrumental analysis. Samples were analyzed by a ZEBRON SV33 column (60 m 0.25 mm 0.25 mm) coupled with an Agilent 7890GC-5975 Mass Spectrometer, operating in the electron impact ionization (EI+) mode at 70eV and a temperature source of 230°C. 2 μL of each sample was injected in split mode, at a temperature of 280 °C. Helium was used as carrier gas. The temperature program for analysis was 40°C for 0.5 min, 10°C/min increase up to 260°C maintained for 8 min.

- *Formaldehyde*

Sample were treated according to the method NIOSH number 2016. Briefly, after eluting the formaldehyde derivative from the cartridge samplers with 10-mL quantities of acetonitrile, an aliquot was analyzed by a liquid chromatograph (equipped with a 3.9x150-mm, stainless steel, packed with 5-μm C-18, Symmetry™ column) coupled with an UV detector. 20 μL of each sample was injected using a 45% acetonitrile/55% water (v/v) as mobile phase, with a flow of 1.3 mL/min.

3.2.2   Brake system

Finely tuning of inorganic friction material formulation and manufacturing process steps modification for inorganic brake pads production, required implementation and testing of a large number of formulations and brake pads prototypes.

Fig.3.12 Organic (on the left) and inorganic (on the right) brake pad

To summarizing the results achieved over this research work in "testing results" section are reported the outcome of the two more significant experimental inorganic materials compared to typical organic materials available on the market.

Mat. name	Matrix	Manufacturing	Description
Inorganic 1	Inorganic	Brembo S.p.A.	Inorganic formulation (with copper) for R&D purpose
Inorganic Cu free	Inorganic	Brembo S.p.A.	Inorganic formulation (copper-free) for R&D purpose
Organic low-met	Organic	Brembo S.p.A.	Organic formulation for R&D purpose
Commercial low-met	Organic	Brembo S.p.A.	Brembo S.p.A. commercial material
Original equipment (OE)	Organic	Available on the market	Alfa 159 original equipment
Original equipment 2 (OE2)	Organic	Available on the market	Alfa 166 original equipment

Tab.3.3 Materials evaluated in "testing results" section

Testing procedures on manufactured brake pads required a full-scale brake dynamometer and a testing vehicle.

Main purpose of the inertia-dynamometer or full-scale brake dynamometer was used to measures the behavior of a brake system under different conditions of speed, pressure and temperature before using new brake system components on real vehicles. For all tests the original components of the Alfa Romeo brake system type 939 were used where the brake caliper was BREMBO M4 42 and the brake disc was Brembo 330x28 code 09.9365.10, see fig.3.13. Brake dynamometer was a TecSA performances/NVH passenger cars.

All dyno-test were conducted in Brembo S.p.A. Adv. R&D testing department.
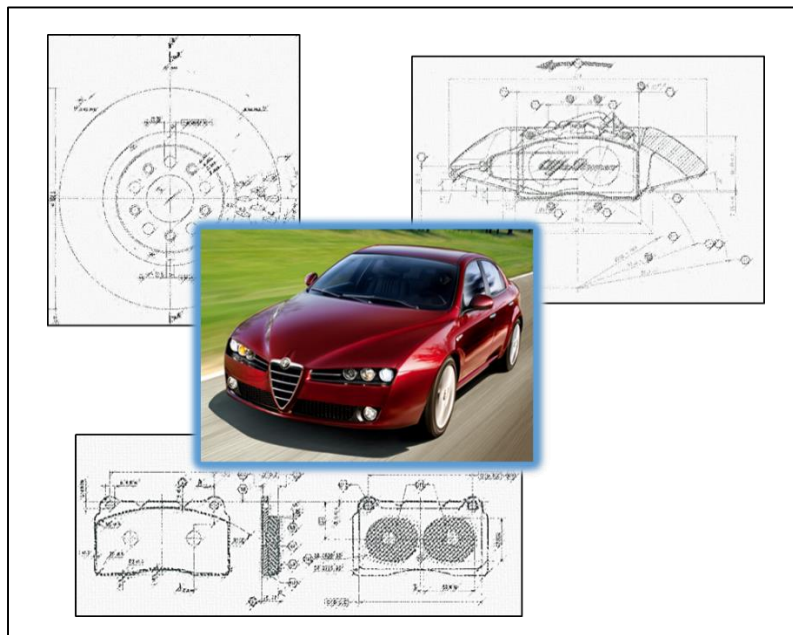
Fig.3.13 Alfa Romeo 159 (center) and general scheme of brake system components, brake disc (top left), caliper (top right) and brake pad (bottom).

Representative car used for this brake system type (mounted on front axle) was Alfa Romeo 159 2,4Jtdm.

3.2.2.1   *Wear particle emission*

The full-scale brake dynamometer was modified according to design proposed by Perricone et al. (248) to generate and collect wear particles.
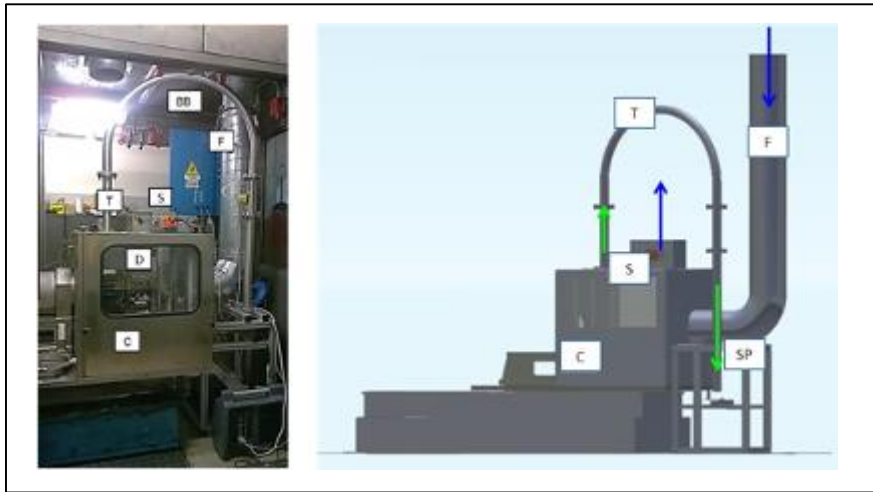
Fig.3.14 Picture on the left and general scheme on the right of dyno-bench tester designed for characterization of wear particles emissions where C is the dust-box chamber, F is the inlet tube, D is the Brake disc, T is the sampling tube, S is the shutter and SP is the Sampling point. Adapted from (248) **and** (237).

A HEPA filter class H13 was used to produce cleaned inlet air (F). Flowrate at sampling tube (T) was regulated at 10 l/min, adjusting the inlet flowrate and the outlet flowrate modulating the shutter (S). On sampling point (SP) a filter holder is connected with the cyclone and serves as support for a 47 mm quartz filter which is used to collect the PM10 wear particles. A vacuum pump is used to pump air (10 l/min) through the PM10 collection line (PM10 cyclone – 47 mm filter holder). Isokinetic sampling was required to ensure that all particle sizes were sampled in an unbiased manner. At sampling point a second device was connected, the electrical low pressure impactor ELPI+® E. The flowrate of 10 l/min at ELPI is guaranteed by a second vacuum pump.

- *Testing procedure*

Testing procedure for wear particle generation used was an internal procedure based on the international standard SAE J2707 "Wear Test Procedure on Inertia Dynamometer for Brake Friction Materials" method B. Indeed, to be representative of urban driving condition, the Highway and hill descent blocks were avoided, moreover the number of brakes along other blocks were reduced respect to the international standard procedure.
Testing cycle for wear particle generation is shown in tab.3.4

Block	Initial speed (km/h)	Final speed (km/h)	Init disc temp. (°C)	Decel (g)	Snubs N.
Burnish (B)	50	4	100	0.25	100
5 min cleaning					
Town block 1 (TB1)	50	4	150	0.25	20
5min cleaning					
Country road block 1 (CRB1)	80	4	200	0.35	20
5min cleaning					

Country road block 2 (CRB2)	100	4	125	0.4	20
5min cleaning					
Town block (TB2)	50	4	150	0.25	20
5min cleaning					
Country road block 3 (CRB3)	100	4	125	0.4	20

Tab.3.4 Dyno-bench testing procedure used for wear particles generation

Every test cycle was repeated on the same components twice. Brake disc and pads were weighted before and after each cycle with a Sartorius master CPA34001P and LA2200P balance respectively, then weight loss of components was calculated. Filters were conditioned 24h in a SCC400L-EPA climatic cabinet at 22° ±1°C and dew point of 9.5° ±1°C and weighted before and after the test with a Sartorius CUBIS MSA2.7S-000-DM balance. New quartz filters were used at each cycle and total amount of PM10 was calculated considering total air flow and collecting air flow and ratio.
ELPI+ collected and measured particle number in a range 0.006 – 10 μm, the total particle number PN10 measured during each test were recorded.

3.2.2.2 *Brake performance*
According to ISO 15484:2008 (Road vehicles — Brake lining friction materials — Product definition and quality assurance), the inertia-dynamometer tests based on performance test /production friction test shall be in accordance with one of following procedures:

- ISO 26867 Road vehicles -- Brake lining friction materials -- Friction behaviour assessment for automotive brake systems
- SAE J2522 (AK-Master) Dynamometer Global Brake Effectiveness
- JASO C406-00 Passenger car - Braking device - Dynamometer test procedures.

3.2.2.2.1 *SAE J2522 (AK-Master)*
The choice of the test procedure is based on regional request, AK-Master has proved useful on the European market for several friction material manufacturers and designers. The "AK Working group", which represents European manufacturers of friction linings and passenger car brakes, has developed AK-Master, the standard procedure consisting of 15 steps and for the car front axle the test is performed as described in tab.3.5

Step n°	Step name	description
1	*Green μ Characteristic*	30 snubs 80 to 30 km/h at 3 000 kPa
2	*Burnish*	64 snubs 80 to 30 km/h at varying pressures
3	*Characteristic Value 1*	6 snubs 80 to 30 km/h at 3 000 kPa
4.1	*Speed/pressure sensitivity 40 km/h*	8 stops 40 to 5 km/h at increasing pressures

4.2	*Speed/pressure sensitivity 80 km/h*	8 snubs 80 to 40 km/h at increasing pressures
4.3	*Speed/pressure sensitivity 120 km/h*	8 snubs 120 to 80 km/h at increasing pressures.
4.4	*Speed/pressure sensitivity 160 km/h*	8 snubs 160 to 130 km/h at increasing pressures.
4.5	*speed/pressure sensitivity 200 km/h*	8 snubs 200 to 170 km/h at increasing pressures
5	*Characteristic Value 2*	6 snubs 80 to 30 km/h at 3 000 kPa
6	*Cold Application*	1 stop 40 to 5 km/h at 3 000 kPa
7	*Motorway Applications*	1 stop and 1 snub at 0.6 g
8	*Characteristic Value 3*	6 snubs 80 to 30 km/h at 3 000 kPa
9	*Fade 1*	15 stops 100 to 5 km/h at 0.4 g and increasing initial temperatures 100 to 550°C log scale
10	*Recovery 1 (Characteristics values)*	18 snubs 80 to 30 km/h at 3000 kPa
11	*Temperature/Pressure Sensitivity 100 °C*	8 snubs 80 to 30 km/h at increasing pressure, initial braking temperature < = 100 °C
12.1	*Increasing temperature 500 °C*	9 snubs 80 to 30 km/h at increasing temperature
12.2	*Pressure line 500 °C*	8 snubs 80 to 30 km/h at increasing pressure, initial brake temperature < = 500°C
13	*Recovery 2 (Characteristics values)*	18 snubs 80 to 30 km/h at 3000 kPa
14	*Fade 2*	15 stops 100 to 5 km/h at 0.4 g and increasing initial temperatures 100 to 550°C log scale
15	*Recovery 3 (Characteristics values)*	18 snubs 80 to 30 km/h at 3000 kPa

Tab.3.5 SAE J2522 (AK-Master) testing procedure

SAE J2522 requires for front axle application to set the dynamometer inertia according to half of 75% of the gross vehicle weight (GVW). The temperature was measured with thermocouples at the friction path centre radius 0.5 mm ± 0.1 mm deep in the disc outer face whilst additional thermocouples could be positioned in the friction material of both pads for further temperature recordings.

As set out in testing procedure "… there are no minimum specifications or requirements for any section or stop on the test. Performance levels and technical requirements depend more upon the specific application for which the brake lining is intended and upon additional criteria that go beyond the reach of this recommended practice. Each customer and vendor should properly define specific requirements as part of their business relationship…".

3.2.2.2.2 Internal fading

The same system components and dynamometer set-up was used to evaluate the materials behavior under heavy-duty thermo-mechanical conditions (high external pressure, torque, tangential forces and high-thermal loads). This high demanding internal fading procedure specifically designed for sport car applications, consisted in an initial bedding block of 60 snubs from 80 km/h to 30 km/h at an imposed

deceleration of 3 m/s^2, with disc initial temperature of 100 °C. The fading block consisted in a series of snubs from 225 to 90 km/h with a applied torque of 200 daN·m for a total of 20 applications. The recovery time after each brake event in the main block was 87 s. Disc and pads temperature, friction coefficient and applied torque was recorded during the test. Temperature during tests was measured on disc with the same set-up of AK-Master and inside friction materials at the height of 3 mm from the backing-plate.

3.2.2.2.3   ECE Regulation 90

Regulation No 90 of the Economic Commission for Europe of the United Nations (UN/ECE) establishes foreseen provisions concerning the approval of replacement brake lining assemblies.

The aim of the activity is to verify if the new inorganic friction material can be released as aftermarket spare parts according to ECE R90 specification for M1 category vehicles (Vehicles used for the carriage of passengers and comprising not more than eight seats in addition to the driver's seat (Passenger car)).

Different requirements have to be met:

- *Performance requirements*

For M1 vehicles brake pads shall be installed and tested in the vehicle according to the prescriptions of Annex 3 of regulation and shall satisfy the requirements stated in this Annex and in the Addendum 12-H: Regulation No. 13-H, see tab.

Block	Block name	Mass and gear	Parameter	Value	Request
1	**Bedding**	Full load	Mileage	min 50 km	T pad 250-500°C at least 3 times
			Initial speed	50-120 km/h	
			T pad max	500°C	
			Deceleration	1-5 m/s^2	
			Stops n.	Min. 100	
2	**Performance check**	Full load	Initial speed	70 km/h	The measured deceleration of the 5 brakes must remain within a tolerance range of ±0,6 m/s^2 If the request is not met the bedding must be extended
			Final speed	0 km/h	
			Initial T	<100°C	
			Brake pressure front	40 bar	
3	**(A) Type-0 test with engine disconnected**	Full load	Initial speed	100 Km/h	Deceleration >6.43 m/s^2 Stop distance ≤ 70m Mean deceleration >6.43 m/s^2
			Final speed	0	
			Initial T	65-100°C	
			Application force	6.5÷50 daN	
	(B) Type-0 test with engine connected	Full load	Initial speed	160 km/h	Pedal force > 6.5N Stop distance ≤ 187.52 m
			Final speed	0	
			Initial T	65-100°C	

				Application force	6.5÷50 daN	Mean deceleration >5.76 m/s²
4.	Type-I test (Fading test)	Full load Highest gear		Initial speed	120 km/h	Deceleration 3m/s²
				Final speed	60 km/h	
				Δt Time elapsing between the initiation of one brak application and the initiation of the next.	45 s	
				Number of brake applications	15	
4.1	Hot Performance: Same conditions as Type-0 test (A)	Full load		Initial speed	100 Km/h	Deceleration >6.43 m/s² stopping distance≤70m
				Final speed	0	
				Initial T	65-100°C	
4.2	Recovery	Full load		Initial speed	50 km/h	No requirements
				Deceleration	3 m/s²	
				Stops interval	1.5km	
4.3	Recovery performance: same conditions as Type-0 test (A)	Full load		Initial speed	100 Km/h	Deceleration >6.43 m/s² Stopping distance≤70m
				Final speed	0	
				Initial T	65-100°C	
5	Cold performance test	Full load		Initial speed	70 km/h	The upper two thirds of the curve must lie within ±15% of the curve found with the original equipment
				Deceleration	Up to 6 m/s² max	
				Number of brake applications	≥6	
				Initial T	<100°C	p*=pressure at 0.5m/s²
6	Speed sensitivity test	Full load		Initial speed	65,100,135 km/h	Dec(135)=dec(65)±15%
				Pressure	p=p*	

Tab3.6 ECE R90 testing procedure

The mean fully developed deceleration d_m shall be calculated according to eq.3.1

$$d_m = \frac{v_b - v_e}{25.92(s_e - s_b)}$$

Eq.3.1

Where v_0= initial vehicle speed in km/h, v_b= vehicle speed at 0.8 v_0 in km/h, v_e= vehicle speed at 0.1 v_0 in km/h, s_b = distance travelled between v_0 and v_b in meters, s_e = distance travelled in between v_0 and v_e in meters.

The vehicle has been set-up with a Brembo S.p.A. internal data logger where different channels corresponded to:

- Brake pressure (front axle)

- Pads temperature are recorded on right pad (CH25-FRP), front left pad (CH26-FLP), rear right pad (CH29-RRP).

- Vehicle deceleration

- Vehicle speed / stopping distance

- Temperature

Test were conducted in Vairano test track (249). During the whole test a total distance of 250 km was covered. Beside the specified tests, also the pedal feeling and noises have been evaluated.

- *Mechanical characteristics (shear force)*

Replacement brake lining assemblies of the type for which approval is requested shall be tested for shear strength according to international standard ISO 6312:2001 "Road vehicles — Brake linings — Shear test procedure for disc brake pad and drum brake shoe assemblies". The standard specifies a method for measuring the strength of the bond connection between the lining material and the backing plate applying a shear load on friction material as described in fig.3.15
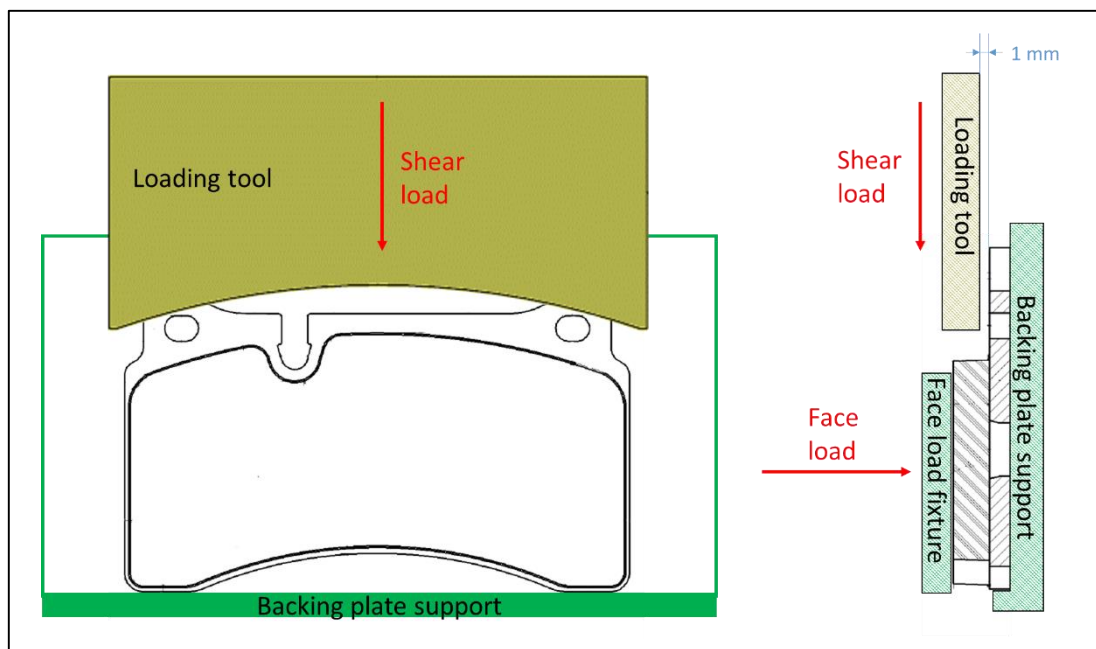
Fig.3.15 Front and side view of disc brake pad test fixture according to ISO 6312:2001

In order to prevent assembly movement under testing, a pressure fixture applies a face load of $0,5 \pm 0,15$ N/mm^2 of the lining area at a right angle to the shear load. The shear load application rate shall be controlled in such a way that the load increases at an average rate of 4500 ± 1000 N/s, in this phase friction has to be minimized at interface between face load fixture and lining. The shear strength at failure τ was calculated as in eq.3.2

$$\tau = \frac{F}{A}$$

Eq.3.2

Where F is the total load applied at the time of shear failure and A contact area between lining and backing plate. The test rig used to measure the shear strength was a Galdabini QUASAR 100 equipped with a special fixture designed to fulfill the international standard requirements. According to ECE R90 for brake pad the minimum acceptable shear strength is $\tau \geq 250N/cm^2$, therefore for Alfa 939 front axe brake pad where $A=77cm^2$ the minimum acceptable shear force is 19,25kN.

- *Mechanical characteristics (compressibility)*

Brake pad which approval is requested shall be tested for compressibility according to standard ISO 6310:2009 "Road vehicles — Brake linings — Compressive strain test methods". The international standard specifies a method for test and measurement of the compressive displacement of brake linings or brake pad assemblies due to loading. Test apparatus is made of uniaxial material-testing load frame to provide a uniform load over the surface of the test sample, the compressibility is the change in the pad thickness caused by a single dimensional pressure load towards the normal plane of the friction surface. Testing apparatus is described in fig.3.16
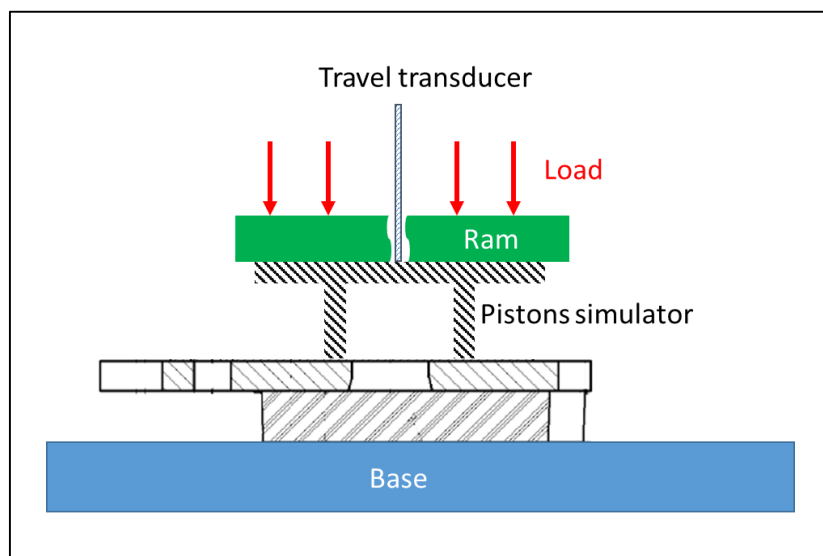
Fig.3.16 testing apparatus for brake linings compressive strain test methods ISO 6310:2009

On the back of brake pad a template simulates a caliper piston configuration. The cold compressibility measurement testing cycle is:

1) A preload of 0,5 MPa is applied for 1 sec, the displacement gauge is set to zero while the sample is held at pre-load.
2) Pressure increases at 8 ±1 MPa/s rate up to a test load of 16 MPa, the test load is maintained for 1 second

3) pressure is decreased at 8 ±1 MPa/s rate to preload pressure
4) Repeat loading and unloading in accordance with points 2 and 3 for five times. the change of the pad thickness against the force on last cycle is the compressibility value

According to ECE R90 for brake pad the compressibility values shall not exceed 2 per cent at ambient temperature. The brake pad height is 15,8 mm therefore cold compressibility have to be d≤316μm.

Even if required by ECE R90, it was not possible to include hot compressibility in this work.

3.3 Testing results

3.3.1   Chemical emission

Qualitative identification of all measured organic compounds sampled on scorching air extraction is shown in tab.3.7

Organic compound name	CAS number	Hazard statement(s)	Hazard statements description
Fluorene	86-73-7	H410	H221 Flammable gas
			H225 Highly flammable liquid and vapor,
Phenantrene	85-01-8	H302, H315, H319, H335, H410	H301 Toxic if swallowed
			H302 Harmful if swallowed.
Anthracene	120-12-7	H315, H319, H335, H410	H304 May be fatal if swallowed and enters airways.
Fluoranthene	206-44-0	H302, H410	H310 Fatal in contact with skin
Pyrene	129-00-0	H341, H372, H410	H311 Toxic in contact with skin
Benzo(a)anthracene	56-55-3	H350, H410	H314 Causes severe skin burns and eye damage.
Chrysene	218-01-9	H341, H350, H410	H315 Causes skin irritation.
Benzo(b)fluoranthene	205-99-2	H350, H410	H317 May cause an allergic skin reaction.
Benzo(k)fluoranthene	207-08-9	H350, H410	H318 - Causes serious eye damage
Benzo(j)fluoranthene	205-82-3	H315, H319, H335, H336, H350, H373, H412	H319 Causes serious eye irritation. H331 Toxic if inhaled. H335 May cause respiratory irritation.
Benzo(e)pyrene	192-97-2	H350, H410	H336 May cause drowsiness or dizziness.
Benzo(a)pyrene	50-32-8	H317, H340, H350, H360FD, H410	H340 May cause genetic defects. H341 Suspected of causing genetic
Indeno[1,2,3-cd]pyrene	193-39-5	H351	defects.

Organic compound name	CAS number	Hazard statement(s)	Hazard statements description
Benzo(g,h,i)perylene	191-24-2	H410	H350 May cause cancer.
Dibenzo[a,h]anthracene	53-70-3	H350	H351 Suspected of causing cancer
Dibenzo(a,e)pyrene	192-65-4	H318, H351, H413	H360FD May damage fertility. May damage the unborn child.
Dibenzo(a,h)pyrene	189-64-0	H340, H350, H372H304	H361d Suspected of damaging the unborn child.
Dibenzo(a,i)pyrene	189-55-9	H225, H310, H340, H350, H372, H304, H315, H319	H370 Causes damage to organs. H372 Causes damage to organs through prolonged or repeated exposure.
Dibenzo(a.l)pyrene	191-30-0	H350, H302	H373 May cause damage to organs (Liver, Blood) through prolonged or repeated exposure if swallowed.
DiChloroMethane	75-09-2	H315, H319, H335, H336, H351, H373	H373 May cause damage to organs (Central nervous system) through prolonged or repeated exposure if inhaled.
TetraHydroFuran	109-99-9	H225, H302, H319, H335, H351	H402 Harmful to aquatic life.
Toluene	108-88-3	H225, H304, H315, H336, H361d, H373	H410 Very toxic to aquatic life with long lasting effects. H411 Toxic to aquatic life with long lasting effects. H412 Harmful to aquatic life with long lasting effects H413 - May cause long lasting harmful effects to aquatic life
Hexanal	66-25-1	H319	
Nonane	111-84-2	H304, H315, H336, H410	
1,3 DiMethylBenzene	108-38-3	H304, H312, H332, H315, H319, H335 , H412	
Heptanal	111-71-7	H315	
2-Hydroxybenzaldehyde	90-02-8	H302, H411	
1,2,3 TriMethylBenzene	526-73-8	H315, H319, H335	
2-MethylPhenol	95-48-7	H301, H311, H314, H411	
Naphthalene	91-20-3	H302, H351, H410	
Biphenyl	92-52-4	H315, H319, H335, H410	
Xylenes	-	H304, H312, H332, H315 , H319, H335, H373, H412	
Phenol	108-95-2	H301, H311, H331, H314,H341, H373, H411	
Benzene 1ethenyl-3ethyl	7525-62-4	na	
Benzene 1-ethenyl-4ethyl	3454-07-07	na	
Tetradecane	629-59-4	H304	
Benzene 1-methyl4 (1methylethyl)	99-87-6	H304, H411	

Organic compound name	CAS number	Hazard statement(s)	Hazard statements description
Formaldehyde	50-00-0	H301, H311, H331, H314, H317, H318, H341, H350, H370, H402	

Tab.3.7 Organic compounds identified by qualitative GC/MS screening analysis + formaldehyde method. CAS number and hazard statements from SDS of compounds are shown.

Semi-quantitative analysis of measured compounds are shown in tab.3.8

	Concentration ($\mu g/m^3$)
PHAs (total)	52.3
Other organic compounds	31.5
Ammonia	26.5
Formaldehyde	0.43

Tab.3.8 semi-quantitative concentration values of compounds measured in scorching air extractor

This results are in accordance with recent studies on identification of organic compounds released from low-metallic automotive model brake pad (250). Part of this emission can be ascribable also to inorganic carbon phases, such as graphite and cokes, present in the friction mix, but most of the hazardous substances released under 500°C was attributed to thermo-oxidative degradation of phenolic resin and other organic components in friction compound.

3.3.2 Brake system

Composition and manufacturing process parameter of tested friction materials are summarized in patents description (233) (234).

3.3.2.1 Inorganic 1

A full inorganic alkali-activated friction material (now on named "*Inorganic 1*") was the final material achieved after first part of formulation work. It was derived from a low-met organic formulation (now on named "*organic low-met*") where all the organic raw materials and all materials incompatible with inorganic alkali-activated binders were removed, see tab.3.9. A fine tuning of binders and other components was necessary to reach AK-Master results as similar as possible to the Alfa Romeo 159 original equipment friction material (now on named "*organic original equipment*").

Constituents of inorganic friction materials	Weight (%) Organic Low-met	Weight (%) Inorganic 1
Dry-Mix		
Abrasive 1	4.0	3.8
Abrasive 2	6.0	-
Abrasive 3	5.0	4.8
Carbonaceous lubricants	17.0	16.3
Lubricant 2	4.0	3.8
Lubricant 3	3.0	2.9
Metal fibers	25.0	23.9
Metal powders with Cu	16.0	15.3
Metal powder Cu free	2	-
Filler 1	7.0	7.7
Functionalizer 1	2.0	-
Organic components	9.0	
Inorganic binder components		
Inorganic binders	-	10.1
Alkaline solution	-	11.4

Tab.3.9 Organic and inorganic friction material formulation, dry mix and inorganic binder components are shown

Organic original equipment, organic low-met and inorganic1 friction materials contained Cu>5 wt.% in form of copper or its compounds.

3.3.2.1.1 Inorganic 1 SAE J2522 (AK-Master) test

AK-Master results are shown in fig.3.17 and characteristic values in tab.3.10

Characteristic values μ		Organic OE		Organic Low-met		Inorganic 1	
		Avg.	Min	Avg.	Min	Avg.	Min
Char. Value (3)	μ0P6	0.40		0.55		0.42	
Speed/pressure (4.3)	μv120	0.40		0.49		0.38	
Speed/pressure (4.5)	μvmax	0.43		0.36		0.31	
Char. Value (5)	μ0 P6	0.44		0.44		0.42	
40°C Brake apply (6)	μT40	0.37		0.38		0.43	
Second motorway apply (7)	μMW2	0.42		0.33		0.29	0.29
Char. Value (8)	μ0P18	0.37		0.45		0.39	
Fade 1 (9)	μF1		0.24		0.25		0.32
Char. Value (10)	μ0P18	0.41		0.42		0.43	
Temperature (12)	μT500		0.32		0.33		0.33
Char.Value (13)	μ0P18	0.41		0.42		0.44	
Fade 2 (14)	μF2		0.42		0.35		0.33
Char. Value (15)	μ0P6	0.40		0.40		0.38	
	μ nom	**0.41**		**0.42**		**0.39**	
	μ min		**0.24**		**0.25**		**0.29**

Tab.3.10 SAE J2522 Characteristic values of Organic original equipment, organic low-met and Inorganic 1 friction material

Fig.3.17 SAE J2522 (AK-Master) results of Alfa Romeo 159 2,4Jtdm original equipment (red), organic low-met (blue) and inorganic-binder based friction material (yellow). Part 1/2
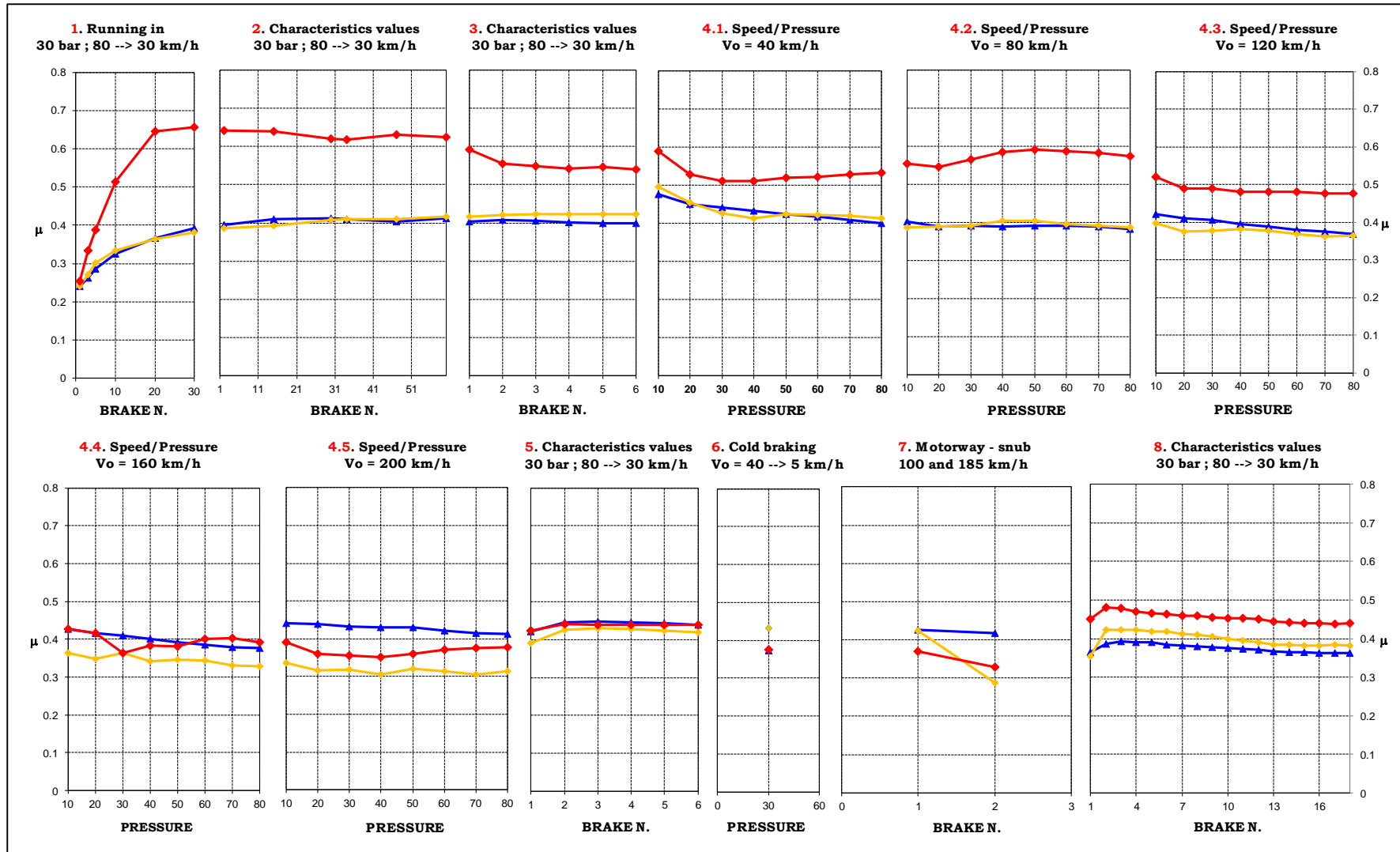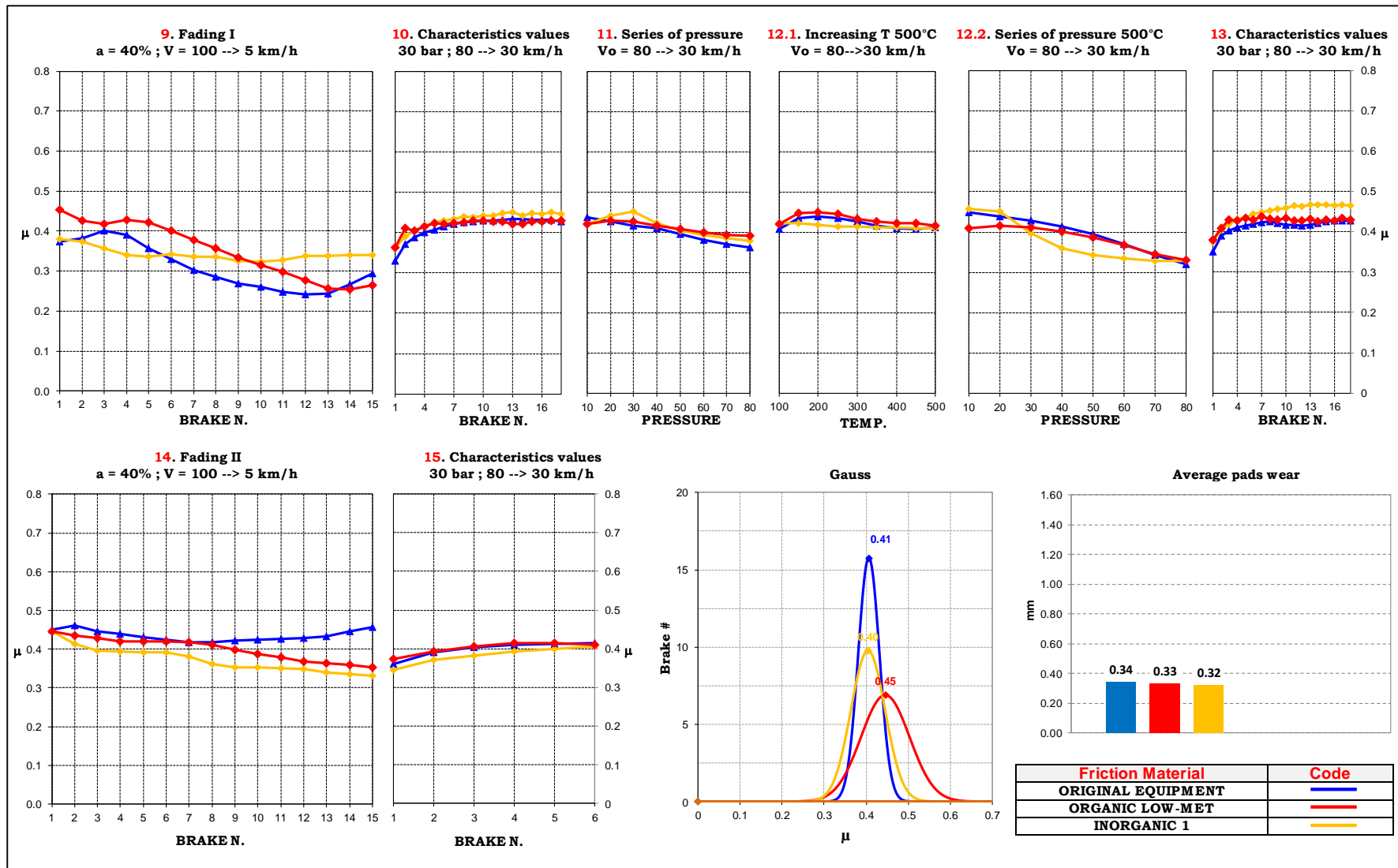
159

Fig.3.17 SAE J2522 (AK-Master) results of Alfa Romeo 159 2,4Jtdm original equipment (red), organic low-met (blue) and inorganic-binder based friction material (yellow). Part 2/2

Characteristic value steps are indicators of friction material behavior after each specific braking condition.

Speed sensitivity of inorganic1 can be seen considering the pressure/speed section; in particular a reduction of the efficiency was recorded for initial speed higher than 160km/h (Fig.3.17 block 4) and in the second motorway application, where the initial speed was 185 km/h and a deceleration of 0.6 g was required (fig.3.17 block 7). Characteristic average values over the whole test resulted stable around 0.38-0.44. Higher value of friction coefficients on inorganic 1 cold braking was recorded respect organic materials.

Similar behavior of inorganic 1 in the first and second fading section was very similar with a minimum friction coefficient 0.33 and 0.32 respectively (Fig block 9 and 14), therefore the material after fading and high temperature blocks had a reproducible behavior.

After SAE J2522 test brake pads didn't present any anomaly in terms of lack of compactness, the average total wear of pads for organic original equipment, organic lo-met and inorganic 1 was 0.34, 0.33 and 0.32 respectively. According to the test results it is import to point out that there are no critical elements in the use of inorganic 1 material on a real vehicle, a good friction coefficient during all blocks where μ nom. was 0.39 and μ min. was 0.29 ensures performance of the material more than enough to satisfy most driving conditions.

3.3.2.1.2 Inorganic 1 internal fading test
After AK-master, organic original equipment, organic low-met and inorganic 1 friction material performances were compared with internal fading procedure. Internal fading results are shown in fig.3.18 and characteristic values in tab.3.11

Characteristic Values	Organic OE	Organic Low-met	Inorganic 1
Max disc T (°C)	634	787	741
Max disc T Avg. after brake n°10 (°C)	612	732	675
Max pads temperatures (°C)	245	261	282
Min friction coefficient μ	0.21	0.18	0.12
Friction coefficient μ Avg. after brake n°10	0.32	0.22	0.14

Tab.3.11 Internal fading test characteristic values for organic original equipment, organic low-met and inorganic-binder based friction material.
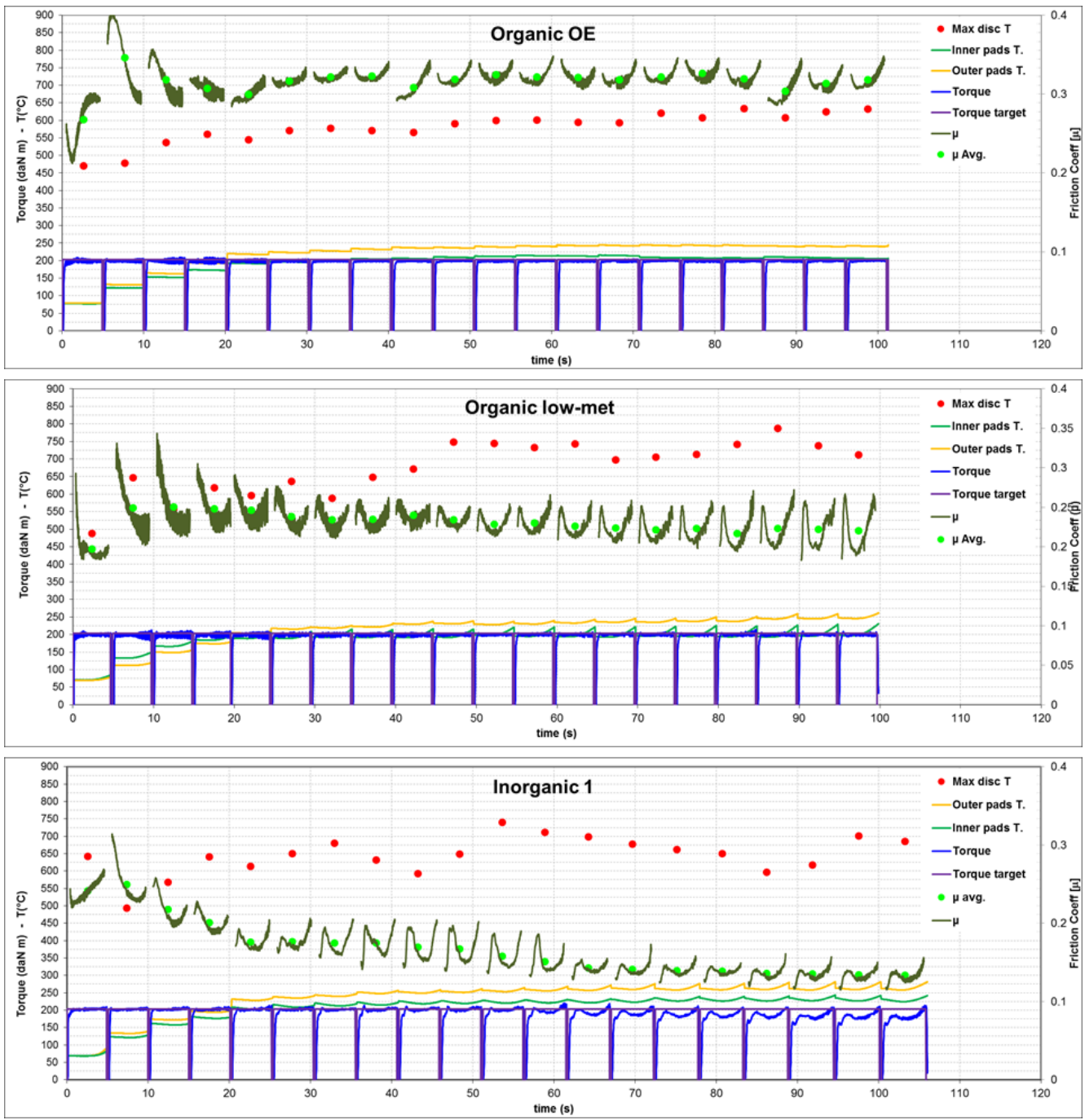
Fig.3.18 Internal fading test results of organic original equipment, organic low-met and inorganic-binder based friction material.

Only organic materials successfully fulfill the test requirements, indeed the dyno-bench applicable pressure is limited to 180 bar, even at this pressure inorganic 1 material could not reach required torque target after brake no.10 due to the insufficient friction coefficient at this severe condition.

3.3.2.1.3 Inorganic 1 wear particle emission
Wear particle emission of inorganic 1 was compared with an organic commercial material (now on named "*commercial low-met*", it was not the Alfa OE). Results in terms of components wear, particulate matter emission PM10 and particle number emission are shown in fig.3.19 and fig.3.20

Fig.3.19 Pads weight loss, disc weight loss, sum of components weight loss and amount of PM10 released during two cycles of the wear particles emission test for commercial low-met and inorganic based materials.
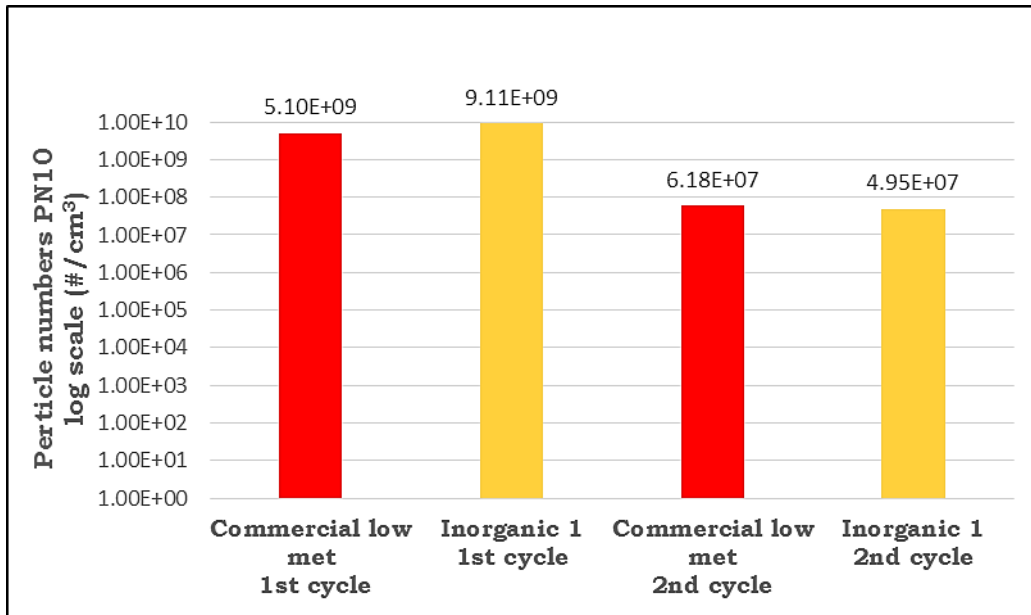
Fig.3.20 PN10 emission during two cycles of the wear particle emission test in commercial low-met and inorganic based materials.

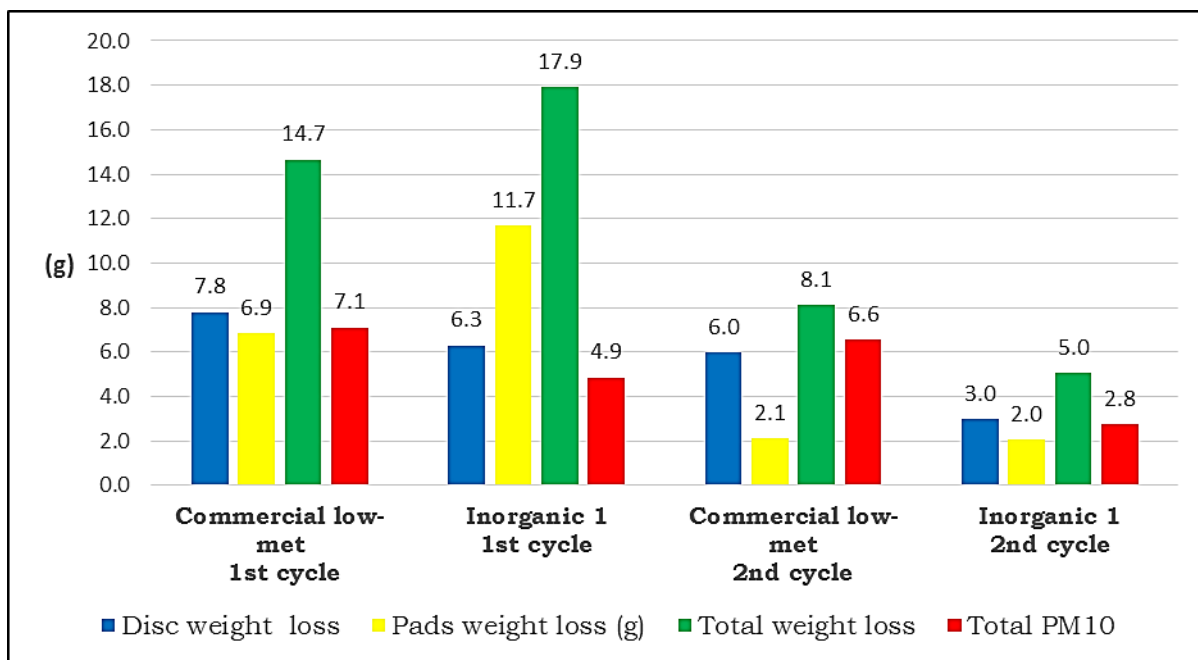As described in testing procedure brake pads and disc were used in two subsequently cycles. At the beginning of the first cycle components were new and during the first part of this cycle the friction layer from pads and disc was formed. Even if inorganic1 pads wear and PN10 emission was higher than commercial pads, in this phase a lower PM10 emission was measured (respectively 11.7g and 6.9g). Indeed on first cycle PM 10 for Inorganic 1 was 27% of total wear and PM10 of commercial low-met was 48%, this means that most of the matter generated by wear of inorganic1 pads was composed by particles with mean aerodynamic diameter higher than 10.

On second cycles components were already run-in, therefore this cycle was more significant respect the every-day brake use. Total wear, PM10 and particles number emission were considerably lower respect first cycle for both materials, but inorganic 1 shown a particular low particle emission in terms of PM10 and PN10 compared to commercial low-met.

3.3.2.2 Inorganic Cu-Free

After copper limitation in friction material comes into force on new legislation in Washington and California States (21) (22), it was therefore necessary to research new copper-free formulation also for inorganic materials.

Starting from Inorganic1 composition, new full inorganic friction compound (now on named "*inorganic Cu-Free*") with Cu<0.5% was exploited.

Constituents of inorganic friction materials	Weight (%) Inorganic 1	Weight (%) Inorganic Cu free
Dry-Mix		
Abrasive 1	3.8	2.7
Abrasive 3	4.8	-
Abrasive 4	-	2.0
Abrasive 5	-	3.4
Carbonaceous lubricants	16.3	9.50
Lubricant 2	3.8	4.7
Lubricant 3	2.9	6.1
Metal fibers	23.9	17.0
Metal powders with Cu	15.3	-
Metal powder Cu free 2	-	6.1
Filler 1	7.7	-
Inorganic binder components		
Inorganic binders	10.1	20.6
Alkaline solution	11.4	27.9

Tab.3.12 Inorganic friction materials formulation, dry mix and inorganic binder components are shown

During this part of the work, best performances of this new inorganic material on thermo-mechanical demanding internal-fading procedure have been researched.

3.3.2.2.1 Inorganic Cu-free, SAE J2522 (AK-Master) test

AK-Master results are shown in fig.3.21 and characteristic values in tab.3.13

Fig.3.21 SAE J2522 (AK-Master) results of Alfa Romeo 159 2,4Jtdm original equipment (blu), inorganic-binder based friction material (yellow) and inorganic-binder based friction material Cu-Free (green) . Part 1/2
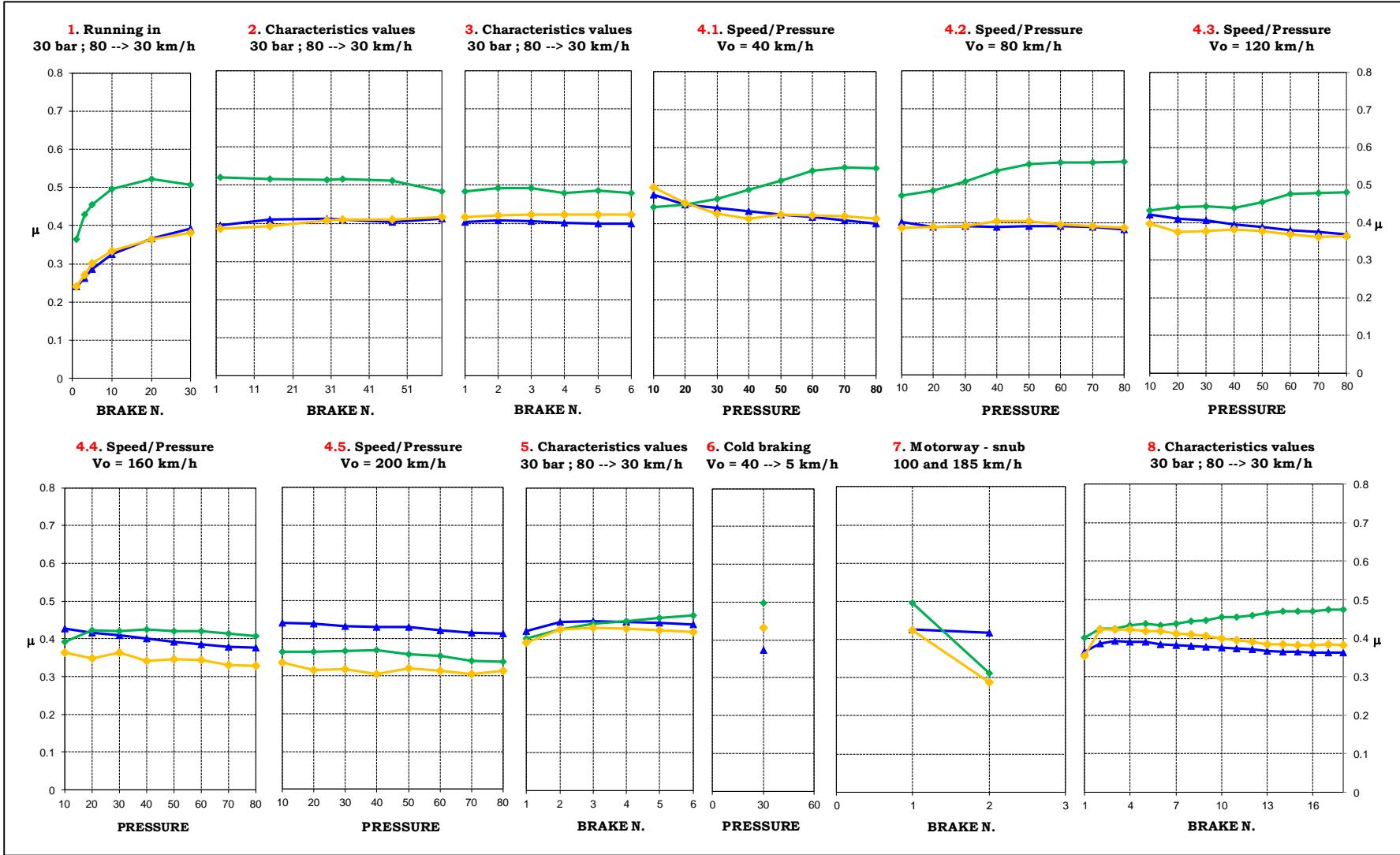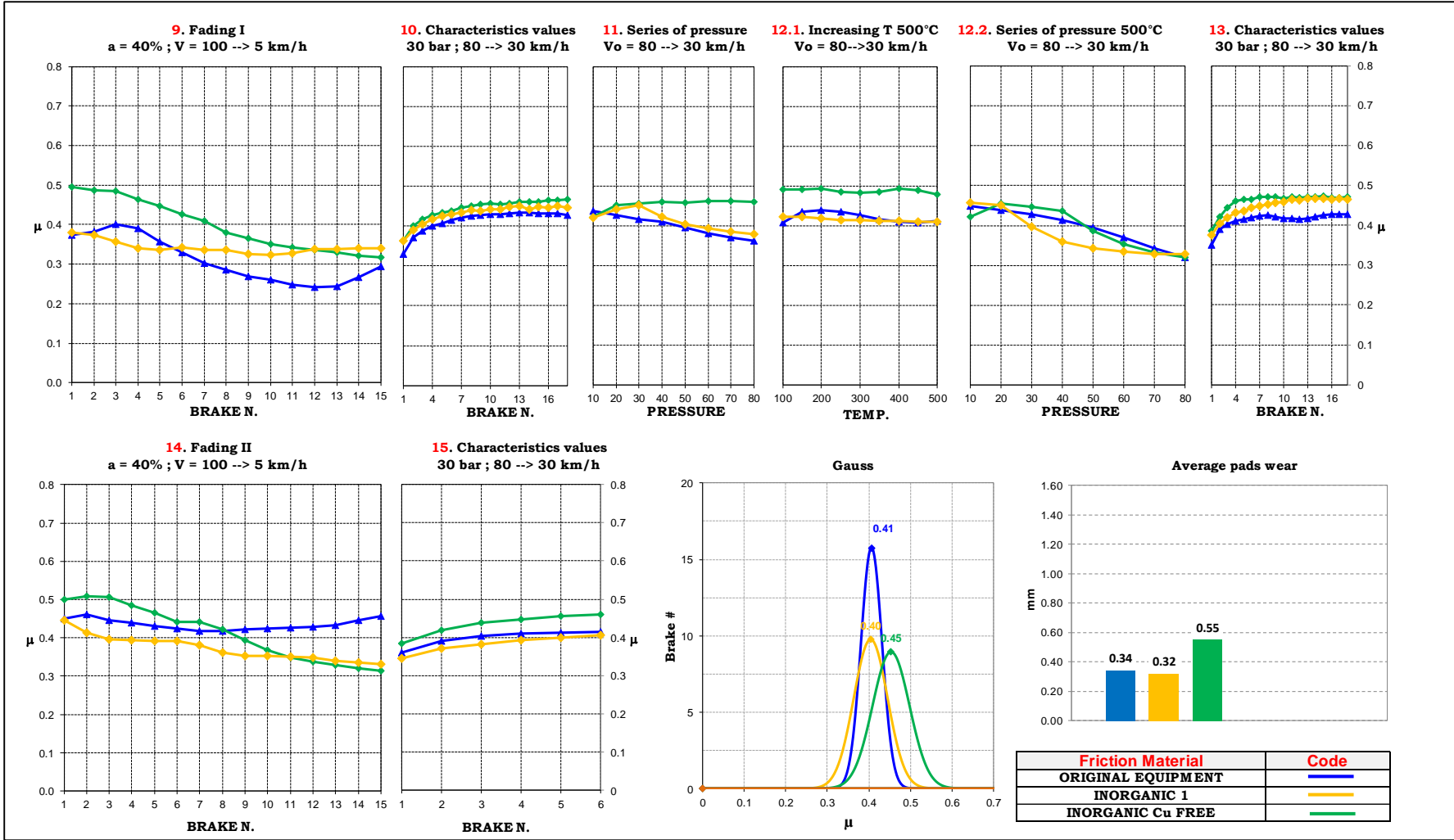
Fig.3.21 SAE J2522 (AK-Master) results of Alfa Romeo 159 2,4Jtdm original equipment (blu), inorganic-binder based friction material (yellow) and inorganic-binder based friction material Cu-Free (green) . Part 2/2

Characteristic values μ		Organic OE		Inorganic 1		Inorganic Cu free	
		Avg.	Min	Avg.	Min	Avg.	Min
Char. Value (3)	μ0P6	0.40		0.42		0.49	
Speed/pressure (4.3)	μv120	0.40		0.38		0.44	
Speed/pressure (4.5)	μvmax	0.43		0.31		0.37	
Char. Value (5)	μ0 P6	0.44		0.42		0.44	
40°C Brake apply (6)	μT40	0.37		0.43		0.50	
Second motorway apply (7)	μMW2	0.42		0.29	0.29	0.31	
Char. Value (8)	μ0P18	0.37		0.39		0.44	
Fade 1 (9)	μF1		0.24		0.32		0.32
Char. Value (10)	μ0P18	0.41		0.43		0.44	
Temperature (12)	μT500		0.32		0.33		0.32
Char. Value (13)	μ0P18	0.41		0.44		0.45	
Fade 2 (14)	μF2		0.42		0.33		0.31
Char. Value (15)	μ0P6	0.40		0.38		0.43	
	μ nom	0.41		0.39		0.43	
	μ min		0.24		0.29		0.31

Tab.3.13 SAE J2522 Characteristic values of organic original equipment, inorganic 1 and inorganic Cu free friction materials

Speed sensitivity of inorganic Cu-free was still present in the pressure/speed section; a reduction of the efficiency was recorded for initial speed higher than 160km/h (fig.3.21 block 4) and in the second motorway application, (fig.3.21 block 7) but friction coefficient values were higher respect inorganic 1. After pressure/speed block characteristic average values resulted stable around 0.43-0.44, at the end of each "char. value" block the friction coefficient switch to a recovery value of 0.48. It is therefore not surprising to record a low speed cold braking as well as a first motorway application friction coefficients of 0.50 (fig.1 block 6) and 0.49 (fig.1 block 7) respectively.

Behavior of inorganic Cu-free in the first and second fading section was very similar with a minimum friction coefficient 0.32 and 0.31 respectively (Fig block 9 and 14), therefore the material after fading and high temperature blocks had a reproducible behavior.

Also for inorganic Cu-free after SAE J2522 test brake pads didn't present any anomaly in terms of lack of compactness. The average total wear of inorganic Cu-free brake pads was higher (but not too high to reject it) compared to organic original equipment and inorganic1 (0.55, 0.34 and 0.32 respectively). A friction coefficient (μ nom. was 0.43 and μ min. was 0.31) ensures performance of the material more than enough to satisfy most driving conditions. According to the test results also for inorganic Cu-free there were no critical elements in the use on a real vehicle.

3.3.2.2.2 Inorganic Cu-free internal fading test

After AK-master, organic original equipment, inorganic 1 and inorganic Cu-free friction material performances were compared with internal fading procedure. Internal fading results are shown in fig.3.22 and characteristic values in tab.3.12
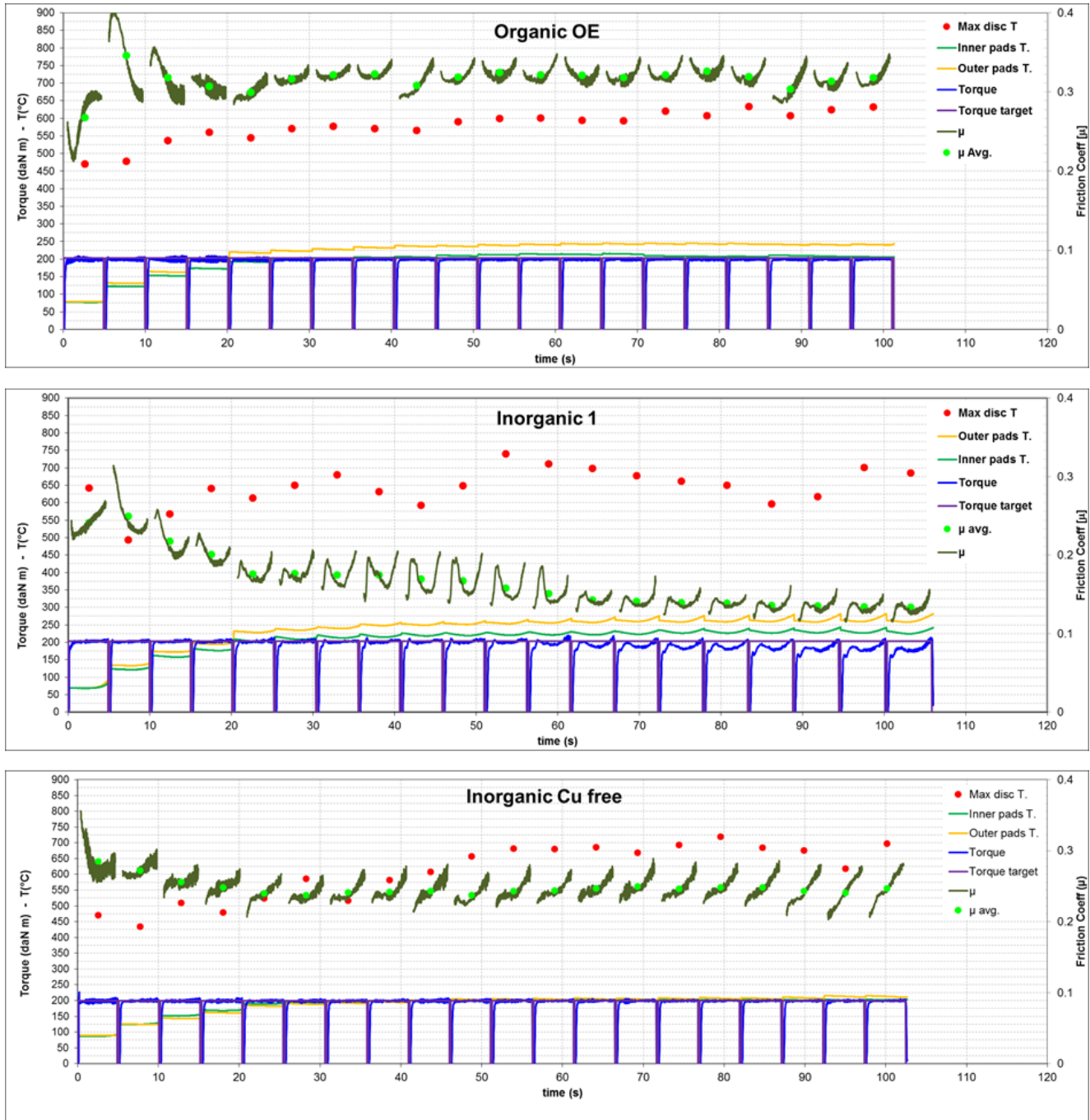

Fig.3.22 Internal fading test results of organic original equipment, inorganic1 and inorganic Cu-free friction materials.

Characteristic Values	Organic OE	Inorganic 1	Inorganic Cu free
Max disc T (°C)	634	741	720
Max disc T Avg. after brake n°10 (°C)	612	675	681
Max pads temperatures (°C)	245	282	215
Min friction coefficient μ	0.21	0.12	0.20
Friction coefficient μ Avg. after brake n°10	0.32	0.14	0.25

Tab.3.14 Internal fading characteristic values of organic original equipment, inorganic 1 and inorganic Cu free friction materials

Considering the obtained results summarized in tab.3.14, it is useful to explain more in detail the temperature of brake pads for the inorganic Cu-free material. Main function of copper and its derivatives is to increase the thermal conductivity of the mix and encourage the heat dispersion from third layer to brake pads. Therefore a lower thermal diffusivity of Cu-free material can explain the strong reduction of brake pads temperature (215°C respect 282°C of inorganic 1).

Regarding the friction coefficient, a lower efficiency at high velocity of inorganic material was confirmed as previously stated when discussing the trend for fading sections in AK-Master test. Despite this trend, however, one important aspect which stands out quite firmly from the internal fading test is the capability of inorganic Cu-free to tolerate the high stresses imposed by the braking conditions. Although less performing respect organic original equipment, inorganic Cu-free friction coefficient is very stable with a good build-up during the brake. At the end of the internal fading test inorganic material presented only few superficial cracks, without any sign of significant material removal, pad side-delamination or structural breakdown.

3.3.2.2.3 Inorganic Cu-free ECE R90 test

In regulation ECE R90 p*erformance* requirements and mechanical characteristics had to be met.

- *Performance requirements*

It was not possible to compare inorganic Cu-free with the organic OE of Alfa 159, so as basis for comparison it was used the original equipment of Alfa 166 "now on named organic OE 2". The Organic OE 2 pads were of same format of 159 OE, plus some NVH

countermeasures such as Rubber shim and chamfer 25 mm wide on the side of disc in and 20 mm wide on the side of disc out. Same machining and finishing was done on inorganic Cu-free.

Block	Block name	Mass and gear	Parameter	Value	Request
1	**Bedding**	Full load	Mileage	min 50 km	T pad 250-500°C at least 3 times
			Initial speed	50-120 km/h	
			T pad max	500°C	
			Deceleration	1-5 m/s²	
			Stops n.	Min. 100	

Fig.3.23 ECE R90 Inorganic Cu-free. Block 1. Bedding.

During the first brake applications a strong airplane noise has been heard. In the same part of the bedding (see red square) the friction level is too high, and therefore not comfortable. After this first part the friction level became constant and acceptable

Block	Block name	Mass and gear	Parameter	Value	Request
2	**Performance check**	Full load	Initial speed	70 km/h	The measured deceleration of the 5 brakes must remain within a tolerance range of ±0,6 m/s² If the request is not met the bedding must be extended
			Final speed	0 km/h	
			Initial T	<100°C	
			Brake pressure front	40 bar	
			Pressure	p=p*	
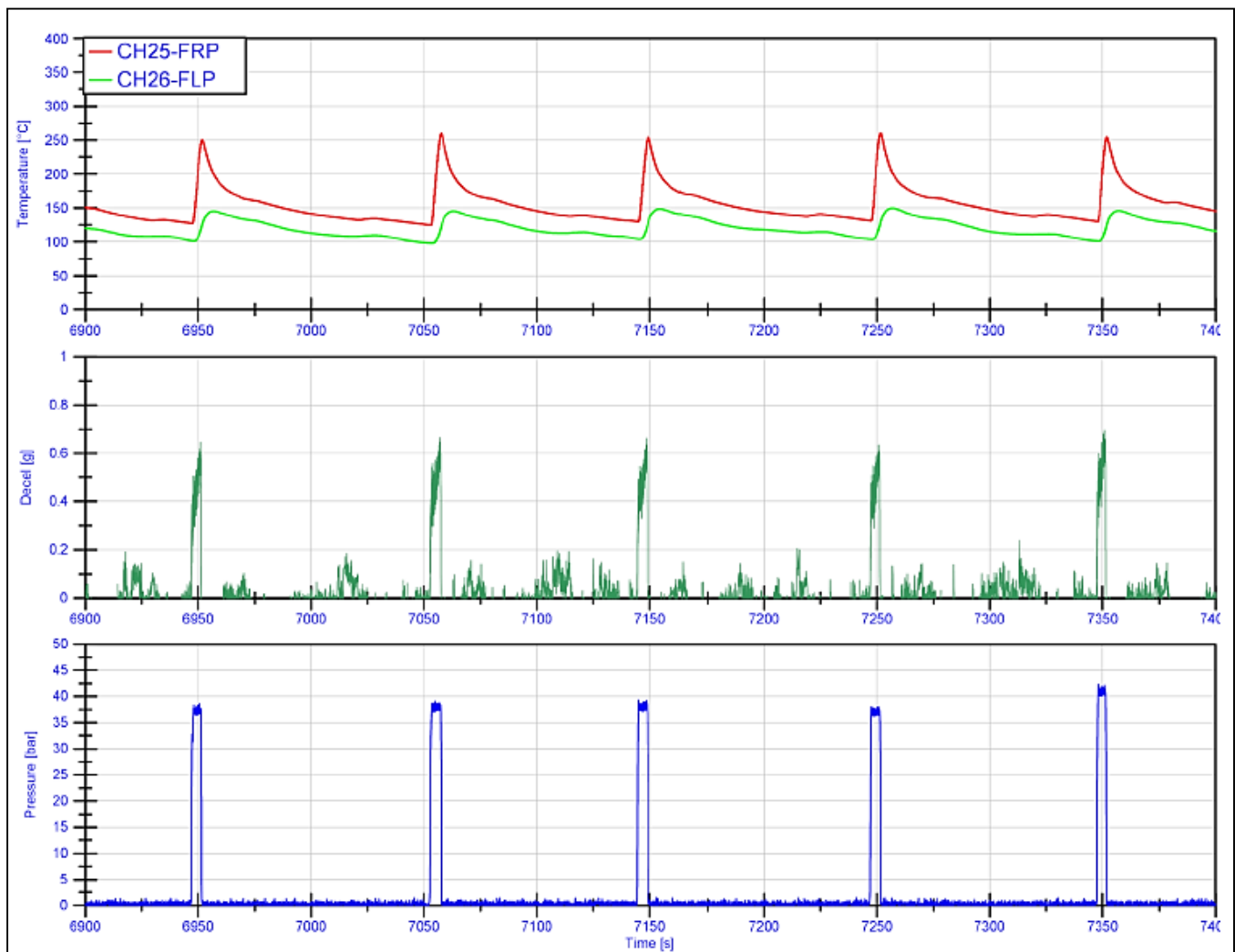
Fig.3.24 ECE R90 inorganic Cu free. Block 2. Performance check
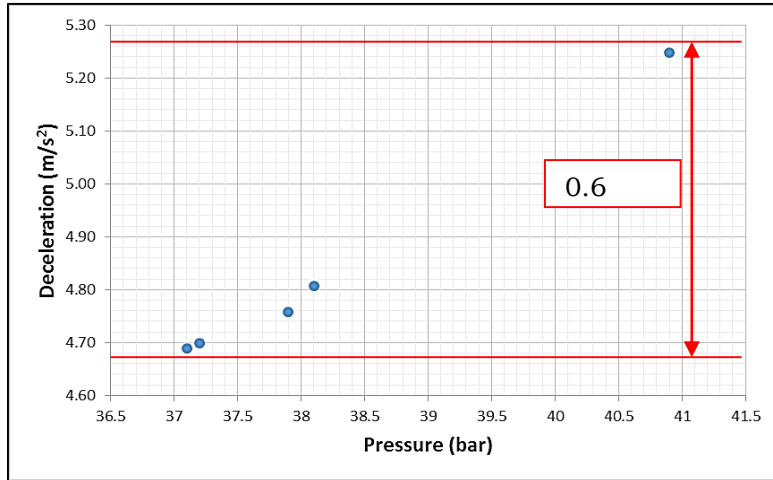
Fig.3.25 ECE R90 inorganic Cu.free. Block 2. Performance check requirements

After the bedding, the friction level must be checked to verify that a constant value has been reached.

The tolerance range has been met, also considering the variability in the brake pressure. During these applications, as a secondary aspect, a not acceptable roughness has been noticed. At the same time an acoustic wire brush has been heard

Block	Block name	Mass and gear	Parameter	Value	Request
3	**(A) Type-0 test with engine disconnected**	Full load	Initial speed	100 Km/h	Deceleration >6.43 m/s² Stop distance ≤ 70m Mean deceleration: more than 6.43 m/s²
			Final speed	0	
			Initial T	65-100°C	
			Application force	6.5÷50 daN	
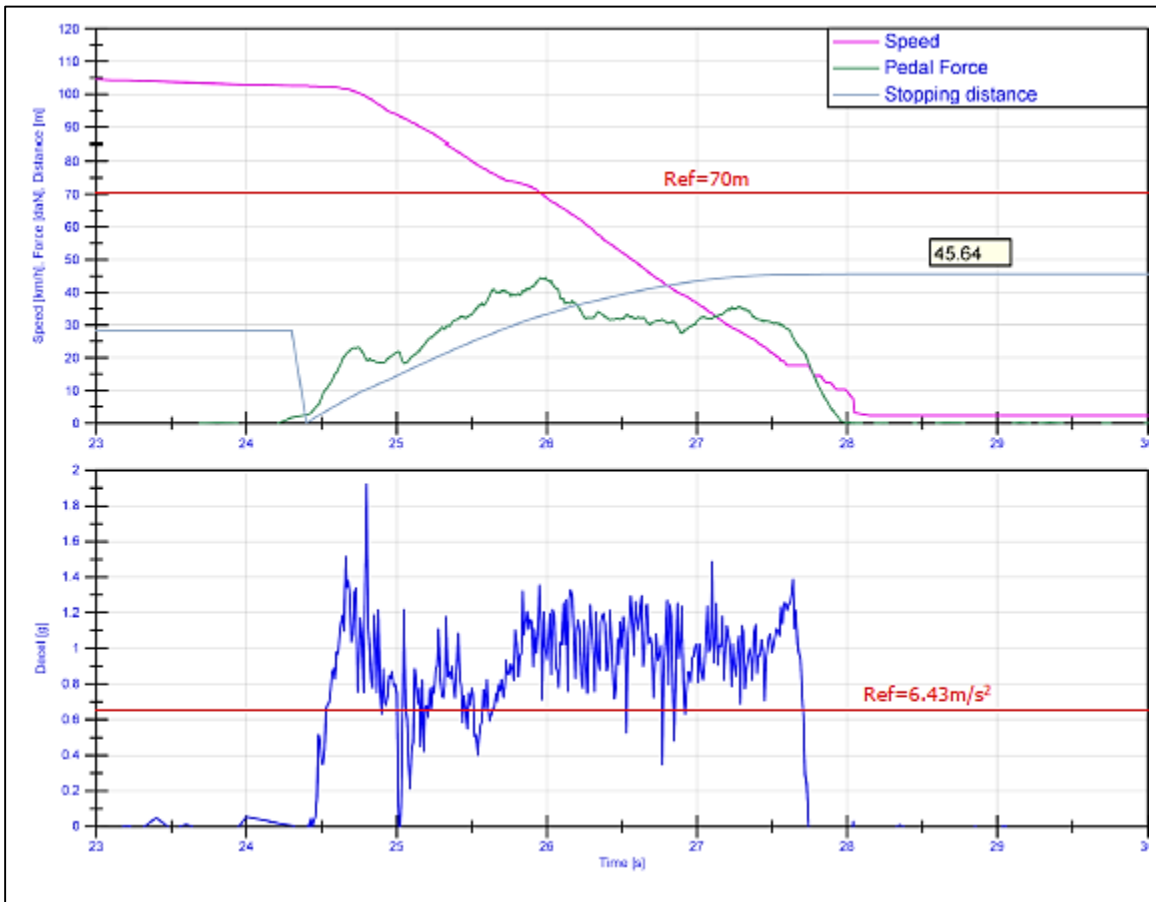
Fig.3.26 ECE R90 inorganic Cu-free. Block 3(A). Type-0 test with engine disconnected

Block	Block name	Mass and gear	Parameter	Value	Request
3	**(B) Type-0 test with engine connected**	Full load	Initial speed	160 km/h	Pedal force > 6.5N
			Final speed	0	Stop distance ≤ 187.52 m
			Application force	6.5÷50 daN	Mean deceleration: more than 5.76 m/s^2
			Initial T	65-100°C	
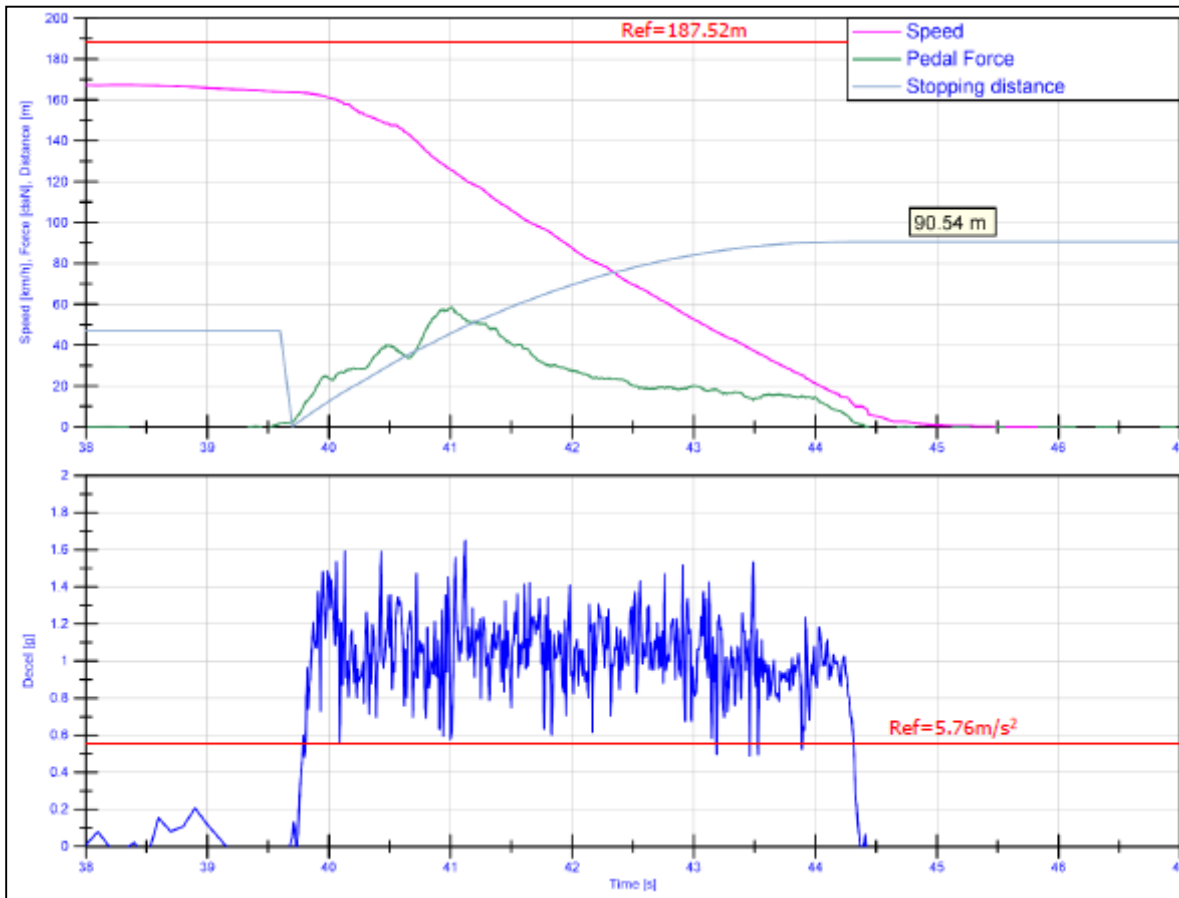
F

ig.3.27 ECE R90 inorganic Cu-free. Block 3(B). Type-0 test with engine connected

Block	Block name	Mass and gear	Parameter	Value	Request
4.	**Type-I test (Fading test)**	Full load Highest gear	Initial speed	120 km/h	Deceleration 3m/s²
			Final speed	60 km/h	
			Δt Time elapsing between the initiation of one brak application and the initiation of the next.	45 s	
			Number of brake applications	15	

Fig.3.28 ECE R90 inorganic Cu-free. Block 4. Type-I test (Fading test)

Block	Block name	Mass and gear	Parameter	Value	Request
4.1	**Hot Performance: Same conditions as Type-0 test (A)**	Full load	Initial speed	100 Km/h	Deceleration >6.43 m/s^2 stopping distance≤70m
			Final speed	0	
			Initial T	65-100°C	

Fig.3.29 ECE R90 inorganic Cu-free. Block 4.1 Hot Performance

Block	Block name	Mass and gear	Parameter	Value	Request
4.2	**Recovery**	Full load	Initial speed	50 km/h	No requirements
			Deceleration	3 m/s^2	
			Stops interval	1.5km	
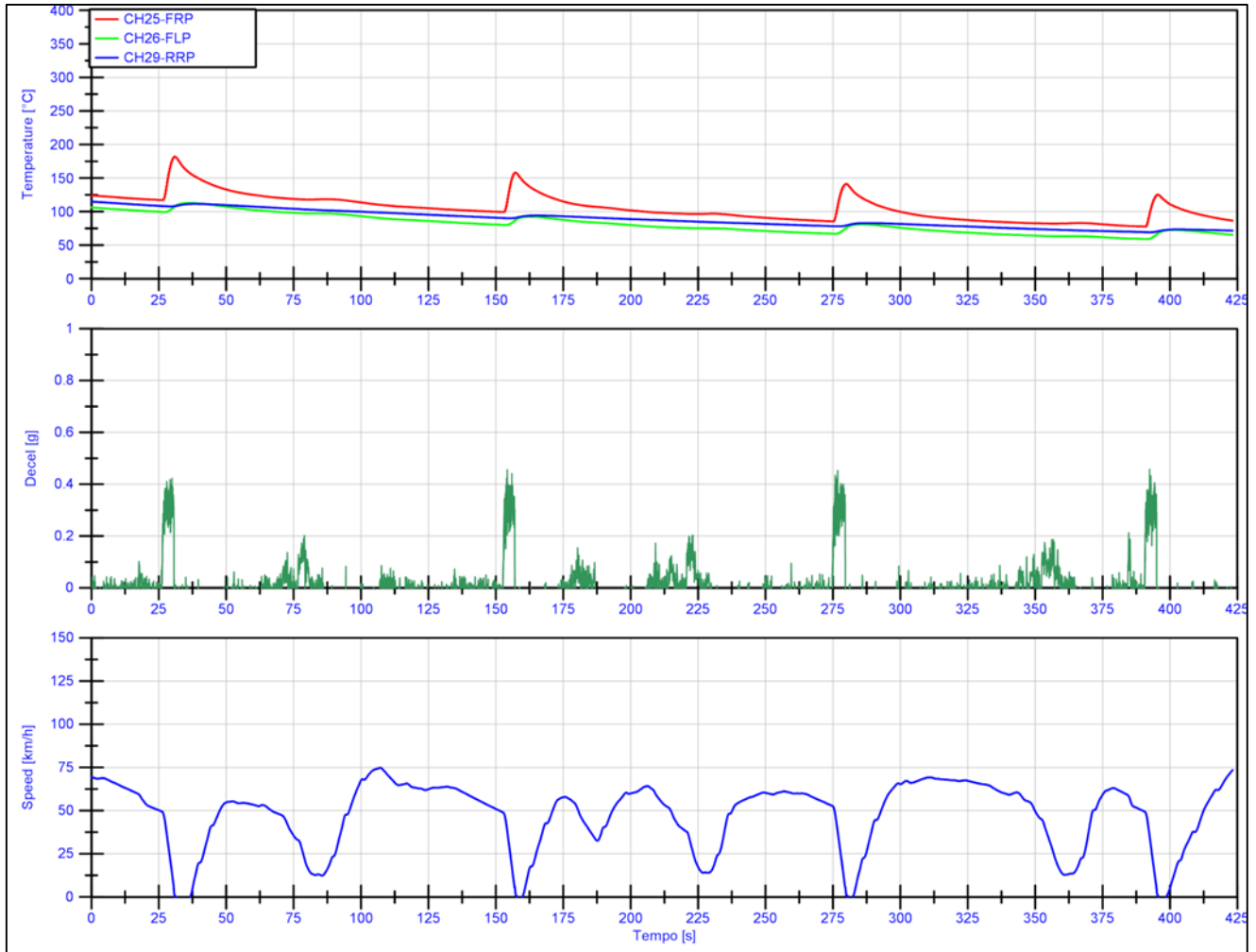
Fig.3.30 ECE R90 inorganic Cu-free. Block 4.2 Recovery

Block	Block name	Mass and gear	Parameter	Value	Request
4.3	**Recovery performance: same conditions as Type-0 test (A)**	Full load	Initial speed	100 Km/h	Deceleration >6.43 m/s² Stopping distance≤70m
			Final speed	0	
			Initial T	65-100°C	
			Pressure	p=p*	

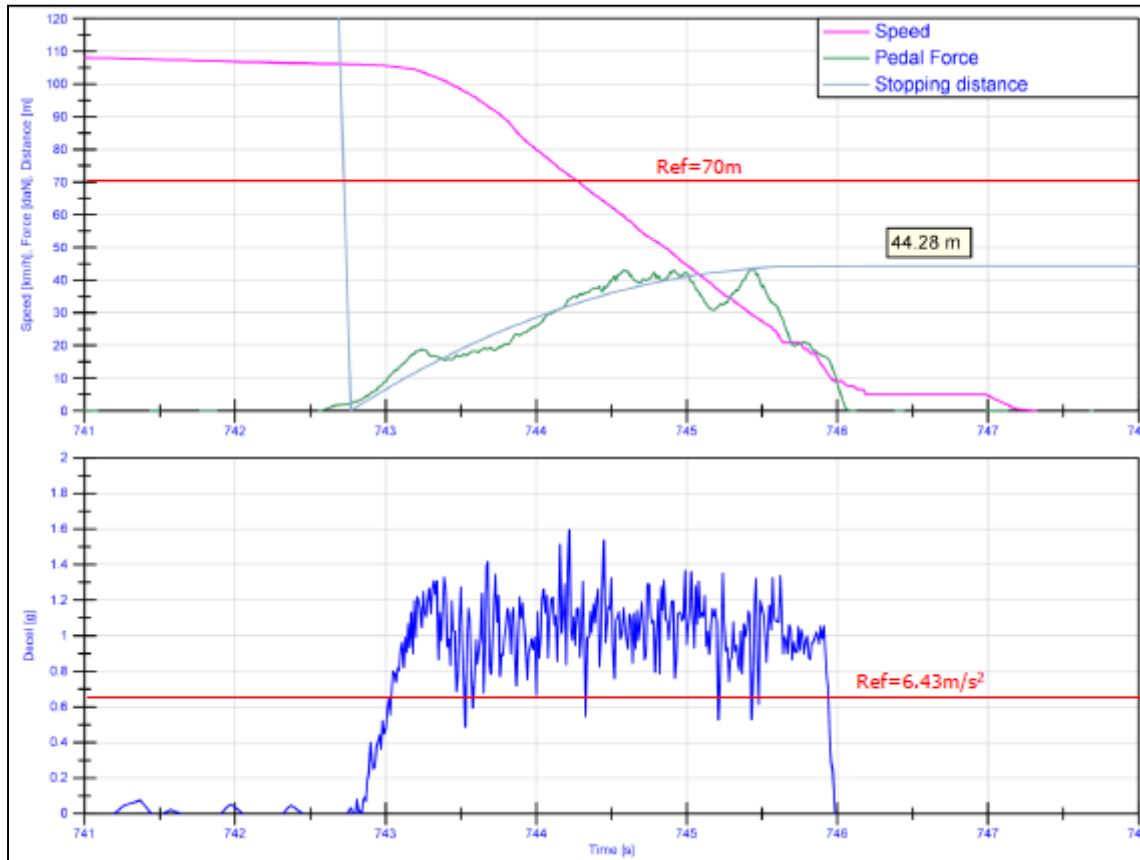**Fig.3.31 ECE R90 inorganic Cu-free. Block 4.3. Recovery performance**

Block	Block name	Mass and gear	Parameter	Value	Request
5	Cold performance test	Full load	Initial speed	70 km/h	The upper two thirds of the curve must lie within ±15% of the curve found with the original equipment
			Deceleration	Up to 6 m/s² max	
			Number of brake applications	≥6	
			Initial T	<100°C	p*=pressure at 0.5m/s²

Fig.3.32 ECE R90 inorganic Cu-free compared with Organic OE2. Block 5. Cold performance test

This requirement was not fulfilled, friction level of inorganic Cu-free was too high compared to organic OE2.

Block	Block name	Mass and gear	Parameter	Value	Request
6	**Speed sensitivity test**	Full load	Initial speed	65,100,135 km/h	Dec(135)=dec(65)±15%
			Pressure	p=p*	
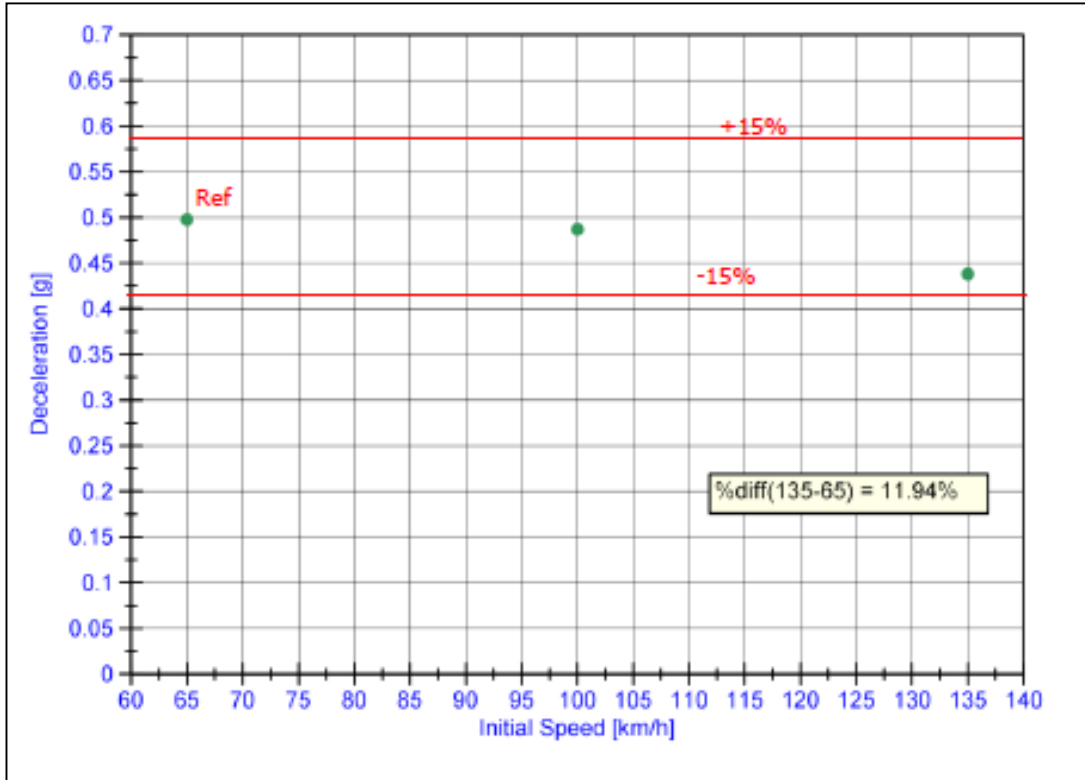
Fig.3.33 ECE R90 inorganic Cu-free. Block 6. Speed sensitivity test

ECE R90 test summary

Step	Result
Bedding	**Positive**
Performance check	**Positive**
Type 0 with engine disconnected	**Positive**
Type 0 with engine connected	**Positive**
Type I (Fading test)	**Positive**
Hot performance	**Positive**
Recovery procedure	**Positive**
Recovery performance	**Positive**
Additional requirements (split axle test)	
Cold performance equivalence test	**Negative**
Speed sensitivity test	**Positive**

Tab 3.15 ECE R90 Performance requirements

Mechanical test	Requirement	Measured	Result
Shear test	F>19,25kN	Min 30.2N Avg.36,7N	**Positive**
Cold compressibility	d≤316μm	Max 74 μm Avg. 63.1 μm	**Positive**

3.16 ECE R90 Mechanical characteristics

The inorganic Cu-free brake pads could not be released according to ECE R90 procedure because of the cold performance equivalence test, this is the only test that has not met the requirements. This can be confirmed comparing the AK-master test results of two materials, see tab.3.17

Characteristic values μ		Organic OE 2		Inorganic Cu free	
		Avg.	Min	Avg.	Min
Char. Value (3)	μ0P6	0.39		0.49	
Speed/pressure (4.3)	μv120	0.37		0.44	
Speed/pressure (4.5)	μvmax	0.34		0.37	
Char. Value (5)	μ0 P6	0.39		0.44	
40°C Brake apply (6)	μT40	0.37		0.50	
Second motorway apply (7)	μMW2	0.35		0.31	
Char. Value (8)	μ0P18	0.39		0.44	
Fade 1 (9)	μF1		0.31		0.32
Char. Value (10)	μ0P18	0.42		0.44	
Temperature (12)	μT500		0.39		0.32
Char. Value (13)	μ0P18	0.42		0.45	
Fade 2 (14)	μF2		0.42		0.31
Char. Value (15)	μ0P6	0.40		0.43	
	μ nom	0.38		0.43	
	μ min		0.31		0.31

Tab.3.17 SAE J2522 Characteristic values of Organic OE2, and inorganic Cu-free friction material

As subjective impression, the feeling of the driver was that the friction level is too high, so it was difficult to handle the brake application in the best way. Low frequency squeals and roughness/wire brush were listened.

3.33 Discussion on testing results

On first part of the work, starting from an R&D organic friction material (*organic low-met*) it was necessary to review ingredients and manufacturing process to produce a full inorganic material with same performance of Alfa 159 original equipment in AK-Master test. To achieve this result all organic raw materials were removed and different inorganic binders in different proportion were attempted, moreover all raw material not compatibles with the new matrix were avoided and, at last, a fine tuning of the other components was required. Despite matrix and were treated separately from other components in manufacturing blending steps, they are not independent in formulation process. Indeed, the ratio between inorganic binders, alkali solution and dry friction mix depended on all selected components. Therefor every modification at friction modifiers, reinforcements, fillers or functionalizers required a tune on inorganic binders.

Not only chemical composition of materials influenced final properties of brake pads, manufacturing process parameters like molding set-up and post curing time were equally significant, for example the special draining system designed for inorganic materials molding affected the amount of water retained by friction mix at selected pressure, modifying material characteristics.

At the end of first part of formulation process, *Inorganic 1* was formulation most similar to the Alfa 159 original equipment in terms of AK-Master performance. *Inorganic 1* compared to the organic *original equipment* demonstrated a lower but stable efficiency ($\mu_{inorganic\ 1}$ =0.39, $\mu_{organic\ OE}$ =0.42)$_{avg.}$ ($\mu_{inorganic\ 1}$ =0.25, $\mu_{organic\ OE}$=0.24)$_{min.}$, furthermore the wear of two materials was comparable. Considering that AK-master procedure was thought to evaluate the behavior of friction material in more than 80% of vehicle use, in this conditions performances of inorganic material and of original equipment were similar. Strong achievement of the first part of this work was that inorganic pads didn't present any anomaly in terms of lack of compactness or cracks evolved during manufacturing and testing,. The critical point on *inorganic 1* was the friction efficiency at high speed, material suffered a speed fading for initial velocity higher than 160 km/h at any pressure. This criticism was highlighted testing the material with a special demanding fading procedure (typically used for sporting car) which submits components to a series of snubs from 225 to 90 km/h at high torque and pressure. In the fading test a good initial friction coefficient μ=0.25 fast dropped during subsequent snubs when temperature raised and friction layer grew up without the possibility of a system recovery. This aspect was evaluated on second part of formulation work.

Regarding chemical emission, it has been demonstrated that manufacturing of inorganic brake pads based on hydraulic binders will have positive effects on the health of workers engaged in the realization of brake pads thanks to the avoidance of hazardous substances generated during manufacturing process on organic brake. Moreover, the use of the innovative pads can reduce the amount of harmful chemicals dispersed into the air during brake events at high temperature, with a subsequent incidence reduction of associated diseases.

Even if non-exhaust airborne particle emission is an interesting topic and is getting growing attention and there is not a test stand for standardized measurements of the brake emissions internationally accepted, in the future is expected that materials particle emission will be regulated. The aim of emission test procedure was to measure particulate matter emission PM10 and particle number emission PN10. Good tribological behavior of *inorganic 1* was confirmed when compared to an organic low-met commercial material. Highest wear rate of disc only in first test step for inorganic material could be explained as a longer running-in time of this new materials. Tribo-layer required more time to be formed at brake pad/disc interface, indeed on second test step, when components were settled their wear was significantly lower. This results should be considered for future regulations on particle emission from brake systems, different tribology behavior of new and used materials due to running-in

phase, possible scorched or green layer (hard surface coating for safe braking after install) can significantly change classification of different materials. Furthermore, beside airborne particle emission, the use of analysis procedure on dyno-bench test as did for manufacturing process could show chemical emission of brake system during the use.

On the second part of formulation work two main aspects were considered. The first aspect was a new regulation on brake pads which provides that in some countries copper in friction materials has to be limited to 5% after January 1, 2021 and to 0.5% after January 1, 2025; the second aspect was the sensitivity of *inorganic 1* at the high speeds. At first all the component containing copper were avoided in friction formulation, copper substitution required a series of countermeasures aimed to replace copper properties in terms of friction stability, wear resistance, heat dissipation and noise damping.

At last, speed sensitivity was considered; results from internal fading of *inorganic 1* shown a low efficiency when submitted at high temperature, speed and pressure. This behavior could be assessed to a formation of an inadequate tribo-layer in this conditions. Low friction coefficients required higher pressure to reach required torque during the test increasing also pad wear rate due to higher shear stress. An excess of third body layer thickness can reduce surfaces contact with abrasives further reducing the friction efficiency. Therefore it was necessary to review compactness of friction material removing fillers and modifying nature and amount of binders, then reducing the amount of tribo-layer formed at brake pad/disc interface substituting abrasive components and lowering the amount of lubricants.

At the end of second part of friction formulation *Inorganic Cu-free* was the material with best performance in AK-Master and internal fading tests. In *Inorganic Cu-free* AK-Master it was measured a contained speed sensitivity, anyway less significant respect *Inorganic 1*. Internal fading requirements were completely satisfied, efficiency of the material at high temperature-speed-torque for the whole test was achieved. According to this data inorganic materials are clearly capable of withstand also the severe thermo-mechanical conditions of a fading test required for sport-car application, providing more than acceptable performances, even more impressive considering the introduced innovations.

Good efficiency of the brake system on dyno bench test guaranteed the possibility of using *Inorganic Cu-free* on a real vehicle. Testing vehicle was the Alfa Romeo 159 2,4Jtdm; for safety reasons trials were conducted in Vairano track. ECE Regulation 90 describe the test procedure concerning the approval of replacement brake lining assemblies. It was not possible to compare *Inorganic Cu-free* with Alfa159 original equipment friction material, therefore it was used as matter of comparison the original equipment of Alfa 166, which had the same brake pad format. All the requirements of ECE R90 procedure in terms of performance and mechanical characteristics were met except the comparison of materials in "cold performance equivalence" block were

inorganic materials exceeded in friction coefficient value respect 166 OE for more than 30%. Since *Inorganic Cu-free* was designed for high demanding internal fading procedure specifically designed for sport car applications, in future activities will be compared with materials for vehicles of different market segment.

The results obtained so far are regarded as particularly promising in view of further development of these new class of friction materials.

Summary/Conclusions

The role of a brake systems is to generate a braking torque to retard the road wheel and thus the vehicle to which it is fitted. The purpose of friction brakes is to decelerate a vehicle transforming the kinetic energy of the vehicle into heat, via friction, and dissipating that heat to the surroundings. Modern light and commercial vehicles brake systems are constituted by a cast iron brake disk integral with the wheel hub which is clamped by brake pads pushed on the disc by slave cylinders inside a caliper fixed to an hub bracket.

State-of-the-art brake pads for passenger cars are constituted nowadays by resin-bonded composite friction materials, they are specially formulated to give good friction and wear performance under the sliding contact conditions of braking. The basis of such formulations is usually a polymeric binder (usually phenolic resin) with addition of components that provide mechanical strength necessary to withstand at generated frictional forces and good friction efficiency during brakes at different conditions.

The aim of this work was investigating the feasibility to produce a new and alternative friction materials for passenger car disk brake pads with a low environmental impact compared to traditional friction materials based on organic binders.

The idea was to substitute organic friction materials focusing on developing new braking materials based upon innovative friction mixes and inorganic hydraulic binders with enhanced properties, and subsequently testing their friction performances. The use of inorganic binders can be considered more environmentally-friendly to the use of traditional organic thermoset resin in terms of brake pad embodied energy and chemical emission during their manufacturing and use.

During this study few important results were achieved as summarized in the following:

1. Raw material selection: only inorganic components were selected for both binder and friction active materials to avoid high temperature VOCs emissions, typical of organic polymers usually employed in ordinary brake pads.

2. New developed friction formulation fully respects the regulations regarding friction materials forbidden elements such as lead, mercury, cadmium and their compounds, chromium (VI)-salts and asbestiform fibers; moreover in some formulation copper content was limited to less than 0.5 w%.

3. The manufacturing process of inorganic materials required only a blending step, and a custom-engineered molding set-up for the press in order to avoid water leakage during manufacturing. Semi-quantitative analysis was carried on chemicals (such as VOCs and SVOCs) generated during scorching process on organic brake pads. It was measured an emission of hazardous substances from organic components which can cause severe human health effects, including causing genetic defects and cancer. No high temperature process was required for new inorganic brake pads, moreover the absence of organic ingredients

assures a lower emission of hazardous volatile chemicals also during the pads use.

4. Wear particle emission of an inorganic low-met and a commercial organic low-met friction material were measured. According to wear particle emission procedure results (a specific procedure which foreseen the use of friction material in urban condition) inorganic lining wear was lower respect to the organic lining wear only after running-in process where friction layer is formed. Particles emission of new inorganic materials were considerably lower in terms of PM10 and PN10 than organic commercial material during the whole test.

5. According to the results obtained during the SAE J2522 AK-Master test, inorganic materials demonstrated good brake efficiency compared to OE organic brake pad specifically designed for the tested braking system. Satisfying material performances during the main driving conditions are therefore fulfilled; it remains still to be enhanced how to stabilize friction coefficient in cold brake and to reduce the sensitivity in the speed and fading blocks.

6. The "internal fading test" specific for sport car applications demonstrated the effectiveness of inorganic brake pad when carefully designed to resist at high thermo-mechanical loads.

7. Regulation No 90 of the Economic Commission for Europe of the United Nations (UN/ECE) establishes foreseen provisions concerning the approval of replacement brake lining assemblies. Novel inorganic material achieved all the request foreseen by regulation when used on Alfa Romeo 159 2,4Jtdm car except for block 5 "cold performance test", indeed friction level of inorganic material was too high compared to the organic. According to this results the use of proposed inorganic brake pads would appear more suitable for sporting car application.

Low level of wear powders and VOCs emission and low embodied energy and water of new full inorganic cold-wet-made brake pads are in line with a large part of the EU regulations and strategies, such as:

- *Climate Action and Energy Strategy:* among others, the objective is to cut EU greenhouse gas emissions to at least 20% below 1990 levels by 2020.

- *Environment and Health Policies:* the goal is to help green the EU economy, protect nature, and safeguard the health and quality of life of people living in

the EU, with particular reference to the improvement of air quality and the reduction or elimination of the effects of harmful chemicals.

References

Andrea Bonfanti ref.43, 123, 233, 234, 236, 237, 247

1. *Tribological surfaces of organic brake pads.* Eriksson, Mikael and Jacobson, Staffan. 12, December 2000, Tribology International, Vol. 33, pp. 817-827.

2. Blau, Peter J. *Compositions, Functions, and Testing of Friction Brake Materials and Their Additives.* Metals and Cerarmics Division, Oak Ridge National Laboratory. 2001. ORNL/TM-2001/64.

3. Chan, D. and Stachowiak, G.W. *Proceedings of the Institution of Mechanical Engineers, Part D: Journal of Automobile Engineering.* 2004. pp. 953-964. Vol. 218.

4. Dante, Roberto C. *Handbook of Friction Materials and Their Applications.* 2015.

5. S. Turani, K. Vikulov, M. Valle and M. Orlandi. *Method for making a ceramic matrix material for friction components of brakes and ceramic matrix material made by such method. 8960384* United States Patent, 2008.

6. *Friction Performance of Eco-Friendly Cu-Free Brake Materials with Geopolymer Matrixes.* Poh Wah Lee, Lin Lee, Peter Filip. 2013-01-2026, Southern Illinois Univ. at Carbondale : s.n., 2013, SAE technical paper.

7. *Identification of Organic Compounds Released from Low-Metallic Automotive Model Brake Pad and its Non-Airborne Wear Particles.* Daniela Plachá, Pavlina Peikertova, Jana Kukutschova, Poh Wah Lee, Kristina Čabanová and Jiří Karas, Jana Kuchařová, Peter Filip. 2015-01-2662, 2015, SAE technical paper.

8. Ashby, Michael F. *Materials and the Environment (Second Edition).* 2013 .

9. Rod Jones, Michael McCarthy and Moray Newlands. Fly Ash Route to Low Embodied CO2 and Implications for Concrete Construction. *2011 World of Coal Ash (WOCA) Conference - May 9-12, 2011 in Denver, CO, USA.*

10. *Alkali-activated binders: A review Part 1. Historical background, terminology, reaction mechanisms and hydration products.* Fernando Pacheco-Torgal, Joa˜o Castro-Gomes, Said Jalali. 2008, Construction and Building MATERIALS, Vol. 22, pp. 1305–1314.

11. *Alkali-activated binders: A review. Part 2. About materials and binders manufacture.* Fernando Pacheco-Torgal, Joao Castro-Gomes, Said Jalali. 2008, Construction and Building MATERIALS, Vol. 22, pp. 1315–1322.

12. M.W Brocklesbya, J.B Davison. The environmental impacts of concrete design, procurement and on-site use in structures. *Construction and Building Materials.* 12 June 2000, Vol. 14, 4, pp. 179–188.

13. Britannica, Encyclopaedia. Power brake system. [Online] http://www.britannica.com/media/full/44957/47836.

14. Nicholson, G. *Facts about Friction: A Friction Material Manual Almost All You Need to Know about Manufacturing.* s.l. : Gedoran, 1995. p. 244 .

15. *Development of materials for automotive disc brakes.* Maluf, Omar, et al. 2007, Minerva, Vol. 4 (2), pp. 149-158.

16. *Metal-Ceramic Composites in High-Energy Friction Applications.* Hooton, A. 1969, Bendix Technical Journal, pp. 55-61.

17. *Fillers in friction materials.* Spurr, R.T. 3, December 1972, Wear, Vol. 22, pp. 367–372.

18. http://www.ameca.org/. [Online]

19. Automotive Manufacturers Equipment Compliance Agency, Inc. *AMECA Compliance List of VESC V-3 Brake Friction Material For Three-Year Period 2012-2015.* 2016.

20. International, SAE. Brake Lining Quality Test Procedure. 2012. SAE J661_201211.

21. Wieckowski, Introduced by Senator. Senate Bill No. 346.

22. BRAKE FRICTION MATERIAL--RESTRICTIONS ON USE. 2010. SUBSTITUTE SENATE BILL 6557.

23. *Composites as Friction Materials: Recent Developments in Non-Asbestos Fiber Reinforced Friction Materials - A Review.* Bijwe, Jayashree. 3, JUNE 1997, POLYMER COMPOSITES, Vol. 18, pp. 378-396.

24. *The use of analytical surface tools in the fundamental study of wear.* BUCKLEY, D. H. 1978, Wear, Vol. 46, pp. 19-53.

25. P.K. ROHATGI, Y. LIU , S.C. LIM. Wear Mapping for Metal and Ceramic Matrix Composites. *Advances in Composite Tribology.* s.l. : K Friedrich.

26. *Two-body and three-body abrasion: A critical discussion.* Gates, J.D. 1998, Wear, Vol. 214, pp. 139-146.

27. *Transitions between two-body and three-body abrasive wear: influence of test conditions in the microscale abrasive wear test.* R.I. Trezona, D.N. Allsopp, I.M. Hutchings. 229, 1999, Wear, Vol. 225, pp. 205–214.

28. *Friction and Molecular Structure: the Behaviour of some Thermoplastics,.* Christine M. Pooley, D. Tabor. [ed.] The Royal Society. 1972, Proc. Roy. Soc., London, Series A., Vol. 329.

29. Moore, M.A. *Abrasive wear, in Fundamentals of Friction and Wear of Materials.* Rigney : D.A., 1981.

30. Gwidon W Stachowiak, Andrew W Batchelor. Abrasive, erosive and cavitation wear. *Engineering Tribology (Fourth Edition).* 12.

31. *Principles of abrasive wear.* Khruschov, M. M. 28, 1974, Wear, pp. 69-88.

32. *A review of two-body abrasive wear.* Moore, M. A. 1974, Wear, Vol. 27, pp. 1 - 17.

33. *The influence of solid state cohesion of metals and non-metals on the magnitude of their abrasive wear.* Ashok, Vijk K. 1975, Wear, Vol. 35, pp. 205 - 209.

34. Hawk, Jeffrey A. and Wilson, R.D. Tribology of Earthmoving, Mining, and Minerals Processing. *Modern trybology handbook.* s.l. : CRC Press LLC, 2001.

35. *Grain size and porosity dependence of ceramic fracture energy and toughness at 22°C.* RICE, R. W. 1996, JOURNAL OF MATERIALS SCIENCE, Vol. 31, pp. 1969-1983.

36. *Mechanisms of abrasive wear in lubricated contacts.* Hyncica, J. A. Williams and A. M. 1992, Wear, Vol. 152, pp. 57-74.

37. *The measurement of abrasive particle.* P.A. Swanson, A.F. Vetter. 2, 1985, A S L E Transactions, Vol. 28.

38. *Description of Abrasive Particle Shape and Its Relation to Two-Body Abrasive Wear.* Michael G. Hamblin, Gwidon W. Stachowiak. 4, 1996, Tribology Transactions, Vol. 39.

39. *A multi-scale measure of particle abrasivity, and its relation to two-body abrasive wear.* M.G. Hamblin, G.W. Stachowiak. 1995, Wear, Vol. 190, pp. 190-196.

40. *Particle angularity and its relationship to abrasive and erosive wear.* Stachowiak, G.W. 2000, Wear, Vol. 241, pp. 214–219.

41. *The effects of particle characteristics on three-body abrasive wear.* G.B. Stachowiak, G.W. Stachowiak. 2001, Wear, Vol. 249, pp. 201–207.

42. *Numerical characterization of wear particles morphology and angularity of particles and surfaces.* Stachowiak, G. W. 1-3, Tribology International, Vol. 98, pp. 139–157.

43. *Role of the friction layer in the high-temperature pin-on-disc study of a brake material.* Piyush Chandra Verma, Rodica Ciudin, **Andrea Bonfanti**, Pranesh Aswath,Giovanni Straffelini, StefanoGialanella. 2016, Wear, Vols. 346-347, pp. 56-65.

44. *Tribological surfaces of organic brake pads.* Mikael Eriksson, Staffan Jacobson. 2000, Tribology International, Vol. 33, pp. 817–827.

45. *Effects of silicon carbide particle sizes on friction-wear properties of friction composites designed for car brake lining applications.* Vlastimil Matějkaa, Yafei Lub, Long Jiaob, Li Huangb, Gražyna Simha Martynkováa, Vladimír Tomášeka. 1-2, 2010, Tribology International, Vol. 43, pp. 144–151.

46. *Effects of alumina in nonmetallic brake friction materials on friction performance.* Vladimır Tomasek, Gabriela Kratosova, Rongping Yun, Yanli Fan, Yafei Lu. 2009, J Mater Sci, Vol. 22, pp. 266–273.

47. *Chemical and microstructural changes induced by friction and wear of brakes.* W. Österle, M. Griepentrog, Th. Gross, I. Urban. 2001, Wear, Vol. 251, pp. 1469–1476.

48. *Morphology and Toughness of Abrasive Particles and Their Effects on the Friction and Wear of Friction Materials: A Case Study with Zircon and Quartz.* E. J. Lee, H. J. Hwang, W. G. Lee, K. H. Cho • H. Jang. 2010, Tribol Lett, Vol. 37, pp. 637–644.

49. *The size effect of zircon particles on the friction characteristics of brake lining materials.* K.H. Choa, H. Jang , Y.-S. Hong, S.J. Kim, R.H. Basch, J.W. Fash. 2008, Wear, Vol. 264, pp. 291–297.

50. *The role of transfer layers on friction characteristics in the sliding interface between friction materials against gray iron brake disks.* M.H. Choa, K.H. Choa, S.J. Kimb, D.H. Kimc and H. Janga. 2, 2005, Tribology Letters, Vol. 20, pp. 101-107.

51. Pierson, Hugh O. *Handbook of Refractory Carbides and Nitrides.* s.l. : William Andrew Inc. , 1996 .

52. Branko Matovi, ToyohikoYano. Silicon Carbide and Other Carbides: From Stars to the Advanced Ceramics (Second Edition). [book auth.] Somiya. *Handbook of Advanced Ceramics: Materials, Applications, Processing, and properties.* s.l. : Shigeyuki, 2013.

53. *Boron Carbide: Structure, Properties, and Stability under Stress.* Vladislav Domnich, Sara Reynaud, Richard A. Haber, and Manish Chhowalla. 11, 2011, J. Am. Ceram. Soc., Vol. 94, pp. 3605–3628.

54. *Polytypism and Properties of Silicon Carbide.* F. Bechstedt, P. Käckell, A. Zywietz, K. Karch, B. Adolph, K. Tenelsen and J. Furthmüller. 1, 1997, physica status solidi (b), Vol. 202, pp. 35-62.

55. *Material selection for hard coatings.* Holleck, H. 2661, 1986, Journal of Vacuum Science & Technology A, Vol. 4.

56. *Raw materials for refractories: SiC and Si3N4.* Ault, Nail N. Alabama : s.n., 1982. Raw Materials for Refractories Conference.

57. Joseph R Smyth, David L Bish. *Crystal Structures and Cation Sites of the Rock-Forming Minerals.* s.l. : Boston ALLEN & UNWIN, 1988.

58. W. a. Deer, R. a. Howie, J. Zussman. *An introduction to the Rock-Forming Minerals: 2nd edition.* 1992.

59. Cox, Roy L. *Engineered tribological composite: The Art of friction materials development.* s.l. : SAE International, 2012.

60. Organization, World Health. *IARC MONOGRAPHS ON THE EVALUATION OF CARCINOGENIC RISKS TO HUMANS.* 1997. Vol. 68.

61. *The mineralogy of bauxite for producing smelter-grade alumina.* M. Authier-Martin, G. Forté, S. Ostap, J. See. 12, Overview Mineralogy, Vol. 53, pp. 36-40.

62. L. KEITH HUDSON, CHANAKYA MISRA, ANTHONY J. PERROTTA, KARL WEFERS, F. S.WILLIAMS,. Aluminum Oxide. *Ullmann's Encyclopedia of Industrial Chemistry.* 2000.

63. AZoM.com. The Different Types of Commercially Available Grades . [Online] 2002. http://www.azom.com/article.aspx?ArticleID=1389#_Smelter_Grade_Alumina.

64. *Metastable Alumina Polymorphs: Crystal Structures and Transition Sequences.* Igor Levin, David Brandon. 8, 1998, J. Am. Ceram. Soc, Vol. 81, pp. 1995–2012.

65. Teruyuki Nagayoshi, Noboru Suzuki, Manabu Ono. *Friction material composition and friction material using the composition. US 20040247847 A1* 12 9, 2004.

66. *Shape memory effect and pseudoelasticity behavior in tetragonal zirconia polycrystals: A phase field study.* Mahmood Mamivand, Mohsen Asle Zaeem, Haitham El Kadiri. 2004, International Journal of Plasticity, Vol. 60, pp. 71–86.

67. *Thermochemical insights into refractory ceramic materials based on oxides with large tetravalent cations.* Navrotsky, Alexandra. 2005, J. Mater. Chem.,, Vol. 15, pp. 1883–1890.

68. *Thermal stability of nanostructurally stabilized zirconium oxide.* Fereydoon Namavar, Gonghua Wang, Chin Li Cheung , Renat F. Sabirianov, Xiao Cheng Zeng, Wai Ning Mei, Jaeil Bai,Joseph R. Brewer, Hani Haider, and Kevin L. Garvin. 2007, Nanotechnology, Vol. 18.

69. *Evaluation of solid lubricant materials for use under extreme environmental conditions review. Recent research developments in materials science.* J.H. Ouyang, S. Sasaki, T. Murakami, K. Umeda. s.l. : S.G. Pandalai, 2004, Vol. 5, pp. 85–103.

70. *Fundamentals of Adhesion.* s.l. : Lieng-Huang Lee, 1991.

71. *Self-Consistent Equations Including Exchange and Correlation Effect.* W. Kohn, L. J. Sham. 4A, 1965, PHYSICAL REVIEW, Vol. 140, pp. A1133-A1138.

72. *Theory of the bimetallic interface.* J. Ferrante, J. R. Smith. 6, 1985, PHYSICAL REVIEW B, Vol. 31, pp. 3427-3434.

73. Stachowiak, A.W. Batchelor. *Engineering Tribology 3rd edn.* Amsterdam : Elsevier Butterworth-Heinemann , 2001.

74. *Solid lubricants: a review.* T. W. Scharf, S. V. Prasad. 2013, J Mater Sci, Vol. 48, pp. 511-513.

75. *A chemical and theoretical way to look at bonding on surfaces.* Hoffmann, Roald. 3, 1988, Rev. Mod. Phys., Vol. 60, p. 601.

76. *Ceramic microstructure and adhesion.* Buckley, D. H. 3, 1985, J. Vac. Sci. Technol., Vol. A3, p. 762.

77. *The adhesion of evaporated metal films on glass.* Weaver, P. Benjamin and C. 1961. Proc. Roy. Soc. London. Vol. A261, p. 516.

78. Jia-Hu Ouyang, Xue-Song Liang. High-Temperature Solid Lubricating Materials . *Encyclopedia of Tribology.* 2013.

79. *A STUDY OF MECHANISMS OF GRAPHITE FRICTION AND WEAR.* P. J. BRYANT, I. L. GUTSHALL, L. H. TAYLOR. 1964, WEAR, Vol. 7.

80. *Transfer Lubrication for High Temperatures: A Review.* Lancaster, J. K. 437, OCTOBER 1985, Journal of Tribology, Vol. 107.

81. Haidou Wang, Binshi Xu, Jiajun Liu. *Micro and Nano Sulfide Solid Lubrication.* s.l. : Science Press Beijing, Springer Heidelberg Dordrecht London New York, 2011.

82. Reynolds, W.N. *Physical properties of graphite.* Amsterdam : Elsevier, 1968.

83. Substech. [Online] http://www.substech.com/dokuwiki/lib/exe/detail.php?id=graphite&cache=cache&media=graphite_ structure.png.

84. *Superlubricity of graphite.* JA Heimberg, HW Zandbergen. 2004, Phys Rev Lett , Vol. 92, pp. 126101–126104.

85. *Influence of water vapor and oxygen on the tribology of carbon materials with sp2 valence configuration.* Yen, BK. 1996, Wear, Vol. 192, pp. 208–215.

86. Clauss, F.J. *Solid Lubricants and Self-Lubricating Solids.* New York : Academic Press, 1972.

87. *Tight-binding density of electronic states of pregraphitic carbon.* Charlier JC, Michenaud JP, Lambin Ph. 1992, Physical Review B, Vol. 46, pp. 4540-4543.

88. *Super low to high friction of turbostratic graphite under various atmospheric test conditions.* N. Kumar, S. Dash, A.K. Tyagi, Baldev Raj. 2011, Tribology International, Vol. 44, pp. 1969–1978.

89. *Load dependent friction coefficient of crystalline graphite and anomalous behavior of wear dimension.* N. Kuma, A.T. Kozakovr, T.R. Ravindran, S. Dash,A.K. Tyagi. Accepted date: 25 March 2015, Tribology International. Author's Accepted Manuscript.

90. *The Role of Raw Material Ingredients of Brake Linings on the Formation of Transfer Film and Friction Characteristics.* Min Hyung Cho, Eun Gap Bae and Ho Jang ,Geunjoong Jeong, Daehwan Kim and Chunrak Choi. New Orleans, Louisiana : SAE International, October 28-31, 2001. Proceedings of the 19th Annual Brake Colloquium & Exhibition.

91. *Graphite, semi-graphite, natural coke, and natural char classification—ICCP system.* B. Kwiecin, H.I. Petersen. 2004, International Journal of Coal Geology, Vol. 57, pp. 99–116.

92. *Advantages of natural microcrystalline graphite filler over petroleum coke in isotropic graphite preparation .* Ke Shen, Zheng-Hong Huang, Kaixin Hu, Wanci Shen, Suyuan Yu, Junhe Yang,. Accepted Manuscript 26 March 2015, Carbon.

93. Asbury, Carbons. Amorphous Graphite. [Online] http://asbury.com/technical-presentations-papers/materials-in-depth/amorphous-graphite/.

94. Inagaki, Michio. Advanced Carbon Materials. *Handbook of Advanced Ceramics.* s.l. : Elsevier Inc., 2013.

95. Weisenfluh, Cortland Eble and Jerry. *Metallurgical Coal Resources in Eastern Kentucky.* Lexington, Kentucky : Department for Energy Development and Independence Energy Research and Development, 2012.

96. Mohamed A. Fahim, Taher A. Alsahhaf, Amal Elkilani. Chapter 6 – Thermal Cracking and Coking. *Fundamentals of Petroleum Refining.* 2010, pp. 123-152.

97. *THE PRODUCTION OF MATERIALS AND CHEMICALS FROM COAL.* Frank Derbyshire, Marit Jagtoyen, You Qing Fei, and Geoff Kimber. University of Kentucky Center for Applied Energy Research, 3572 Iron Works Pike, Lexington KY 40511-8433 : s.n., 1994, American Chemical Society, Fuel Division Preprints., Vol. 39 (1), pp. 113-120.

98. Tamashausky, Albert V. *An Introduction to Synthetic Graphite.* Technical Services Department , Asbury Graphite Mills Inc. s.l. : Asbury Graphite Mills Inc, 2006.

99. Marsh H., Heintz E. A., Rodríguez-Reinoso F. *Introduction to Carbon Technologies.* 1997.

100. Tamashausky, Albert V. *Synthetic Graphite Advanced Topics; Morphology.* Technical Services Department, Asbury Graphite Mills Inc. s.l. : Asbury Graphite Mills Inc, 2006.

101. *Analysis of load-speed sensitivity of friction composites based on various synthetic graphites.* Dilip Kolluri, Anup K. Ghosh, Jayashree Bijwe. 266, 2009, Wear, pp. 266–274.

102. Blau., Peter J. *Friction science and technology.* 1996.

103. *Poly(carbon monofluoride): A solid layered fluorocarbon.* Peter Kamarchik Jr., John L. Margrave. 8, 1978, Acc. Chem. Res., Vol. 11, pp. 296–300.

104. *Graphite fluoride as a solid lubricant.* 3, 1973, Industrial Lubrication and Tribology, Vol. 25 , pp. 118 - 118.

105. *Analytical Evaluation of Graphite Fluoride and Its Lubrication Performance Under Heavy Load.* MeConnell B.D., Snyder C.E. and Strang J.R. 4, April 1977, Lubrication Engineering, Vol. 33, pp. 184-190.

106. *A Comprehensive Study of Chemical and Physical Properties of Metal Sulfides.* Bernhard Melcher, Peter Faullant. 2000, SAE TECHNICAL PAPER SERIES. 2000-01-2757.

107. *Effect of zinf sulfide on the formation of an antiseizing layer in the sintered antifriction materials.* V. T. Bondar, B. V. Fenochka, i. A. Kossko, V. S. Ageeva. 4, 1992, Soviet Powder Metallurgy and Metal Ceramics, Vol. 31, pp. 357-363.

108. *The effects of antimony trisulfide (Sb2S3) and zirconium silicate (ZrSiO4) in the automotive brake friction material on friction characteristics.* Ho Jang, Seong Jin Kim. 2000, Wear, Vol. 239, pp. 229–236.

109. Geringer, Michael. *Solid lubricant, especially for friction linings, friction lining mixtures . US5958846 A* Apr 12, 1999.

110. *Friction Science and Technology: From Concepts to Applications, Second Edition.* Blau, Di Peter J. s.l. : Taylor and Francis group, LLC, 2009.

111. *Molybdenum disulfide as a lubricant a review of the fundamental knowledg.* Winer, W.O. 7, 1967, Wear, Vol. 10, pp. 422-452.

112. Ronald Hüner, Bernhard Melcher, Roman Milczarek, Herbert Kienleitner, (Chemetall Ges. M.B.H.). *Solid lubricants with a tin sulphide and carbon base. US 6303545 B1* oct 16, 2001.

113. ITRI Ltd. *Feasibility of a New Approach to Tin-Based Material Blends for Brake Pads.* 2004. SUSTAINABLE TECHNOLOGIES INITIATIVE.

114. *A Review of the Contribution of Solid Lubricants to Performance Improvement of Friction Linings.* Holinski, R. Denver, Colorado : s.n., August 5, 1984. 3rd ASLE International Solid Lubricants Conference.

115. *Materials, Use of Hexagonal Boron Nitride in Automotive Friction.* Lee P.W., Leist J., Filip P. 2010, Society of Automotive Engineers technical paper series. 2010-01-1676.

116. *A new strain path to inducing phase transitions in semi-crystalline polymers.* E.N. Brown, D.M. Dattelbaum, D.W. Brown, P.J. Rae, B. Clausen. 2007, Polymer, Vol. 48, pp. 2531e-536.

117. *X-ray diffraction study of crystal transformation and molecular disorder in poly(tetrafluoroethylene).* Takashi Yamamoto, Tetsuhiko Hara. s.l. : Butterworth & Co (Publishers) Ltd, 1982, POLYMER,, Vol. 23.

118. *Friction and wear of PTFE - a review.* S. K. Biswas, Kalyani Vijayan. 1992, Wear, Vol. 158, pp. 193-211.

119. *Transfer film evolution and its role in promoting ultra-low wear of a PTFE nanocomposite.* J. Ye, H.S.Khare,D.L.Burris. 2013, Wear, Vol. 297, pp. 1095–1102.

120. *Solid lubricants for applications at elevated temperatures.* Allam, I.M. 1991, JOURNAL OF MATERIALS SCIENCE, Vol. 26, pp. 3977-3984.

121. *Localization of Plastic Deformation in Calcium Fluoride Crystals at Elevated Temperatures.* N. P. Skvortsova, E. A. Krivandina, and D. N. Karimov. 4, 2008,, Physics of the Solid State, Vol. 50, pp. 665–669.

122. *On the role of copper in brake friction materials.* W. O sterle, C. Prietzel, H.Kloß , A.I.Dmitriev. 12, 2010, TribologyInternational, Vol. 43, pp. 2317–2326.

123. *Braking pad-disc system: Wear mechanisms and formation of wear fragments.* Piyush Chandra Vermaa, Luca Menapacea, **Andrea Bonfanti**, Rodica Ciudina, Stefano Gialanellaa, Giovanni Straffelini. 2015, Vols. 322-323, pp. 251–258.

124. Limiting the use of certain substances in brake friction material. Washington : s.n., 2010. SUBSTITUTE SENATE BILL 6557.

125. *A crystal-chemical approach to lubrication by solid oxides.* Erdemir, Ali. 8, 2000, Tribology Letters, pp. 97–102.

126. U.S. TEWARI, J. BIJWE. Recent Developments in Tribology of Fibre Reinforced Composites with Thermoplastic and Thermosetting Matrices. *Advances in Composite Tribology.* s.l. : K Friedrich, 1993.

127. McGraw-Hill. *Encyclopedia of Science and Technology,.* New York : s.n., 1960. p. 243. Vol. 5.

128. Wallenberger, F. T. CHAPTER 1 FIBERS FROM THE VAPOR, LIQUID AND SOLID PHASE. *Advanced Inorganic Fibers.* 2000.

129. IN, ADVANCES. Recent Developments in Tribology of Fibre Reinforced Composites with Thermoplastic and Thermosetting Matrices. [book auth.] U.S. TEWARI and J. BIJWE. *ADVANCES IN COMPOSITE TRIBOLOGY.* s.l. : Klaus Friedrich, 1993.

130. cambridge, University of. Mechanics of Fibre-Reinforced Composites. *DoITPoMS.* [Online] http://www.doitpoms.ac.uk/tlplib/fibre_composites/printall.php.

131. IARC Monographs on the Evaluation of Carcinogenic Risks to Humans. 100 C.

132. *Asbestos and the Pleura; A Review.* David W. Cugell, MD, FCCP and and David W. Kamp, MD. 2004, CHEST, Vol. 125, pp. 1103–1117.

133. Jean-Baptiste Donnet, Emmanuel Custodero. Reinforcement of Elastomers by Particulate Fillers. *The Science and Technology of Rubber (Fourth Edition).* 2013.

134. S. Yashima, Y. Kanda, S. Sano. Relationships between particle size and fracture energy or impact velocity required to fracture as estimated from single particle crushing. *Powder Technology.* 1987, Vol. 51, 3, pp. 277–282.

135. *Effect of aspect ratios of aramid fiber on mechanical and tribological behaviors of friction materials.* Peng Cai, Zhenlian Li , Tingmei Wang, Qihua Wang. 2015, Tribology International, Vol. 92, pp. 109–116.

136. *A review of heat treatment on polyacrylonitrile fiber.* M.S.A. Rahaman, A.F. Ismail, A. Mustafa. 2007, Polymer Degradation and Stability, Vol. 97, pp. 1421-1432.

137. *Friction characteristics of brake pads with aramid fiber and acrylic fiber.* Jung Hwan Park, Jin Oh Chung, Hyang Rae Kim. 2, 2010 : s.n., Industrial lubrication and tribology, Vol. 62.

138. *Natural Fiber Polymer Composites: A Review.* JOG, D. NABI SAHEB and J. P. 4, 1999, Advances in Polymer Technology, Vol. 18, pp. 351–363.

139. *Selection and verification of kenaf fibres as an alternative friction material using Weighted Decision Matrix method.* Ashafi'e Mustafa, Mohd Fadzli Bin Abdollah, Fairuz Fazillah Shuhimi, Nurhidayah Ismail,Hilmi Amiruddin , Noritsugu Umehara. 2015, Materials and Design, Vol. 67, pp. 577–582.

140. *Natural fiber in friction materials.* M.Sloan, L.Savage, K.Evans, B.Hooper. 2006. SAE technical paper. 2006-01-3187.

141. *Jute fibers and powderized hazelnut shells as natural fillers in non-asbestos organic non-metallic friction composites.* Vlastimil Matejka, Zhezhen Fu, Jana Kukutschová, Shicheng Qi, Shengling Jiang, Xiaoa Zhang, Rongping Yun , Miroslav Vaculík, Marie Heliová , Yafei Lu. 2013, Materials and Design, Vol. 51, pp. 847–853.

142. *State of the art on tribological behavior of polymer matrix composites reinforced with natural fibers in the green materials world - review.* Emad Omrani, Pradeep L. Menezes, Pradeep K. Rohatgi. 2015, Engineering Science and Technology, an International Journal.

143. *Performance of friction materials based on variation in nature of organic fibres Part I. Fade and recovery behaviour.* B.K. Satapathy, J. Bijwe. 257, 2004, Wear, pp. 573–584.

144. Michel Cartier, Georges Cros. *Organic filler of animal origin to be used in the preparation of friction materials offering a very low rate of wear. US 4491542 A* 1 1, 1985.

145. *The thermal transformation of Man Made Vitreous Fibers (MMVF) and safe recycling as secondary raw materials (SRM).* A.F. Gualtieri, E. Foresti , I.G. Lesci, N. Roveri, M. Lassinantti Gualtieri, M. Dondi, M. Zapparoli. 2009, Journal of Hazardous Materials, Vol. 162, pp. 1494–1506.

146. *The effect of metal fibers on the friction performance of automotive brake friction materials.* H. Jang, K. Ko, S.J. Kima, R.H. Basch, J.W. Fash. 2004, Wear, Vol. 256, pp. 406–414.

147. Tabor, David. FRICTION, LUBRICATION,AND WEAR. [book auth.] Thomas H. Brown Harold Rothbart. *Mechanical Design Handbook, Measurement, Analysis, and Control of Dynamic Systems.* 2006.

148. Cox, Roy L. *ENGINEERED TRYBOLOGICAL COMPOSITE.* Warrendale, Pennsylvania, USA : SAE International, 2012.

149. *Copper Substitution and Noise Reduction in Brake Pads: Graphite Type Selection.* Raffaele Gilardi, Luigi Alzati , Mamadou Thiam, Jean-François Brunel , Yannick Desplanques , Philippe Dufrénoy , Sanjeev Sharma, Jayashree Bijwe. 2012, Materials, Vol. 5, pp. 2258-2269.

150. *Feasibility study of replacing copper in NAO/NON-Steel Disc Pads by a thermally conductive Roxul®1000 fibre and synthetic iron sulphide.* B. van de Worp, L. Smeets. 2013. EuroBrake . EB2013-FRM-007.

151. G. CROSA, I.J.R. BAUMVOL. Chapter 16 Tribology of Polymer Composites Used as Frictional Materials. *Advances in Composite Tribology.* 1993.

152. *Effects of Ceramic Fiber on the Friction Performance of Automotive Brake Lining Materials.* Ye Han, Xiaofeng Tian, Yansheng Yin. 6, 2008, Tribology Transactions , Vol. 51, pp. 779-783.

153. F.R.Jones, N.T.Huff. 9 - The structure and properties of glass fibres. *Handbook of Textile Fibre Structure.* s.l. : S. Eichhorn, J.W.S. Hearle, M. Jaffe and T. Kikutani.

154. Erich Fitzer, Andrew Foley, Wilhelm Frohs, Tilo Hauke, Michael Heine, Hubert Jager, Sandra Sitter. Fibers, 5. Synthetic Inorganic. *Ullmann's Encyclopedia of Industrial Chemistry.* s.l. : Wiley-VCH Verlag GmbH & Co. KGaA, 2008.

155. Employment, Social Affairs & Inclusion. European Commission. *Recommendation from the Scientific Committee on Occupational Exposure Limits for man made-mineral fibres (MMMF) with no indication for carcinogenicity and not specified elsewhere.* 2012. SCOEL/SUM/88.

156. *Assessment of braking performance of lapinus–wollastonite fibre reinforced friction composite materials.* Tej Singh, Amar Patnaik, Ranchan Chauhan, Ankit Rishiraj. Received 8 January 2015; accepted 2 June 2015, Journal of King Saud University – Engineering Sciences.

157. *Structural, electronic and elastic properties of potassium hexatitanate crystal.* Hua Manyu, LiYimin, LongChunguang, LiXia. 2012, Physica B, Vol. 407, pp. 2811–2815.

158. *Methods of manufacturing of potassium titanate fibres and whiskers. A review.* T.ZAREMBA, D.WITKOWSKA. 1, 2010, Materials Science-Poland, Vol. 28.

159. *Tribological Properties of Potassium Titanate in the Brake Friction Material; Morphological Effects.* Keun Hyung Cho, Min Hyung Cho, Seong Jin Kim, Ho Jang. 32, 2008, Tribol Lett, pp. 59–66.

160. *Synergistic effects of aramid pulp and potassium titanate whiskers in the automotive friction material.* S.J. Kim, M.H. Cho, D.S. Lim, H. Jang. 2001, Wear, Vol. 251, pp. 1484–1491.

161. *Hybrid composite friction materials reinforced with combination of potassium titanate whiskers and aramid fibre: Assessment of fade and recovery performance.* Mukesh Kumar, Bhabani K. Satapathy, Amar Patnaik, Dilip K.Kolluri , Bharat S.Tomar. 4, 2001, Tribology International, Vol. 44.

162. *Methods of manufacturing of potassium titanate fibres and whiskers. A review.* T. ZAREMBA, D. WITKOWSKA. 1, 2010, Materials Science-Poland, Vol. 28.

163. *Carbon fibers for composites.* CHAND, S. 2000, JOURNAL OF MATERIALS SCIENCE, Vol. 35, pp. 1303 – 1313.

164. *Carbon fibres from cellulosic precursors: a review.* Ahu Gu¨mrah Dumanlı, Alan H. Windle. 2012, J Mater Sci, Vol. 47, pp. 4236–4250.

165. *Production of Mesophase Pitch from Coal Tar and Petroleum Pitches using Supercritical Fluid Extraction.* Mustafa Z. OZEL, Keith D. BARTLE. 2002, Turk J Chem, Vol. 26, pp. 417-424.

166. Erik Frank, Michael R. Buchmeiser. Carbon Fibers. *Encyclopedia of Polymeric Nanomaterials.* 2015.

167. Yoong Ahm Kim, Takuya Hayashi, Morinobu Endo, Mildred S. Dresselhaus. Carbon nanofibres. *Springer Handbook of Nanomaterials.* s.l. : Vajtai, Robert , 2013.

168. *Post spinning and pyrolysis processes of polyacrylonitrile (PAN)-based carbon fiber and activated carbon fiber: A review.* N. Yusofa, A.F. Ismaila,. 2012, Journal of Analytical and Applied Pyrolysis, Vol. 93, pp. 1–13.

169. *A Review of Methods for Improving the Interfacial Adhesion Between Carbon Fiber and Polymer Matrix.* LONG-GUI TANG, JOHN L. KARDOS. 1, 1997, POLYMER COMPOSITES, Vol. 18.

170. *Tribological performance of brake friction materials containing carbon nanotubes.* H.J. Hwang, S.L. Jung, K.H. Cho. 3-4, 2010, Wear, Vol. 268, pp. 519–525.

171. *Multiwall carbon nanotube elastomeric composites: A review.* Bokobza, Liliane. 17, 2007, Polymer, Vol. 48, pp. 4907–4920.

172. Inagaki, Michio. Advanced Carbon Materials. *Handbook of Advanced Ceramics.*

173. John Accorsi, Michael Yu. Carbon black. *Plastics Additives An A-Z reference.* s.l. : Geoffrey Pritchard, 1998.

174. *Evaluation of the material constants of nitrile butadiene rubbers (NBRs) with different carbon black loading (CB): FE-simulation and experimental.* M.A. Hassan, A. Abouel-Kasem, Mahmoud A. El-Sharief, F. Yusof. 2012, Polymer, Vol. 53, p. 3807e3814.

175. *Composites based on carbon black reinforced NBR/EPDM rubber blends.* Vojislav Jovanovic, Suzana Samarz-Jovanovic, Jaroslava Budinski-Simendic, Gordana Markovic. 2013, Composites: Part B, Vol. 45, pp. 333–340.

176. Michio INAGAKI, Feiyu KANG, Masahiro TOYODA, Hidetaka KONNO. Glass-like Carbon. *Advanced Materials Science and Engineering of Carbon.* s.l. : Tsinghua University Press Limited, 2014.

177. Materials, Composite. Composite Materials. [book auth.] JOSEPH K. LEES, ASHOK K. DHINGRA, R. L. MCCULLOUGH, BERNHARD ILSCHNER. *Ullmann's Encyclopedia of industrial chemistry.* 2012.

178. *FILLERS IN FRICTION MATERIALS.* SPURR, R. T. 1972, Wear, Vol. 22.

179. *Review of automotive brake friction materials.* D Chan, G W Stachowiak. Automobile Engineering, Vol. 218 D. Proc. Instn Mech. Engrs.

180. Katz, Harry S. Particulate fillers. *HANDBOOK OF COMPOSITE SECOND EDITION.* s.l. : S.T. Peters, 1998.

181. *The saturation state of the world's ocean with respect to (Ba,Sr)SO4 solid solutions.* Christophe Monnin, Damien Cividini. 2006, Geochimica et Cosmochimica Acta, Vol. 70, pp. 3290–3298.

182. *Correlation Analysis between Friction Material Parameters and the NVH Behavior.* 2015-01-2686, 2015, SAE Technical papers.

183. *Introduction to Brake Noise & Vibration.* Pfeifer, Weiming Liu & Jerome L.

184. Measurement of Disc Brake Friction Material Underlayer Distribution. *SAE standard .* J2724A WIP.

185. *Factors Influencing Acoustic Performance of Sound Absorptive Materials.* Seddeq, Hoda S. 4, 2009, Australian Journal of Basic and Applied Sciences, Vol. 3, pp. 4610-4617.

186. Sergienko Vladimir P., Bukharov Sergey N. *Noise and Vibration in Friction Systems.* 2015.

187. *Sound absorption characteristics of a high-temperature sintering porous ceramic material.* Duan Cuiyun, Cui Guang, Xu Xinbang, Liu Peisheng. 73, 2012, Applied Acoustics.

188. Robert C. Lam, Yih-Fang Chen, Kenji Maruo. *Friction material with nanoparticles of friction modifying layer . US 7294388 B2*

189. *Investigation of using natural zeolite in brake pad.* Keskin, Ahmet. 23, 2011, Scientific Research and Essays, Vol. 6, pp. 4893-4904.

190. *Reduced cost and improved performance of NAO/non-steel and Low-steel disc pads by using Promaxon®-D.* Lapinus in collaboration with Promat. 2012. Eurobrake 2012 Technical Paper.

191. Yukinori Yamashita, Mitsuhiko Nakagawa, Masanori Ibuki, Hiroya Kishimoto. *Friction material for making brake pads. US5266395 A* 1993.

192. Asbury Graphite Mills, Inc. Mica for Friction Materials. [Online]

193. *High-temperature study and thermal expansion of phlogopite.* phlogopite, High-temperature study and thermal expansion of. 9, 2000, Physics and Chemistry of Minerals, Vol. 27, pp. 599-603.

194. *Mineral Resource of the Month: Mica.* Hedrick, James B. 2008, Geotime.

195. *A REVIEW OF ASBESTOS SUBSTITUTE MATERIALS IN INDUSTRIAL APPLICATIONS.* PYE, A.M. 3, 1979, Journal of Hazardous Materials, pp. 125-147.

196. *Synthesis of nano-layered vermiculite of low density by thermal treatment.* Y. El Mouzdahir, A. Elmchaouri, R. Mahboub, A. Gil, S.A. Korili. 189, Powder Technology, Vol. 2009, pp. 2-5.

197. *Improvements in Performance of Vermiculite-Containing Non Asbestos Organic Brake Friction Materials.* Ou C., Bablouzian L., Trainor J. 1991, SAE Technical Paper . 912655.

198. De, Gaugue Charles Louis Ernest. *Dry mix friction material comprising butadiene acrylonitrile rubber, phenol formaldehyde resin and filler. US 3344094 A* 1967.

199. *Antioxidant properties of carbon black in unsaturated elastomers. Studies with cis-polybutadiene.* J. T. GRUVER, K. W. ROLLMAKN. 3, 1964, Journal of Applied Polymer Science, Vol. 8.

200. CORAN, AUBERT Y. Vulcanization. *Science and Technology of Rubber (Third Edition).* 2005.

201. Hewitt, Peter A. Ciullo Norman. COMPOUNDING MATERIALS. *The Rubber Formulary.* 1999.

202. *SPECTROSCOPIC CHARACTERIZATION OF THE MOLECULAR STRUCTURE OF ELASTOMERIC NETWORKS.* Koenig, Jack L. 3, 2000, Rubber Chem, Vol. 73, pp. 385-404.

203. *Recent Advances in Structural Characterization of Elastomers.* Tanaka, Yasuyuki. 3, 1991, Rubber Chemistry and Technology , Vol. 64.

204. *VULCANIZATION AND CROSSLINKING IN ELASTOMERS.* M. AKIBA, A. S. HASHIM. 1997, Prog. Polym. Sci, Vol. 22, pp. 475- 521.

205. CORAN, A.Y. Chapter 7 – Vulcanization. [book auth.] Frederick R. Eirich. *Science & Technology of Rubber.* 1978, pp. 291–338.

206. Shigetoshi Kinouchi, Yasuhiro Hara, Junya Yamaguchi. *Friction material composition, production of the same and friction material. US 6372817 B1* 2002.

207. Knop, Andre, Böhmer, Volker and Pilato, Louis A. *Comprehensive Polymer Science and Supplements.* 1989.

208. Pilato, Louis. *Phenolic Resins: A Century of Progress.* Bound Brook New Jersey : Pilato Consulting, 2010.

209. Andre Knop, Louis A. Pilato. *Phenolic Resins: Chemistry, Applications and Performance.* 1985.

210. T. Takeichi, N. Furukawa. Epoxy Resins and Phenol-Formaldehyde Resins. *Polymer Science: A Comprehensive Reference.* s.l. : Elsevier B.V., 2012, pp. 723-751.

211. *The condensation of trimethylolphenol.* Jones, Robert T. 6, 1984, Journal of Polymer Science: Polymer Chemistry Edition, Vol. 21, pp. 1801–1817.

212. H. U. Wagner, G. Gompper. *The Chemistry of The Quinoid Compounds.* New York : S. Patai, Wiley, 1974, Vol. 2, 18.

213. *Controlled synthesis of high-ortho-substitution phenol-formaldyhde.* Jianying Huang, Miaoqing Xu, Qiang Ge, Minghua Lin, Qiang Lin, Yihong Chen, Jiayan Chu, Lizong Dai, Yousi Zou. 2, July 15, 2005, Journal of Applied Polymer Science, Vol. 97, pp. 652–658.

214. *Effect of molecular weight and molecular weight distribution on cure reaction of novolac with hexamethylenetetramine and properties of related composites.* Jintao Wana, Songsong Wang, Cheng Li , Dapeng Zhou, Jianguo Chen, Zheng Liu, Liqiong Yu,Hong Fana, Bo-Geng Li. 1012, Thermochimica Acta, Vol. 530, pp. 32-41.

215. E. Frollini, C. G. Silva, E. C. Ramires. Phenolic resins as a matrix material in advanced fiber-reinforced polymer (FRP) composites. *Advanced Fibre-Reinforced Polymer (FRP) Composites for Structural Applications.* s.l. : Elsevier, 2013 .

216. *Modified PF resins for composite structures with improved mechanical properties.* F. Cardona, T. Aravinthan, C. Moscou. 6, 2010, Polym Polym Compos, Vol. 18, pp. 297-306.

217. *CNSL: an environment friendly alternative for the modern coating industry.* Dinesh Balgude, Kiran Konge, Anagha Sabnis. 2, 2014, Journal of Coatings Technology and Research , Vol. 11, pp. 169-183 .

218. *Review of automotive brake friction materials.* D Chan, G W Stachowiak. 2004, Proc. Instn Mech. Engrs Part D: J. Automobile Engineering, Vol. 218.

219. Zeitsch, Di K.J. *The Chemistry and Technology of Furfural and its Many By-Products.* s.l. : Elsevier, 2000. p. 376.

220. *Studies On The Synthesis And Curing Of Thermosetting.* Riya Srivastava, Deepak Srivastava. 5, 2013, International Journal of ChemTech Research, Vol. 5, pp. 2575-2581.

221. *Thermal stability of boron-containing phenol formaldehyde resin.* Jungang Gao, Yanfang Liu, Liting Yang. 1999, Polymer Degradation and Stability, Vol. 63, pp. 19-22.

222. *Synthesis of a boron modified phenolic resin.* Aparecida M. Kawamoto, Luiz Cláudio Pardini, Milton Faria Diniz, Vera Lúcia Lourenço, Marta Ferreira K. Takahashi. 2, 2010, J. Aerosp.Technol. Manag, Vol. 2, pp. 169-182.

223. *An Acrylic Rubber Modified Phenolic Resin Which Has Good Flexibility at Low Temperature.* Imai, J. 2008, SAE Technical Papers. 2008-01-2539.

224. John F. Kane, Norman R. Mowrer. *Phenolic resin compositions with improved impact resistance . EP0821711 B1* USA, 2003.

225. *Modification of epoxy resin with siloxane containing phenol.* Tsung-Han Ho, Chun-Shan Wang. 2001, European Polymer Journal, Vol. 37, pp. 267-274.

226. Kandelbauer, Andreas. *Handbook of Thermoset Plastics (Third Edition).* 2014.

227. Fink, Johannes Karl. *Reactive Polymers Fundamentals and Applications (Second Edition).* 2013.

228. *Silicone containing copolymers: Synthesis, properties andapplications.* Emel Yilgor, Iskender Yilgor. 2014, Progress in Polymer Science, Vol. 39, pp. 1165-1195.

229. *The chemistry and properties of silicone resins.* Mayer, H. 1999, Surface coating international, Vol. 2, pp. 77-83.

230. Cox, Roy L. Inorganic Binder Systems. *Engineered Tribological Composites The Art of Friction Material Development.* 2012.

231. Kapl, Gerhard and Hinterwaldner, Rudolph. *FRICTION LINING AND PROCESS FOR THE PRODUCTION THEREOF. US005433774A* Jul. 18, 1995.

232. M. L. Wilson, S. H. Kosmatka. *Design and Control of Concrete Mixtures.* 2002.

233. Roberta Alfani, Fabio Corazza, Flavio RAMPINELLI, **Andrea BONFANTI**, Paolo VAROTTO, Laura SAMMARELLI, Arianna BELOTTI. *Friction material for brake pads and related brake pads . WO2014203142 A1* 24 dic 2014.

234. Alfani Roberta, **Bonfanti Andrea**, Cividini Giovanni, Manganelli Giuseppe, Rampinelli Flavio, Sanguineti Alessandro, Tosi Federico. *Materiali di attrito migliorati per pastiglie frenanti a base di composizioni leganti e relative pastiglie frenanti. Domanda 102015000065027 (UB2015A005005)* 10 03, 2015.

235. *Brake wear particle emissions: a review.* Theodoros Grigoratos, Giorgio Martini. 4, 2015, Environ Sci Pollut Res Int., Vol. 22, pp. 2491-2504.

236. *Alkali-activated inorganic matrix for automotive brake pads application: realization and performances of novel and alternative friction materials.* Alessandro Sanguineti, Federico Tosi, Flavio Rampinelli, **Andrea Bonfanti**. 2016. SAE 2016 Brake Colloquium & Exhibition.

237. *Dependency of pm10 particles emission on stability of friction coefficient and character of friction surface.* Vlastimil, Matějka, Metinöz Ibrahim, Alemani Mattia, Wahlström Jens and **Bonfanti Andrea**, Oloffson Ulf, Perricone Guido. Manuscript accepted. Eurorake 2016.

238. *Characterization of Short Fibers.* Andreas Bartl, Davide Pico. 2009. Conference: 9th International Conference on Chemical and Process Engineering. Vol. 17.

239. Dante, Roberto C. *Handbook of Friction Materials and their Applications.* 2015.

240. http://www.rubbermixingmachinery.com/products.html. [Online]

241. *An experimental study on the effects of manufacturing parameters on the tribological properties of brake lining.* Rukiye Ertan, Nurettin Yavuz. 2010, Wear, Vol. 268, pp. 1524–1532.

242. *Impact of post-curing duration on mechanical, thermal and tribological behavior of an organic friction material.* Hentati, Nesrine, et al. 2014, Materials and Design, Vol. 63, pp. 699–709.

243. *Mechanism of Brake Fade in Organic Brake Pad Linings.* Herring, J.M. 670146, 1967, SAE technical paper.

244. *Determination of Tribological History and Wear through Visualisation in Lubricated Contacts using a Carbon-based Composite.* A. Jullien, M.H. Meurisse and Y. Berthier. 1996, Wear, Vol. 194, pp. 116–125.

245. http://www.rubore.com/en/products_and_applications/shims___insulators/shims___insulators_1.html. [Online]

246. http://nucap.com/. [Online] 2016.

247. Marco Lodi, Emilio Benfenati, **Andrea Bonfanti**. *Indagine d'Igiene Industriale per la ricerca di sostanze organiche ed inorganiche rilasciate da pastiglie di freni durante le lavorazioni in officina.* Unità d'Igiene Industriale ed Ambientale e Laboratorio di Chimica e Tossicologia dell'Ambiente IRFMN. 2015. Confidential report.

248. *Towards a test stand for standardized measurements of the brake emissions.* Perricone G., Wahlström J., Olofsson U. 2015, Proc IMechE Part D: J Automobile Engineering, Vols. 1–8.

249. M.G. Consonni, L. Corgatelli. *ALFA ROMEO 159 2.4jtdm: "Cobra".* Testing dep., Brembo S.p.A. 2015. T FA8Y1 J EB.

250. *Identification of Organic Compounds Released from Low-Metallic Automotive Model Brake Pad and its Non-Airborne Wear Particles.* Daniela Plachá, Pavlina Peikertova, Jana Kukutschova, Poh Wah Lee, Kristina Čabanová, Jiří Karas, Jana Kuchařová, Peter Filip. 1, 2016, SAE Int. J. Mater. Manf., Vol. 9. 2015-01-2662.

Acknowledgments